

W84-24975

**COLLEGE**  
OF  
**ENGINEERING**



**VIRGINIA**  
**POLYTECHNIC**  
**INSTITUTE** AND  
**STATE**  
**UNIVERSITY**



**BLACKSBURG,**  
**VIRGINIA**

INPUT FILTER COMPENSATION  
FOR SWITCHING REGULATORS

FINAL REPORT

Grant NAG 3-220  
National Aeronautics and Space Administration  
Lewis Research Center

by

Professor F. C. Lee  
Department of Electrical Engineering  
Virginia Polytechnic Institute & State University  
Blacksburg, Virginia 24061

## CONTENTS

<u>Chapter</u>	<u>page</u>
I. INTRODUCTION . . . . .	1
II. INPUT FILTER RELATED PROBLEMS AND CONVENTIONAL DESIGN TECHNIQUES . . . . .	5
Input Filter Related Problems . . . . .	5
Input Filter Design Considerations . . . . .	16
III. CONCEPT OF POLE-ZERO CANCELLATION USED IN TOTAL STATE CONTROL . . . . .	31
Concept of Pole-Zero Cancellation. . . . .	31
Total State Control . . . . .	35
IV. MODELING OF THE POWER STAGE WITH INPUT FILTER . .	38
Buck-boost converter small signal model derivation . . . . .	39
Buck converter small signal model derivation . . . . .	49
Boost converter small signal model derivation . . . . .	56
V. IMPLEMENTATION OF THE FEEDFORWARD LOOP FOR A BUCK REGULATOR . . . . .	68
State Space Model of Buck Regulator . . . . .	68
Generalized Small Signal Model of Buck Regulator . . . . .	71
Design of the Feedforward Loop. . . . .	80
Implementation of Feedforward . . . . .	83
VI. ANALYTICAL AND EXPERIMENTAL VERIFICATION OF THE FEEDFORWARD DESIGN . . . . .	91
Measurements of the nonadaptive feedforward control . . . . .	92
Adaptive Feedforward Measurements. . . . .	100
Measurements of Closed Loop Input-to-Output Transfer Function (Audiosusceptibility). . . . .	124
Measurements of Output Impedance. . . . .	140

	Measurement of Transient Response and Starting of the Regulator. . . . .	145
	Conclusions . . . . .	160
VII.	DIGITAL SIMULATION OF BUCK REGULATOR FOR TRANSIENT ANALYSIS . . . . .	162
	Description of the method . . . . .	162
	Description of the program . . . . .	171
	Simulation Results . . . . .	178
VIII.	DISCRETE TIME DOMAIN STABILITY ANALYSIS OF BUCK REGULATOR . . . . .	213
	Analytical Investigation of Stability . . . . .	214
	Experimental Verification of Stability Analysis. . . . .	258
	Conclusions . . . . .	264
IX.	EXTENSIONS OF THE CONCEPT OF INPUT FILTER COMPENSATION TO OTHER CONVERTER TYPES . . . . .	266
	Extension to other types of regulator control . . . . .	266
	Feedforward compensation for the buck-boost and boost regulators . . . . .	271
	Remarks . . . . .	292
X.	CONCLUSIONS AND FUTURE WORK . . . . .	293
	Conclusions . . . . .	293
	Suggestions for future work . . . . .	296
 <u>Appendix</u>		
		<u>page</u>
A.	. . . . .	298
B.	. . . . .	325
BIBLIOGRAPHY . . . . .		353

LIST OF TABLES

<u>Table</u>	<u>page</u>
1. Eigenvalues and Closed Loop Poles for various values of L1. . . . .	239
1. continued . . . . .	240
1. continued . . . . .	241
2. Eigenvalues for different values of $R_{f2}$ . . . . .	255
2. continued . . . . .	256
2. continued . . . . .	257

## LIST OF FIGURES

<u>Figure</u>	<u>page</u>
1. Buck Converter with an Input Filter . . . . .	6
2. Negative resistance oscillation. . . . .	8
3. Small-signal model using the dual-input describing function. . . . .	9
4. Duty cycle-to-output voltage characteristic with and without input filter (a) gain (b) phase. . . . .	12
5. Audiosusceptibility with and without input filter. . . . .	15
6. Buck type switching regulator with a two stage input filter. . . . .	17
7. Open loop gain and phase characteristics without the input filter damping resistance $R_D$ . . . . .	18
8. Single-stage input filters . . . . .	21
9. Interaction between output impedance $Z(s)$ of input filter and input impedance $Z_i(s)$ of regulator. . . . .	23
10. Two-stage input filter. . . . .	25
11. Duty cycle-to-output describing function of power stage with two-stage input filter. . . . .	26
12. Interaction between the switching regulator and its preregulator. . . . .	30
13. Two loop controlled switching buck regulator. . . . .	32
14. Total State Control. . . . .	36
15. Buck-boost converter power stage. . . . .	40
16. Buck-boost converter power stage model: (a) during $T_{ON}$ and (b) during $T_{OFF}$ . . . . .	41
17. Buck-boost converter power stage small signal state space model . . . . .	47

18.	Buck-boost converter power stage small signal equivalent circuit . . . . .	48
19.	Buck converter power stage. . . . .	51
20.	Buck converter power stage model during: (a) $T_{ON}$ and (b) $T_{OFF}$ . . . . .	52
21.	Buck converter power stage small signal state space model. . . . .	57
22.	Buck converter power stage small signal equivalent circuit. . . . .	58
23.	Boost converter power stage . . . . .	60
24.	Boost converter power stage models during : (a) $T_{ON}$ and (b) $T_{OFF}$ . . . . .	61
25.	Boost converter power stage small signal state space model. . . . .	66
26.	Boost converter power stage small signal equivalent circuit. . . . .	67
27.	State space model of the buck regulator . . . . .	70
28.	Generalized Small Signal Model . . . . .	72
29.	Small signal equivalent circuit with $\hat{d} = 0$ . . . . .	76
30.	Small signal equivalent circuit with $\hat{v}_1 = 0$ . . . . .	78
31.	Buck regulator with feedforward used to obtain experimental results . . . . .	84
32.	Nonadaptive Feedforward Circuit . . . . .	88
33.	Adaptive feedforward implementation for a variable voltage supply. . . . .	89
34.	Buck regulator with feedforward used to obtain experimental results . . . . .	93
35.	Open loop transfer function measurements with single-stage input filter. (a) gain (b) phase margin. . . . .	96
36.	Two- stage input filter. . . . .	98

37.	Open loop transfer function measurements with two-stage input filter. (a) gain (b) phase margin. . . . .	99
38.	(a) Open loop gain at $V_I=25v$ : Calculated values and measured values ( $\Delta$ ) without feedforward . . . . .	103
38.	(b) Open loop phase margin at $V_I=25v$ : Calculated values and measured values ( $\Delta$ ) without feedforward . . . . .	104
38.	(c) Open loop gain at $V_I=25v$ : Calculated values and measured values ( $\Delta$ ) with feedforward . . . . .	105
38.	(d) Open loop phase margin at $V_I=25v$ : Calculated values and measured values ( $\Delta$ ) with feedforward . . . . .	106
39.	(a) Open loop gain at $V_I=30v$ : Calculated values and measured values ( $\Delta$ ) without feedforward . . . . .	107
39.	(b) Open loop phase margin at $V_I=30v$ : Calculated values and measured values ( $\Delta$ ) without feedforward . . . . .	108
39.	(c) Open loop gain at $V_I=30v$ : Calculated values and measured values ( $\Delta$ ) with feedforward . . . . .	109
39.	(d) Open loop phase margin at $V_I=30v$ : Calculated values and measured values ( $\Delta$ ) with feedforward . . . . .	110
40.	(a) Open loop gain at $V_I=35v$ : Calculated values and measured values ( $\Delta$ ) without feedforward . . . . .	111
40.	(b) Open loop phase margin at $V_I=35v$ : Calculated values and measured values ( $\Delta$ ) without feedforward . . . . .	112
40.	(c) Open loop gain at $V_I=35v$ : Calculated values and measured values ( $\Delta$ ) with feedforward . . . . .	113
40.	(d) Open loop phase margin at $V_I=35v$ : Calculated values and measured values ( $\Delta$ ) with feedforward . . . . .	114
41.	(a) Open loop gain at $V_I=40v$ : Calculated values and measured values ( $\Delta$ ) without feedforward . . . . .	115
41.	(b) Open loop phase margin at $V_I=40v$ : Calculated values and measured values ( $\Delta$ ) without feedforward . . . . .	116

41.	(c)	Open loop gain at $V_I = 40v$ : Calculated values and measured values ( $\Delta$ ) with feedforward . . .	117
41.	(d)	Open loop phase margin at $V_I = 40v$ : Calculated values and measured values ( $\Delta$ ) with feedforward . . .	118
42.	(a)	Open loop gain at $V_I = 25v$ : Calculated values and measured values ( $\Delta$ ) without feedforward . . .	120
42.	(b)	Open loop phase margin at $V_I = 25v$ : Calculated values and measured values ( $\Delta$ ) without feedforward . . . . .	121
42.	(c)	Open loop gain at $V_I = 25v$ : Calculated values and measured values ( $\Delta$ ) with feedforward . . .	122
42.	(d)	Open loop phase margin at $V_I = 25v$ : Calculated values and measured values ( $\Delta$ ) with feedforward . . .	123
43.		Measurement of audiosusceptibility [ $\hat{V}_o(s)/\hat{V}_x(s)$ ] with and without feedforward at $V_I = 25v$ . . . .	126
44.		Audiosusceptibility with and without feedforward at $V_I = 30v$ . . . . .	127
45.		Audiosusceptibility with and without feedforward at $V_I = 35v$ . . . . .	128
46.		Audiosusceptibility with and without feedforward at $V_I = 40v$ . . . . .	129
47.		$H(s)$ of two stage input filter, with $R_3 = 0.2$ ohm . . .	132
48.		$Z$ of two stage input filter, with $R_3 = 0.2$ ohm . . .	133
49.		Audiosusceptibility with and without feedforward at $V_I = 25v$ . . . . .	134
50.		Audiosusceptibility with and without feedforward at $V_I = 30v$ . . . . .	135
51.		Audiosusceptibility with and without feedforward at $V_I = 35v$ . . . . .	136
52.		Audiosusceptibility with and without feedforward at $V_I = 40v$ . . . . .	137
53.		$H(s)$ of two stage input filter, $R_3 = 0.075$ ohm . . .	138

54.	Z of two stage input filter, $R_3=0.075$ ohm . . . . .	139
55.	Output impedance with and without feedforward (X) at $V_I=25v$ . . . . .	141
56.	Output impedance with and without feedforward (X) at $V_I=30v$ . . . . .	142
57.	Output impedance with and without feedforward (X) at $V_I=35v$ . . . . .	143
58.	Output impedance with and without feedforward (X) at $V_I=40v$ . . . . .	144
59.	Output voltage ripple (a) and input filter capacitor voltage (b) without feedforward . . . . .	148
60.	Output filter inductor current (a) and control voltage (b) without feedforward . . . . .	149
61.	Output voltage ripple (a) and input filter capacitor voltage (b) with feedforward . . . . .	150
62.	Output filter inductor current (a) and control voltage (b) with feedforward . . . . .	151
63.	Output voltage without feedforward (a) and with feedforward (b) . . . . .	153
64.	Output voltage without feedforward (a) and with feedforward (b) . . . . .	156
65.	Output voltage (a) and output filter inductor current (b) without feedforward . . . . .	158
66.	Output voltage (a) and output filter inductor current (b) with feedforward . . . . .	159
67.	Nonadaptive feedforward circuit . . . . .	170
68.	Flow chart for discrete simulation . . . . .	172
68.	continued . . . . .	173
68.	continued . . . . .	174
68.	continued . . . . .	175
68.	continued . . . . .	176

68.	continued . . . . .	177
69.	(a) Output voltage during steady state operation.	180
69.	(b) Input filter inductor current during steady state operation . . . . .	181
69.	(c) Input filter capacitor voltage during steady state operation . . . . .	182
69.	(d) Output filter inductor current during steady state operation . . . . .	183
69.	(e) Feedforward voltage during steady state operation . . . . .	184
69.	(f) Control voltage during steady state operation	185
69.	(g) Voltage $e_R$ during steady state operation . . .	186
70.	(a) Output voltage simulation without feedforward	188
70.	(b) Input filter capacitor voltage simulation without feedforward . . . . .	189
70.	(c) Output filter inductor current simulation without feedforward . . . . .	190
70.	(d) Control voltage simulation without feedforward . . . . .	191
71.	(a) Output voltage simulation with feedforward .	192
71.	(b) Input filter capacitor voltage simulation with feedforward . . . . .	193
71.	(c) Output filter inductor current simulation with feedforward . . . . .	194
71.	(d) Control voltage simulation with feedforward	195
72.	Measurement without feedforward: output voltage (a) and input filter capacitor voltage (b) . . . . .	196
72.	Measurement without feedforward: output filter inductor current (c) and control voltage (d) .	197

73.	Measurement with feedforward: output voltage (a) and input filter capacitor voltage (b) . . . . .	198
73.	Measurement with feedforward: output filter inductor current (c) and control voltage (d) . . . . .	199
74.	(a) Output voltage simulation without feedforward	202
74.	(b) Input filter capacitor voltage simulation without feedforward . . . . .	203
74.	(c) Output filter inductor current simulation without feedforward . . . . .	204
74.	(d) Control voltage simulation without feedforward . . . . .	205
75.	(a) Output voltage simulation with feedforward .	206
75.	(b) Input filter capacitor voltage simulation with feedforward . . . . .	207
75.	(c) Output filter inductor current simulation with feedforward . . . . .	208
75.	(d) Control voltage simulation with feedforward	209
76.	Measured output voltage ripple without (a) and with (b) feedforward . . . . .	210
77.	Notation regarding time $t_K$ . . . . .	218
78.	Flowchart for stability analysis. . . . .	222
79.	Flowchart for calculating matrix $\psi$ . . . . .	225
79.	continued . . . . .	226
79.	continued . . . . .	227
79.	continued . . . . .	228
80.	Eigenvalues without input filter . . . . .	236
81.	Closed loop poles without input filter . . . . .	237
82.	Eigenvalues with input filter, without feedforward	242

83.	Closed loop poles with input filter, without feedforward . . . . .	243
84.	Eigenvalues with feedforward . . . . .	246
85.	(a) Open loop gain: calculated values without feedforward, with $R_{f2} = 220$ ohm and $R_{f2} = 210$ ohm . . . . .	249
85.	(b) Open loop phase margin: calculated values without feedforward, with $R_{f2} = 220$ ohm and $R_{f2} = 210$ ohm . . . . .	250
85.	(c) Open loop gain: calculated values without feedforward, with $R_{f2} = 220$ ohm and $R_{f2} = 240$ ohm . . . . .	251
85.	(d) Open loop phase margin: calculated values without feedforward, with $R_{f2} = 220$ ohm and $R_{f2} = 240$ ohm . . . . .	252
85.	(e) Open loop gain: calculated values without feedforward, with $R_{f2} = 220$ ohm and $R_{f2} = 300$ ohm . . . . .	253
85.	(f) Open loop phase margin: calculated values without feedforward, with $R_{f2} = 220$ ohm and $R_{f2} = 300$ ohm . . . . .	254
86.	(a) Open loop gain: measured values without input filter, with (•) and without feedforward . . . . .	259
86.	(b) Open loop phase margin: measured values without input filter, with (•) and without feedforward . . . . .	260
87.	Output voltage ripple without feedforward: (a) Y:0.2v/div X:5 msec/div. (b) Y:0.2v/div X:10 msec/div. . . . .	262
88.	Output voltage ripple with feedforward: (a) Y:0.2v/div X:5 msec/div. (b) Y:0.2v/div X:10 msec/div. . . . .	263
89.	Generalized small signal model for single loop control . . . . .	270
90.	State space model of the buck-boost regulator . . . . .	273
91.	Generalized small signal model . . . . .	275
92.	Small signal equivalent circuit with $\hat{d}=0$ . . . . .	277

93.	Small signal equivalent circuit with $\hat{v}_I = 0$	279
94.	Schematic of a buck-boost regulator	285
95.	(a) Open loop gain: Calculated values without input filter, with ( $\Delta$ ) and without feedforward	287
95.	(b) Open loop phase margin: Calculated values without input filter, and ( $\Delta$ ) and without feedforward	288
96.	(a) Open loop gain: Measured values without input filter, with ( $\bullet$ ) and without feedforward	290
96.	(b) Open loop phase margin: Measured values without input filter, with ( $\bullet$ ) and without feedforward	291

## Chapter I

### INTRODUCTION

Switching-mode dc-dc regulators are coming into increasing use as power supplies because of the significant reduction of weight, size and increase in equipment efficiency that can be attained. The dissipative regulators used earlier had the advantage of design simplicity, but suffer from low efficiency and higher weight due to the large transformer and filter needed to achieve the required voltage/current regulation.

Since the late sixties, the rapid expansion of the computer and communication industries and increasing complexity and sophistication of various systems necessitated the development of higher performance switched mode power supplies. The incentive for performance improvement prompted the initial development of multiple loop control schemes, such as the standardized control module (SCM) for dc-dc converters [2,7,8] and the current-injected control scheme [9]. The ever continuing search for performance improvement forms the underlying theme of this dissertation.

The work presented in this dissertation is mainly concerned with developing a control scheme to alleviate the

problem brought about due to the use of an input filter in switching regulators. The switching regulator input current has a substantial ripple component at the switching frequency and this necessitates the use of an input filter to smooth the pulsating current drawn from the supply. Furthermore the input filter also serves to attenuate noise present in the supply voltage from being propagated through the regulator to the payload downstream. The presence of the input filter, however, often results in various performance difficulties such as loop instability, degradation of transient response, audiosusceptibility (closed loop input-to-output gain) and output impedance characteristics [3,4,5,6,10]. These problems are caused mainly by the interaction between the resonant peaking of the output impedance of the input filter and the regulator control loop. Conventional single-stage and two-stage input filters can be designed such that the peaking effect is minimized, however such a design is often accompanied with a penalty of weight and loss in the input filter [3,4,5,6,10]. This dissertation presents a different approach via a feedforward control scheme to mitigate the undesirable interaction between the input filter and the regulator control loop.

The concept of pole-zero cancellation is used, in this dissertation, to develop a novel feedforward control loop

that senses the input filter state variables and processes this information in a manner designed to cancel the detrimental effect of peaking of the output impedance of the input filter. The feedforward loop working in conjunction with the feedback loops developed earlier [2,7,8] constitute a total state control scheme that eliminates the interaction between the input filter and the regulator control loop. Employing the novel feedforward compensation scheme presented in this dissertation, a high performance converter together with an effective input filter design (minimum weight and loss) can be accomplished concurrently. A buck regulator employing a feedforward control loop working in conjunction with the feedback loops was used to obtain measurements that showed significant improvement in the following performance categories:

1. Loop stability (open loop gain and phase margins);
2. Audiosusceptibility;
3. Output impedance; and
4. Transient response.

In this dissertation the problem caused by input filter interaction and conventional input filter design techniques are discussed in Chapter 2 followed in Chapter 3 by the concept of pole-zero cancellation developed earlier [2,7,8]. Chapters 4 and 5 present the modeling of the power stage

with input filter and the implementation of the feedforward for a buck regulator respectively. Measurements of open loop gain and phase that confirm the analytical prediction of performance improvement using the feedforward scheme developed, are discussed in Chapter 6 along with other measurements of audiosusceptibility, output impedance and transient response. Chapter 7 presents experimental and analytical results pertaining to transient response while Chapter 8 discusses the use of the feedforward loop in stabilizing a regulator system made unstable due to input filter interaction. Chapter 9 is concerned with extending the concept of feedforward compensation to other types of control and to other types of regulators i.e. the buck-boost regulators. Finally, Chapter 10 presents the conclusions and suggestions for future work.

## Chapter II

### INPUT FILTER RELATED PROBLEMS AND CONVENTIONAL DESIGN TECHNIQUES

#### 2.1 INPUT FILTER RELATED PROBLEMS

An input filter is often required between a switching regulator and its power source. A buck type switching regulator with a single-stage input filter is shown in Figure 1. The regulator input current has a substantial pulsating current component at the switching frequency as a result of the opening and closing of the switch and this component should be prevented from being reflected back into the source; an input filter is required to provide high attenuation at switching frequency and thus smooth the current drawn from the source. The input filter also serves to isolate source voltage disturbances from being propagated to the switching regulator payload downstream.

A presumably well-designed input filter, satisfying the above mentioned requirements, when used with a switching regulator can often cause significant performance degradations [3,4,5,6,10]. This is due primarily to the complex interaction between the switching regulator control loop, the input filter and the regulator output filter [3,4,5,6,10].

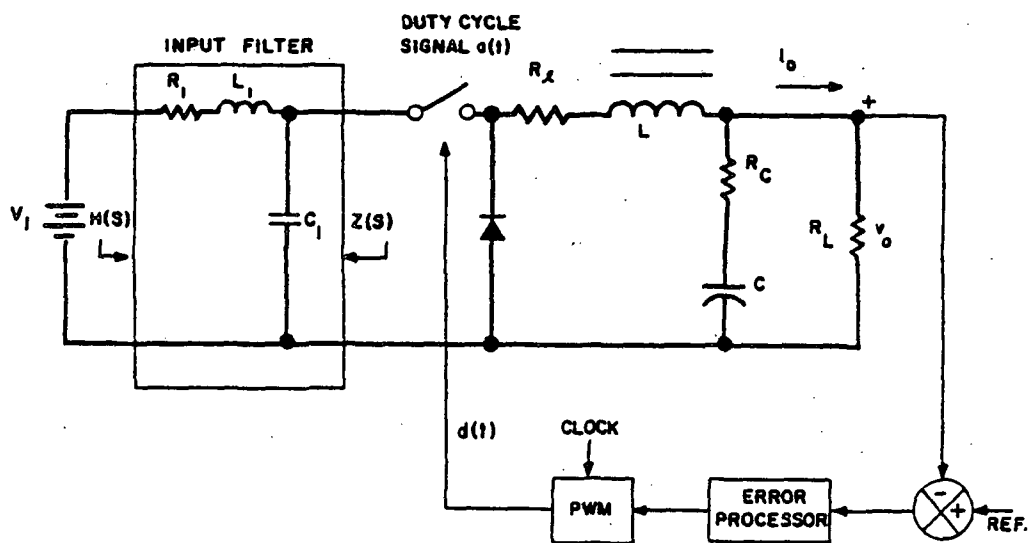


Figure 1: Buck Converter with an Input Filter

$$\begin{array}{llll}
 V_I = 12\text{v} & V_o = 5\text{v} & R_L = 0.86 \text{ ohm} & L = 200 \text{ microH} \\
 R_L = 20\text{mohm} & C = 1540\text{microF} & R_c = 7\text{mohm} & T_p = 50\text{microsecs} \\
 L_1 = 77 \text{ microH} & R_1 = 39.6 \text{ mohm} & C_1 = 412 \text{ microF} &
 \end{array}$$

The interaction between the control loop and the input filter is illustrated in Figure 2 . The switching regulator has been shown to have a nonlinear negative resistance, as illustrated in the figure, [3]. The input current  $i_r$  to the switching regulator is related nonlinearly to the input voltage  $e_r$  and the input resistance  $\frac{di_r}{de_r} = -\frac{1}{r}$  . Under certain conditions the input filter-switching regulator combination can become a negative resistance oscillator, producing large amplitude voltage excursions across capacitor C. When this happens serious degradation of regulator performance could occur, [3], including loss of stability.

The effect of the input filter is more clearly seen using a small signal model.

The averaging technique [1] is used to relate the low frequency modulation component of the source voltage and control signal to the corresponding frequency components of the converter output voltage. Using the continuous inductor current buck regulator with input filter of Figure 1 , as an example, a small signal model using the dual-input describing function can be developed, as shown in Figure 3 , [6]. In this model the effect of the input filter is characterized by the following two parameters: the forward transfer characteristic of the input filter  $H(s)$  and the output impedance of the input filter  $Z(s)$ .

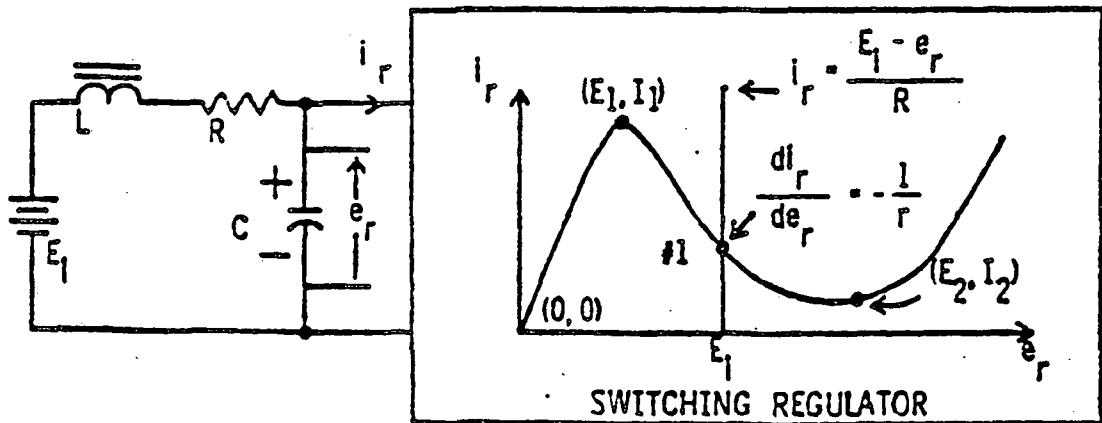


Figure 2: Negative resistance oscillation.



In Figure 1 the output filter is made up of  $R_L$ ,  $L$ ,  $R_C$  and  $C$ ,  $R_L$  is the load resistance,  $D$  is the steady state duty cycle ratio  $D = T_{on}/T$ ,  $V_I$  and  $I_I$  are the steady state regulator input voltage and current respectively, and the lower case letters with a caret above them denote modulation signals.

The small signal model of Figure 3 is used to illustrate briefly the complex interaction between the input filter, output filter and the control loop and the problems caused by the interaction. For detailed analysis please refer to [6].

### 2.1.1 Input Filter Interaction -- Loop Stability and Transient Response

The stability of a switching regulator can be examined by the open loop gain  $G_T(s)$ :

$$G_T(s) = F_C(s)F_p(s)F_E(s)F_M(s) \quad (2-1)$$

where  $F_C(s)F_p(s)$  is the duty cycle-to-output describing function  $\hat{v}_o/\hat{d}$ , and  $F_E(s)$ ,  $F_M(s)$  are the transfer functions of the error processor and the pulse modulator respectively. The peaking of the output impedance of the input filter  $Z(s)$  has the following effects:

- (1) The duty-cycle power stage gain  $F_C(s)$  includes the output impedance  $Z(s)$  --

$$F_C(s) = V_I - Z(s)I_I \quad \text{or} \quad (2-2)$$

$$F_C(s) = I_I \left[ \frac{V_I}{I_I} - Z(s) \right] \quad (2-3)$$

The first term in the brackets  $\frac{V_I}{I_I}$  is the negative input impedance of the regulator. At the input filter resonant frequency,  $Z(s)$  reaches a peak value and if this value is large enough the result could be a reduction in loop gain or even worse a negative duty cycle power stage gain  $F_C(s)$ . Reduction in loop gain could lead to loop instability, whereas a negative  $F_C(s)$  together with the negative feedback loop will result in a positive feedback unstable system.

(2) The power stage transfer function  $F_p(s)$  includes the output impedance  $Z(s)$  --

$$F_p(s) = \frac{[R_C + 1/sC] // R_L}{D^2 Z(s) + Z_i(s)} \quad \text{where} \quad (2-4)$$

$$Z_i(s) = R_f + sL + [R_C + 1/sC] // R_L \quad (2-5)$$

= input impedance of the regulator.

Excessive  $Z(s)$  at the input filter resonant frequency can significantly reduce  $F_p(s)$ , and thus the loop gain.

Figures 4 [6], illustrate the effect of peaking of  $Z(s)$  on the duty cycle-to-output transfer function  $F_C(s)F_p(s)$  if an improperly designed input filter is employed.

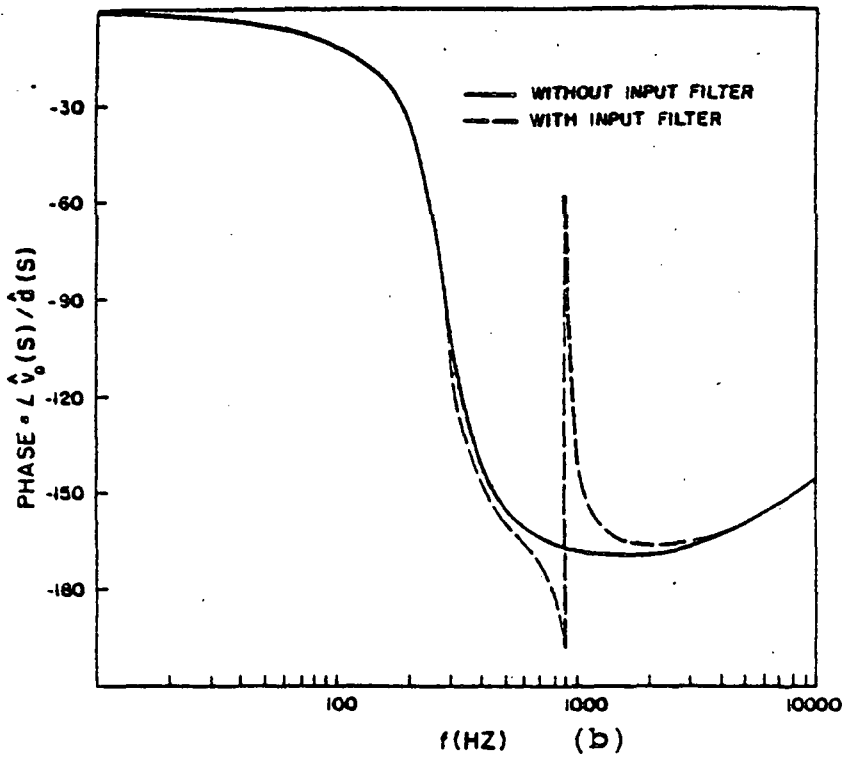
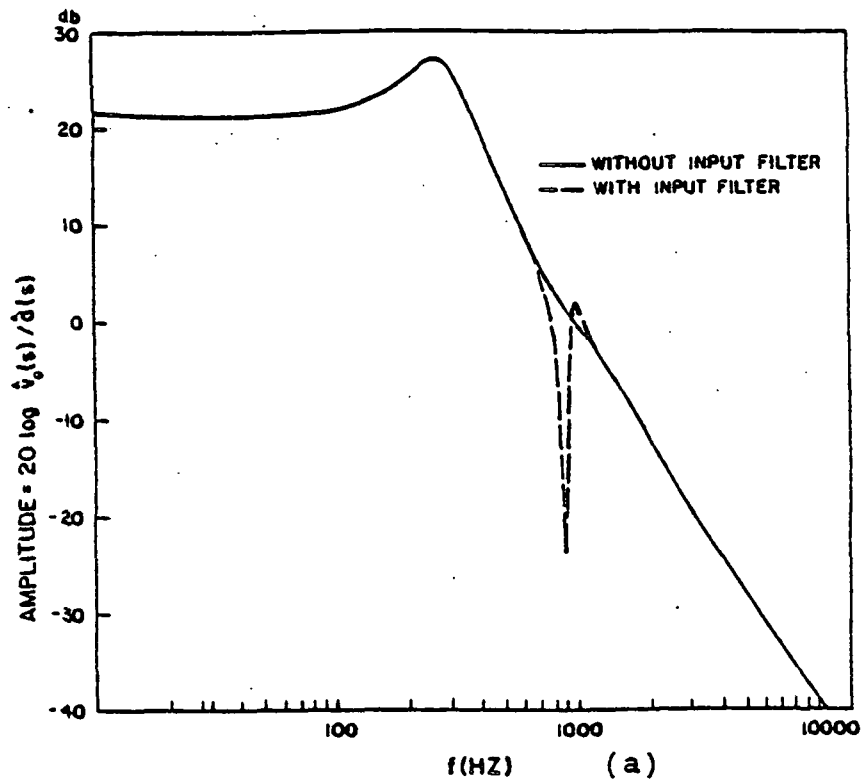


Figure 4: Duty cycle-to-output voltage characteristic with and without input filter (a) gain (b) phase. (parameter values are as shown in Fig.1)

At the input filter resonant frequency the peaking of the output impedance  $Z(s)$  causes a sharp change in the gain and phase of the duty cycle-to-output transfer function. This could result in loop instability and degradation of transient response from a presumably well damped system to an oscillatory one; control of the peaking effect of the output impedance  $Z(s)$  is necessary to avoid these problems.

### 2.1.2 Input Filter Interaction--Audiosusceptibility and Output Impedance

The audiosusceptibility refers to the switching regulator's ability to attenuate small signal sinusoidal disturbances present at the input so as not to affect the regulated output voltage. The audiosusceptibility performance is of considerable importance, as the regulator generally shares the input bus with other on-line equipment. The operation of this equipment generates noise voltages on the input line which must be attenuated by the closed-loop regulator so that operation of the various payloads at the regulator output will not be adversely affected. The audiosusceptibility is expressed in terms of the closed loop input-to-output transfer function  $G_A(s)$ :

$$G_A(s) = \frac{v_O(s)}{v_I(s)} = \frac{F_I(s)F_P(s)}{1+F_C(s)F_P(s)F_E(s)F_M(s)} = \frac{F_I(s)F_P(s)}{1+G_T(s)} \quad (2-6)$$

where  $F_I(s) = DH(s) =$  input voltage gain of the power stage.  $G_A(s)$  and thus the audiosusceptibility are affected by the resonant peaking of the output impedance  $Z(s)$  and of the forward transfer function of the input filter with the regulator disconnected  $H(s)$ , because  $F_I(s)$  is a function of  $H(s)$  whereas  $F_C(s)$  and  $F_p(s)$  are functions of  $Z(s)$ . The reduction of loop gain at the resonant frequency can thus severely degrade the audiosusceptibility. Figure 5, [6], illustrates the audiosusceptibility of the buck regulator with and without an input filter.

The output impedance of the regulator should be small so that the regulator behaves like an ideal voltage source, however the output impedance is increased by the peaking of the output impedance of the input filter.

$$Z_O(s) = \frac{Z_p(s)}{1 + G_T(s)} \quad (2-7)$$

where  $Z_p(s)$  is the output impedance of the power stage with the control loop open.

At the resonant frequency the output impedance of the regulator  $Z_O(s)$  is increased. This is a consequence of the loss of loop gain  $G_T(s)$  as a result of peaking.

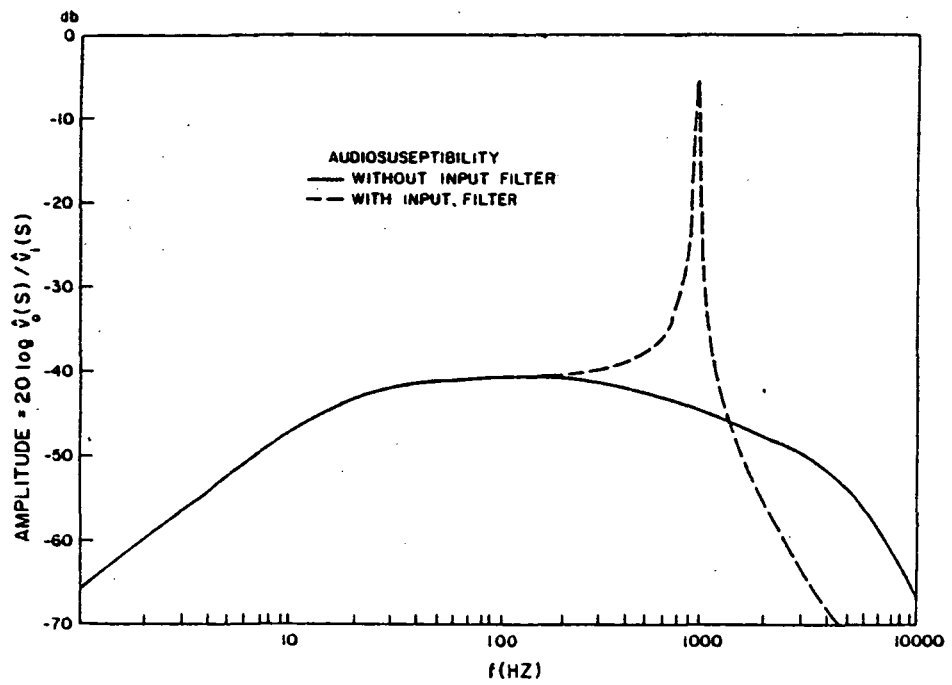


Figure 5: Audiosusceptibility with and without input filter.

(parameters values are as shown in Fig.1)

The peaking of  $H(s)$  and  $Z(s)$  of the input filter thus results in a reduction in the loop gain, this in turn affects stability, transient response, audiosusceptibility and the output impedance of the regulator.

A buck type switching regulator with a two stage input filter is shown in Figure 6 . Figure 7 , [6], shows the measured values of open loop gain and phase as a function of the frequency. ( The input filter damping resistance  $R_D$  is not employed to purposely illustrate the effect of input filter interaction with the regulator control loop.) Significant changes in the open loop gain and phase characteristics at the resonant frequencies of both the first stage and the second stage of the input filter are observed, [6]. Thus it is seen that the peaking of the output impedance at resonant frequency of the two stage input filter can also cause serious performance degradation.

## 2.2 INPUT FILTER DESIGN CONSIDERATIONS

The design of the input filter is made more complicated by the necessity of satisfying the following constraints, which result from the interaction between the input filter and the regulator control loop discussed in section 2.1 :

1. The amount of regulator switching current reflected back into the source should be limited (conducted interference requirement).

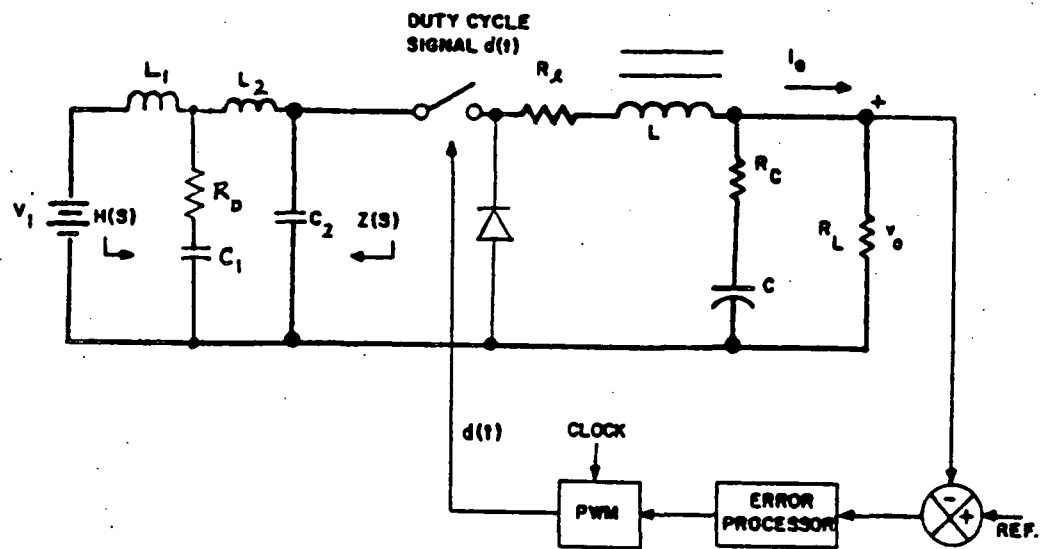


Figure 6: Buck type switching regulator with a two stage input filter.

$$\begin{array}{llll}
 V_1 = 40\text{v} & V_0 = 20\text{v} & R_L = 7 \text{ ohm} & R_2 = 0.05 \text{ ohm} \\
 L = 1 \text{ mH} & C = 455 \text{ microF} & R_c = 0.068 \text{ ohm} & T_p = 50 \text{ microsecs} \\
 L_1 = 1.1 \text{ mH} & R_1 = 0.05 \text{ mohm} & L_2 = 0.27 \text{ mH} & \\
 R_2 = 0.02 \text{ ohm} & C_1 = 225 \text{ microF} & C_2 = 20 \text{ microF} & 
 \end{array}$$

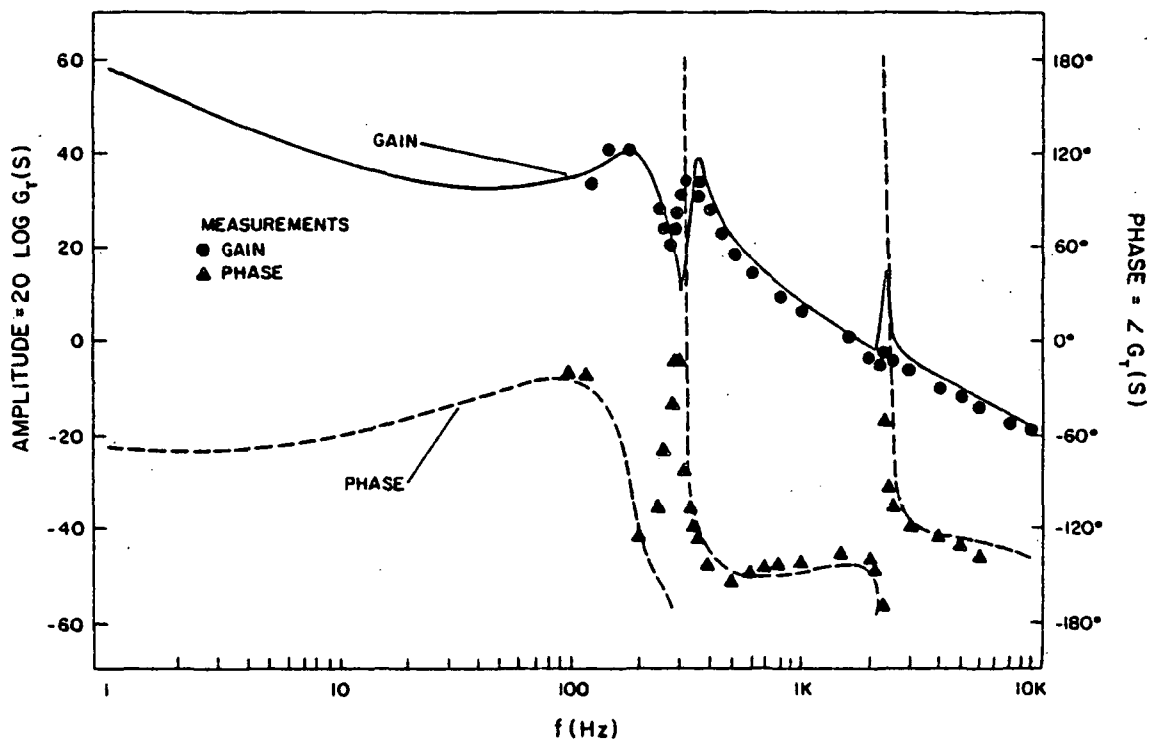


Figure 7: Open loop gain and phase characteristics without the input filter damping resistance  $R_D$ .

(parameter values used are as shown in Fig.6)

2. The peaking of the output impedance of the input filter  $Z(s)$  should be limited to a safe value to avoid significant loop gain reduction.
3. The peaking of the transfer function of the input filter  $H(s)$  should be limited to achieve a satisfactory rejection rate of audio signals propagating from input to output.
4. The input filter weight and energy loss should be limited to low values.
5. The Nyquist stability criterion has to be satisfied; thus the closed loop poles should be in the left half plane for stable operation -

$$|1 + E_C(s)E_P(s)E_E(s)E_M(s)| > 0$$

6. The closed-loop input-to-output transfer characteristic (audiosusceptibility) and transient response due to a sudden line/load change should not be degraded by a noticeable amount.

An input filter design that satisfies one constraint may often result in violating some other constraint. For example, an input filter design that limits performance degradation (degradation of stability, transient response and audiosusceptibility) often results in higher weight and increased losses in the input filter. A satisfactory input filter design trades off one or more of the performance deg-

radations for size, weight and loss. A near-to-optimal design thus requires many trial and error design attempts. Some of the conventional input filter design techniques are presented next.

### 2.2.1 Conventional Input Filter Design Techniques

A single stage input filter as shown in Figure 8(a) can be designed to avoid performance degradation -- but this would result in larger filter  $L_1$  and  $C_1$  thus resulting in weight and size increase. The filter is simple and commonly used but it cannot often satisfy the stringent requirement on audiosusceptibility without size/weight penalty. Resonant peaking of the filter of Figure 8(b), [3], is lowered by adding resistance  $R$ , but this lowers efficiency because the pulse current flowing through  $C_1$  increases losses. Another design uses a resistance  $R$  in parallel across  $C_1$ , [4], but this results in a large  $C_1$ .

The optimal design of a single stage input filter thus is rather difficult without tradeoff between performance degradations and the weight and loss limitations.

The degradation of the power stage transfer function  $E_p(s)$  due to peaking of  $Z(s)$  can be avoided if there is sufficient separation of the input filter resonance frequency  $\omega_1 = \frac{1}{\sqrt{L_1 C_1}}$  and the output filter resonant frequency

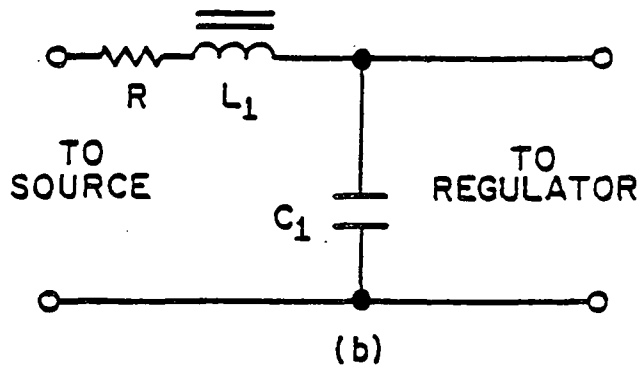
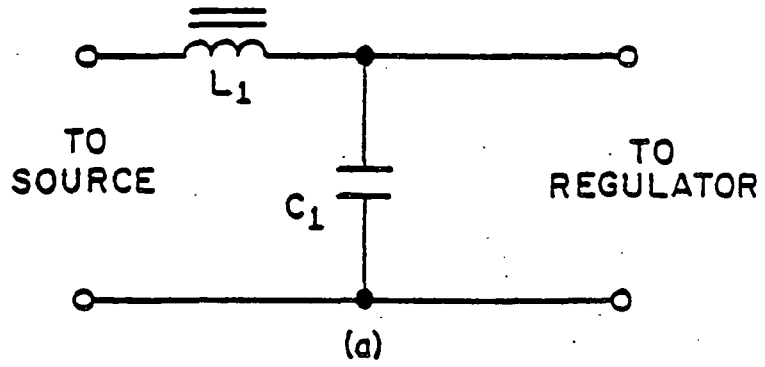


Figure 8: Single-stage input filters

$\omega_0 = \frac{1}{\sqrt{LC}}$  , [4,5,10]. Figure 9 , [4,5,10], shows three possible combinations of  $\omega_0$  and  $\omega_1$ .  $F_p(s)$  is related to both  $Z(s)$  and the input impedance of the regulator  $Z_i(s)$  thus

$$F_p(s) = \frac{[R_C + 1/sC]//R_L}{D^2 Z(s) + Z_i(s)} \quad (2-8)$$

where  $Z_i(s) = R_2 + sL + [R_C + 1/sC]//R_L$   
 = input impedance of the regulator.

$Z(s)$  and  $Z_i(s)$  peak at the frequencies  $\omega_0$  and  $\omega_1$  respectively. If the two resonance frequencies are the same as in Figure 9 then both  $Z(s)$  and  $Z_i(s)$  peak at the same frequency and thus at that frequency the transfer function  $F_p(s)$  would be affected, i.e. reduced, to the maximum possible extent. Shifting the two frequencies  $\omega_0$  and  $\omega_1$  apart as shown in Figure 9 will result in reducing the effect of peaking on  $F_p(s)$ . Reducing  $\omega_1$  would result in increasing the size and weight of the input filter. A high value of  $\omega_1$  is desirable from the point of view of weight and size reduction but this can result in severe performance degradation -- from Figure 4 it is clear that the gain of the duty cycle-to-output transfer function  $F_C(s)F_p(s)$  decreases with increasing frequency and thus the effect of peaking of  $Z(s)$  on the gain of  $F_C(s)F_p(s)$  would be more pronounced if  $Z(s)$  peaks at a higher  $\omega_1$ .

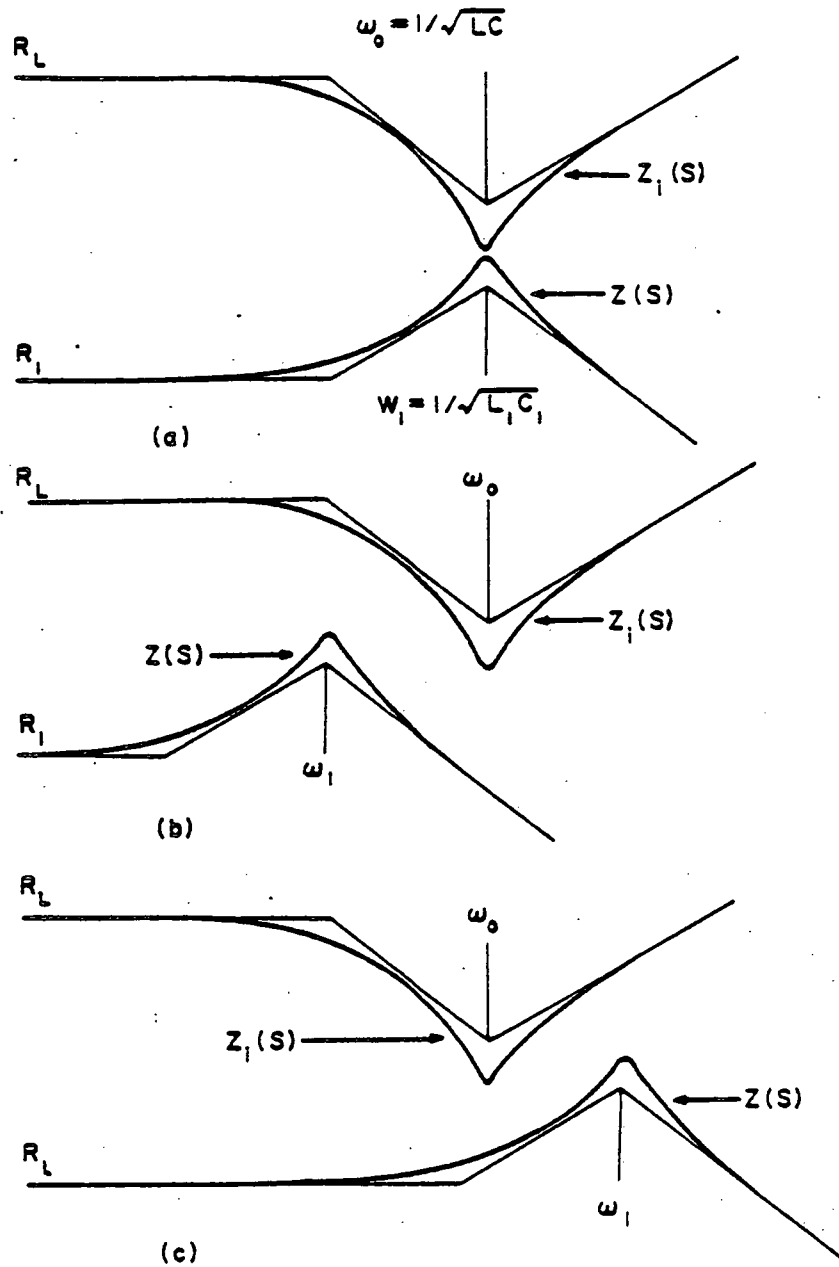


Figure 9: Interaction between output impedance  $Z(s)$  of input filter and input impedance  $Z(s)$  of regulator.

The reduction of the loop gain at higher input filter resonant frequency  $\omega_1$  often results in poor audiosusceptibility, oscillatory transient response or even an unstable system. The choice of  $\omega_1$  thus involves a trade off between meeting performance specifications and size/weight.

### 2.2.2 An Optimal Configuration

A two-stage input filter configuration has been described, [3,6] and is shown in Figure 10 . The first stage consisting of  $L_1, C_1, R_3$  and  $R_1$  controls the resonant peaking of the filter. The second stage consisting of  $L_2, C_2$  supplies most of the pulse current required by the regulator. As shown in the literature, [6], the two-stage input filter is capable of reducing  $H(s)$  and  $Z(s)$  at resonant frequency without significantly increasing weight and loss, unlike the single-stage input filter. Computer optimization techniques have been utilized to optimally design the two-stage filter[6]. It has been shown that the two-stage filter is much lighter than its single-stage counterpart under identical design constraints. Also it has been shown that for the same filter weight the single stage filter has a significantly higher peaking of  $H(s)$  and  $Z(s)$ . Figure 11 shows the gain and phase of the duty cycle-to-output describing function of a power stage with a two stage input filter, [6].

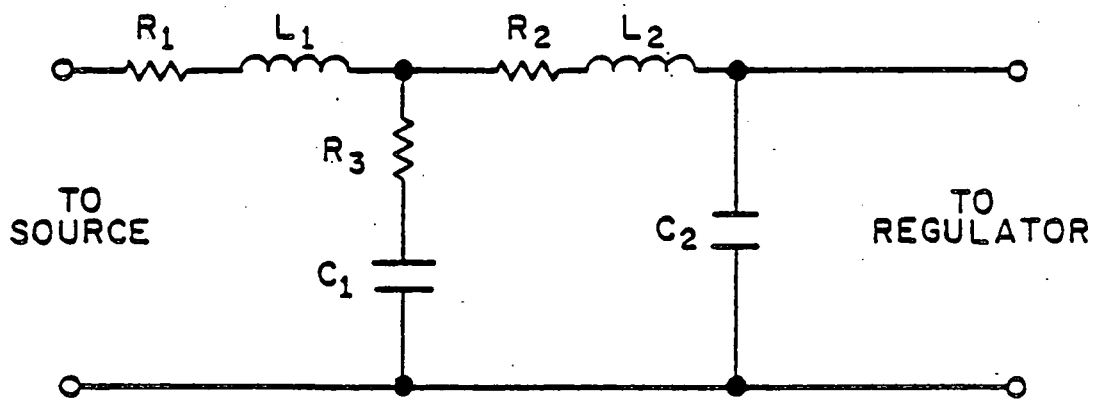


Figure 10: Two-stage input filter.

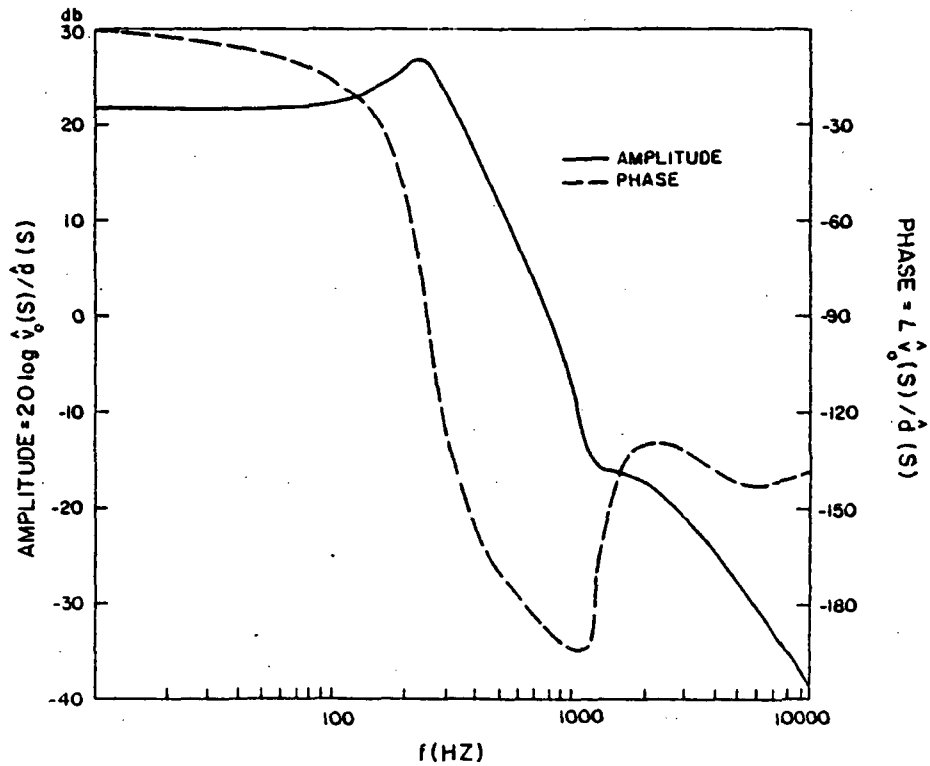


Figure 11: Duty cycle-to-output describing function of power stage with two-stage input filter.

(parameter values used are as shown in Fig.1 with the following two-stage input filter parameters --  
 $L_1=232$  microH       $R_1=0.0276$  ohm       $L_2=77$  microH  
 $R_2=0.0119$  ohm       $C_1=100$  microF       $R_3=1.73$  ohm  
 $C_2=30$  microF )

Figure 4 shows the gain and phase of the duty cycle-to-output describing function of a power stage with a single-stage input filter, and the two-stage filter of Figure 11 was designed to have the same weight as the single-stage input filter of Figure 4. Comparing the two figures the improvement in performance regarding the duty cycle-to-output transfer function is dramatic.

It can therefore be concluded that the two-stage filter provides the best compromise among the conflicting requirements of an input filter.

### 2.2.3 Input Filter Compensation Via a Feedforward Loop

Limiting interaction between the input filter and the regulator control loop is possible with the addition of a feedforward control loop. At this point it is important to emphasize that such a scheme is designed to eliminate the effect of peaking of the output impedance of the input filter  $Z(s)$ , since the peaking of  $Z(s)$  interacts with the control loop. The forward transfer function  $H(s)$  does not interact with the regulator control loop, as is evident from Figure 3 and therefore the peaking of  $H(s)$  cannot be controlled in any way by adding a feedforward loop. The peaking of  $H(s)$  can only be controlled by proper filter design. In this dissertation a feedforward loop is implemented for a

switching buck regulator employing multiple control loops. The feedforward loop will be designed to cancel the detrimental effect of input filter interaction and thus improve the regulator performance and stability. The use of the feedforward control loop thus removes some of the conflicting design constraints mentioned above and makes an optimal input filter design more easily attainable.

#### 2.2.4 Objectives of Feedforward Loop Design

The proposed feedforward loop will be designed such that :

1. It will eliminate input filter interaction with the regulator loop. This will result in improvement in stability margins, audiosusceptibility, output impedance and transient response of the regulator.
2. It will allow the input filter to be optimized. Some of the design constraints that make an optimal filter design difficult to attain are removed with the addition of feedforward.
3. It will eliminate equipment interaction. Figure 12 shows a switching regulator and its preregulator which may be a rectifier and a filter. The dynamic output impedance of the preregulator will interact with the switching regulator and may cause problems like loop instability, degradation of audiosuscepti-

bility, output impedance and transient response. The addition of a feedforward loop will eliminate such interaction, thus isolating the switching regulator from equipment upstream.

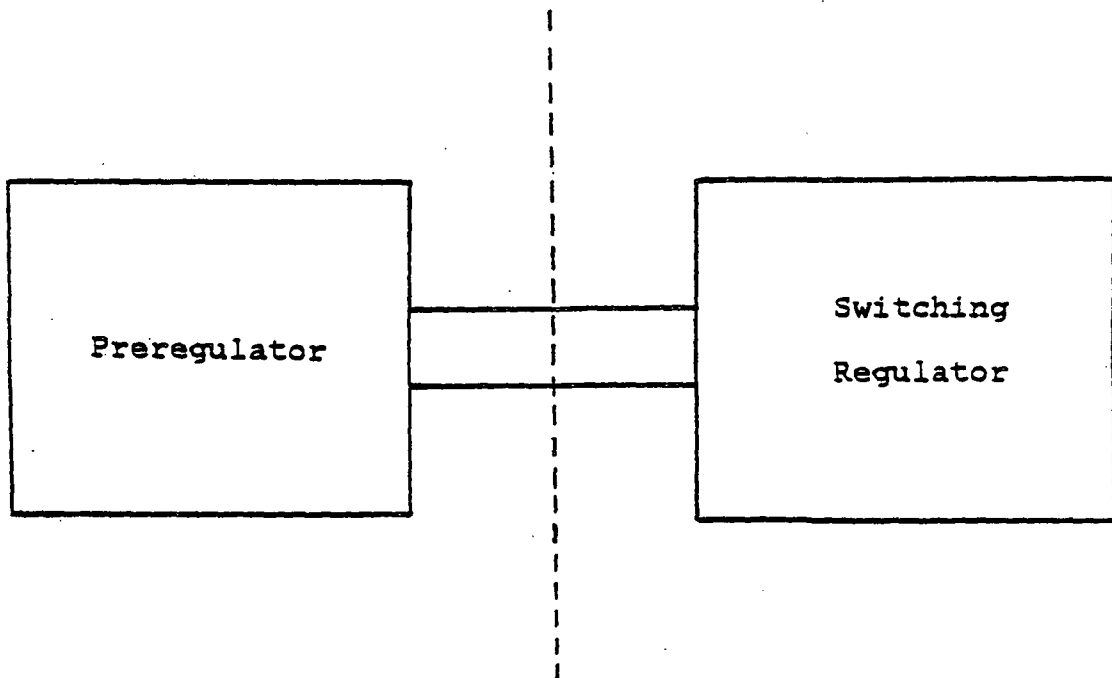


Figure 12: Interaction between the switching regulator and its preregulator.

## Chapter III

### CONCEPT OF POLE-ZERO CANCELLATION USED IN TOTAL STATE CONTROL

#### 3.1 CONCEPT OF POLE-ZERO CANCELLATION.

The concept of pole-zero cancellation that was developed earlier [2,7,8] was implemented by feedback loops that sense the regulator output filter state variables and process this information to achieve better performance, and a control adaptive to filter parameter and load changes.

Figure 13 [2], shows a two-loop controlled switching buck regulator. The dc loop senses the converter output voltage and compares it with the reference voltage to generate a dc error signal for voltage regulation. The ac loop senses the ac voltage across the output filter inductor to generate an ac signal. Both ac and dc signals are processed through an operational amplifier summing junction to provide a total error signal at the output of the operational amplifier integrator. It is apparent that the error signal at the output of the integrator contains information regarding the output filter state variables -- the inductor current and the capacitor voltage.

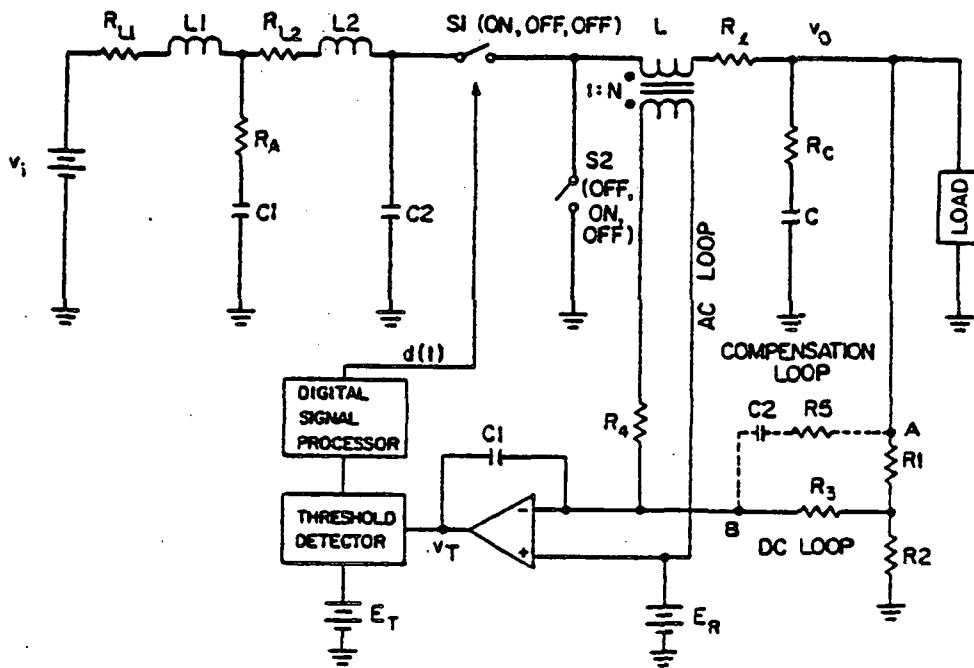


Figure 13: Two loop controlled switching buck regulator.

It was shown, [2], that the feedback control loops when properly designed can provide complex zeros to cancel completely the complex poles presented by the low-pass output filter of the power stage. It was also shown that the feedback control loop has the ability to sense filter parameter changes and automatically provide pole-zero cancellation. To examine the adaptive nature of the control loops the open loop regulator transfer function  $G_T(s)$  is used

$$G_T(s) = \frac{KZ(j\omega)}{sP(j\omega)} \quad (3-1)$$

where  $K$  is a constant determined by the power stage and control loop parameters and

$$Z(j\omega) = 1 + j2\zeta_1 \omega/\omega_{n1} - \omega^2/\omega_{n1}^2 \quad (3-2)$$

$$P(j\omega) = 1 + j2\zeta_2 \omega/\omega_{n2} - \omega^2/\omega_{n2}^2 \quad (3-3)$$

$P(j\omega)$  has complex poles corresponding to the output filter and  $Z(j\omega)$  has complex zeros produced by the two loop feedback control.

$$\omega_{n1} = \sqrt{\frac{\alpha}{LC}} \quad (3-4)$$

$$\omega_{n2} = \frac{1}{\sqrt{LC}} \quad (3-5)$$

$$\zeta_1 = \frac{\omega_{n1}}{2} \tau_z \quad (3-6)$$

$$\zeta_2 = \frac{\omega_{n2}}{2} \left( \frac{L}{R_L} + R_C C + R_2 C \right) \quad (3-7)$$

$$\alpha = \frac{R_4}{NR_Y} \quad (3-8)$$

$$\tau_z = (R_Y + R_5)C_2 + \frac{L}{\alpha R_L} \quad (3-9)$$

$$R_Y = \left[ (R_1/R_2) + R_3 \right] \frac{(R_1 + R_2)}{R_2} \quad (3-10)$$

$L$ ,  $C$ ,  $R_2$  and  $R_C$  form the output filter as in Figure 13 . The control parameters can be chosen such that

$$\omega_{n1} = \omega_{n2} \quad (3-11)$$

$$\zeta_1 = \zeta_2 \quad (3-12)$$

thus resulting in

$$P(j\omega) = Z(j\omega) \quad (3-13)$$

and

$$G_T(s) = \frac{K}{s} \quad (3-14)$$

The open loop transfer function is of first order and is completely independent of output filter parameters. The adaptive nature of the control loop is apparent from the fact that the complex zeros imitate the change in the complex poles due to component tolerance, aging or temperature variations, thus preserving the pole-zero cancellation.

### 3.2 TOTAL STATE CONTROL

The concept of pole-zero cancellation of the output filter characteristics led to the idea of using similar means to control the effect of peaking of the output impedance of the input filter. The objective of the work reported in this dissertation is thus to develop a feedforward loop that senses the input filter state variables and uses the information contained therein to eliminate the interaction between the input filter and the regulator control loop. Such a feedforward loop working in conjunction with existing feedback loops forms a total state control scheme, which is illustrated in Figure 14 . The feedforward loop senses the input filter state variables and feeds this information to the error processor.

The other inputs to the error processor are the ac voltage across the output filter inductor and the output voltage - as shown in section 3.1 these contain information regarding the output filter state variables.

The pulse modulator thus has as its input information regarding the state variables of the output filter and also the input filter. The duty cycle signal  $d(t)$ , which controls the switch in the power stage, is thus also affected by the input filter state variables. It is shown later in this dissertation, in Chapters 4 and 5, that the feedforward loop

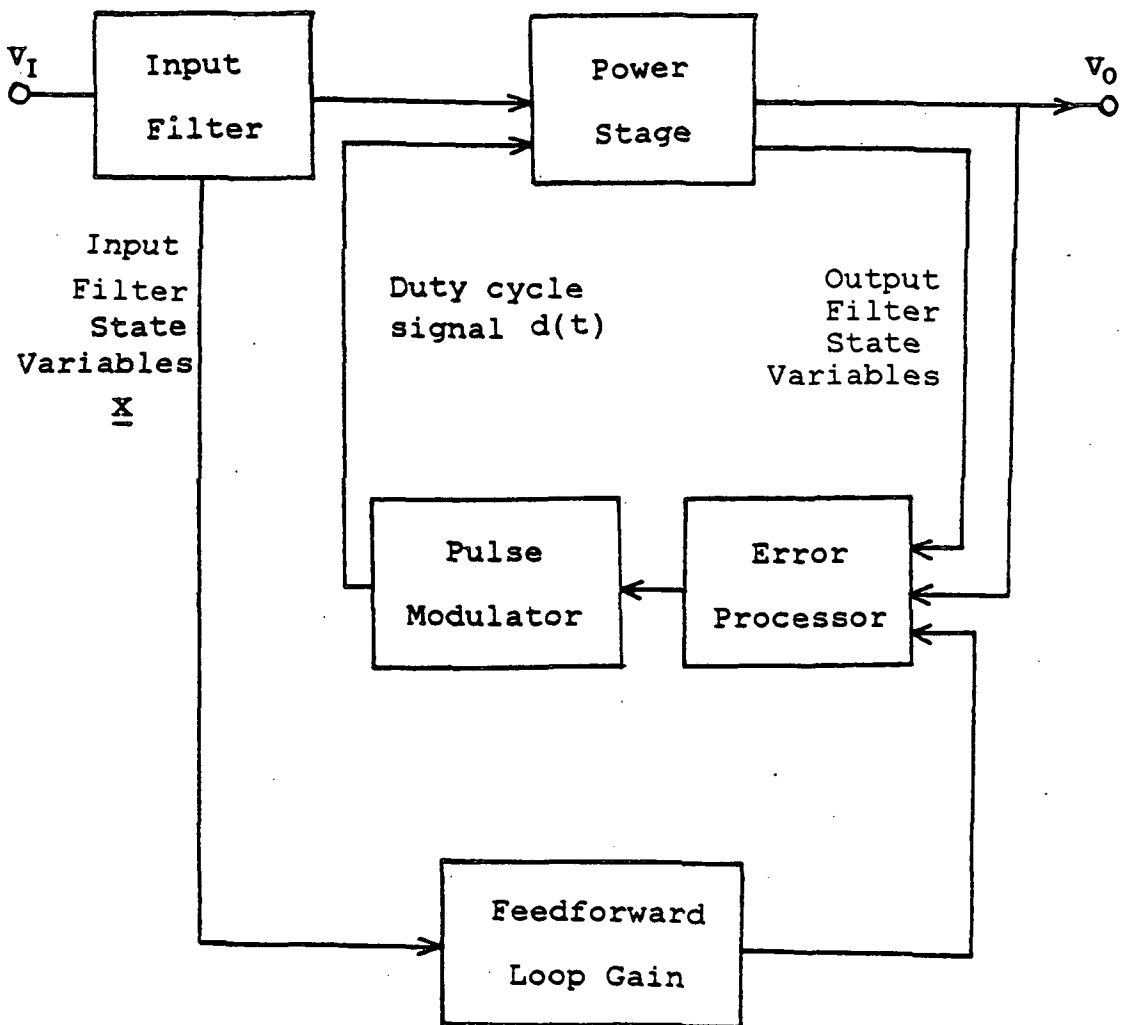


Figure 14: Total State Control.

can be designed such that interaction between the input filter and the regulator is eliminated.

## Chapter IV

### MODELING OF THE POWER STAGE WITH INPUT FILTER

The first step in the design and analysis of the feed-forward loop is to develop the small signal model of the power stage with input filter for the buck-boost, buck and boost type of switching regulators, using the averaging technique, [1]. The modeling is carried out in the continuous conduction operating mode, in which the inductor current is always nonzero. This mode is the prevalent operating mode for most dc-dc converters. The discontinuous conduction operating mode in which the inductor current is zero for some time during the cycle occurs at light loads and is seldom used as the intended design at full load.

The modeling is carried out in the following steps --

1. State space equation formulation during  $T_{ON}$  and  $T_{OFF}$ .
2. State space averaging and perturbation.
3. Linearization and derivation of the small signal equations and the small signal equivalent circuit and state space model.

#### 4.1 BUCK-BOOST CONVERTER SMALL SIGNAL MODEL DERIVATION

The buck-boost converter is shown in Figure 15 . In the buck-boost converter shown the input filter is composed of  $R_{L1}$ ,  $L1$ ,  $R_{C1}$  and  $C1$ . The load is represented by  $R_L$  while  $V_I$  and  $V_O$  are the input and output voltages respectively. During  $T_{ON}$ , the switch  $S$  is on and the circuit as shown in Figure 16 (a).

The equations describing the circuit are

$$i_p = \frac{N_p}{L_p} \phi \quad \phi = \text{flux in core} \quad (4-1)$$

$$\frac{di_{L1}}{dt} = \frac{i_{L1}}{L1} (-R_{L1} - R_{C1}) + \frac{R_{C1}}{L1} \frac{N_p}{L_p} \phi - \frac{v_{C1}}{L1} + \frac{v_I}{L1} \quad (4-2)$$

$$\frac{d\phi}{dt} = \frac{v_{C1}}{N_p} + \frac{R_{C1}}{N_p} i_{L1} - \frac{\phi}{L_p} (R_{C1} + R_p) \quad (4-3)$$

$$\frac{dv_{C1}}{dt} = \frac{i_{L1}}{C1} - \frac{N_p}{C1L_p} \phi \quad (4-4)$$

$$\frac{dv_C}{dt} = \frac{-v_C}{C(R_L + R_C)} \quad (4-5)$$

$$v_O = \frac{R_L v_C}{R_C + R_L} \quad (4-6)$$

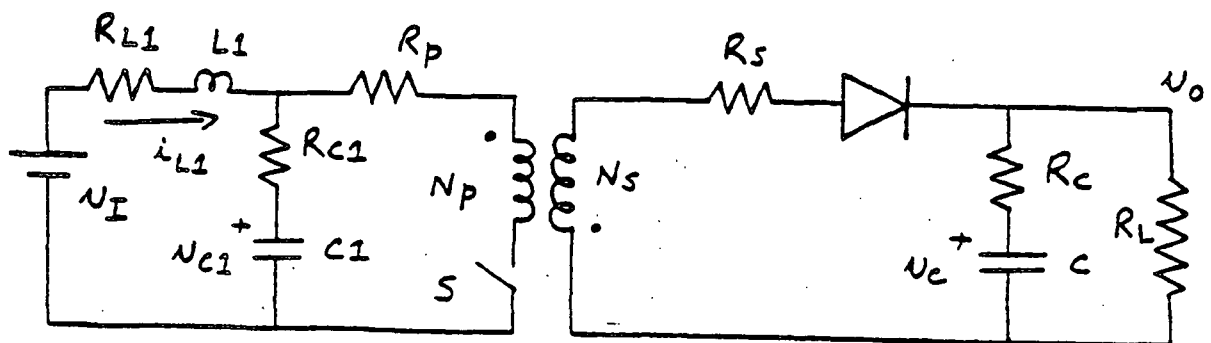
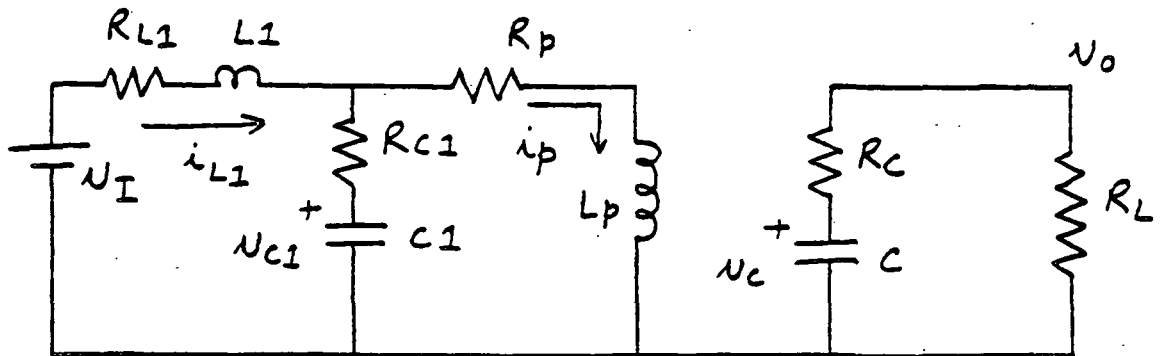
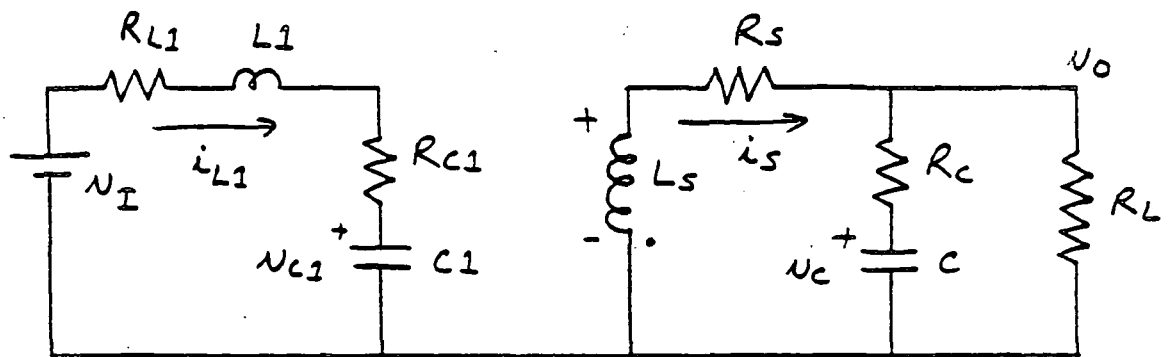


Figure 15: Buck-boost converter power stage.



(a)



(b)

Figure 16: Buck-boost converter power stage model: (a) during  $T_{ON}$  and (b) during  $T_{OFF}$ .

During  $T_{OFF}$  the switch S is off and the circuit is as shown in Figure 16 (b).

The equations describing the circuit are

$$i_S = \frac{N_S}{L_S} \phi \quad (4-7)$$

$$\frac{di_{L1}}{dt} = \frac{i_{L1}}{L1} (-R_{L1} - R_{C1}) - \frac{v_{C1}}{L1} + \frac{v_I}{L1} \quad (4-8)$$

$$\frac{d\phi}{dt} = \frac{-(R_S R_C + R_S R_L + R_C R_L)\phi}{L_S(R_C + R_L)} - \frac{R_L v_C}{N_S(R_C + R_L)} \quad (4-9)$$

$$\frac{dv_{C1}}{C1} = \frac{i_{L1}}{C1} \quad (4-10)$$

$$\frac{dv_C}{dt} = \frac{N_S R_L \phi}{C L_S (R_C + R_L)} - \frac{v_C}{C(R_C + R_L)} \quad (4-11)$$

$$v_0 = \frac{R_L v_C}{R_C + R_L} + \frac{R_C R_L N_S \phi}{L_S (R_C + R_L)} \quad (4-12)$$

The following vectors are defined

$$\underline{x} = \begin{bmatrix} i_{L1} \\ \phi \\ v_{C1} \\ v_C \end{bmatrix} \quad \begin{array}{l} \underline{u} = [v_I] \\ \underline{y} = [v_0] \end{array} \quad (4-13)$$

resulting in the following state space equations

$$\begin{aligned}
 \overset{T_{ON}}{\dot{\underline{x}}} &= A_1 \underline{x} + B_1 \underline{u} & \overset{T_{OFF}}{\dot{\underline{x}}} &= A_2 \underline{x} + B_2 \underline{u} \\
 \underline{y} &= C_1 \underline{x} & \underline{y} &= C_2 \underline{x}
 \end{aligned} \tag{4-14}$$

where

$$A_1 = \begin{bmatrix} -\frac{(R_{L1} + R_{C1})}{L1} & \frac{R_{C1}N_p}{L1L_p} & \frac{-1}{L1} & 0 \\ \frac{R_{C1}}{N_p} & \frac{-(R_{C1} + R_p)}{L_p} & \frac{1}{N_p} & 0 \\ \frac{1}{C1} & \frac{-N_p}{C1L_p} & 0 & 0 \\ 0 & 0 & 0 & \frac{-1}{C(R_L + R_C)} \end{bmatrix} \tag{4-15}$$

$$A_2 = \begin{bmatrix} -\frac{(R_{L1} + R_{C1})}{L1} & 0 & \frac{-1}{L1} & 0 \\ 0 & \frac{-R_1}{L_s} & 0 & \frac{-R_L}{N_s(R_C + R_L)} \\ \frac{1}{C1} & 0 & 0 & 0 \\ 0 & \frac{N_s R_L}{C L_s (R_C + R_L)} & 0 & \frac{-1}{C(R_C + R_L)} \end{bmatrix} \tag{4-16}$$

$$B_1 = \left[ \frac{1}{L1} \quad 0 \quad 0 \quad 0 \right]^T \tag{4-17}$$

$$B_2 = B_1 \tag{4-18}$$

$$C_1 = \left[ 0 \quad 0 \quad 0 \quad \frac{R_L}{R_C + R_L} \right] \tag{4-19}$$

$$C_2 = \left[ 0 \quad \frac{R_C R_L N_S}{L_S (R_C + R_L)} \quad 0 \quad \frac{R_L}{R_C + R_L} \right] \quad (4-20)$$

$$R_1 = \frac{R_S R_C + R_S R_L + R_C R_L}{R_C + R_L} \quad (4-21)$$

The state space averaged model over the entire period  $T$  is

$$\dot{\underline{x}} = [dA_1 + d'A_2] \underline{x} + [dB_1 + d'B_2] \underline{u} \quad (4-22)$$

$$\underline{y} = [dC_1 + d'C_2] \underline{x}$$

where  $d = \text{duty cycle ratio} = T_{ON} / (T_{ON} + T_{OFF})$

$$d' = 1 - d \quad (4-23)$$

$$T = T_{ON} + T_{OFF}$$

The state space averaged model is perturbed thus -

$$\begin{aligned} d &= D + \hat{d} \\ d' &= D' - \hat{d} \\ \underline{u} &= \underline{U} + \hat{\underline{u}} \\ \underline{y} &= \underline{Y} + \hat{\underline{y}} \\ \underline{x} &= \underline{X} + \hat{\underline{x}} \end{aligned} \quad (4-24)$$

Assuming that the perturbation is small

$$\frac{\hat{d}}{D} \ll 1, \frac{\hat{\underline{x}}}{\underline{X}} \ll 1 \text{ etc. leads to the following small}$$

signal linearized model

$$\begin{aligned}
\mathbf{0} &= [DA_1 + D'A_2] \underline{\mathbf{x}} + [DB_1 + D'B_2] \mathbf{v}_I \\
\mathbf{v}_0 &= [DC_1 + D'C_2] \underline{\mathbf{x}} \\
\dot{\underline{\mathbf{x}}} &= [DA_1 + D'A_2] \hat{\underline{\mathbf{x}}} + [DB_1 + D'B_2] \hat{\mathbf{v}}_I \\
&\quad + [A_1 - A_2] \underline{\mathbf{x}} + (B_1 - B_2 \mathbf{v}_I] \hat{d} \\
\hat{\mathbf{v}}_0 &= [C_1 - C_2] \underline{\mathbf{x}} \hat{d} + [DC_1 + D'C_2] \hat{\underline{\mathbf{x}}}
\end{aligned} \tag{4-25}$$

Defining

$$\begin{aligned}
A &= DA_1 + D'A_2 \\
B &= DB_1 + D'B_2 \\
C &= DC_1 + D'C_2
\end{aligned} \tag{4-26}$$

results in

$$\begin{aligned}
\dot{\underline{\mathbf{x}}} &= A \hat{\underline{\mathbf{x}}} + B \hat{\mathbf{v}}_I \\
&\quad + [A_1 - A_2] \underline{\mathbf{x}} + (B_1 - B_2) \mathbf{v}_I] \hat{d} \\
\hat{\mathbf{v}}_0 &= [C_1 - C_2] \underline{\mathbf{x}} \hat{d} + C \hat{\underline{\mathbf{x}}}
\end{aligned} \tag{4-27}$$

Using Laplace transforms results in

$$\begin{aligned}
\hat{\underline{\mathbf{x}}}(s) &= [SI - A]^{-1} B \hat{\mathbf{v}}_I(s) \\
&\quad + [SI - A]^{-1} [(A_1 - A_2) \underline{\mathbf{x}} + (B_1 - B_2) \mathbf{v}_I] \hat{d}(s) \\
\hat{\mathbf{v}}_0(s) &= [C_1 - C_2] \underline{\mathbf{x}} \hat{d}(s) + C \hat{\underline{\mathbf{x}}}(s)
\end{aligned} \tag{4-28}$$

The state space model is derived from the two equations above, and is shown in Figure 17 .

To derive the small signal equivalent circuit, it is first necessary to use the equation for  $\hat{v}_0$  to substitute for  $\hat{v}_c$  in terms of  $\hat{v}_0$ , in the small signal equations described above. Simplifying, the four equations are obtained

$$\hat{v}_I = (R_{Cl} + R_{L1})i_{L1} - \frac{R_{Cl}N_P D}{L_P} \hat{\phi} + L1 \frac{di_{L1}}{dt} \quad (4-29)$$

$$+ \hat{v}_{Cl} - \frac{R_{Cl}N_P}{L_P} \phi \hat{d}$$

$$Cl \frac{d\hat{v}_{Cl}}{dt} = i_{L1} - \frac{DN_P}{L_P} \hat{\phi} - \frac{N_P}{L_P} \phi \hat{d} \quad (4-30)$$

$$C \frac{d\hat{v}_C}{dt} = \frac{D'N_S}{L_S} \hat{\phi} - \frac{\hat{v}_0}{R_L} - \frac{N_S}{L_S} \phi \hat{d} \quad (4-31)$$

$$D \frac{\hat{v}_{Cl} N_S}{N_P} = \frac{N_S d\hat{\phi}}{dt} - \frac{R_{Cl}N_S D}{N_P} i_{L1} + \frac{DR_{Cl}N_S}{L_P} \hat{\phi} \quad (4-32)$$

$$+ \frac{R_S N_S}{L_S} \hat{\phi} + \frac{DD'R_C R_L N_S}{L_S (R_C + R_L)} \hat{\phi} + D' \hat{v}_0$$

$$- \frac{R_{Cl} L_{L1} N_S}{N_P} \hat{d} + \frac{R_{Cl} \hat{d} \phi N_S}{L_P} - \hat{d} v_0$$

$$- \frac{R_C R_L N_S \phi \hat{d} (D - D')}{L_S (R_C + R_L)} - \frac{V_{Cl} N_S}{N_P} \hat{d}$$

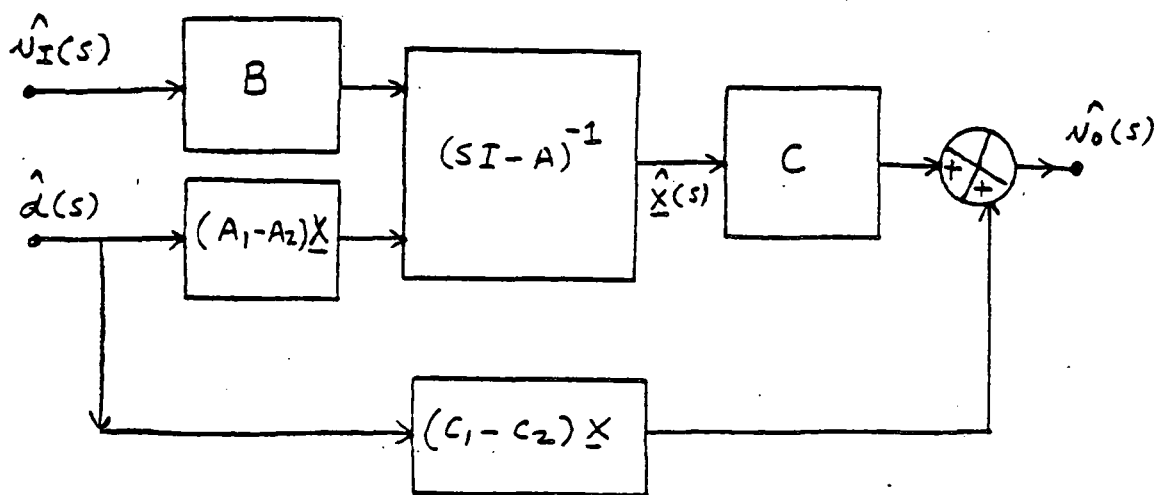
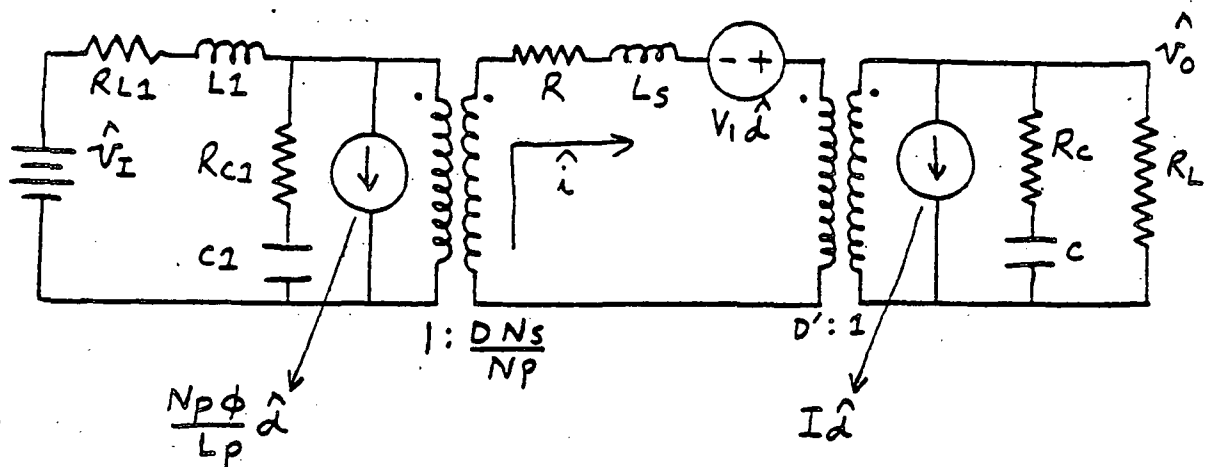


Figure 17: Buck-boost converter power stage small signal state space model



$$R = \frac{DD'R_{C1}L_S}{L_P} + \frac{DD'R_C R_L}{R_C + R_L} + R_S$$

$$V_1 = \left[ \frac{R_{C1}I_{L1}N_S}{N_P} - \frac{R_{C1}I_{L_S}}{L_P} + \frac{R_C R_L I(D-D')}{(R_C + R_L)} + \frac{V_{C1}N_S}{N_P} + V_O \right]$$

Figure 18: Buck-boost converter power stage small signal equivalent circuit

Using a fictitious current  $i$  described by

$$L_S i = N_S \phi \quad (4-33)$$

an equivalent circuit can be made up that is described by the four equations given above. This circuit will use the current  $i$  flowing through  $L_S$  and it is thus the small signal equivalent circuit for the buck-boost converter, as shown in Figure 18.

#### 4.2 BUCK CONVERTER SMALL SIGNAL MODEL DERIVATION

The procedure used in deriving the small signal model for the buck converter is exactly similar to that used for the buck-boost converter. The buck converter is shown in Figure 19 .

During  $T_{ON}$  the switch  $S$  is on and the circuit is as shown in Figure 20 (a).

The equations describing the circuit are

$$\frac{di_{L1}}{dt} = \frac{-(R_{L1} + R_{C1})}{L1} i_{L1} + \frac{R_{C1}}{L1} i_L - \frac{v_{C1}}{L1} + \frac{v_I}{L1} \quad (4-34)$$

$$\frac{di_L}{dt} = \frac{R_{C1}}{L} i_{L1} - \frac{R_L}{L} i_L + \frac{v_{C1}}{L} - \frac{R_L v_C}{L(R_C + R_L)} \quad (4-35)$$

$$\frac{dv_{C1}}{dt} = \frac{i_{L1}}{C1} - \frac{i_L}{C1} \quad (4-36)$$

$$\frac{dv_C}{dt} = \frac{R_L i_L}{C(R_C + R_L)} - \frac{v_C}{C(R_C + R_L)} \quad (4-37)$$

$$v_0 = \frac{R_L R_C i_L}{R_L + R_C} + \frac{R_L v_C}{R_L + R_C} \quad (4-38)$$

During  $T_{OFF}$ , the switch S is off, and the circuit is shown in Figure 20 (b). The equations describing the circuit are

$$\frac{di_{L1}}{dt} = \frac{-(R_{L1} + R_{C1})}{L1} i_{L1} - \frac{v_{C1}}{L1} + \frac{v_I}{L1} \quad (4-39)$$

$$\frac{di_L}{dt} = \frac{-R_2 i_L}{L} - \frac{R_L v_C}{L(R_L + R_C)} \quad (4-40)$$

$$\frac{dv_{C1}}{dt} = \frac{i_{L1}}{C1} \quad (4-41)$$

$$\frac{dv_C}{dt} = \frac{R_L i_L}{C(R_L + R_C)} - \frac{v_C}{C(R_L + R_C)} \quad (4-42)$$

$$v_0 = \frac{R_L R_C i_L}{R_L + R_C} + \frac{R_L v_C}{R_L + R_C} \quad (4-43)$$

$$R_2 = R_2 + \frac{R_C R_L}{R_C + R_L} \quad (4-44)$$

$$R_1 = R_{C1} + R_2 + \frac{R_C R_L}{R_C + R_L} \quad (4-45)$$

The following vectors are defined

$$\begin{aligned} \underline{u} &= [v_I] \\ \underline{y} &= [v_0] \end{aligned} \quad \underline{x} = \begin{bmatrix} i_{L1} \\ i_L \\ v_{C1} \\ v_C \end{bmatrix} \quad (4-46)$$

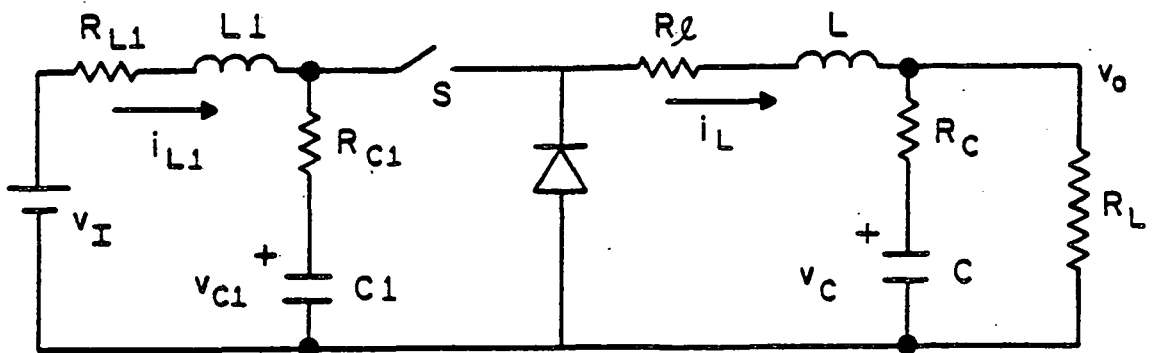
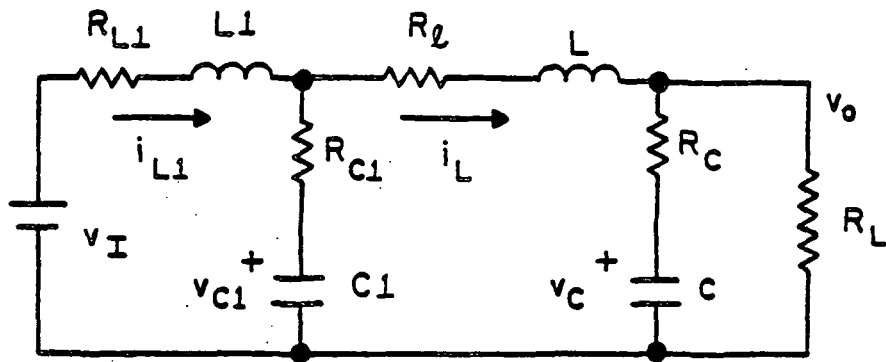
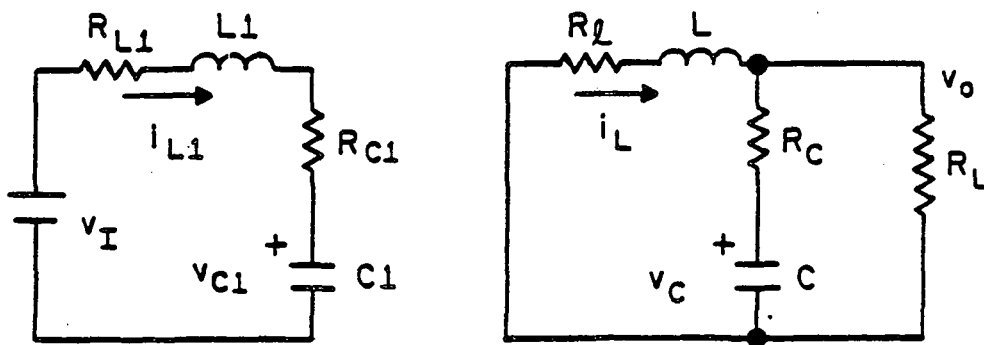


Figure 19: Buck converter power stage.



(a)



(b)

Figure 20: Buck converter power stage model during: (a)  $T_{ON}$  and (b)  $T_{OFF}$ .



$$B_1 = \begin{bmatrix} \frac{1}{Ll} & 0 & 0 & 0 \end{bmatrix}^T \quad (4-50)$$

$$B_2 = B_1 \quad (4-51)$$

$$C_1 = \begin{bmatrix} 0 & \frac{R_L R_C}{R_L + R_C} & 0 & \frac{R_L}{R_L + R_C} \end{bmatrix} \quad (4-52)$$

$$C_2 = C_1 \quad (4-53)$$

The state space averaged model over the entire period  $T$  is

$$\dot{\underline{x}} = [dA_1 + d'A_2]\underline{x} + [dB_1 + d'B_2]u \quad (4-54)$$

$$y = [dC_1 + d'C_2]\underline{x}$$

where  $d = \text{duty cycle ratio} = T_{ON} / (T_{ON} + T_{OFF})$

$$d' = 1 - d \quad (4-55)$$

$$T = T_{ON} + T_{OFF}$$

The state space averaged model is perturbed and linearized in exactly the same way as for the buck-boost converter. The resulting small signal linearized model is

$$\begin{aligned} \underline{0} &= [DA_1 + D'A_2]\underline{x} + [DB_1 + D'B_2]V_I \\ \dot{\underline{x}} &= [DA_1 + D'A_2]\hat{\underline{x}} + [DB_1 + D'B_2]\hat{v}_I \\ &\quad + [(A_1 - A_2)\underline{x} + (B_1 - B_2)V_I]\hat{d} \end{aligned} \quad (4-56)$$

$$V_0 = [DC_1 + D'C_2]\underline{x}$$

$$\hat{v}_0 = [C_1 - C_2]\underline{x}\hat{d} + [DC_1 + D'C_2]\hat{\underline{x}}$$

Defining

$$\begin{aligned}
 A &= DA_1 + D'A_2 \\
 B &= DB_1 + D'B_2 \\
 C &= DC_1 + D'C_2
 \end{aligned}
 \tag{4-57}$$

results in

$$\begin{aligned}
 \dot{\underline{\hat{x}}} &= A\underline{\hat{x}} + B\hat{v}_I \\
 &+ [(A_1 - A_2)\underline{\hat{x}} + (B_1 - B_2)v_I]\hat{d} \\
 \hat{v}_O &= [C_1 - C_2]\underline{\hat{x}}\hat{d} + C\underline{\hat{x}}
 \end{aligned}
 \tag{4-58}$$

Using Laplace transforms gives

$$\begin{aligned}
 \underline{\hat{x}}(s) &= [sI - A]^{-1}B\hat{v}_I(s) \\
 &+ [sI - A]^{-1}[(A_1 - A_2)\underline{\hat{x}} + (B_1 - B_2)v_I]\hat{d}(s) \\
 v_O(s) &= [C_1 - C_2]\underline{\hat{x}}\hat{d}(s) + C\underline{\hat{x}}(s)
 \end{aligned}
 \tag{4-59}$$

The state space model is derived from the above two equations and is shown in Figure 21 .

The procedure for deriving the small signal equivalent circuit is exactly similar to the one used for the buck-boost converter. The four equations that result are

$$\begin{aligned}
 \hat{v}_I &= (R_{L1} + R_{C1})\hat{i}_{L1} - DR_{C1}\hat{i}_L + L1\frac{d\hat{i}_{L1}}{dt} \\
 &+ \hat{v}_{C1} - R_{C1}L\hat{d}
 \end{aligned}
 \tag{4-60}$$

$$\begin{aligned}
 D\hat{v}_{C1} &= (DR_{C1} + R_L)\hat{i}_L - DR_{C1}\hat{i}_{L1} + \hat{v}_O \\
 &+ L\frac{d\hat{i}_L}{dt} - (R_{C1}L1 - R_{C1}L + v_{C1})\hat{d}
 \end{aligned}
 \tag{4-61}$$

$$C1 \frac{d\hat{v}_{C1}}{dt} = \hat{i}_{L1} - D\hat{i}_L - \hat{d}i_L \quad (4-62)$$

$$C \frac{d\hat{v}_C}{dt} = \hat{i}_L - \frac{\hat{v}_O}{R_L} \quad (4-63)$$

The small signal equivalent circuit is described by the four equations above, as in the buck-boost converter, and is shown in Figure 22 .

#### 4.3 BOOST CONVERTER SMALL SIGNAL MODEL DERIVATION

The procedure used in deriving the small signal model for the boost converter is exactly similar to that used for the buck-boost converter. The boost converter is shown in Figure 23 .

During  $T_{ON}$ , the switch S is on, and the resulting circuit is shown in Figure 24 (a).

The equations describing the circuit are

$$\frac{di_{L1}}{dt} = \frac{-(R_{L1} + R_{C1})}{L1} i_{L1} + \frac{R_{C1}}{L1} i_L - \frac{v_{C1}}{L1} + \frac{v_I}{L1} \quad (4-64)$$

$$\frac{dv_{C1}}{dt} = \frac{i_{L1}}{C1} - \frac{i_L}{C1} \quad (4-65)$$

$$\frac{di_L}{dt} = \frac{R_{C1}}{L} i_{L1} - \frac{(R_{C1} + R_L)}{L} i_L + \frac{v_{C1}}{L} \quad (4-66)$$

$$\frac{dv_C}{dt} = \frac{-v_C}{C(R_C + R_L)} \quad (4-67)$$

$$v_O = \frac{v_C R_L}{R_C + R_L} \quad (4-68)$$

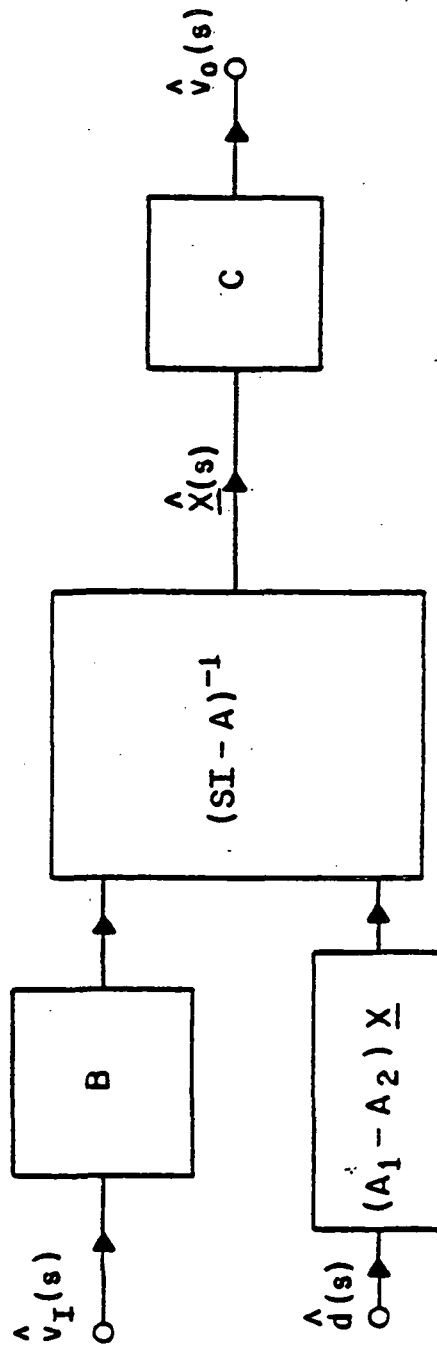
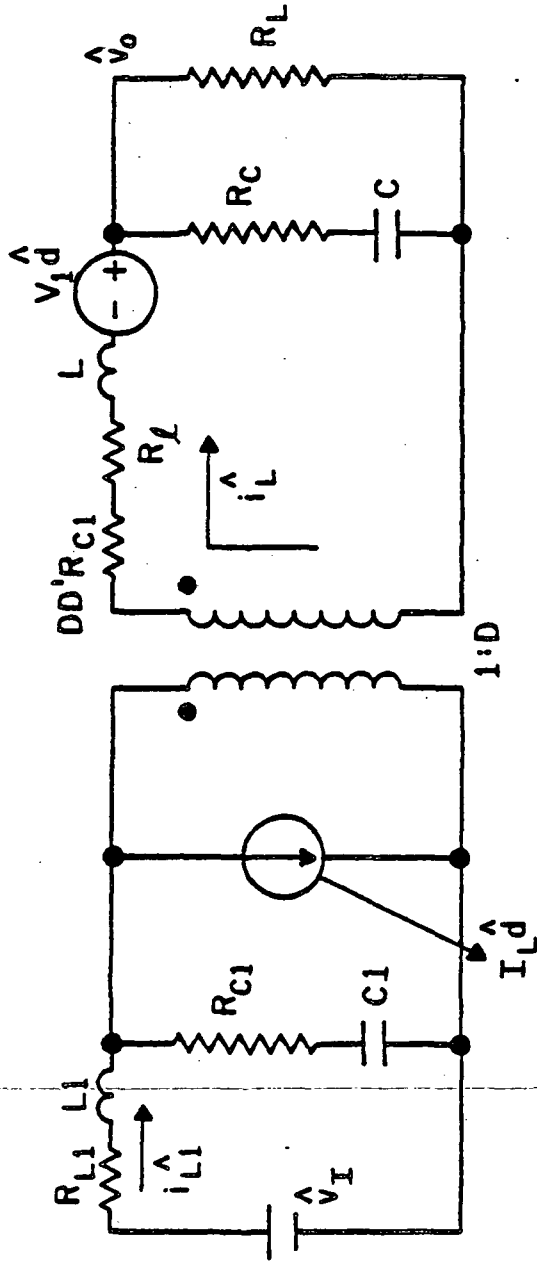


Figure 21: Buck converter power stage small signal state space model.



$$V_I = V_{C1} - D'R_{C1}I_L + R_{C1}I_{L1}$$

Figure 22: Buck converter power stage small signal equivalent circuit.

During  $T_{OFF}$  the switch S is off and the resulting circuit is shown in Figure 24 (b).

The equations describing the circuit are

$$\frac{di_{L1}}{dt} = \frac{-(R_{L1} + R_{C1})}{L1} i_{L1} + \frac{R_{C1}}{L1} i_L - \frac{v_{C1}}{L1} + \frac{v_I}{L1} \quad (4-69)$$

$$\frac{dv_{C1}}{dt} = \frac{i_{L1}}{C1} - \frac{i_L}{C1} \quad (4-70)$$

$$\begin{aligned} \frac{di_L}{dt} = & \frac{R_{C1}}{L} i_{L1} - \frac{i_L}{L} (R_{C1} + R_L + \frac{R_C R_L}{R_C + R_L}) \\ & - \frac{R_L v_C}{L(R_C + R_L)} + \frac{v_{C1}}{L} \end{aligned} \quad (4-71)$$

$$\frac{dv_C}{dt} = \frac{R_L i_L}{C(R_C + R_L)} - \frac{v_C}{C(R_C + R_L)} \quad (4-72)$$

$$v_O = \frac{R_C R_L}{R_C + R_L} i_L + \frac{R_L v_C}{R_C + R_L} \quad (4-73)$$

The following vectors are defined

$$\underline{x} = \begin{bmatrix} i_{L1} \\ i_L \\ v_{C1} \\ v_C \end{bmatrix} \quad \begin{aligned} \underline{u} &= [v_I] \\ \underline{y} &= [v_O] \end{aligned} \quad (4-74)$$

resulting in the following state space equations.

$$\begin{aligned} \underline{\dot{x}} &= A_1 \underline{x} + B_1 \underline{u} & \underline{\dot{x}} &= A_2 \underline{x} + B_2 \underline{u} \\ \underline{y} &= C_1 \underline{x} & \underline{y} &= C_2 \underline{x} \end{aligned} \quad (4-75)$$

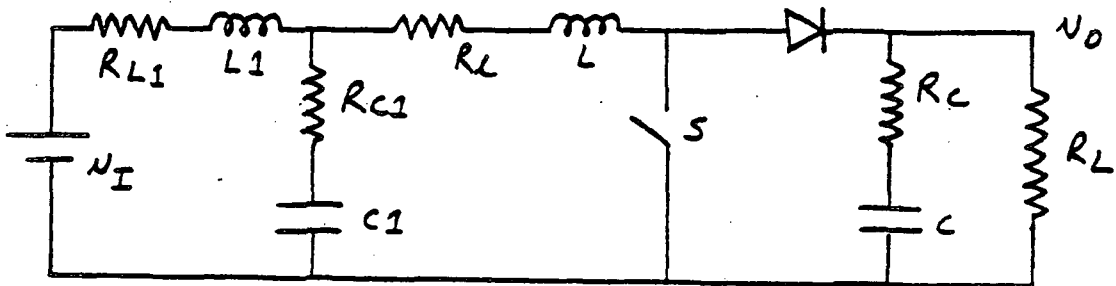
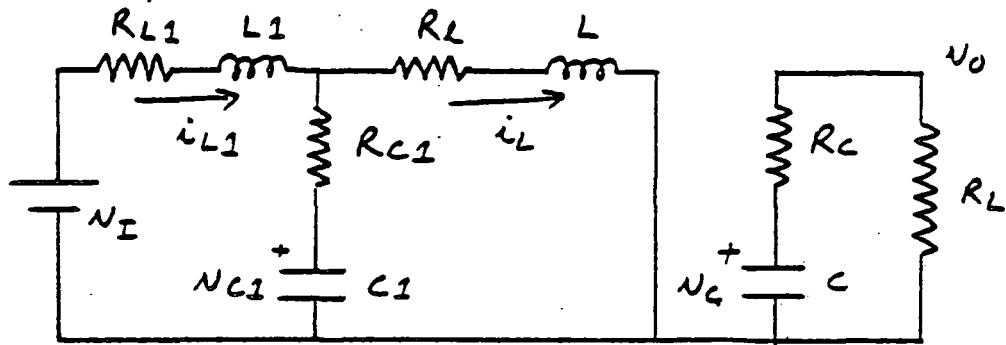
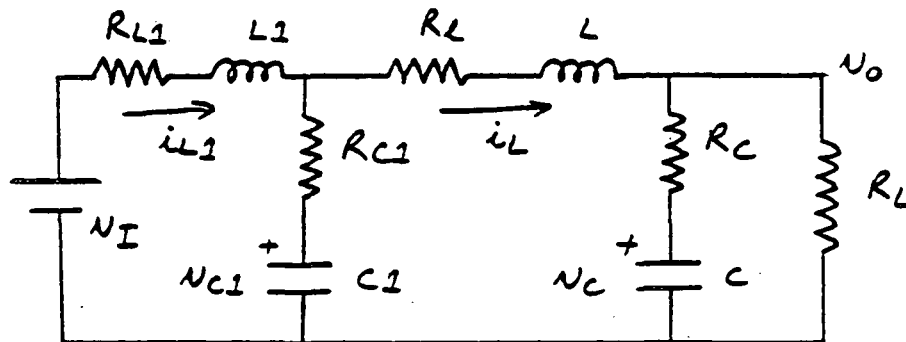


Figure 23: Boost converter power stage



(a)



(b)

Figure 24: Boost converter power stage models during : (a)  $T_{ON}$  and (b)  $T_{OFF}$ .

where

$$A_1 = \begin{bmatrix} \frac{-(R_{L1} + R_{C1})}{L1} & \frac{R_{C1}}{L1} & \frac{-1}{L1} & 0 \\ \frac{R_{C1}}{L} & \frac{-(R_{C1} + R_2)}{L} & \frac{1}{L} & 0 \\ \frac{1}{C1} & \frac{-1}{C1} & 0 & 0 \\ 0 & 0 & 0 & \frac{-1}{C(R_C + R_L)} \end{bmatrix} \quad (4-76)$$

$$A_2 = \begin{bmatrix} \frac{-(R_{L1} + R_{C1})}{L1} & \frac{R_{C1}}{L1} & \frac{-1}{L1} & 0 \\ \frac{R_{C1}}{L} & \frac{-R_1}{L} & \frac{1}{L} & \frac{-R_L}{L(R_C + R_L)} \\ \frac{1}{C1} & \frac{-1}{C1} & 0 & 0 \\ 0 & \frac{R_L}{C(R_C + R_L)} & 0 & \frac{-1}{C(R_C + R_L)} \end{bmatrix} \quad (4-77)$$

$$R_1 = R_{C1} + R_2 + \frac{R_C R_L}{R_C + R_L} \quad (4-78)$$

$$B_1 = \begin{bmatrix} \frac{1}{L1} & 0 & 0 & 0 \end{bmatrix}^T \quad (4-79)$$

$$B_2 = B_1 \quad (4-80)$$

$$C_1 = \begin{bmatrix} 0 & 0 & 0 & \frac{R_L}{R_C + R_L} \end{bmatrix} \quad (4-81)$$

$$C_2 = \begin{bmatrix} 0 & \frac{R_L R_C}{R_L + R_C} & 0 & \frac{R_L}{R_C + R_L} \end{bmatrix} \quad (4-82)$$

The state space averaged model over the entire period T is

$$\dot{\underline{x}} = [dA_1 + d'A_2]\underline{x} + [dB_1 + d'B_2]\underline{u} \quad (4-83)$$

$$Y = [dC_1 + d'C_2]\underline{x}$$

where  $d = \text{duty cycle ratio} = T_{ON}/(T_{ON} + T_{OFF})$

$$d' = 1 - d$$

$$T = T_{ON} + T_{OFF}$$

(4-84)

The state space averaged model is perturbed and linearized in exactly the same way as for the buck-boost converter. The resulting small signal linearized model is

$$\underline{0} = A \underline{X} + B V_I \quad (4-85)$$

$$\dot{\underline{x}} = A \hat{\underline{x}} + B \hat{V}_I + [(A_1 - A_2) \underline{x} + (B_1 - B_2) V_I] \hat{d}$$

$$V_0 = C \underline{X} \quad (4-86)$$

$$\hat{V}_0 = [C_1 - C_2] \underline{x} \hat{d} + C \hat{\underline{x}} \quad (4-87)$$

where  $A = DA_1 + D'A_2$

$$B = DB_1 + D'B_2 \quad (4-88)$$

$$C = DC_1 + D'C_2$$

Using Laplace transforms gives

$$\begin{aligned} \hat{\underline{x}}(s) &= [SI - A]^{-1} B \hat{v}_I(s) \\ &\quad + [SI - A]^{-1} [(A_1 - A_2)\underline{X} + (B_1 - B_2)V_I] \hat{d}(s) \end{aligned} \quad (4-89)$$

$$\hat{v}_0(s) = [C_1 - C_2]\underline{X} \hat{d}(s) + C\hat{\underline{x}}(s)$$

The state space model is derived from the above two equations and is shown in Figure 25 .

The procedure for deriving the small signal equivalent circuit is exactly similar to the one used for the buck-boost converter. The four equations that result are --

$$L_1 \frac{d\hat{i}_{L1}}{dt} = -(R_{L1} + R_{C1})\hat{i}_{L1} + R_{C1}\hat{i}_L - \hat{v}_{C1} + \hat{v}_I \quad (4-90)$$

$$\begin{aligned} L \frac{d\hat{i}_L}{dt} &= R_{C1}\hat{i}_{L1} - (R_{C1} + R_L)\hat{i}_L - DD' \frac{R_C R_L}{R_C + R_L} \hat{i}_L \\ &\quad + \hat{v}_{C1} - D'\hat{v}_0 + \frac{R_C R_L L \hat{d}(D - D')}{R_C + R_L} + v_0 \hat{d} \end{aligned} \quad (4-91)$$

$$C_1 \frac{d\hat{v}_{C1}}{dt} = \hat{i}_{L1} - \hat{i}_L \quad (4-92)$$

$$C \frac{d\hat{v}_C}{dt} = D'\hat{i}_L - \frac{\hat{v}_0}{R_L} - L_L \hat{d} \quad (4-93)$$

The small signal equivalent circuit is described by the four equations above as in the buck-boost converter, and is shown in Figure 26 .

The power stage small signal models developed include the input filter state variables, whereas earlier models [3,4,5,6] had treated the input filter only in terms of its output impedance and transfer function. The models developed in this chapter are used to analyze and design a feedforward loop that includes the input filter state variables.

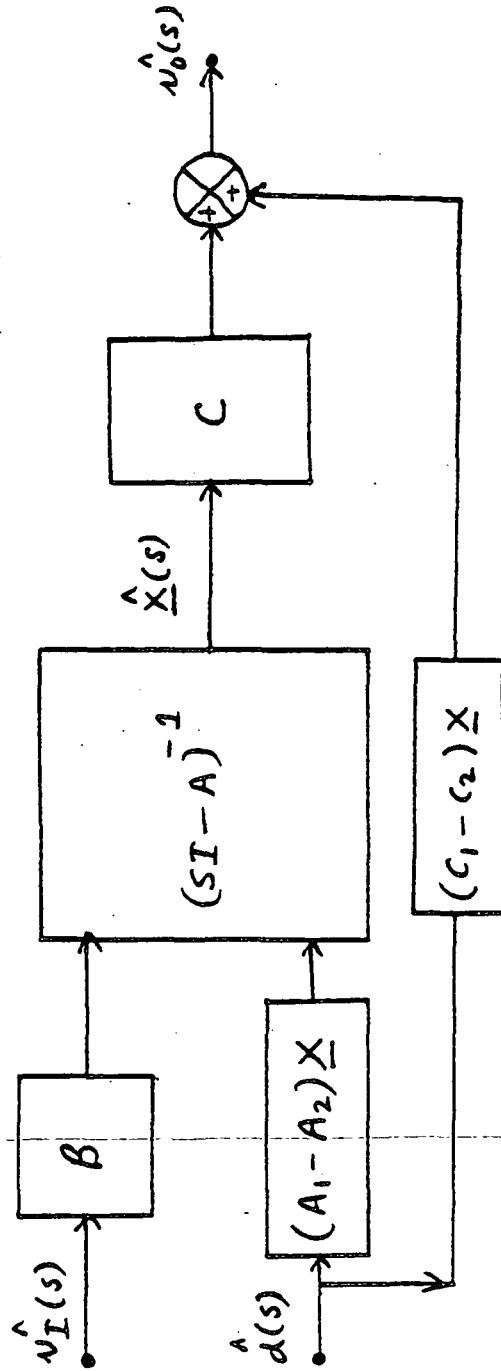
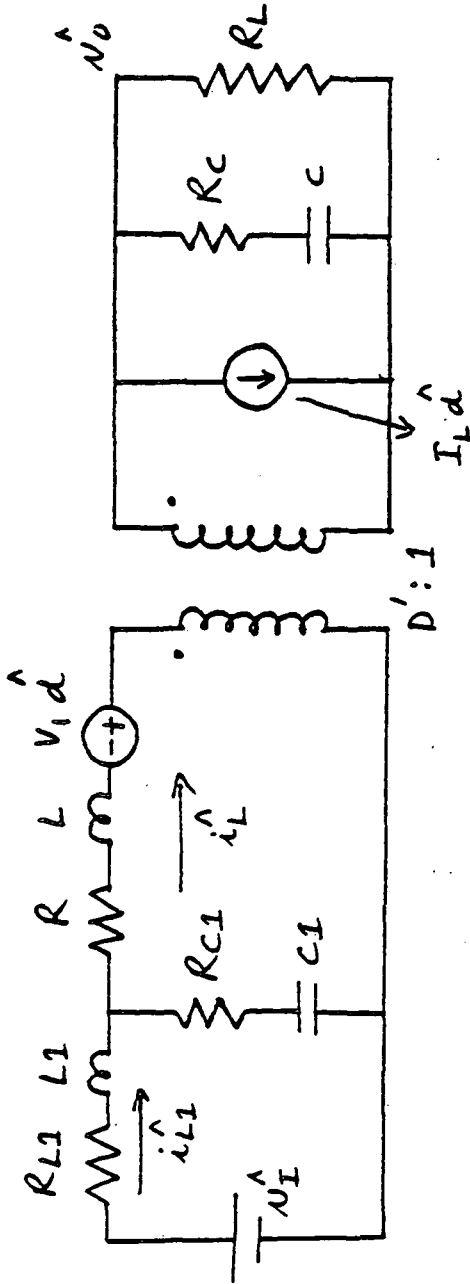


Figure 25: Boost converter power stage small signal state space model.



$$R = R_L + \frac{D D' R_C R_L}{R_C + R_L}$$

$$V_1 = V_0 + \frac{R_C R_L I_L (D - D')}{R_C + R_L}$$

Figure 26: Boost converter power stage small signal equivalent circuit.

## Chapter V

### IMPLEMENTATION OF THE FEEDFORWARD LOOP FOR A BUCK REGULATOR

This chapter first presents an analysis that leads to a design of the feedforward loops for a buck regulator. A small signal model that includes a general form of the feedforward loops is developed first. Analysis of the small signal model leads to a design of the feedforward loop. Implementation of the design is next discussed and two feedforward circuits are presented. The buck regulator alone is treated in this chapter, however the analysis and design procedure would be similar for the boost and the buck-boost regulators.

#### 5.1 STATE SPACE MODEL OF BUCK REGULATOR

The state space model of the buck regulator is shown in Figure 27 . In the figure the feedforward loop has as its input the input filter state variables  $\hat{i}_{L1}$  and  $\hat{v}_{C1}$  (the input filter inductor current and capacitor voltage respectively). These two inputs are multiplied by the transfer functions  $c_2(s)$  and  $c_3(s)$  whose properties are yet to be determined. The feedback loop has as its inputs the output voltage and the output filter inductor current. The feedback control in this case is the two loop control (the standardized control

module or SCM) developed earlier [2,7,8] and discussed in Chapter 3. The error processor in Figure 27 is thus composed of the blocks labelled  $c_2$ ,  $c_3$  and the feedback, and has as its input information regarding the output filter and input filter state variables. The pulse modulator is represented by its transfer function  $F_M$  [2,8]. The rest of Figure 27 is the state space model of the buck power stage developed in Chapter 4.

The feedforward and feedback signals are added and fed to the pulse modulator. In physical terms this means sensing the small signal variations in input filter inductor current and capacitor voltage, processing these variations (as represented by the blocks  $c_2(s)$  and  $c_3(s)$  in Figure 27) and adding the processed variations to the feedback signal. The total state feedforward/feedback error signal is then used to modulate the duty cycle of the switch for loop gain correction.

The transfer function  $\hat{v}_0(s)/\hat{v}_x(s)$ , Figure 27, is used to design the feedforward because it expresses clearly what the feedforward does; also the resulting design is independent of the feedback loop parameters. The generalized small signal model for the buck regulator is developed next and used to write the transfer function  $\hat{v}_0(s)/\hat{v}_x(s)$ .

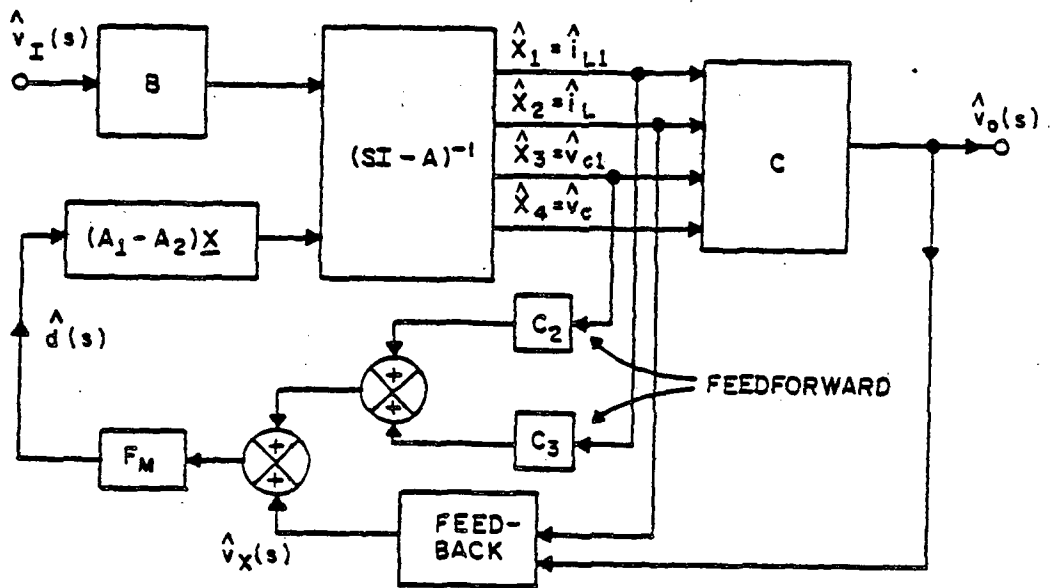


Figure 27: State space model of the buck regulator

## 5.2 GENERALIZED SMALL SIGNAL MODEL OF BUCK REGULATOR

The generalized small signal model of the buck regulator is shown in Figure 28 . The regulator is modelled according to the three basic functional blocks: power stage, error processor and duty cycle pulse modulator. The power stage model consists of two inputs: disturbances from the line  $\hat{v}_I$  and the duty cycle control  $\hat{d}$ , and four outputs: the output voltage  $\hat{v}_O$ , the output filter inductor current  $\hat{i}_L$ , the input filter capacitor voltage  $\hat{v}_{C1}$  and the input filter inductor current  $\hat{i}_{L1}$ . The error processor has as its input information regarding the output filter and the input filter state variables. The transfer functions  $F_3$ ,  $F_{AC}$  and  $F_{DC}$  constitute the two loop standardized control module (SCM) developed earlier [2,7,8], whereas the feedforward loop gains  $c_2$  and  $c_3$  are as yet unknown. The error processor processes information regarding the state variables of the input and output filters and feeds a total error signal to the pulse modulator, whose transfer function  $F_M$  was developed earlier [2,7,8].

The power stage transfer functions  $F_{11}$  etc. are written using the following equations:

$$\begin{aligned}
 T_{11}\hat{v}_I + T_{12}\hat{d} &= \hat{v}_O \\
 T_{21}\hat{v}_I + T_{22}\hat{d} &= \hat{i}_L \\
 T_{31}\hat{v}_I + T_{32}\hat{d} &= \hat{v}_{C1} \\
 T_{41}\hat{v}_I + T_{42}\hat{d} &= \hat{i}_{L1}
 \end{aligned}
 \tag{5-1}$$

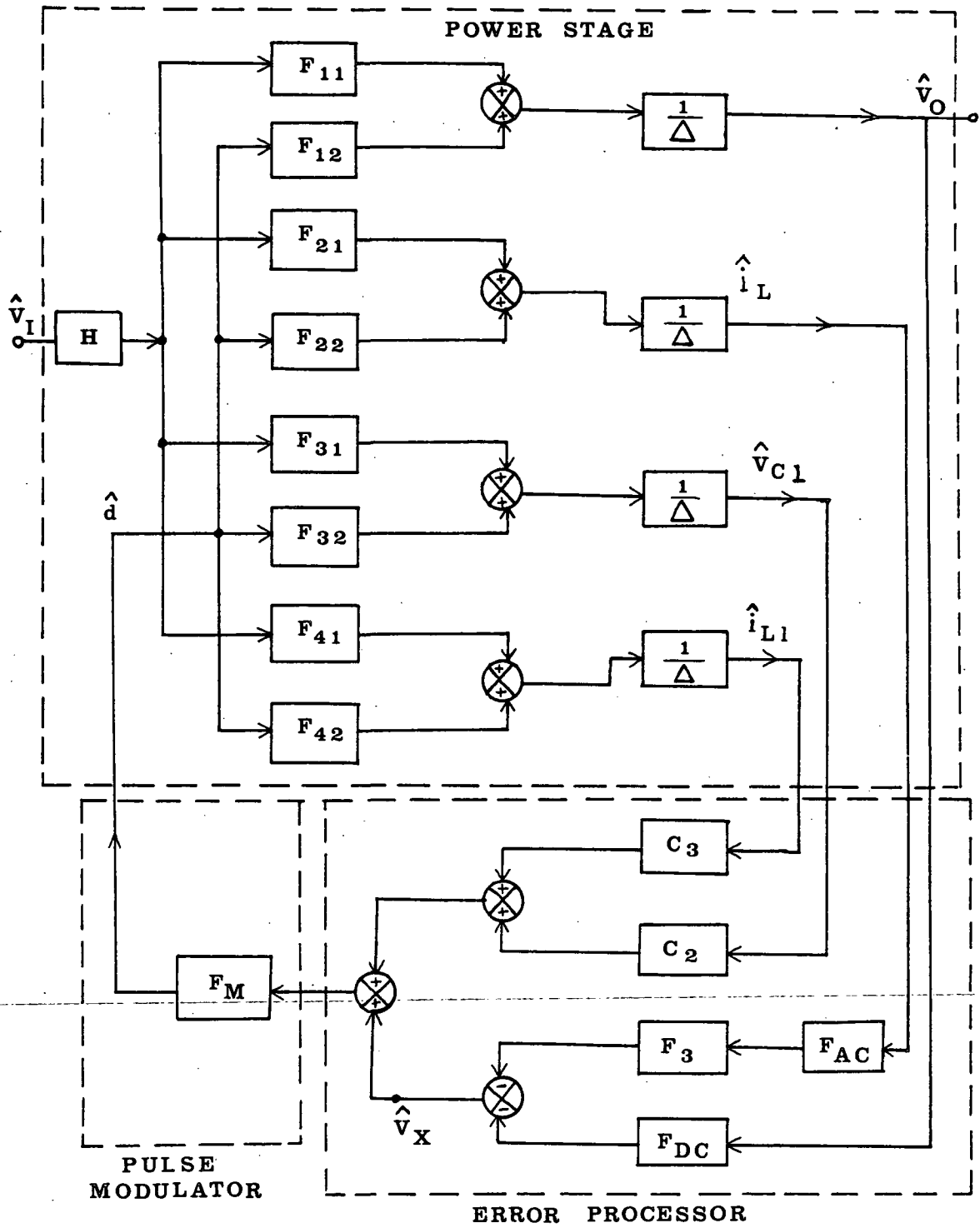


Figure 28: Generalized Small Signal Model

Thus it can be seen that

$$T_{11} = \left. \frac{\hat{v}_O}{\hat{v}_I} \right|_{\hat{d} = 0} \quad (5-2)$$

and

$$\begin{aligned} T_{11} &= \frac{H F_{11}}{\Delta} \\ T_{12} &= \frac{F_{12}}{\Delta} \end{aligned} \quad (5-3)$$

### 5.2.1 Development of Power Stage Transfer Functions

As can be seen from equations (5-1)  $T_{11}$ ,  $T_{21}$ ,  $T_{31}$  and  $T_{41}$  can be evaluated with  $\hat{d} = 0$  and the other four with  $\hat{v}_I = 0$ . The starting point for the evaluation of the transfer functions is the small signal equivalent circuit model for the buck regulator power stage developed in Chapter 4, Figure 22

#### 5.2.1.1 Evaluation of $T_{11}$ , $T_{21}$ , $T_{31}$ and $T_{41}$

These transfer functions are evaluated with  $\hat{d} = 0$  in Figure 22. The resulting circuit is shown in Figure 29. In Figure 29 the input filter has been replaced by its forward transfer function  $H(s)$  and its output impedance  $Z(s)$ .

$$H(s) = \frac{1 + sC_1 R_{C_1}}{s^2 L_1 C_1 + sC_1 (R_{L_1} + R_{C_1}) + 1} \quad (5-4)$$

$$Z(s) = \frac{s^2 L_1 C_1 R_{C1} + s C_1 R_{C1} R_{L1} + s L_1 + R_{L1}}{s^2 L_1 C_1 + s C_1 (R_{L1} + R_{C1}) + 1} \quad (5-5)$$

From the equivalent circuit of Figure 29 the following can be derived:

$$\begin{aligned} T_{11} &= \frac{\hat{v}_O}{\hat{v}_I} = \frac{D R_L (1 + s C R_C) H}{\Delta} \\ T_{21} &= \frac{\hat{i}_L}{\hat{v}_I} = \frac{D (1 + s C R_L) H}{\Delta} \\ T_{31} &= \frac{\hat{v}_{C1}}{\hat{v}_I} = \frac{a_1 H}{\Delta} \\ T_{41} &= \frac{\hat{i}_{L1}}{\hat{v}_I} = \frac{\Delta - a_1 H}{(R_{L1} + s L_1) \Delta} \end{aligned} \quad (5-6)$$

where

$$\begin{aligned} a_1 &= s^2 L C R_L + s C R_L (R_\ell + R_C + \frac{L}{C R_L}) + R_L \\ \Delta &= a_1 + D^2 Z (1 + s C R_L) \\ D &= \text{duty cycle} = \frac{V_O}{V_I}, \quad V_I = \text{supply voltage} \end{aligned} \quad (5-7)$$

$$R_L + R_\ell \approx R_L$$

Using equations (5-3) and (5-6) the following are derived:

$$\begin{aligned} F_{11} &= DR_L(1 + sCR_C) \\ F_{21} &= D(1 + sCR_L) \\ F_{31} &= a_1 \\ F_{41} &= \frac{\Delta/H - a_1}{R_{L1} + sL1} \end{aligned} \quad (5-8)$$

In the derivation of equations (5-6) the resistance  $R_{C1}$  has been assumed negligibly small. This is not an unrealistic assumption since the ESR of the input filter capacitor ( $R_{C1}$ ) can be assumed negligibly small compared with the other resistances; also in the derivation of  $T_{41}$  the following is used:

$$\frac{\hat{v}_I - \hat{v}_{C1}}{R_{L1} + sL1} = \hat{i}_{L1} \quad (5-9)$$

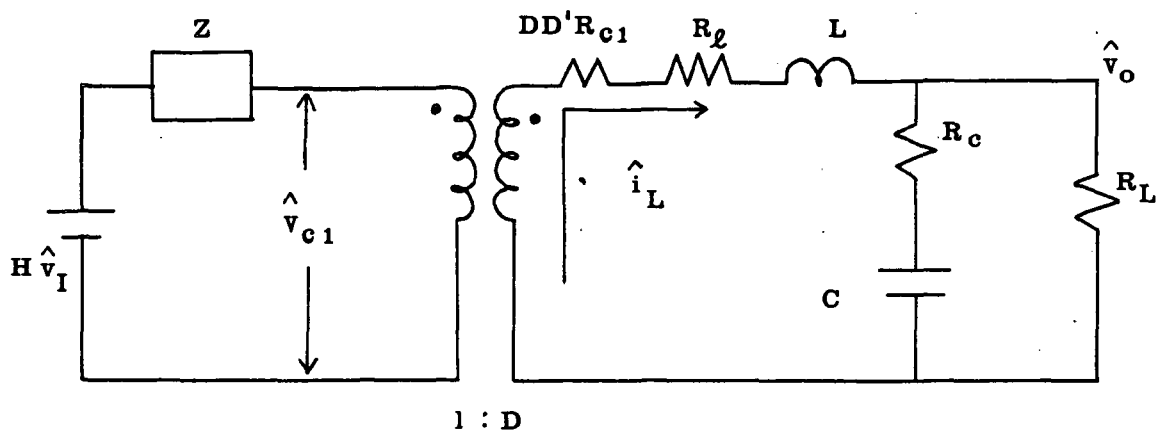


Figure 29: Small signal equivalent circuit with  $\hat{d} = 0$

### 5.2.1.2 Evaluation of $T_{12}$ , $T_{22}$ , $T_{32}$ and $T_{42}$ .

These transfer functions are evaluated with  $\hat{V}_I = 0$  in Figure 22. The resulting circuit is shown in Figure 30.

From the equivalent circuit of Figure 30 the following are derived:

$$\begin{aligned}
 T_{12} &= \frac{\hat{V}_O}{\hat{d}} = \frac{V_O (R_L - D^2 Z) (1 + sCR_C)}{D\Delta} \\
 T_{22} &= \frac{\hat{i}_L}{\hat{d}} = \frac{V_O (R_L - D^2 Z) (1 + sCR_L)}{DR_L \Delta} \\
 T_{32} &= \frac{v_{C1}}{\hat{d}} = \frac{-zV_O [a_1 + R_L (1 + sCR_L)]}{R_L \Delta} \\
 T_{42} &= \frac{\hat{i}_{L1}}{\hat{d}} = \frac{zV_O [a_1 + R_L (1 + sCR_L)]}{(R_{L1} + sL1)R_L \Delta}
 \end{aligned} \tag{5-10}$$

Using equations (5-1) and (5-10) the following are derived:

$$\begin{aligned}
 F_{12} &= \frac{V_O (R_L - D^2 Z) (1 + sCR_C)}{D} \\
 F_{22} &= \frac{V_O (R_L - D^2 Z) (1 + sCR_L)}{DR_L} \\
 F_{32} &= \frac{-zV_O [a_1 + R_L (1 + sCR_L)]}{R_L}
 \end{aligned} \tag{5-11}$$

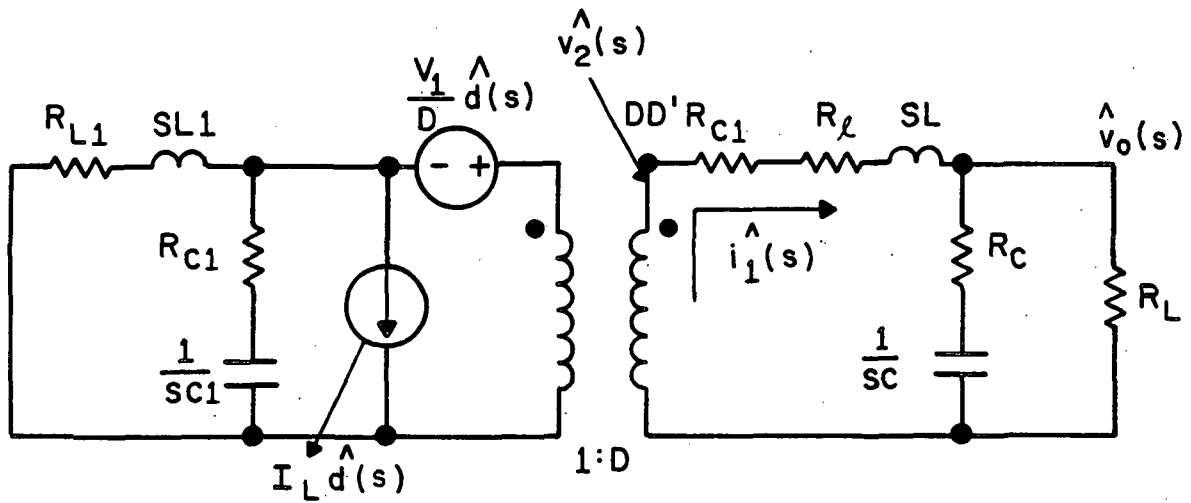


Figure 30: Small signal equivalent circuit with  $\hat{v}_I = 0$

$$F_{42} = \frac{zV_O [a_1 + R_L (1 + sCR_L)]}{(R_{L1} + sL1)R_L}$$

where  $\Delta$  and  $a_1$  are as defined in equation (5-7) and

$$V_1 \approx \frac{V_O}{D}$$

(5-12)

$$R_{C1} \approx 0$$

### 5.2.2 Feedback Transfer Functions

Transfer functions  $F_3$ ,  $F_{AC}$ ,  $F_M$  and  $F_{DC}$  constitute the feedback. A two loop standardized control module (SCM) controlled [2,7,8] buck regulator was used to obtain experimental results that are discussed later in this dissertation. The buck regulator used is shown in Figure 31, and with reference to that figure the following are defined [2,7,8] :

$$F_3 = snL$$

$$F_{AC} = \frac{1}{sC_1 R_4}$$

$$F_{DC} = \frac{1}{sC_1} \left( \frac{g}{R_{14} + R_x} + \frac{1}{Z_C} \right) \quad (5-13)$$

$$R_x = R_{11} // R_{12}, \quad g = \frac{R_x}{R_{11}}$$

$$Z_C = R_{13} + \frac{1}{sC_2}$$

$$F_M = \frac{2R_4 C_1'}{nM} \quad (\text{Pulse Modulator Transfer Function})$$

$M =$  Constant depending on the type of control used.

### 5.3 DESIGN OF THE FEEDFORWARD LOOP.

The transfer function  $\hat{v}_0/\hat{v}_x$  is used to design the feedforward. With  $\hat{v}_1 = 0$  the following equations are derived from Figure 28 :

$$[\hat{v}_x + c_2 \hat{v}_{C1} + c_3 \hat{i}_{L1}] F_M = \hat{d} \quad (5-14)$$

and

$$\begin{aligned} \frac{\hat{d}F_{12}}{\Delta} &= \hat{v}_0 \\ \hat{v}_{C1} &= \frac{\hat{d}F_{32}}{\Delta} \\ \hat{i}_{L1} &= \frac{\hat{d}F_{42}}{\Delta} \end{aligned} \quad (5-15)$$

Substituting for  $\hat{v}_{C1}$ ,  $\hat{i}_{L1}$  and  $\hat{d}$  from (5-15) in (5-14) results in

$$\frac{\hat{v}_0}{\hat{v}_x} = \frac{(\frac{F_{12}}{\Delta}) F_M}{1 - c_2 (\frac{F_{32}}{\Delta}) F_M - c_3 (\frac{F_{42}}{\Delta}) F_M} \quad (5-16)$$

In the absence of feedforward i.e. with  $c_2 = c_3 = 0$  it can be seen that:

$$\frac{\hat{v}_O}{\hat{v}_X} = \frac{V_O (R_L - D^2 Z) (1 + sCR_C) F_M}{a_1 + D^2 Z (1 + sCR_L)} \quad (5-17)$$

The effect of peaking of the output impedance of the input filter  $Z$  is to cause a reduction in the term  $(R_L - D^2 Z)$  and also an increase in the denominator, thus resulting in a substantial loss of loop gain.

With feedforward the detrimental effect of peaking of  $Z$  could be avoided by a proper choice of the feedforward loop gains  $c_2$  and  $c_3$ . Choosing

$$c_2 = \frac{-D^2}{V_O F_M} \quad (5-18)$$

$$c_3 = 0$$

leads to

$$\frac{\hat{v}_O}{\hat{v}_X} = \frac{V_O F_M (R_L - D^2 Z) (1 + sCR_C)}{D\Delta} \quad (5-19)$$

$$1 + \frac{D^2}{V_O F_M} F_M \left\{ \frac{-ZV_O [a_1 + R_L (1 + sCR_L)]}{R_L \Delta} \right\}$$

which can be simplified to

$$\frac{\hat{v}_O}{\hat{v}_X} = \frac{V_{OM} (R_L - D^2 Z) (1 + sCR_C) R_L \Delta}{D \Delta a_1 (R_L - D^2 Z)} \quad (5-20)$$

Cancellation of the two terms leads to

$$\frac{\hat{v}_O}{\hat{v}_X} = \frac{V_{OM} (1 + sCR_C) R_L}{D a_1} \quad (5-21)$$

Thus a proper choice of the feedforward loop gains has resulted in the transfer function  $\hat{v}_O/\hat{v}_X$  being completely independent of the input filter output impedance  $Z$ . It is also noted from equations (5-11) and (5-16) that at frequencies other than the resonant frequencies at which  $Z$  peaks, the gain of  $F_{32}$  is fairly small since  $Z$  would be small at those frequencies. Thus the addition of feedforward would not affect, in any noticeable manner, the open loop gain and phase margin at any frequency other than those at which  $Z$  peaks.

The following points regarding the feedforward loop design can be made:

1. It has been shown analytically that a proper choice of feedforward loop gains results in eliminating completely the effect of peaking of  $Z$  on the loop gain.

2. The gain  $c_3 = 0$ , thus the inductor current information is not needed, only the input filter capacitor voltage information is used.
3. The feedforward loop gains are independent of the input filter parameter values, and are free of any frequency dependent term.
4. The feedforward loop gains are independent of the type of feedback control used. The pulse modulator transfer function  $F_M$  is, however, an integral part of the design and thus the compensation depends on the type of duty cycle control used. The feedforward loop design process is independent of the particular type of control used and thus the same design can be used for other types of control, for example for single loop control, current injected control and others.

#### 5.4 IMPLEMENTATION OF FEEDFORWARD

The buck regulator used to obtain experimental results that are discussed later is shown in Figure 31 . The feedforward circuit processes the small signal variation across the input filter capacitor and adds this processed information to the feedback signal.

Two circuit implementations of the feedforward design were used in making measurements and they are discussed next.

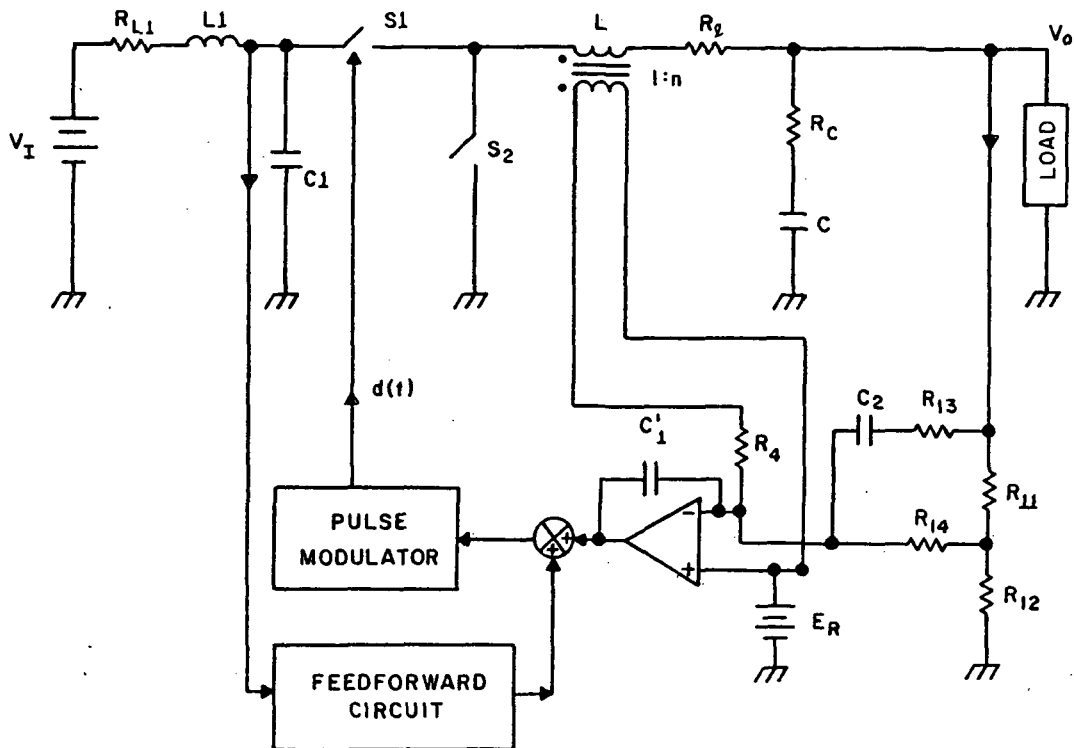


Figure 31: Buck regulator with feedforward used to obtain experimental results

#### 5.4.1 Nonadaptive Feedforward Circuit

It was shown earlier that the feedforward loop gain is

$$c_2(s) = -D^2/V_0 F_M \quad , \text{ equation (5-18)}$$

The nonadaptive feedforward circuit was developed for the buck regulator of Figure 31. The key parameters of the regulator are as follows -

##### Input-Output Parameters

$$V_I = 25-40 \text{ volts} \quad V_O = 20 \text{ volts} \quad P_O = 40 \text{ watts}$$

##### Power Stage Parameters

$$L = 230 \text{ micro H} \quad C = 300 \text{ micro F} \quad R_l = 0.2 \text{ ohm}$$

$$R_C = 0.067 \text{ ohm (nominal)} \quad R_L = 20 \text{ ohm (load)}$$

##### Pulse Modulator Parameters

$$M = V_I T_{ON} = 0.88 * 10^{-3} \text{ V-sec}$$

##### Control Circuit Parameters

$$E_R = 6.7 \text{ volts} \quad R_{11} = 33.3 \text{ Kohm} \quad R_{12} = 16.7 \text{ Kohm}$$

$$R_{13} = 2 \text{ Kohm} \quad R_{14} = 47 \text{ Kohm} \quad R_4 = 40.7 \text{ Kohm}$$

$$n = 0.65 \quad C_1' = 5600 \text{ picoF} \quad C_2 = 0.01 \text{ microF}$$

The buck regulator was operated in a predetermined duty cycle control mode (constant  $V_I T_{ON}$  control), [2,7,8]. Substituting for  $F_M$ , [2,8] and for  $D$  leads to

$$c_2(s) = \frac{-V_o nM}{2V_I^2 R_4 C_1'} \quad (5-22)$$

where  $M = V_I T_{ON}$  is constant.

For the nonadaptive design the input voltage was kept constant at  $V_I = 30$  volts. Substituting in equation (5-22) it is calculated that  $c_2(s) = -0.03$ . The nonadaptive feedforward circuit implementation is shown in Figure 32. The input to the circuit is the input filter capacitor voltage and a series capacitor (27 microF) blocks out the dc component. The input is then multiplied by the gain of 0.03 implemented by the 5.1 Kohm and 164 ohm resistances. The feedforward signal available at the potential divider network is then subtracted from the feedback signal available at the output of the integrator in the feedback loop. The result is then fed to the pulse modulator. The capacitor voltage fed into the operational amplifier subtracting circuit consists of two components - a small signal variation and a component corresponding to the switching frequency. The feedback signal is also at the switching frequency, but the amplitude of the feedback signal is large compared to the switching frequency information in the capacitor voltage, and thus the second component has negligible effect. It is to be noted

that the circuit of Figure 32 constitutes the feedforward circuit and also the summing junction shown in Figure 31 .

The nonadaptive circuit has the advantage of being extremely simple and easy to implement. The gain of the potential divider in the feedforward circuit is, however, a function of supply voltage and thus the circuit of Figure 32 cannot be used at any other value of supply voltage. Measurements made using this circuit are discussed in the next chapter.

#### 5.4.2 Adaptive Feedforward Circuit

The adaptive feedforward circuit is shown in Figure 33 . From equation (5-22) it is clear that changes in supply voltage  $V_I$  will change the gain  $c_2$  of the feedforward loop, the circuit of Figure 33 implements the feedforward of equation (5-22) and adjusts the gain automatically as  $V_I$  changes.

The input voltage in Figure 33 is allowed to vary between 25v and 40v. It is fed to a voltage divider and then squared. The input filter capacitor voltage consists of a large dc component and this is blocked out by the 27 microF capacitor in series with the feedforward path. The small signal variation and the small magnitude component at switching frequency are then divided by the squared input voltage. A pair of resistances provides the final gain; the

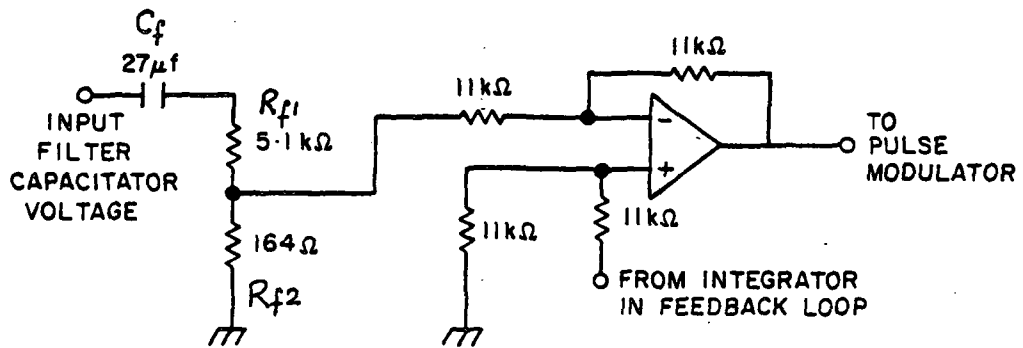


Figure 32: Nonadaptive Feedforward Circuit

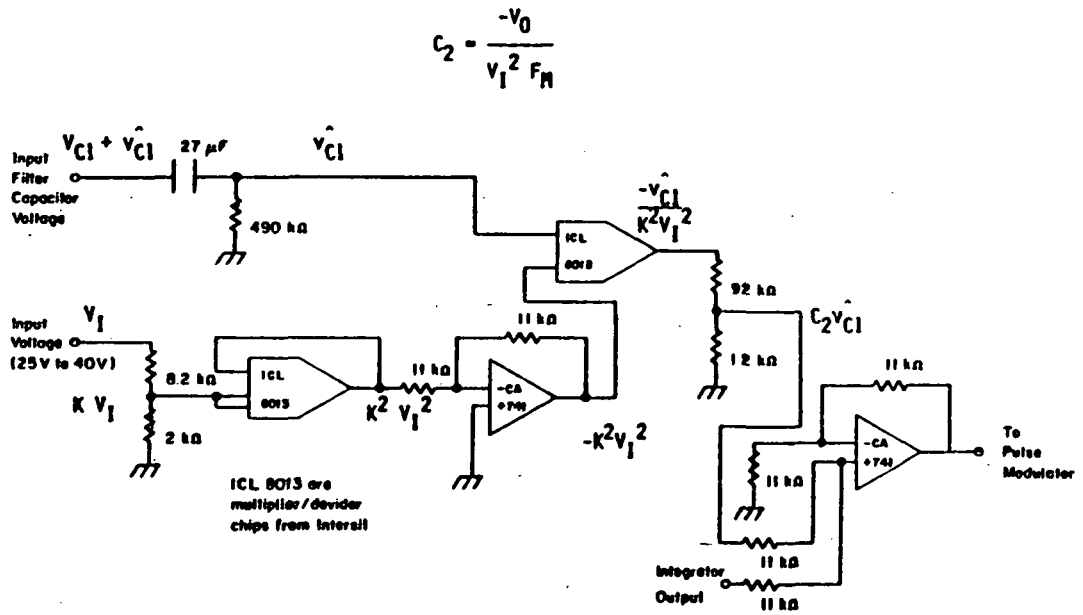


Figure 33: Adaptive feedforward implementation for a variable voltage supply.

feedforward signal now available is then added to the feedback signal at the output of the integrater. As for the nonadaptive circuit the switching frequency component in the input filter capacitor voltage is small compared to the corresponding component in the feedback signal and thus its effect on the duty cycle implementation is negligible.

The gain of the feedforward circuit is thus a function of input voltage  $V_I$  and is made adaptive to changes in  $V_I$ . The feedforward is thus capable of tracking any variations in supply voltage.

## Chapter VI

### ANALYTICAL AND EXPERIMENTAL VERIFICATION OF THE FEEDFORWARD DESIGN

This chapter presents extensive measurement data that was made to verify experimentally the feedforward design outlined earlier. The feedforward control was designed for a buck regulator and the same regulator is used in obtaining measurements.

Measurement data pertaining to the open loop gain and phase margin are presented first; data made using the adaptive feedforward circuit designed earlier confirm the adaptive nature of the circuit. The audiosusceptibility and output impedance measurements presented next show that the feedforward significantly improves performance in both categories. Lastly, measurements of transient response are included that show that the feedforward improves the transient response.

### 6.1 MEASUREMENTS OF THE NONADAPTIVE FEEDFORWARD CONTROL

The buck regulator with feedforward used to obtain experimental results is shown in Figure 34 , and is the same as that presented earlier in Chapter V. The parameters of the regulator are the same as given earlier in Chapter V with the single-stage input filter parameters specified as:

$$R_{L1} = 0.2 \text{ ohm} \quad L1 = 116 \text{ micro-H} \quad C1 = 20 \text{ micro-F}$$

The feedforward circuit used was the nonadaptive feedforward circuit for a fixed input voltage discussed in Chapter V, with  $V_I = 30 \text{ V}$ . The small signal open loop transfer function of the multiloop controlled buck regulator of Figure 34 without feedforward can be expressed as [2,7,8]

$$G_T(s) = E_{DC} E_M F_{12} + E_3 E_{AC} F_{22} E_M \quad (6-1)$$

In equation (6-1)  $F_{12}$  and  $F_{22}$  are the power stage transfer functions,  $E_{DC}$ ,  $E_M$ ,  $E_3$  and  $E_{AC}$  are the feedback control loop transfer functions, as discussed in Chapter 5 (section 5.2). The peaking of the output impedance of the input filter,  $Z(s)$ , affects the transfer functions  $F_{12}$  and  $F_{22}$  as is seen below:

$$F_{12} = \frac{V_O(R_L - D^2 Z) (1 + sCR_C)}{D[ D^2 Z( 1 + sCR_L) + a_1 ]} \quad (6-2)$$

$$F_{22} = \frac{V_O(R_L - D^2 Z)( 1 + sCR_L)}{DR_L[ D^2 Z( 1 + sCR_L) + a_1 ]} \quad (6-3)$$

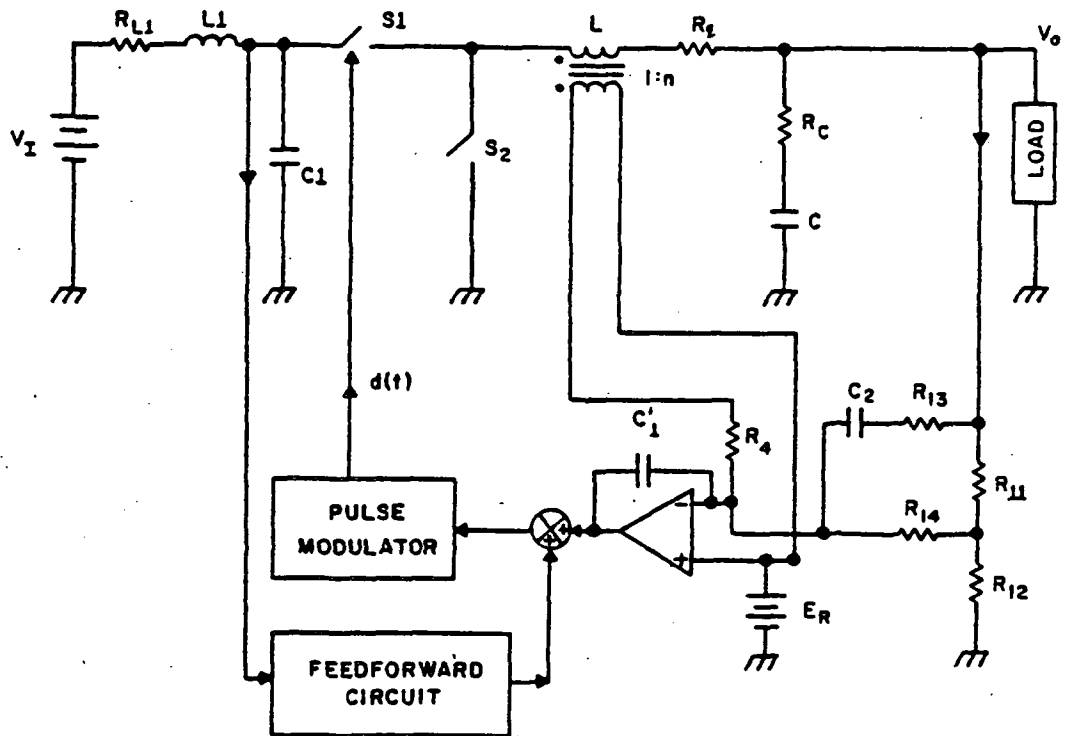


Figure 34: Buck regulator with feedforward used to obtain experimental results

The peaking of  $Z(s)$  reduces the gain of both  $F_{12}$  and  $F_{22}$  and thus reduces the open loop gain at the resonant frequency of the input filter.

The addition of the feedforward loop modifies the open loop transfer function as shown below --

$$G'_T(s) = \frac{E_{DC} E_M V_O R_L (1 + sCR_C)}{D a_1} + \frac{E_3 E_{AC} E_M V_O (1 + sCR_L)}{D a_1} \quad (6-4)$$

The addition of feedforward modifies the transfer functions  $F_{12}$  and  $F_{22}$  and thus it can be seen from equation (6-4) that the open loop gain with feedforward is not affected by the peaking of the input filter output impedance  $Z(s)$ .  $G'_T(s)$  is now independent of  $Z(s)$  and is a function only of the feedback loop parameters and the power stage parameters, unlike  $G_T(s)$  of equation (6-1) which is affected by the peaking of  $Z(s)$ . Equation (6-4) is also the open loop gain of the buck regulator without input filter, as can be seen from equations (6-1), (6-2) and (6-3) by setting  $Z(s) = 0$ , and it can thus be concluded that the addition of the feedforward loop should eliminate completely the peaking effect of the input filter output impedance and that the open loop gain with

feedforward should be identical with the open loop gain without the input filter [10,11].

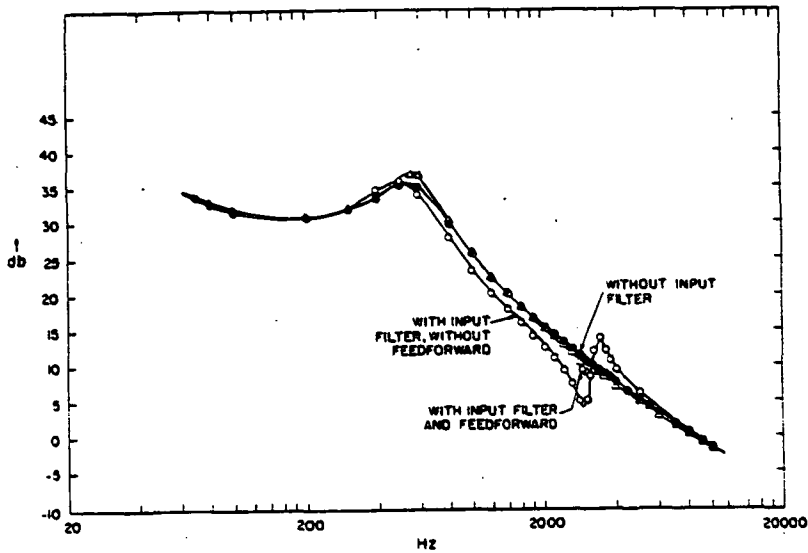
#### SINGLE STAGE INPUT FILTER

Measurements of the open loop gain and phase margin of the buck regulator of Figure 34 were made with and without feedforward, and are presented in Figure 35 (a) and (b). The input filter resonates at around 3 KHz and results in disturbances in the open loop gain and phase margin at that frequency. The feedforward eliminates all these undesirable disturbances as is evident in the figures, thus providing close agreement with theory. It can also be seen from Figure 35 that the characteristics with feedforward are almost identical to the gain and phase margin plots of the buck regulator without input filter, thus providing close agreement with the analytical prediction made earlier.

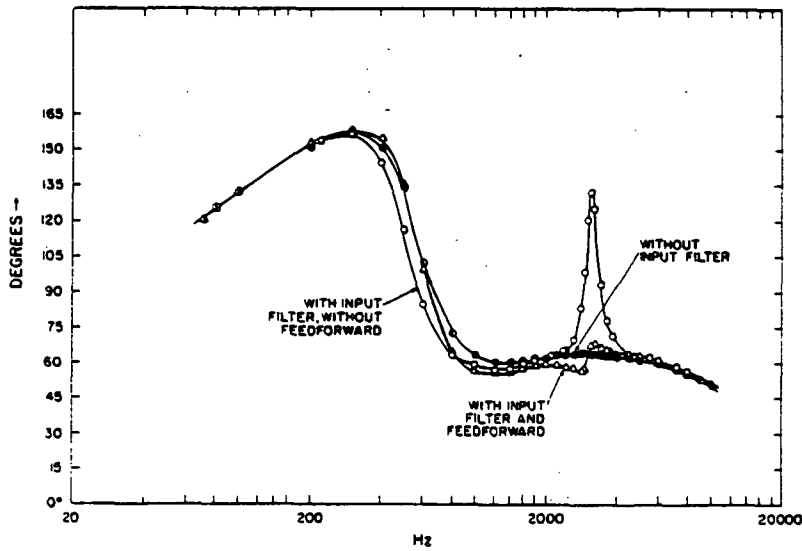
#### TWO-STAGE INPUT FILTER

The experiment was further extended to the buck regulator with a two-stage input filter. The two-stage filter of Figure 36 was used with the following parameter values:

$$\begin{array}{lll}
 R_1 = 0.2 \text{ ohm} & L_1 = 325 \text{ micro H} & C_1 = 200 \text{ micro F} \\
 R_2 = 0.02 \text{ ohm} & L_2 = 116 \text{ micro H} & C_2 = 20 \text{ micro F} \\
 R_3 = 0.075 \text{ ohm} & \text{(ESR of } C_1\text{)}. & 
 \end{array}$$



(a)



(b)

Figure 35: Open loop transfer function measurements with single-stage input filter. (a) gain (b) phase margin.

The feedforward circuit used was the same nonadaptive feedforward circuit used to obtain the measurements of Figure 35 with the feedforward input being the voltage at capacitor  $C_2$ .

The other parameters of the circuit are the same as used to obtain Figure 35. Measurements of the open loop gain and phase margin were made with and without feedforward and the results are shown in Figure 37 (a) and (b). The open loop gain and phase are affected at the resonant frequencies of the two stages of the input filter because the output impedance of the input filter  $Z(s)$  peaks at both resonant frequencies. The use of the feedforward circuit eliminates the detrimental effects of the input filter, as is evident from Figure 37.

#### REMARKS

The following points regarding the above measurements are noteworthy:

- (1) Measurements of the open loop gain and phase margin show that the input filter output impedance causes disturbances in the gain and phase margin at the filter resonant frequencies and the addition of feedforward eliminates these disturbances, providing close agreement with theory.
- (2) The feedforward compensation circuit is independent of the input filter parameter values.

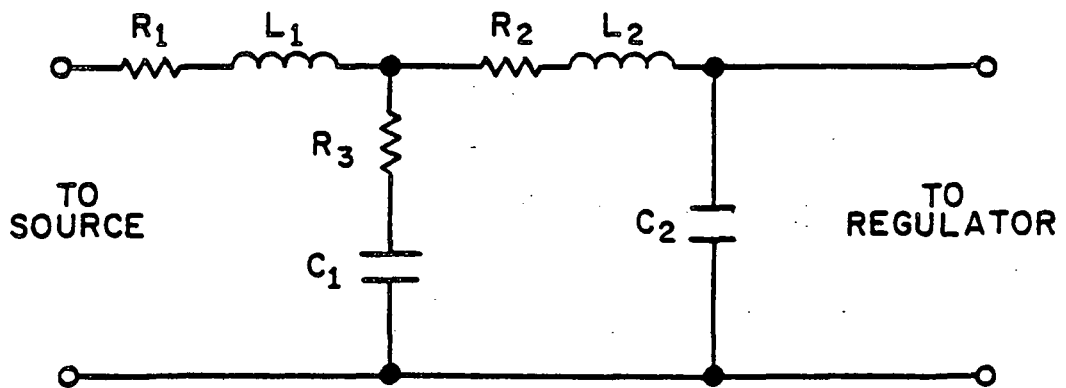
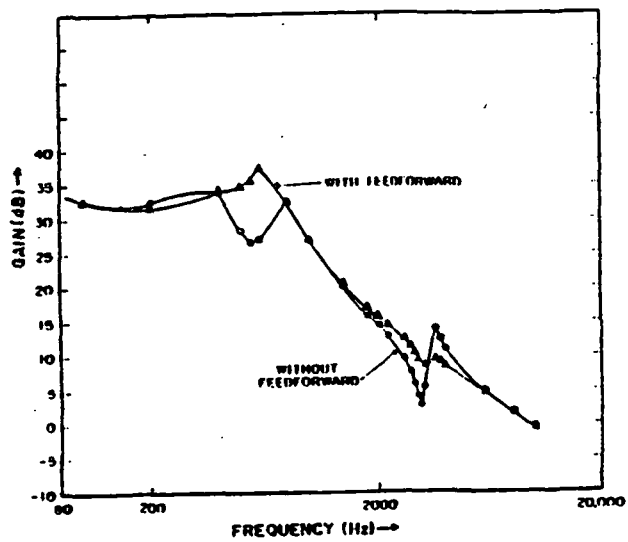
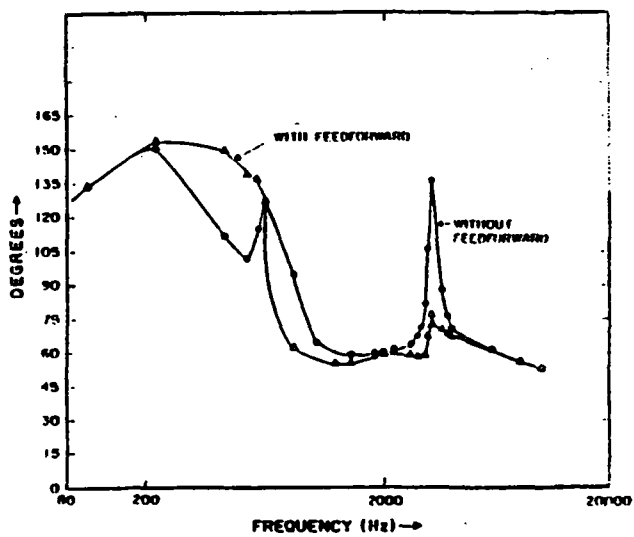


Figure 36: Two-stage input filter.



(a)



(b)

Figure 37: Open loop transfer function measurements with two-stage input filter. (a) gain (b) phase margin.

(3) The feedforward compensation scheme is independent of the input filter configuration. It was demonstrated above that the same feedforward compensation network is equally applicable to a single stage input filter and a two-stage input filter. These observations lead to a stronger conclusion that the feedforward can provide effective compensation for an unknown source impedance. For example, a preregulator which often has an unknown, dynamic output impedance can interact with a DC-DC converter downstream and result in system instability. The feedforward compensation scheme outlined can be used to isolate the switching converter from the source thus preventing interaction between the switching converter and equipment upstream.

## 6.2 ADAPTIVE FEEDFORWARD MEASUREMENTS.

The buck regulator with feedforward used to obtain experimental results is shown in Figure 34 and the parameters of the circuit are as specified in section 6.1. The adaptive feedforward circuit for variable input voltage presented in Chapter 5 was used in obtaining measurements. The two-stage input filter of Figure 36 was used with the same parameter values as in section 6.1 with the feedforward input being the voltage at capacitor  $C_2$ . The value of  $R_3$  was changed to-

$$R_3 = 0.2 \text{ ohm (ESR of } C_2 \text{ plus external damping resistance)}$$

Measurements were obtained at four values of supply voltage using the same adaptive feedforward circuit in all cases - this was done to confirm the adaptive nature of the feedforward circuit.

A computer program was written to calculate the gain and phase margin of the open loop transfer function with and without two-stage input filter, at various input voltages. Equation (6-1) was used to calculate the gain and phase margin; setting  $Z(s) = 0$  in the equation gives the gain and phase margin without input filter. The following expression for the two-stage input filter was used:

$$Z(s) = \frac{Z_1 + R_2 + sL_2}{1 + sC_2(Z_1 + R_2) + s^2L_2C_2} \quad (6-5)$$

where

$$Z_1(s) = (R_1 + sL_1) // (R_3 + 1/sC_1) \quad (6-6)$$

Figures 38 - 41 show the computed values of open loop gain and phase margin with and without the two-stage input filter for input voltages  $V_I = 25v, 30v, 35v$  and  $40v$ . It can be seen that the two-stage input filter resonates at two frequencies and at each frequency the output impedance  $Z(s)$  peaks, thus causing sharp fluctuations in the open loop gain and phase margin. Measurements of the open loop gain and

phase margin at each of the above values of supply voltage were obtained with and without feedforward and are also plotted on the figures. It can be seen clearly that the addition of feedforward removes the sharp fluctuations in open loop gain and phase margin caused by the input filter, providing close agreement with theoretical prediction made earlier. The analytical prediction that the open loop gain and phase margin with feedforward are identical to the characteristics without input filter is also confirmed, as examination Figures 38 - 41 show.

The two stage input filter was modified so that  $R_3 = 0.075$  ohm (ESR of  $C_2$ ) and measurements of the open loop gain and phase margin with and without feedforward were made. Figure 42 shows the calculated values of open loop gain and phase margin together with the measured values at  $V_I = 25$ v. With the external damping resistance set to zero the effect of the input filter is seen to be more pronounced. Measurements without feedforward shown plotted on the figure also show the pronounced effect of the input filter. The addition of feedforward effectively eliminates the sharp fluctuations in gain and phase margin caused by the undamped input filter.

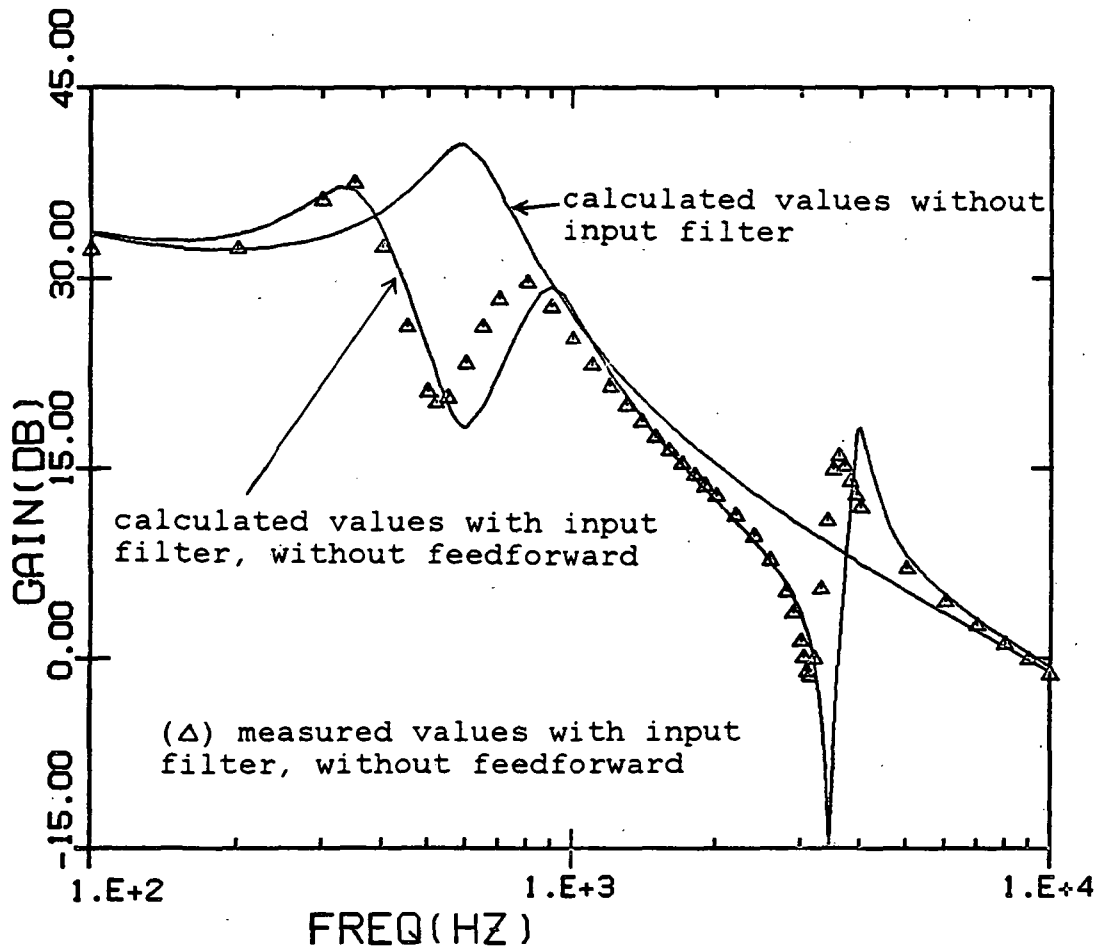


Figure 38: (a) Open loop gain at  $V_I=25v$ : Calculated values and measured values ( $\Delta$ ) without feedforward

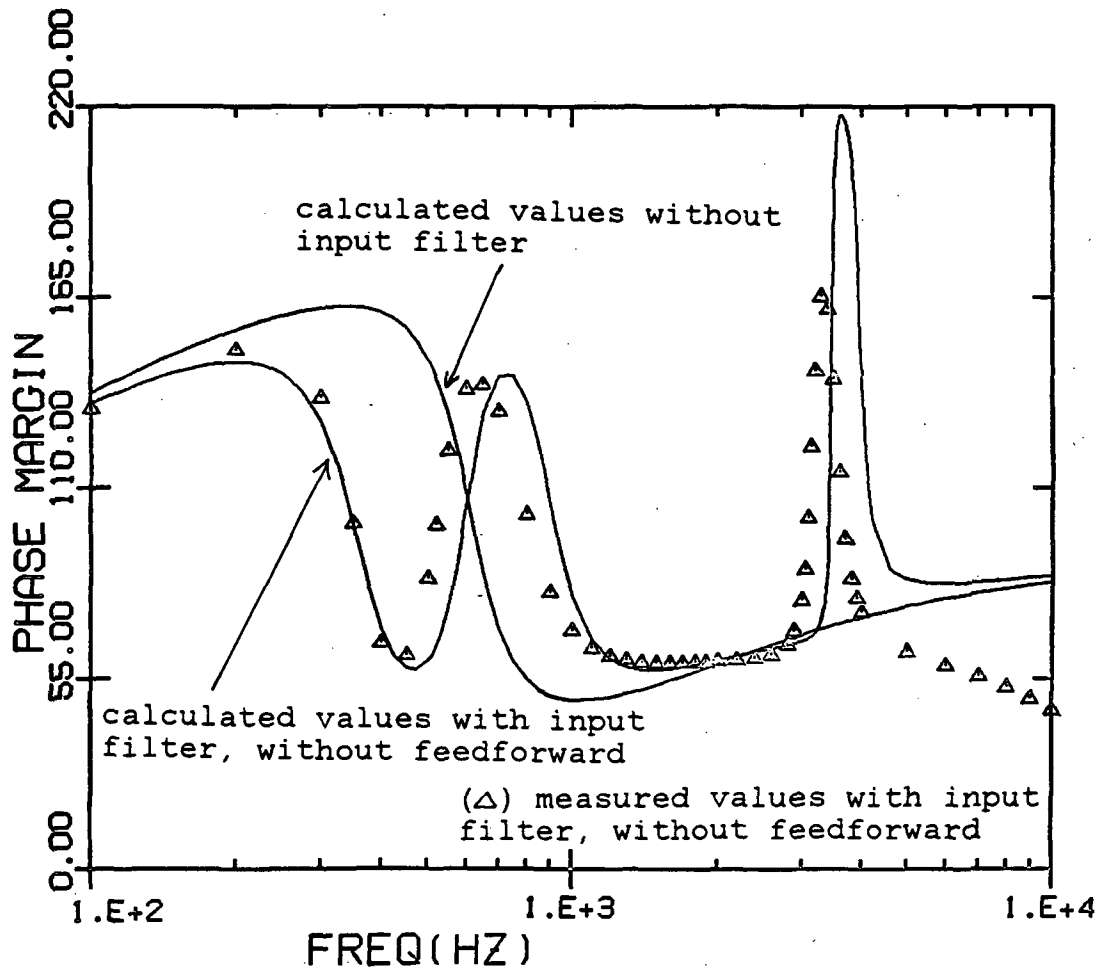


Figure 38: (b) Open loop phase margin at  $V_I=25v$ : Calculated values and measured values ( $\Delta$ ) without feedforward

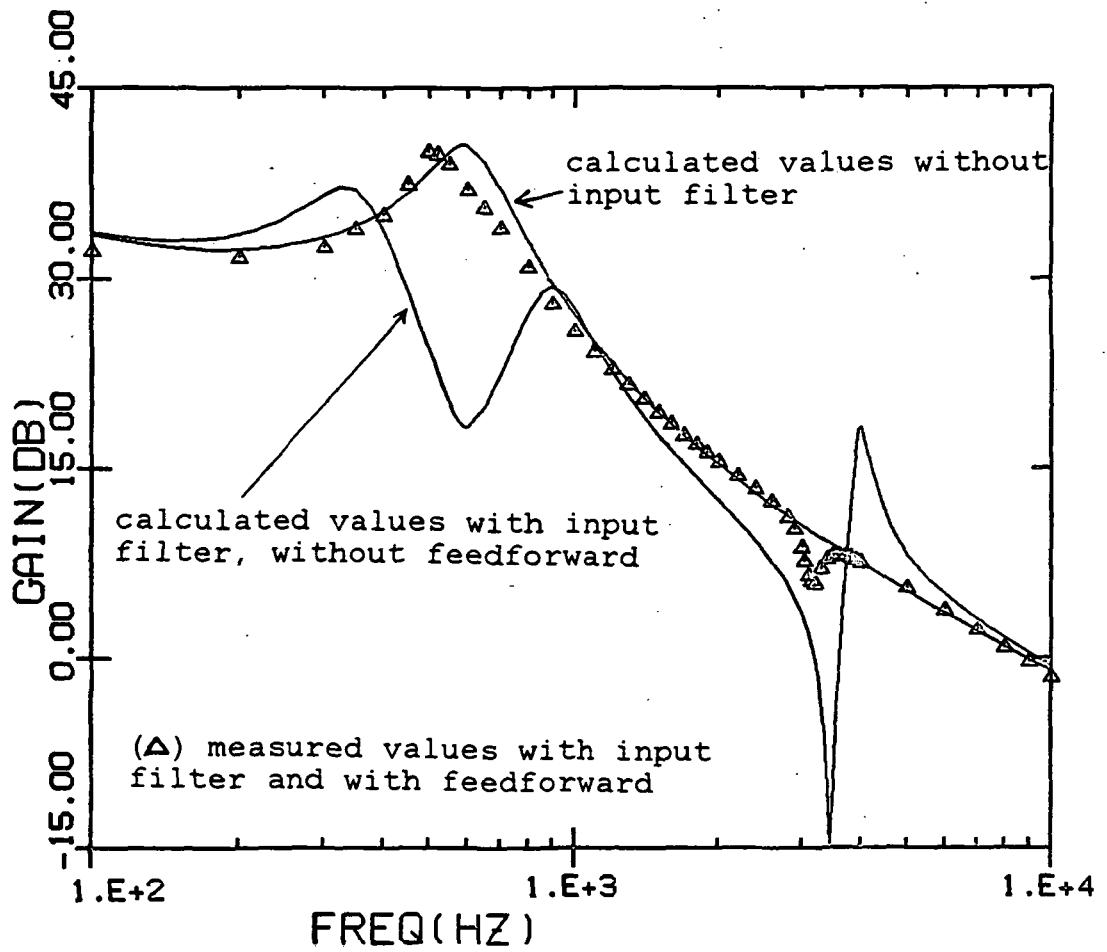


Figure 38: (c) Open loop gain at  $V_I=25v$ : Calculated values and measured values ( $\Delta$ ) with feedforward

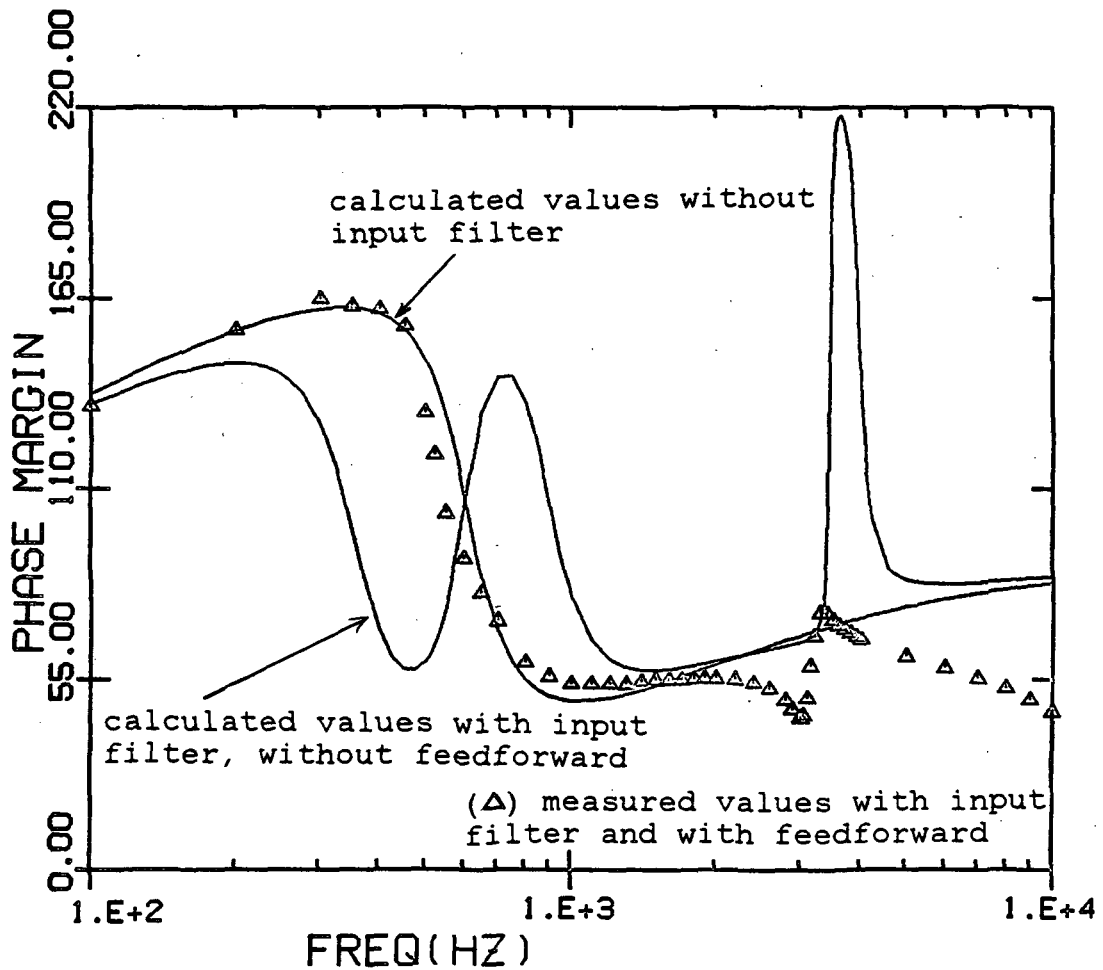


Figure 38: (d) Open loop phase margin at  $V_I=25v$ : Calculated values and measured values( $\Delta$ ) with feedforward

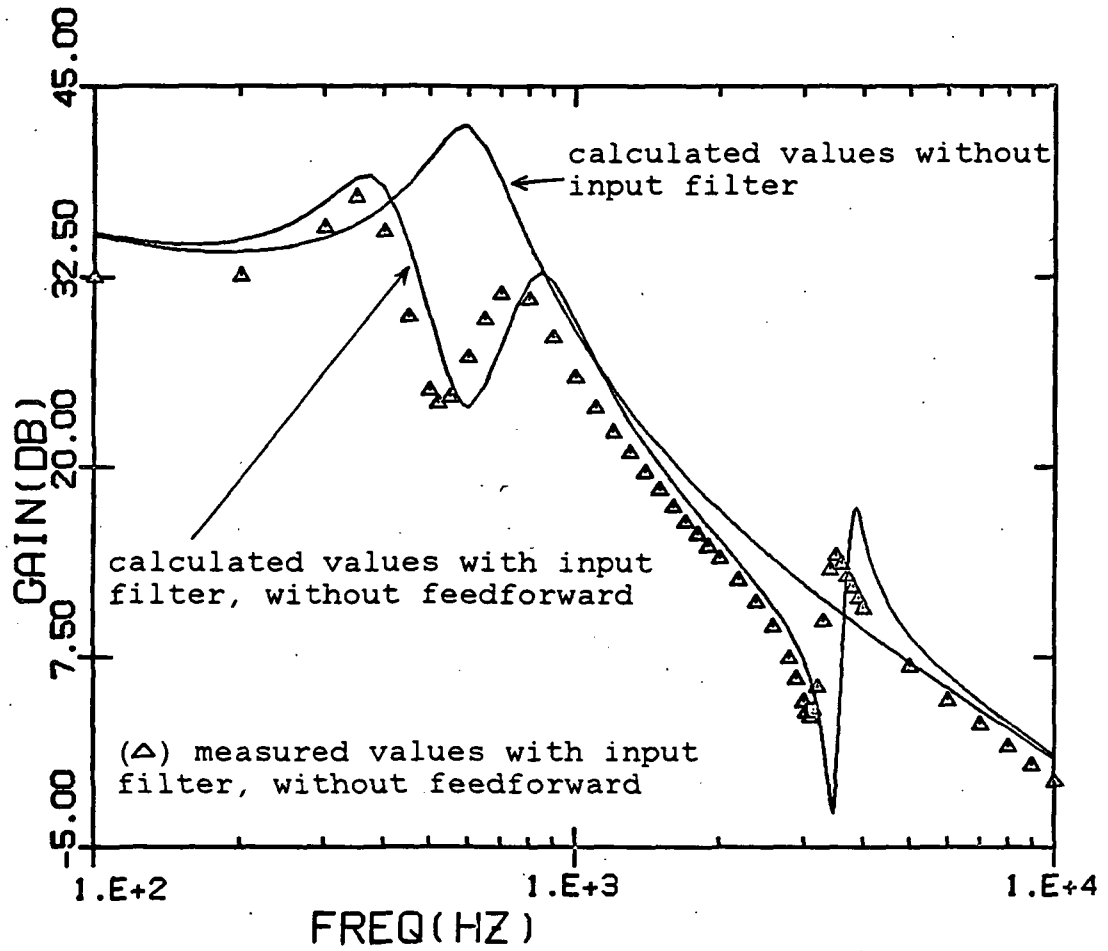


Figure 39: (a) Open loop gain at  $V_I=30v$ : Calculated values and measured values ( $\Delta$ ) without feedforward

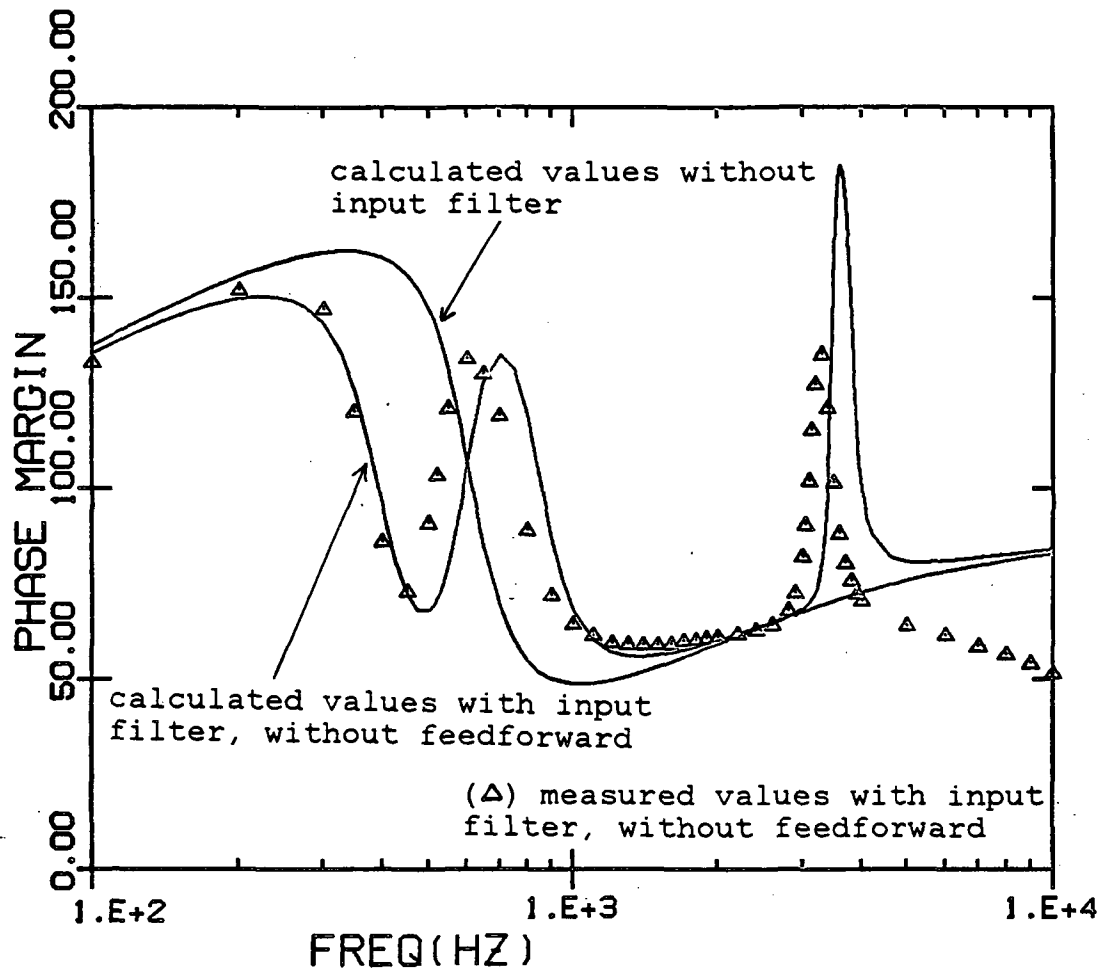


Figure 39: (b) Open loop phase margin at  $V_I=30v$ : Calculated values and measured values ( $\Delta$ ) without feedforward

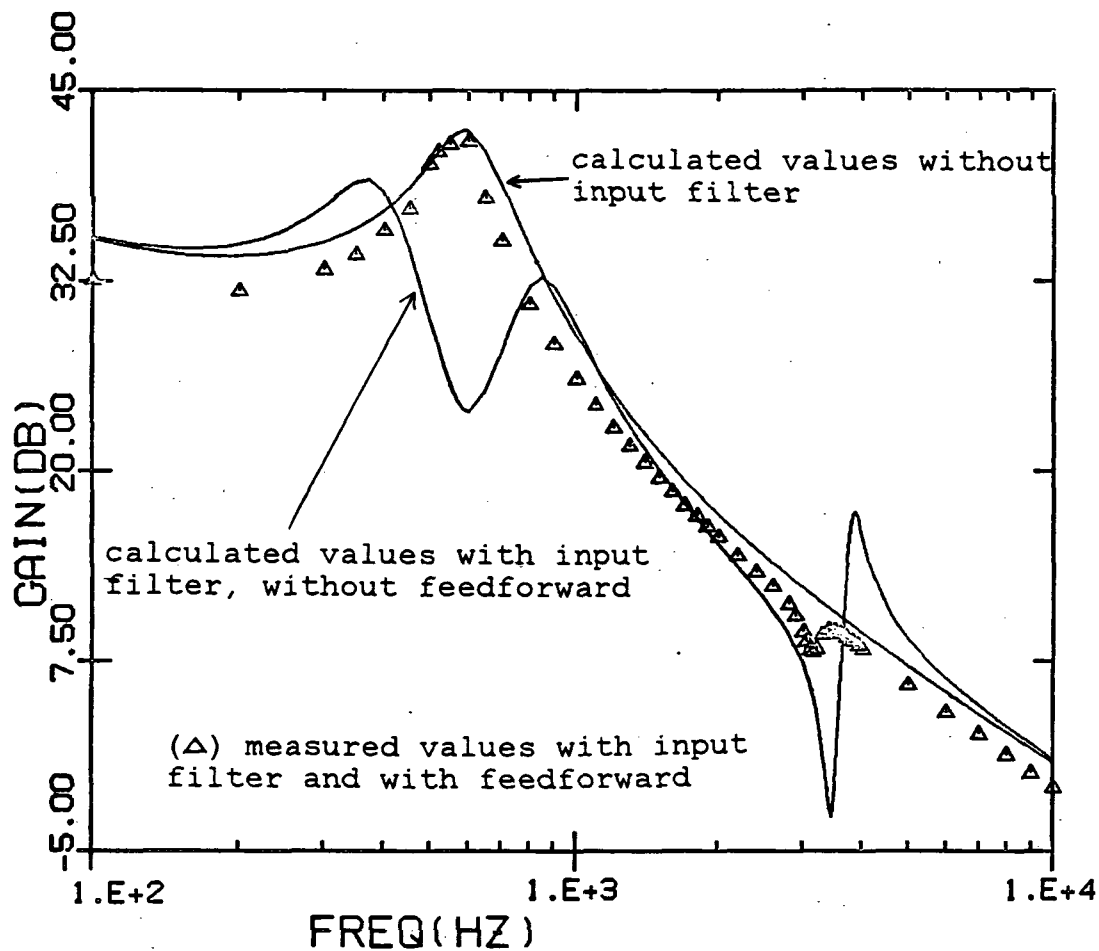


Figure 39: (c) Open loop gain at  $V_I=30v$ : Calculated values and measured values ( $\Delta$ ) with feedforward

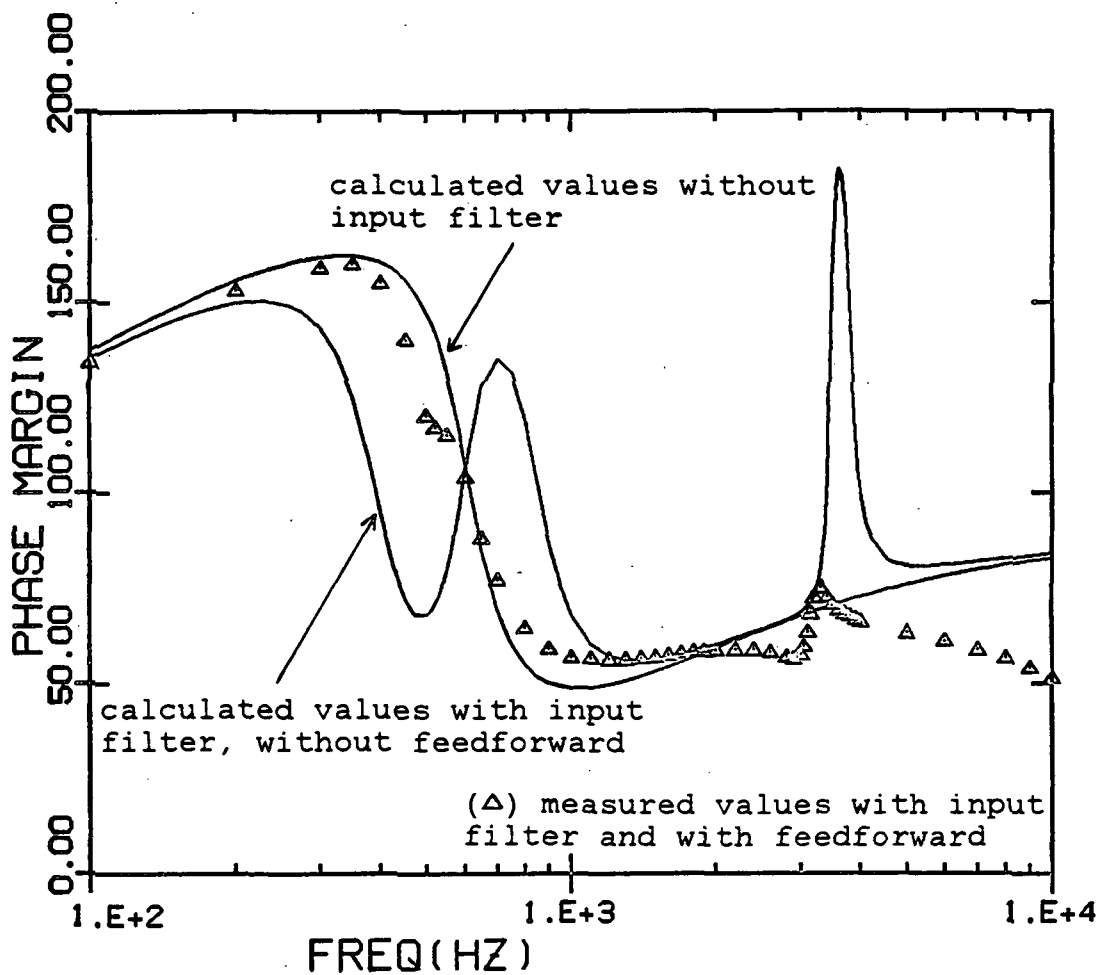


Figure 39: (d) Open loop phase margin at  $V_I=30\text{v}$ : Calculated values and measured values ( $\Delta$ ) with feedforward

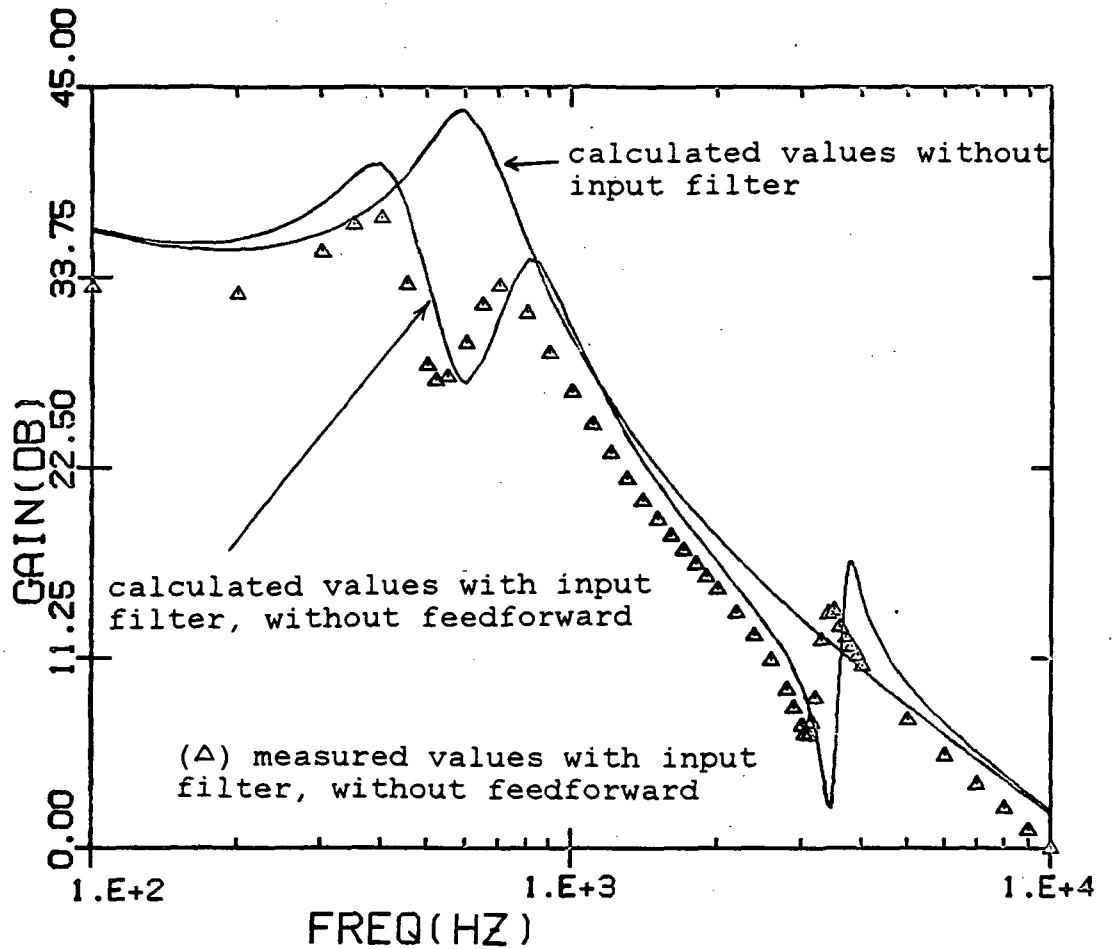


Figure 40: (a) Open loop gain at  $V_I=35v$ : Calculated values and measured values ( $\Delta$ ) without feedforward

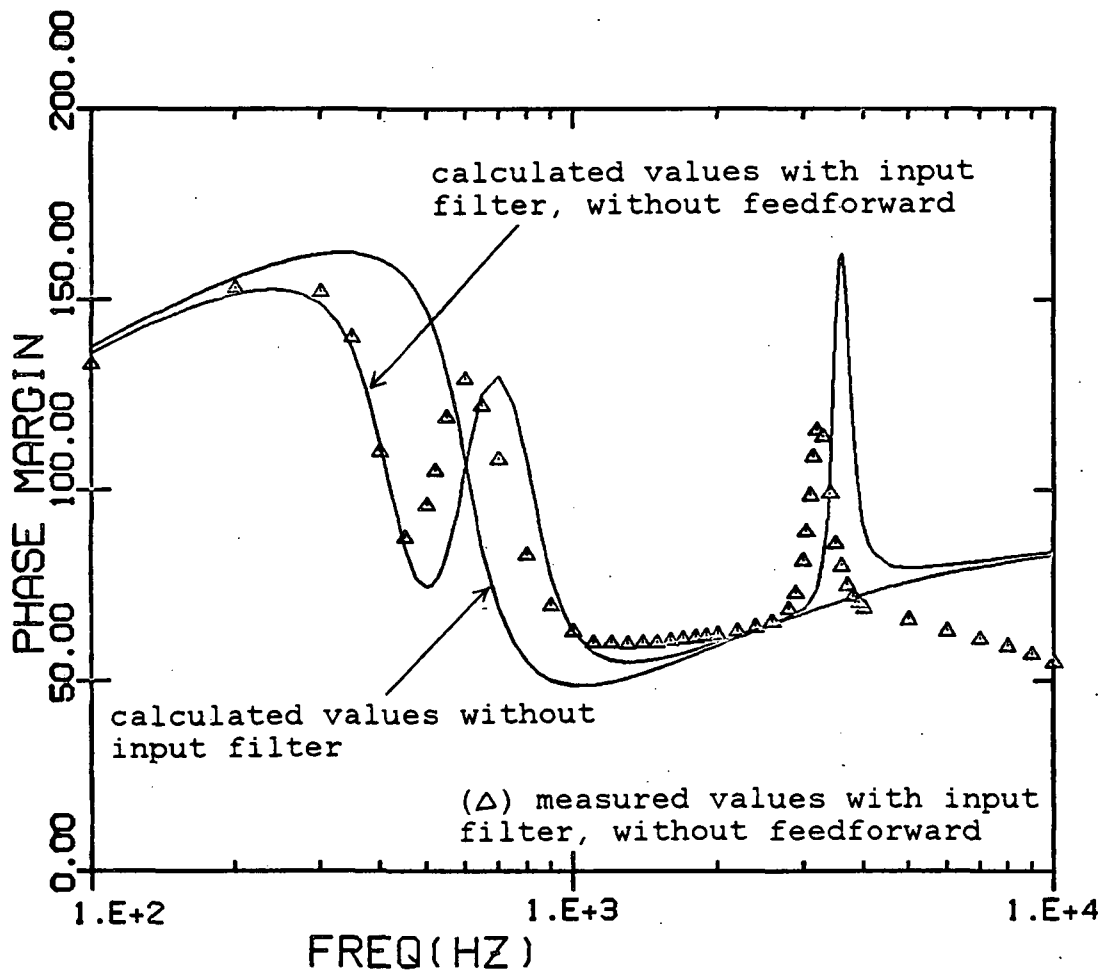


Figure 40: (b) Open loop phase margin at  $V_I=35v$ : Calculated values and measured values ( $\Delta$ ) without feedforward

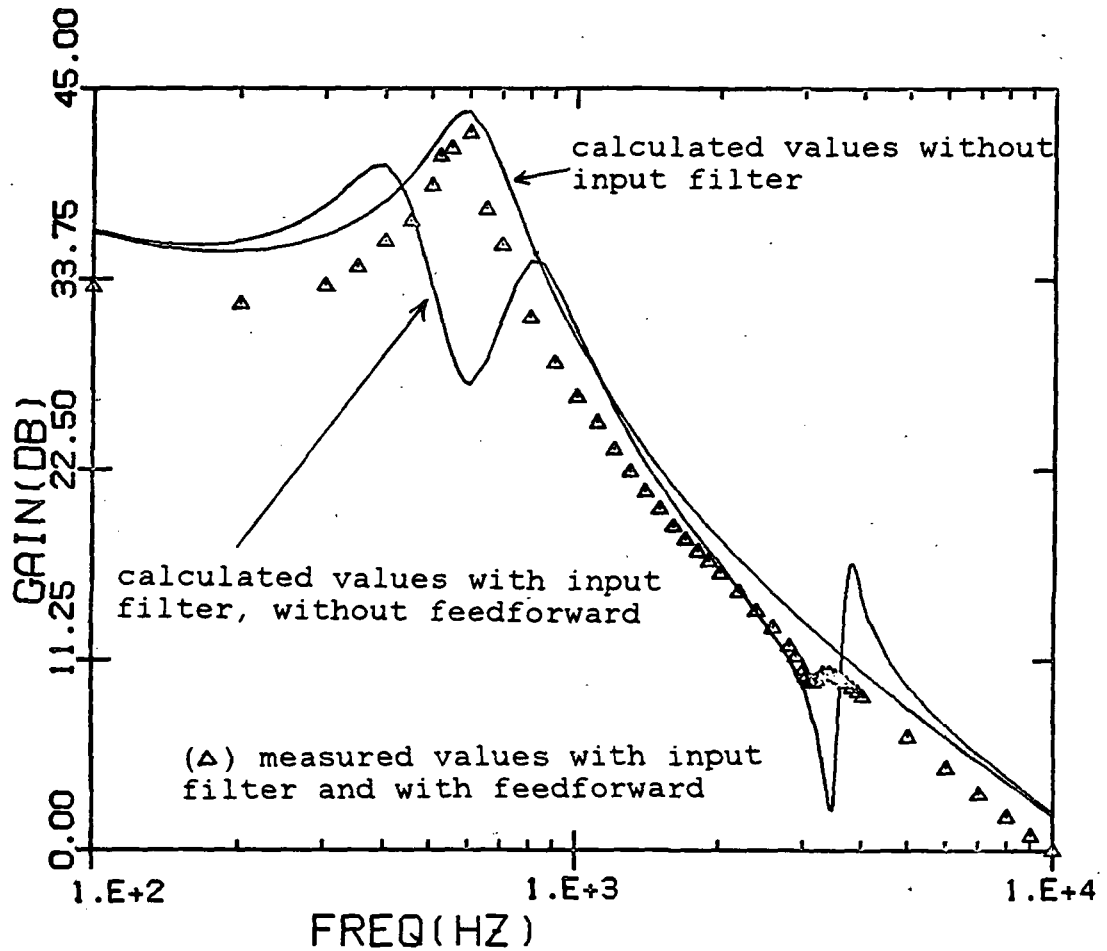


Figure 40: (c) Open loop gain at  $V_I = 35\text{v}$ : Calculated values and measured values ( $\Delta$ ) with feedforward

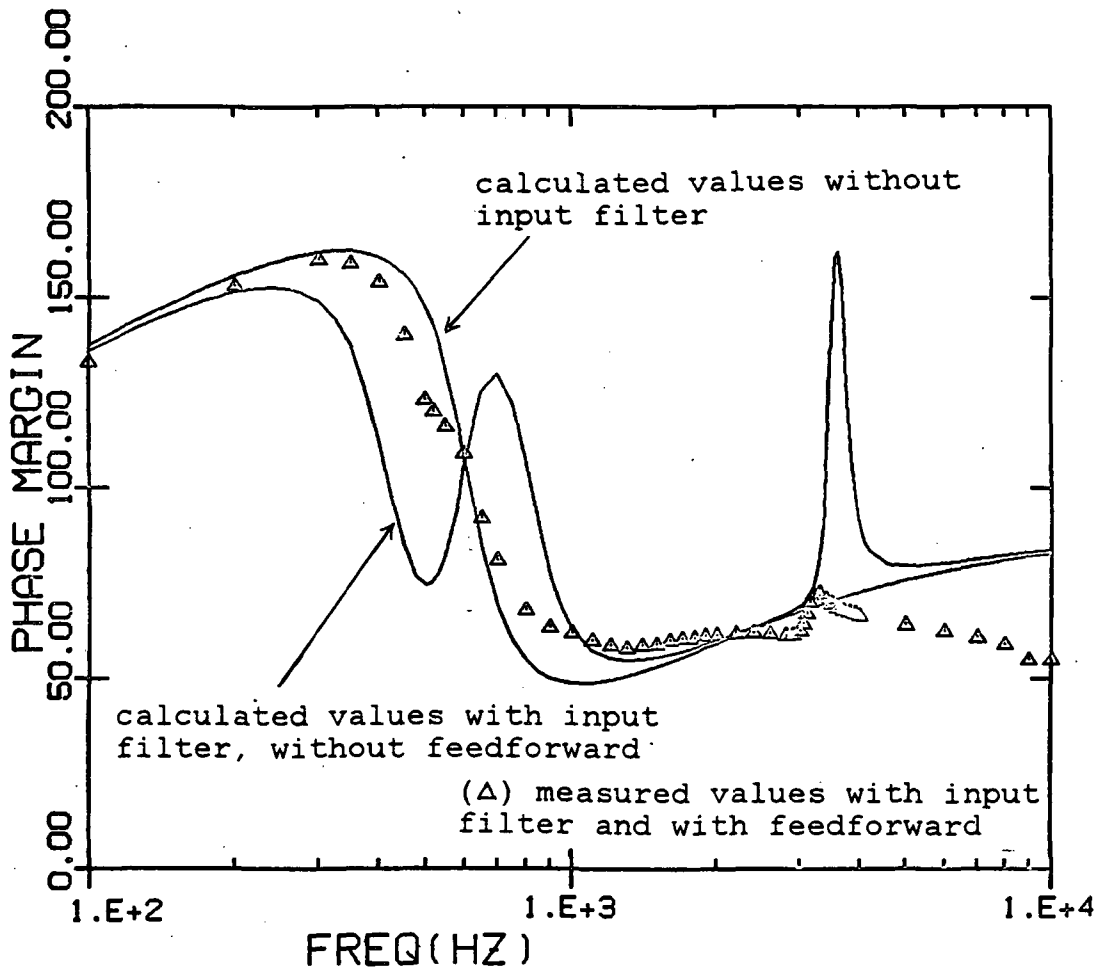


Figure 40: (d) Open loop phase margin at  $V_I=35v$ : Calculated values and measured values ( $\Delta$ ) with feedforward

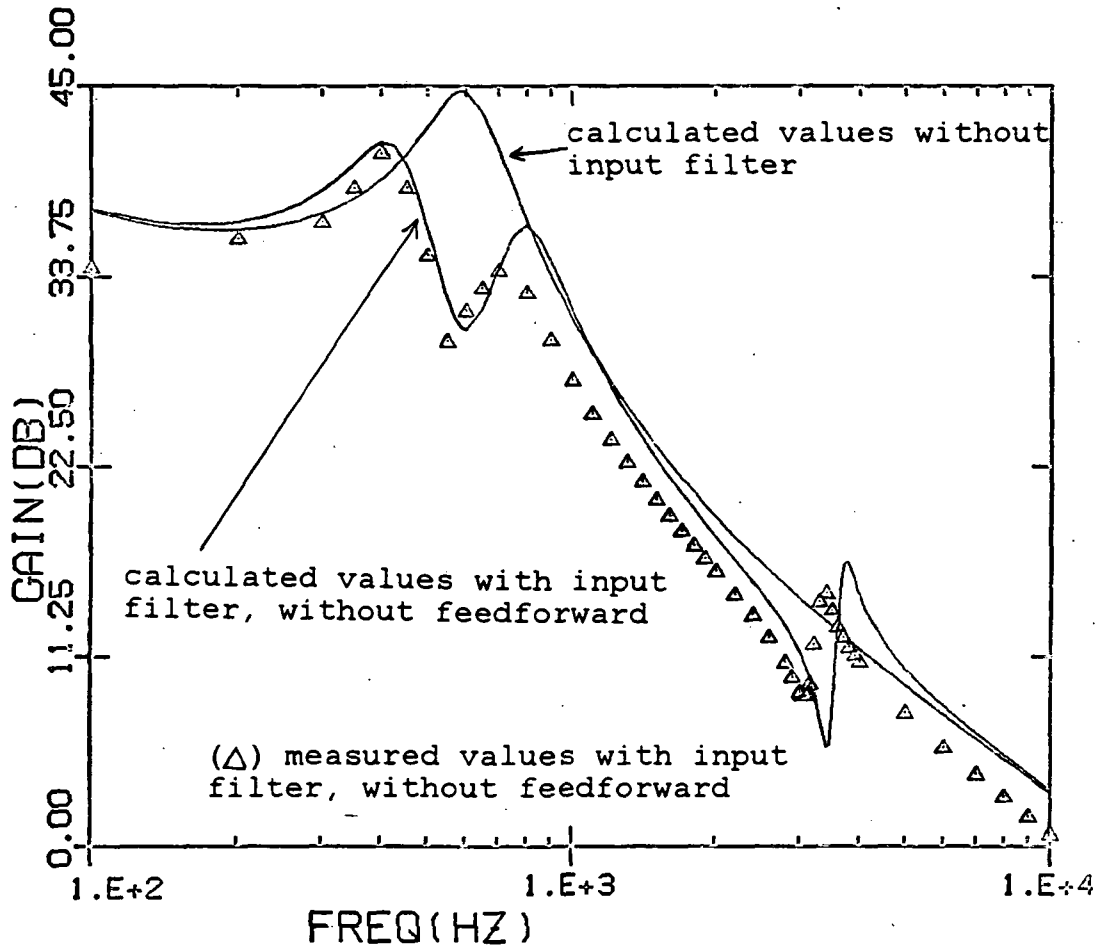


Figure 41: (a) Open loop gain at  $V_I=40v$ : Calculated values and measured values ( $\Delta$ ) without feedforward

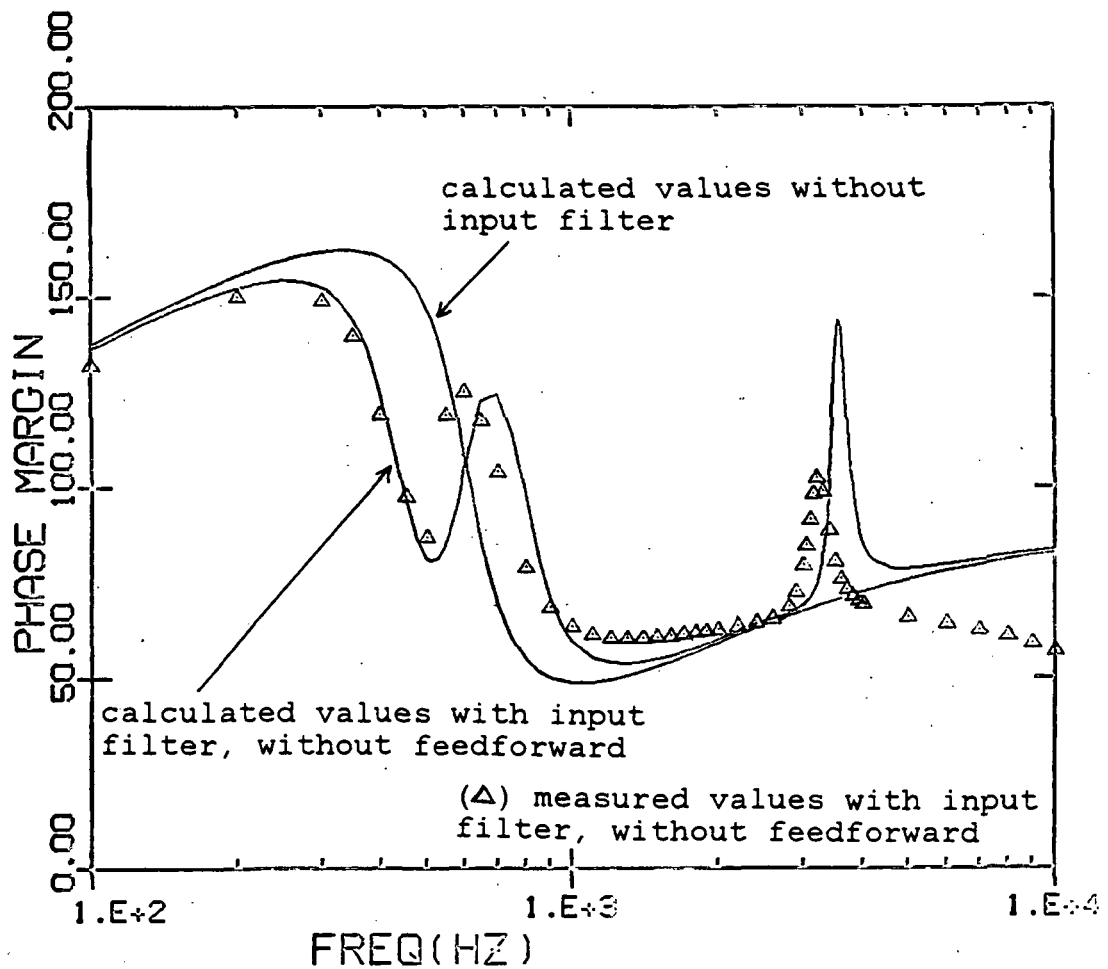


Figure 41: (b) Open loop phase margin at  $V_I=40v$ : Calculated values and measured values ( $\Delta$ ) without feedforward

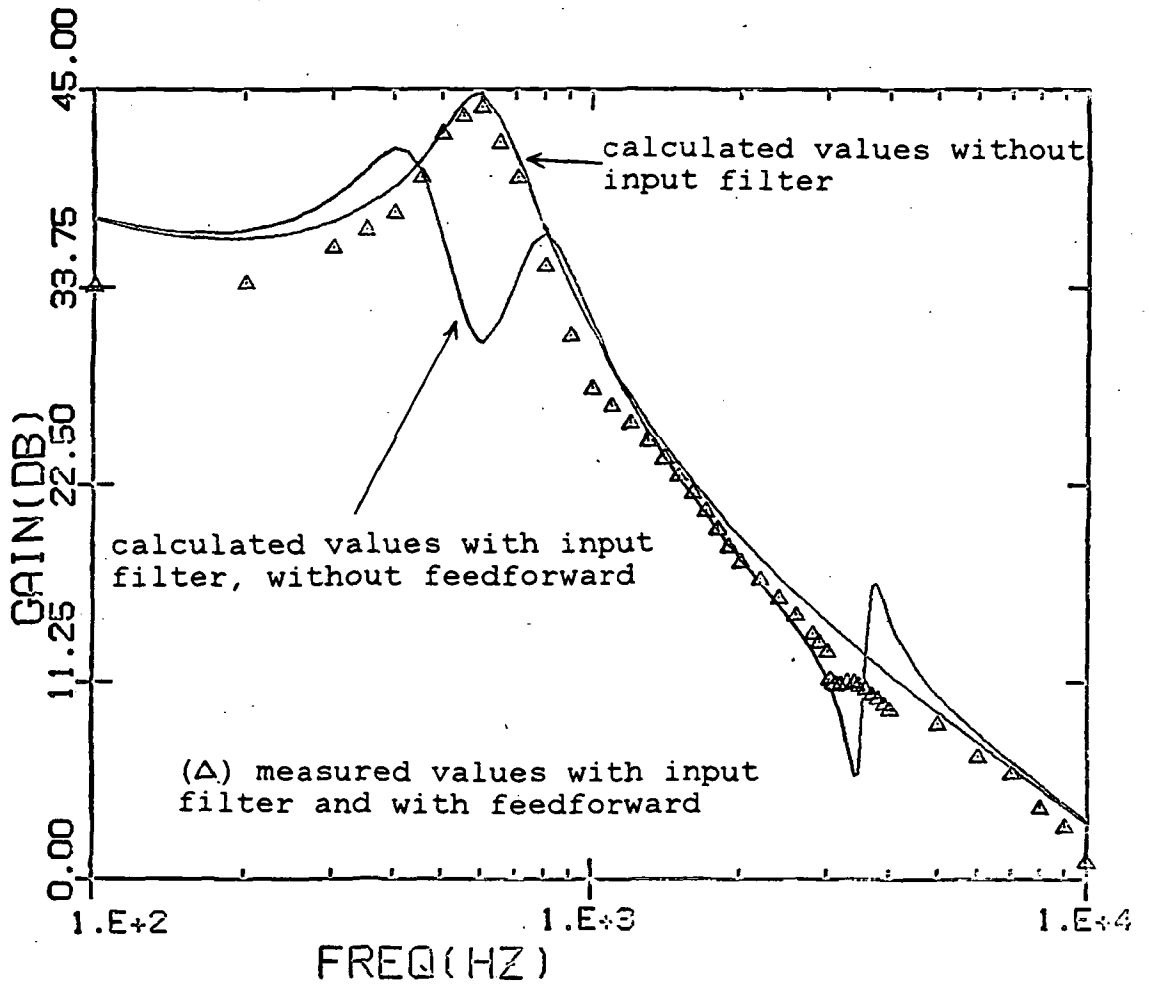


Figure 41: (c) Open loop gain at  $V_I = 40v$ : Calculated values and measured values ( $\Delta$ ) with feedforward

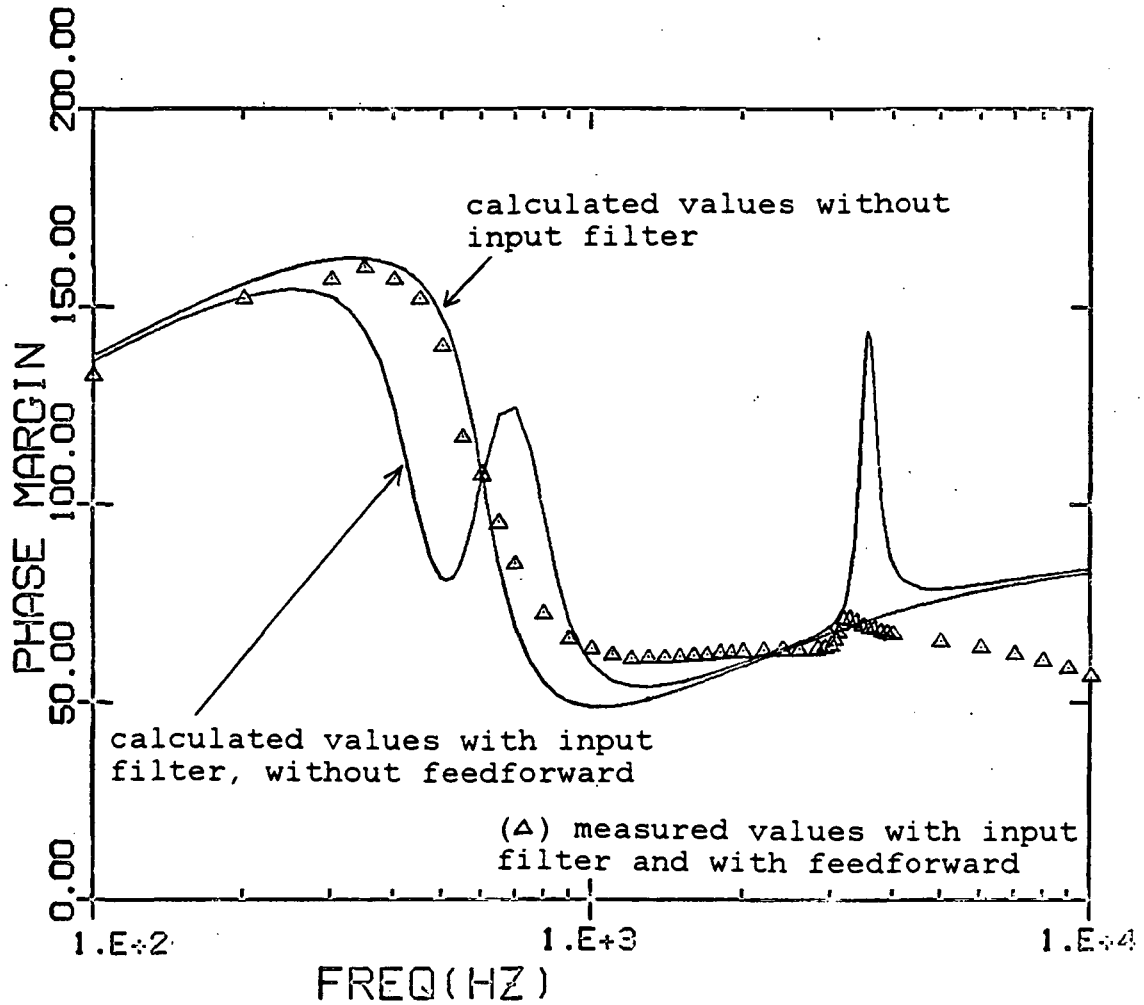


Figure 41: (d) Open loop phase margin at  $V_I=40v$ : Calculated values and measured values ( $\Delta$ ) with feedforward

The following observations regarding the measurements are made:

(1) The peaking of the output impedance of the first stage is more pronounced and has a greater effect on the regulator than the peaking of the second stage.

(2) Both analysis and measurement results indicate that the open loop gain is higher at lower values of duty cycle  $D$ . This is further manifested by examining equation (6-4). It shows that a lower value of  $D$  results in a higher gain.

(3) The effect of input filter peaking varies with the input voltage. This is explained by noting that both  $F_{12}$  and  $F_{22}$ , equations (6-2) and (6-3) depend on the duty cycle  $D$ . The effect of peaking of  $Z(s)$  is to cause a reduction in the term  $(R_L - D^2 Z)$  and the amount of reduction would be greater if  $D$  is larger. Consequently it is expected that at small values of  $V_I$ , when  $D$  is larger, the effect of peaking would be more pronounced. This is confirmed by examination of Figures 38 - 41 .

(4) The addition of the feedforward loop effectively eliminates the perturbation in open loop gain and phase caused by the input filter. The feedforward works effectively at all four values of supply voltage  $V_I$ . Since the same feedforward circuit was used in making all the measurements of Figures 38 - 42 the adaptive nature of the feedforward circuit is confirmed.

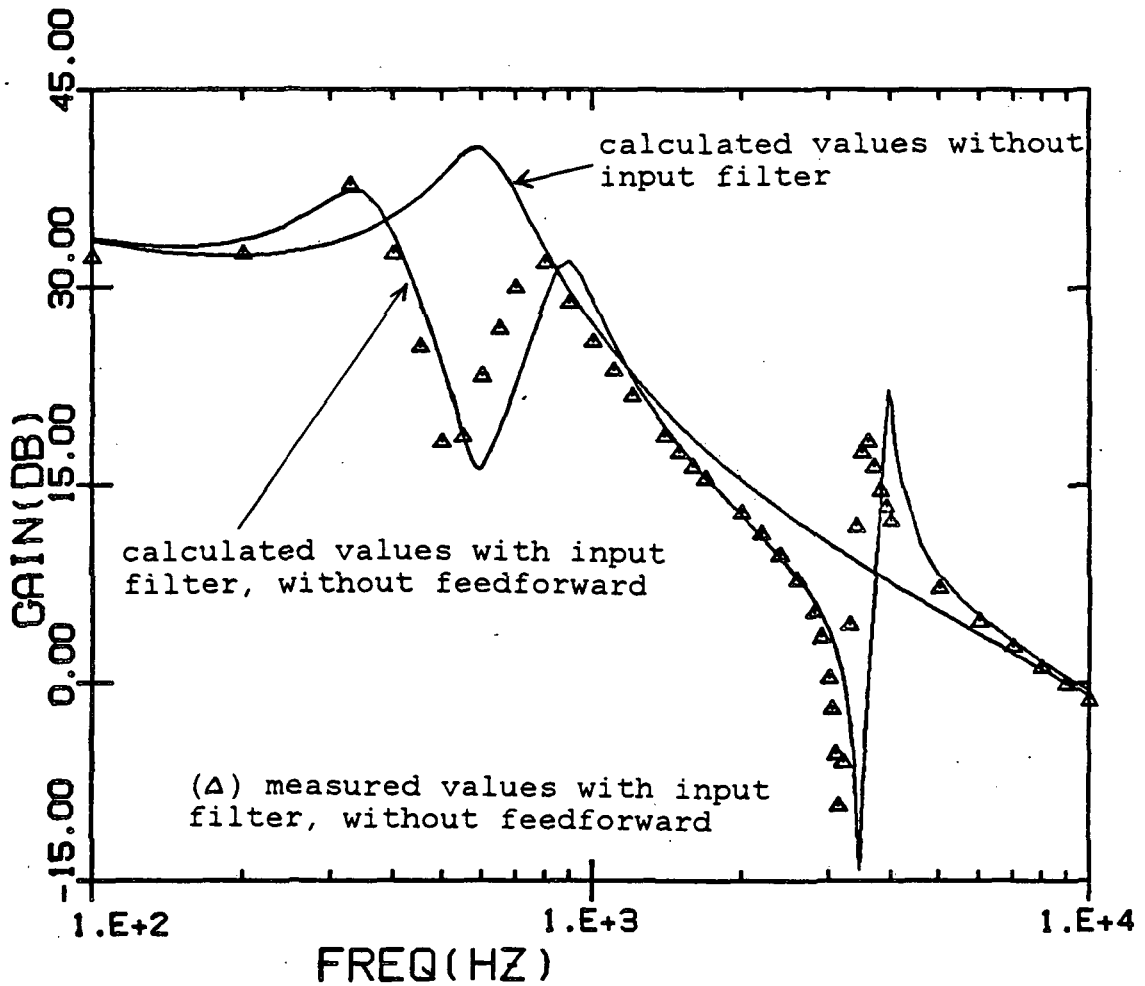


Figure 42: (a) Open loop gain at  $V_I=25v$ : Calculated values and measured values ( $\Delta$ ) without feedforward

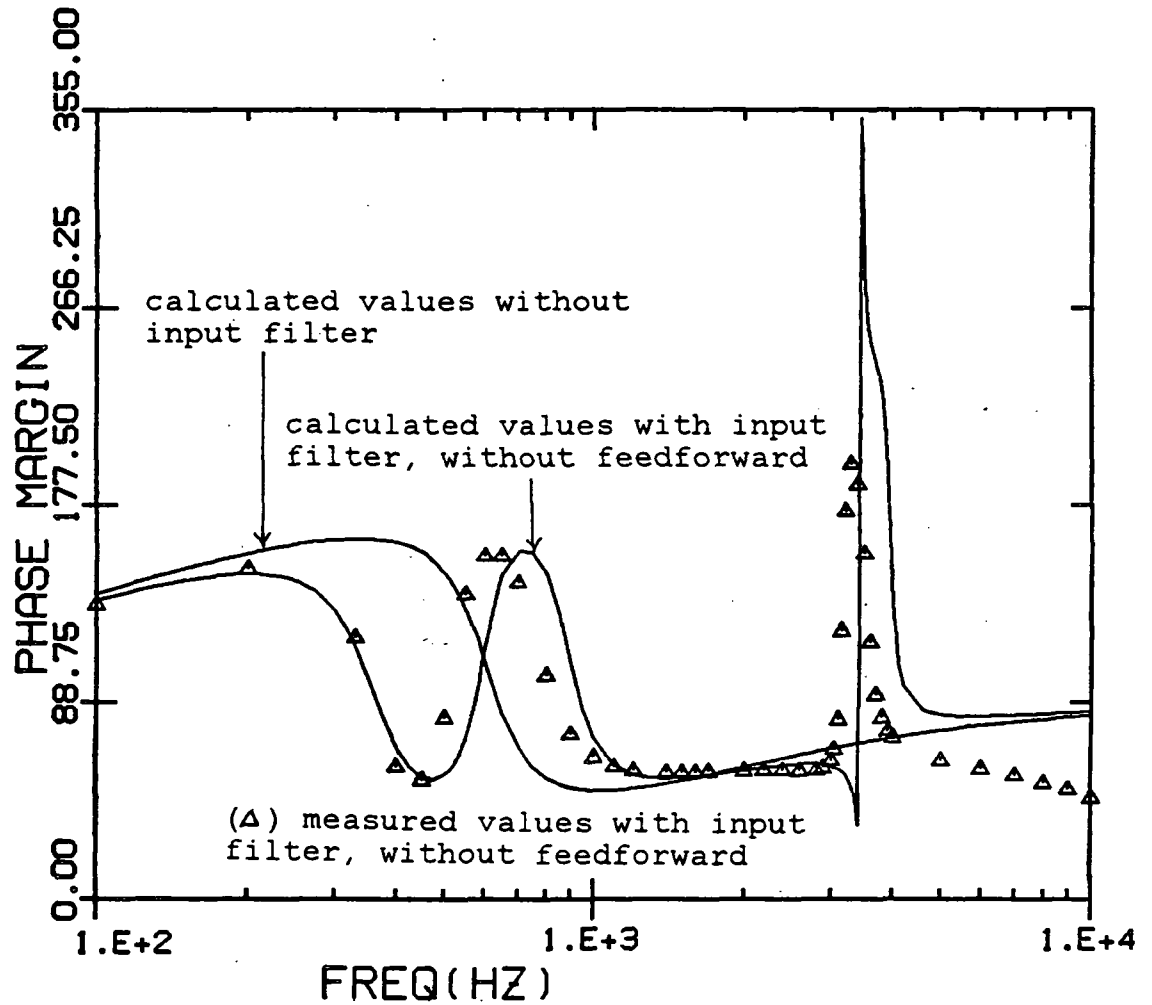


Figure 42: (b) Open loop phase margin at  $V_I=25v$ : Calculated values and measured values ( $\Delta$ ) without feedforward

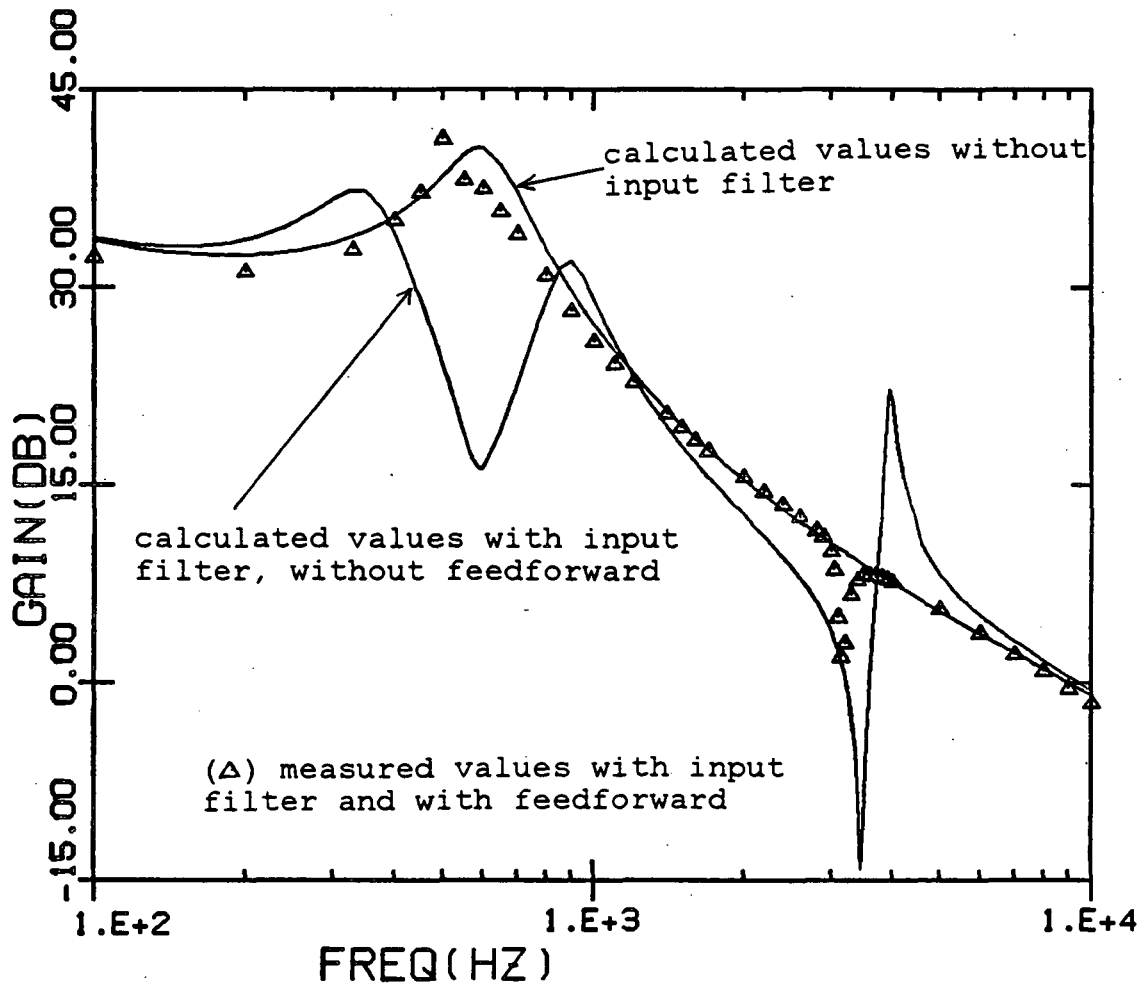


Figure 42: (c) Open loop gain at  $V_I = 25\text{v}$ : Calculated values and measured values ( $\Delta$ ) with feedforward

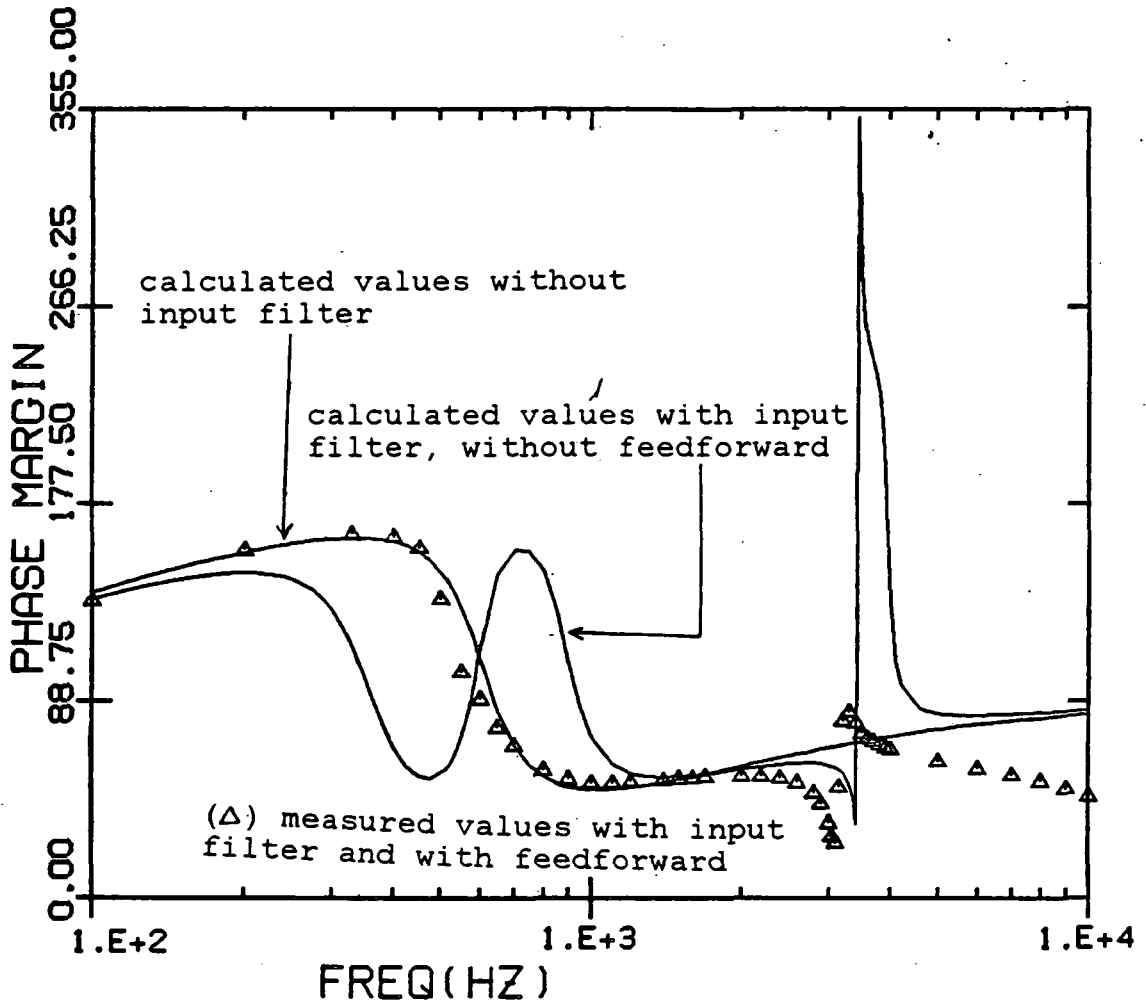


Figure 42: (d) Open loop phase margin at  $V_I = 25\text{v}$ : Calculated values and measured values ( $\Delta$ ) with feedforward

(5) From the results presented in section 6.1 and from measurements presented in this section it is logical to conclude that the adaptive feedforward circuit can provide effective compensation for an arbitrary, unknown source impedance for a variable supply voltage. The adaptive feedforward circuit has been shown to be able to track the supply voltage and adjust the gain in accordance with supply voltage changes. The adaptive feedforward circuit can effectively isolate the switching regulator from its source impedance, thus preventing any interaction between the switching converter and equipment upstream.

### 6.3 MEASUREMENTS OF CLOSED LOOP INPUT-TO-OUTPUT TRANSFER FUNCTION (AUDIOSUSCEPTIBILITY).

The closed loop input-to-output transfer function (audiosusceptibility) of a switching regulator is an important characteristic. It refers to the regulator's ability in attenuating small signal sinusoidal disturbances propagating from the regulator input to its output. The gain of the closed loop input-to-output transfer function should be as small as possible; thus the regulator will effectively attenuate noise at the input so as not to affect operation of the regulator payloads. Unfortunately, as pointed out in Chapter 2, the peaking of the output impedance of the input filter

and the peaking of the forward transfer function of the input filter increase the audiosusceptibility. Measurements of audiosusceptibility with and without feedforward were made using the two-stage input filter of Figure 36 with a damping resistor so that  $R_3 = 0.2$  ohm. Measurements were made by injecting a small sinusoidal signal at the input to the converter and then using a HP network analyser to measure the audiosusceptibility [8]. The feedforward circuit used was the adaptive feedforward circuit of Figure 33 and the buck regulator used is shown in Figure 34, with its parameters as specified in section 6.1.

Figures 43 - 46 show the measured values of audiosusceptibility with and without feedforward at four values of supply voltage  $V_I = 25v, 30v, 35v$  and  $40v$  using the same feedforward circuit in all cases. The top trace in each figure is the plot without feedforward and it can be seen clearly that the audiosusceptibility is degraded

at the two resonant frequencies where the output impedance  $Z(s)$  and the transfer function  $H(s)$  of the input filter peak, with the first stage resonating around 600 Hz and the second stage around 3 KHz. It is also evident from the figures that the audiosusceptibility is dependent on duty cycle  $D$  or the supply voltage. At higher values of supply voltage when the duty cycle is low the audiosusceptibility is lower, specially at the lower frequencies.

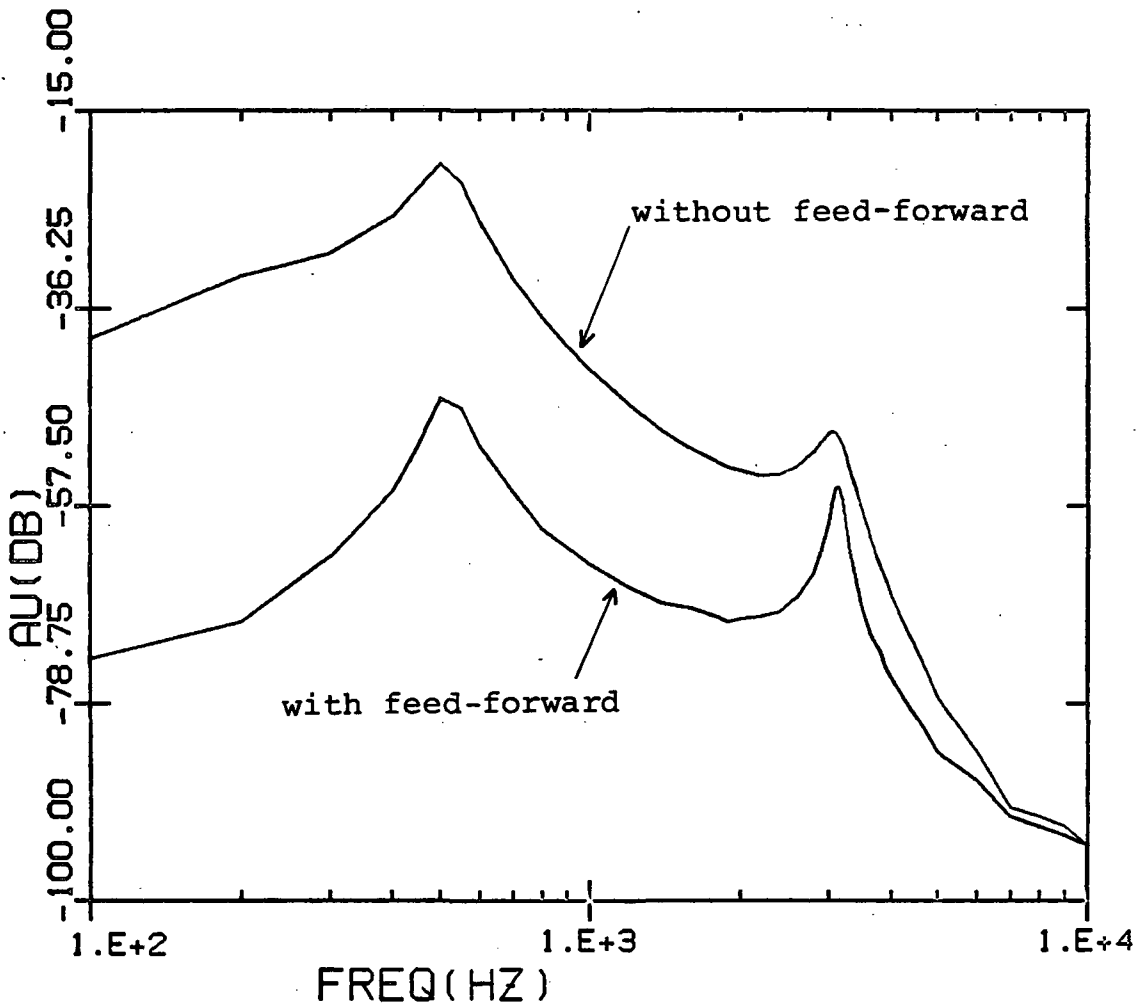


Figure 43: Measurement of audiosusceptibility  $[\hat{v}_o(s)/\hat{v}_x(s)]$  with and without feedforward at  $V_I=25v$

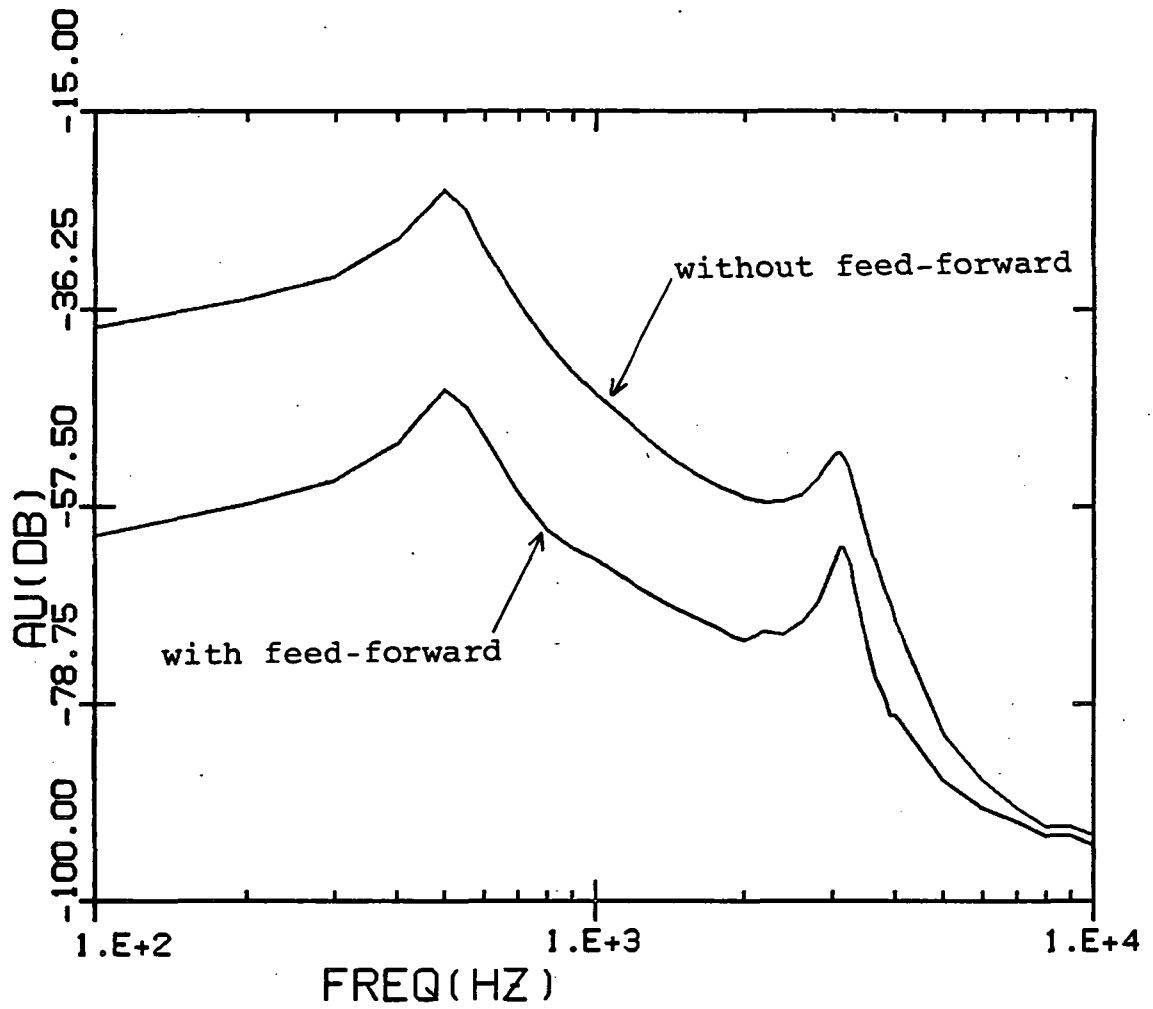


Figure 44: Audiosusceptibility with and without feedforward at  $V_I=30v$  (measurements)

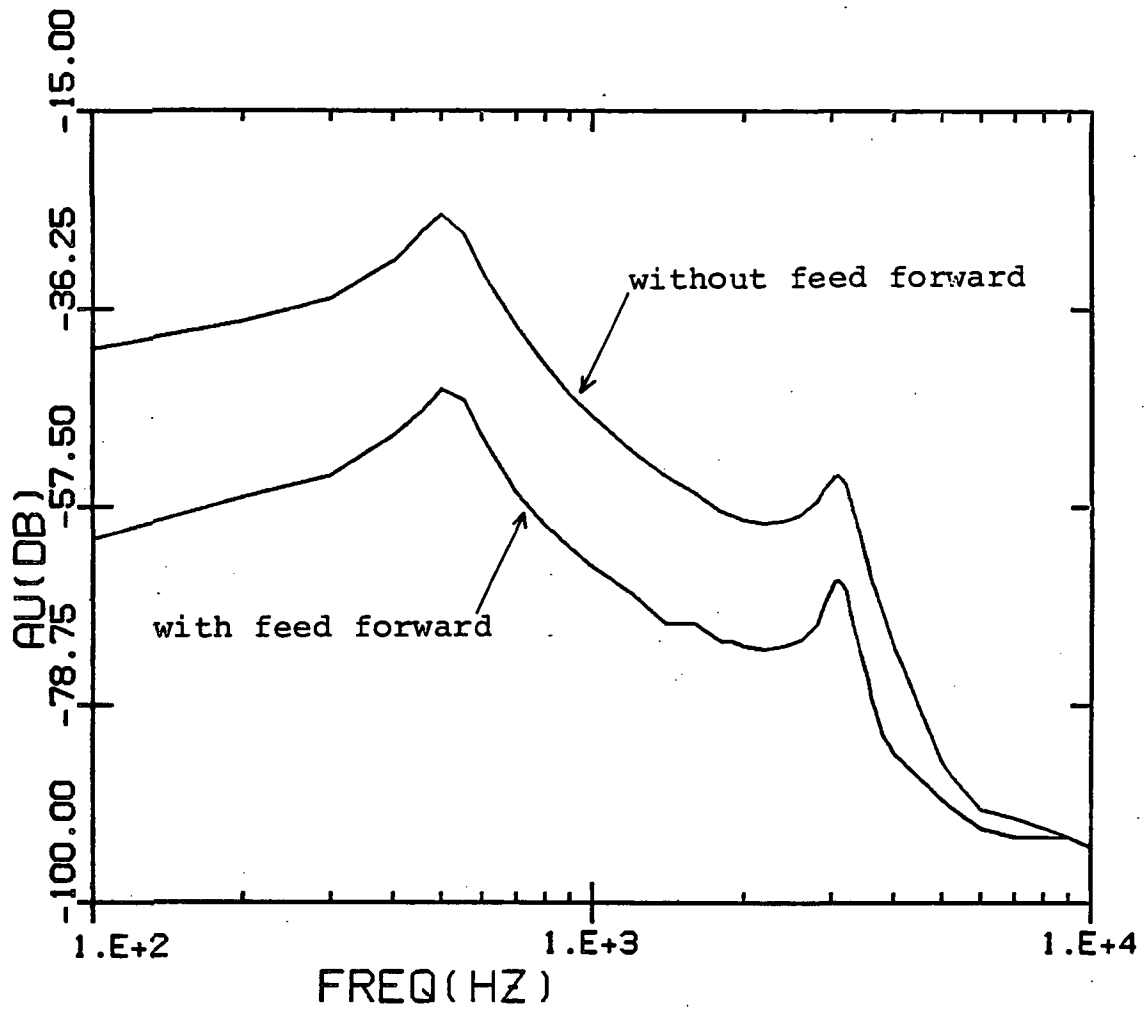


Figure 45: Audiosusceptibility with and without feedforward at  $V_I=35v$  (measurements)

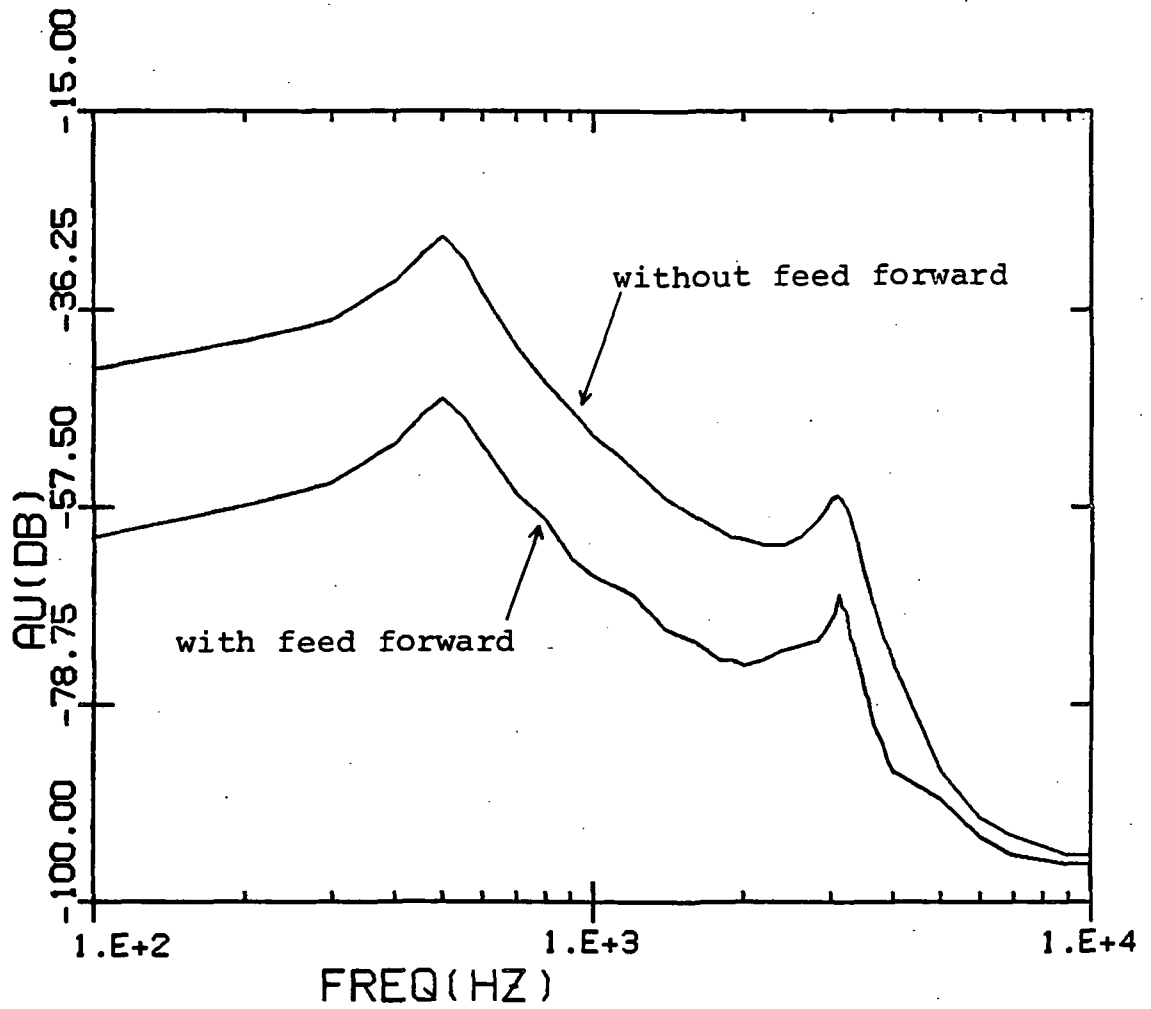


Figure 46: Audiosusceptibility with and without feedforward at  $V_I=40v$  (measurements)

The addition of feedforward substantially improves the audiosusceptibility, specially at the lower frequencies, as is evident upon examination of Figures 43 - 46 . The peaking effect of audiosusceptibility with feedforward loop is however, more pronounced at the two resonant frequencies of the two-stage input filter; this is explained by noting that in equation (2-6), Chapter 2, the audiosusceptibility is shown to be affected both by the peaking of  $Z(s)$  and by the peaking of the forward transfer function  $H(s)$  of the input filter. The peaking of  $H(s)$  cannot be controlled in any fashion by the addition of a feedforward loop since the control loop is not affected by  $H(s)$ ; thus the feedforward loop is effective in cancelling  $Z(s)$  while the peaking effect of  $H(s)$  is manifested in audiosusceptibility. Figures 47 and 48 show the transfer functions  $H(s)$  and  $Z(s)$  of the two-stage input filter used. The peaking of  $H(s)$  at the two resonant frequencies is clearly seen.

The two-stage input filter was modified by removing the damping resistor so that  $R_3 = 0.075$  ohm. Measurement data of the audiosusceptibility with and without feedforward are shown in Figures 49 - 52 . The top trace in all these figures is the closed loop input-to-output transfer function without feedforward and it can be seen that the gain is higher than in the earlier case (with damping resistance).

Figures 53 and 54 show the forward transfer function  $H(s)$  and the output impedance  $Z(s)$  of the input filter used. Comparing Figures 47 and 48 with Figures 53 and 54 it can be seen clearly that both  $Z(s)$  and  $H(s)$  peak at significantly higher values when the external damping resistance is removed.

The addition of feedforward substantially improves the audiosusceptibility as is evident from Figures 49 - 52 . The audiosusceptibility with feedforward peaks at the two resonant frequencies of the two-stage input filter as before, but in this case the peaks are higher. This is explained by noting that  $H(s)$  of the two-stage input filter without damping resistance peaks at a significantly higher value, as shown in Figures 53 and 54 , than that with a damping resistance as shown in Figures 47 and 48 ; thus the effect of  $H(s)$  on the closed loop gain would be expected to be greater in the former case.

It can therefore be concluded that the addition of feedforward significantly improves the audiosusceptibility, specially at the lower frequencies. The audiosusceptibility with feedforward is affected by the peaking of  $H(s)$  since the effect of peaking cannot be eliminated via any control means. The same adaptive feedforward circuit was used in making all the closed loop gain measurements mentioned

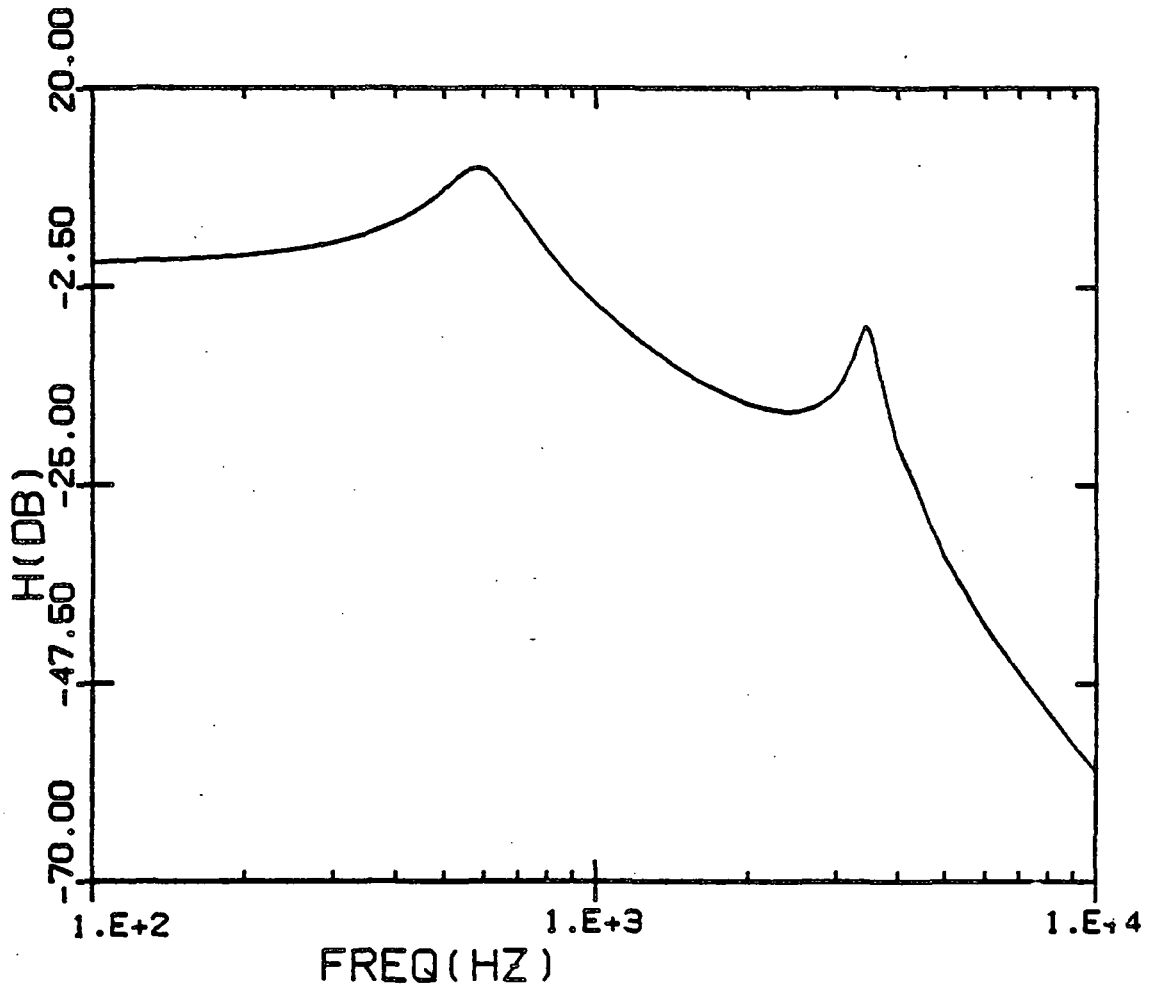


Figure 47:  $H(s)$  of two stage input filter, with  $R_3=0.2$  ohm

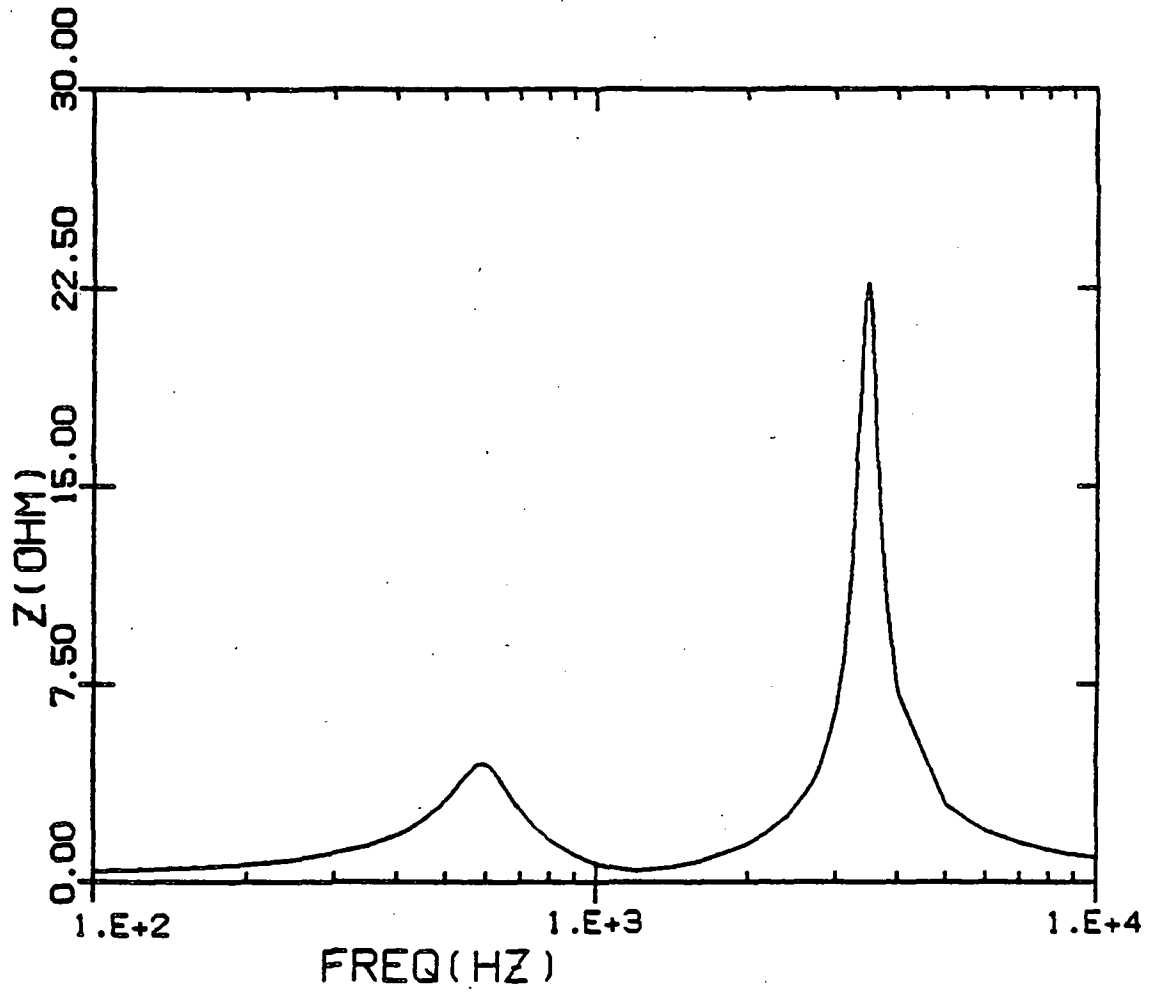


Figure 48:  $Z$  of two stage input filter, with  $R_3=0.2$  ohm

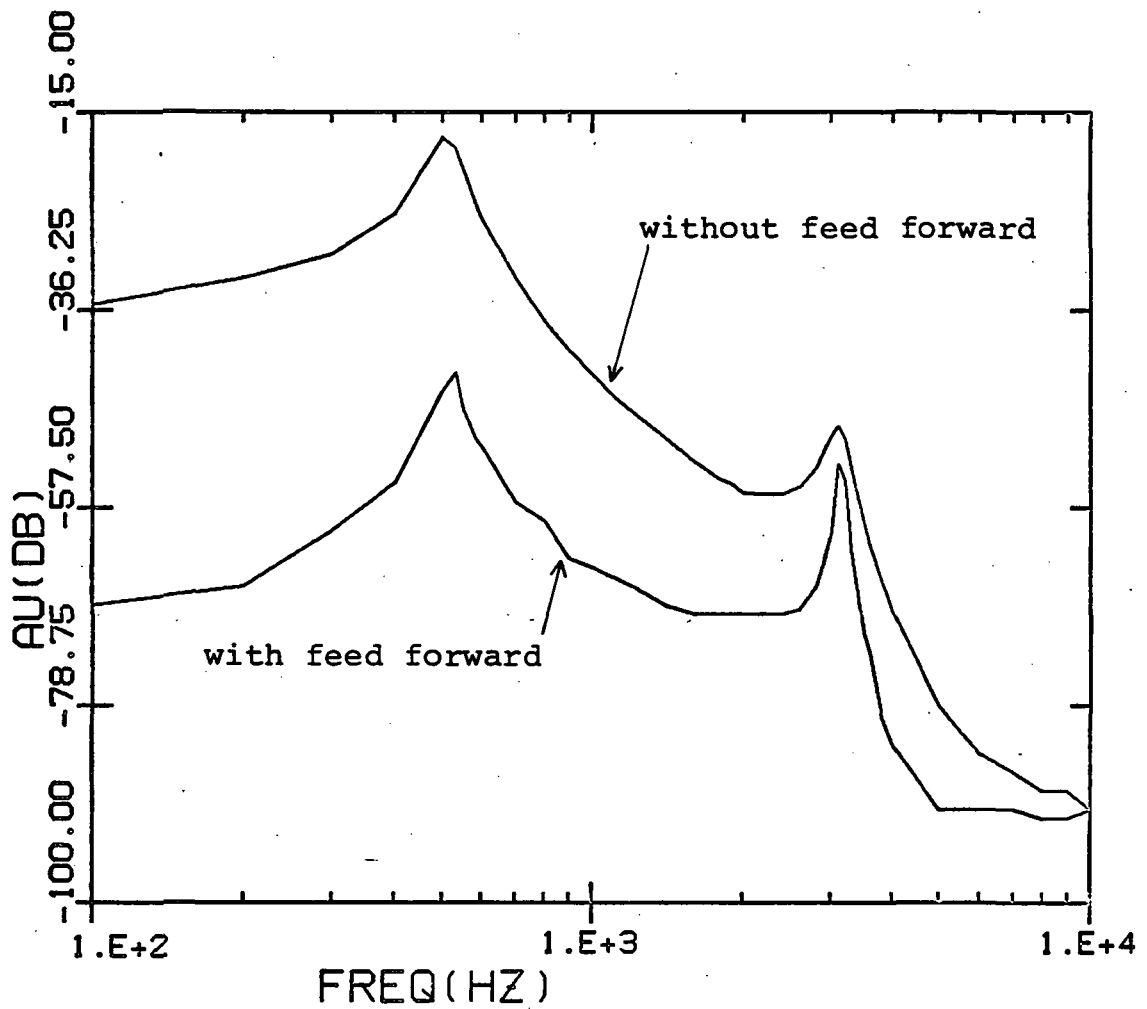


Figure 49: Audiosusceptibility with and without feedforward at  $V_I=25v$  (measurements)

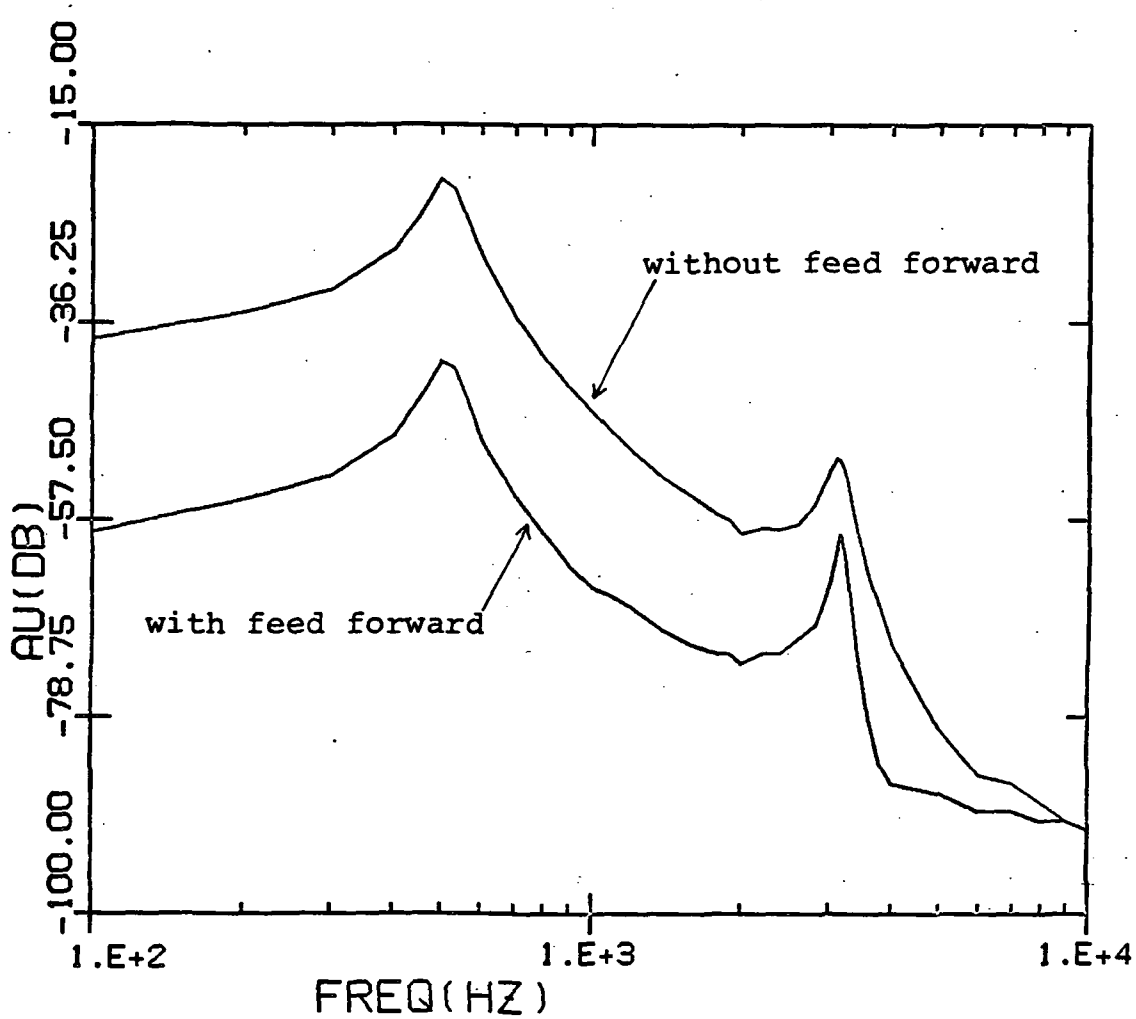


Figure 50: Audiosusceptibility with and without feedforward at  $V_I=30v$  (measurements)

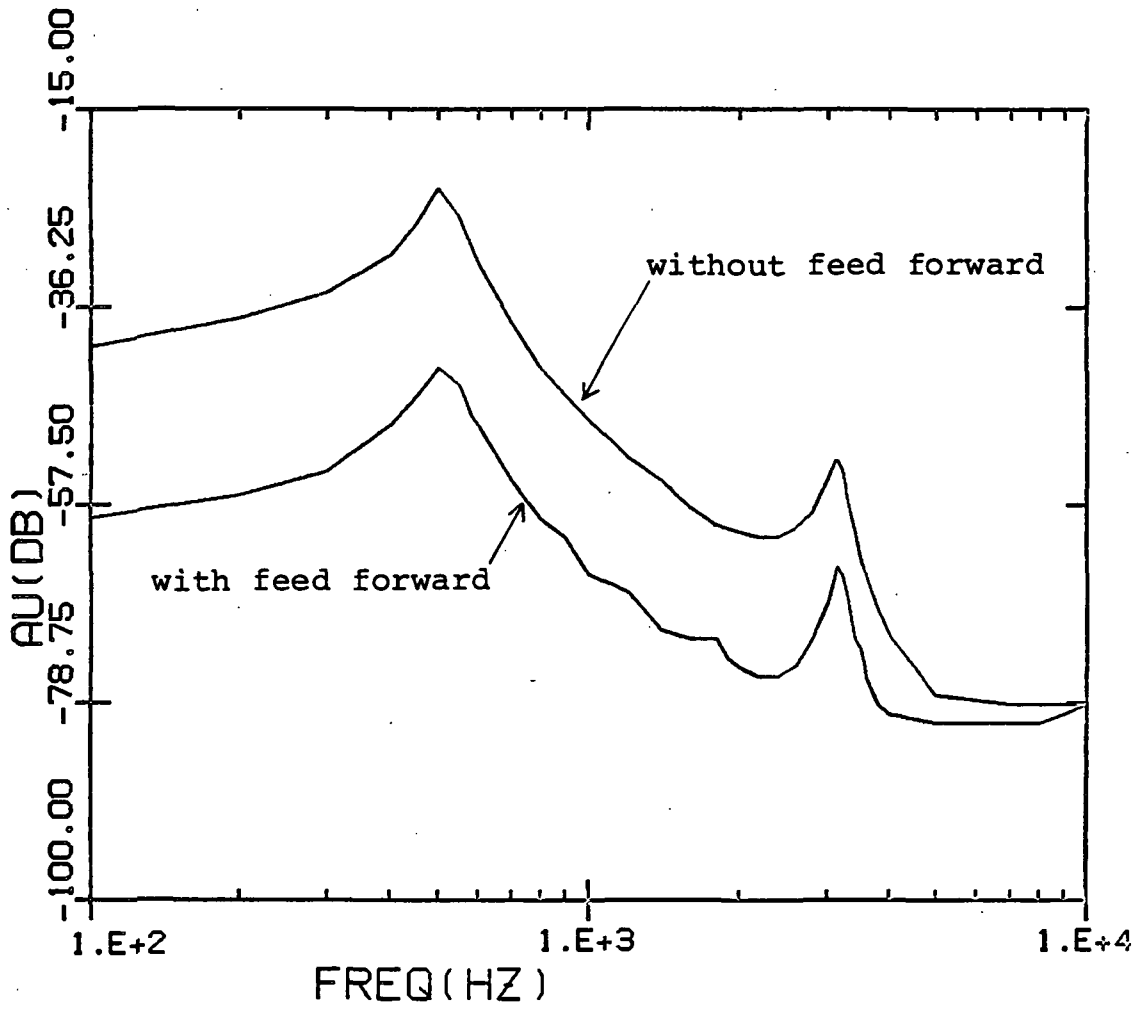


Figure 51: Audiosusceptibility with and without feedforward at  $V_I=35v$  (measurements)

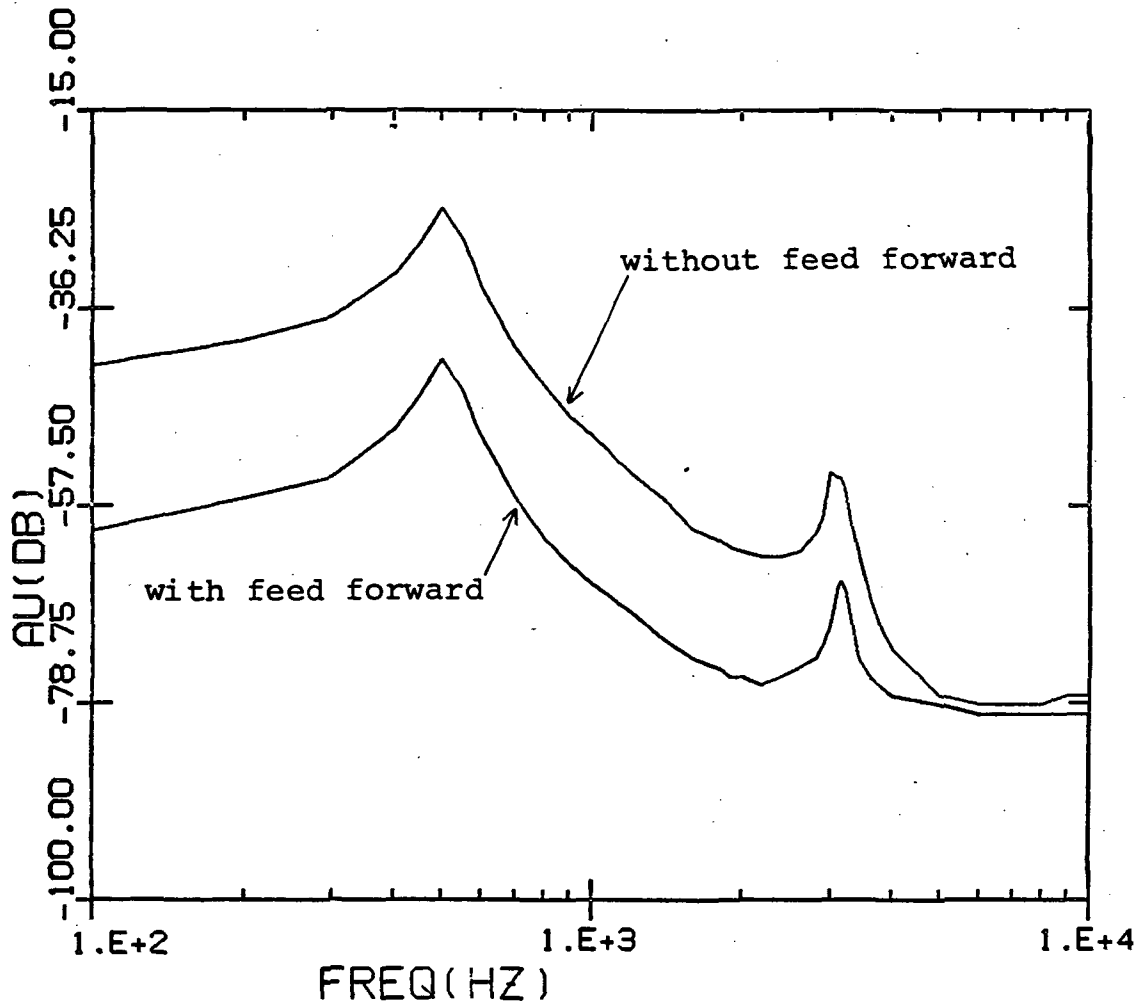


Figure 52: Audiosusceptibility with and without feedforward at  $V_I=40v$  (measurements)

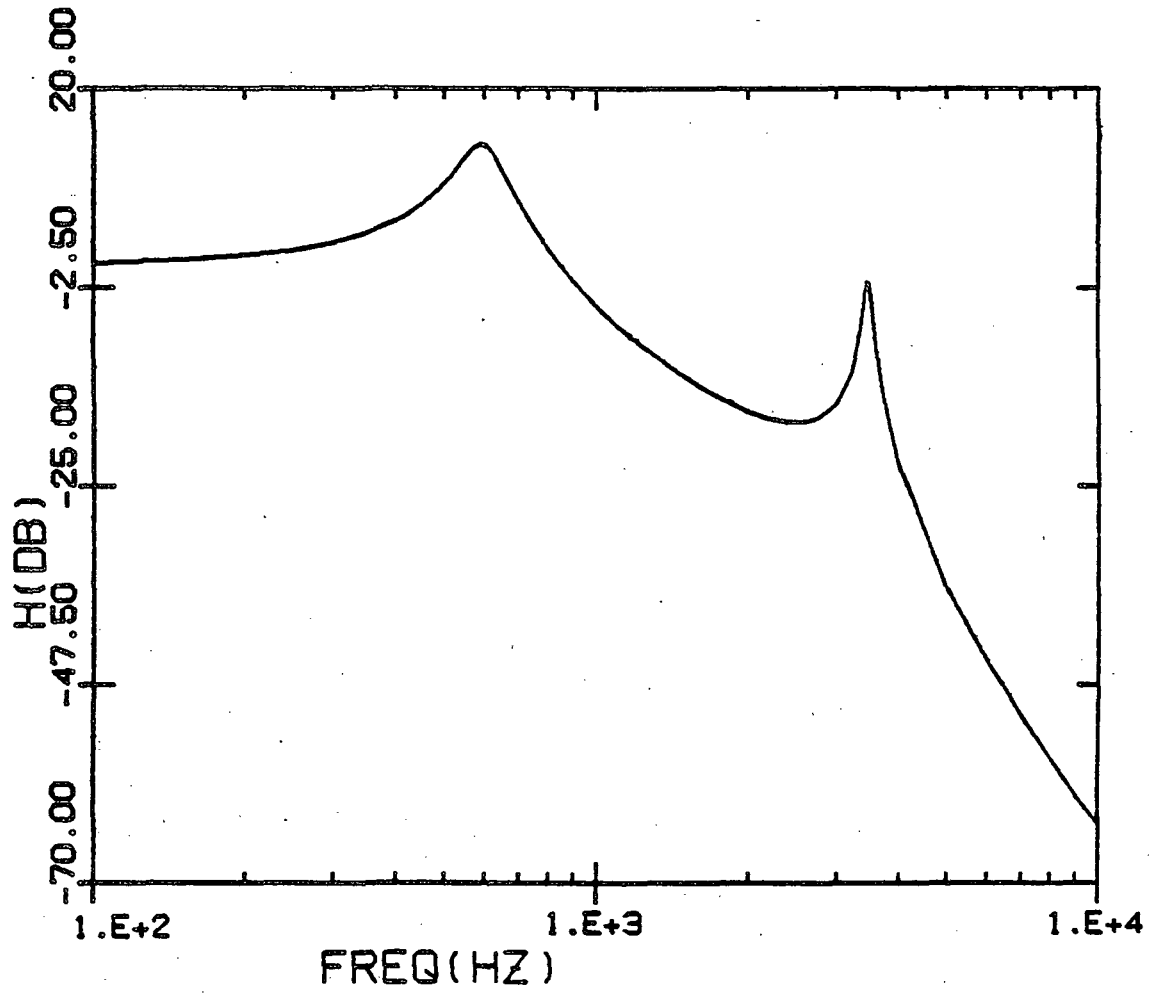


Figure 53:  $H(s)$  of two stage input filter,  $R_3=0.075$  ohm

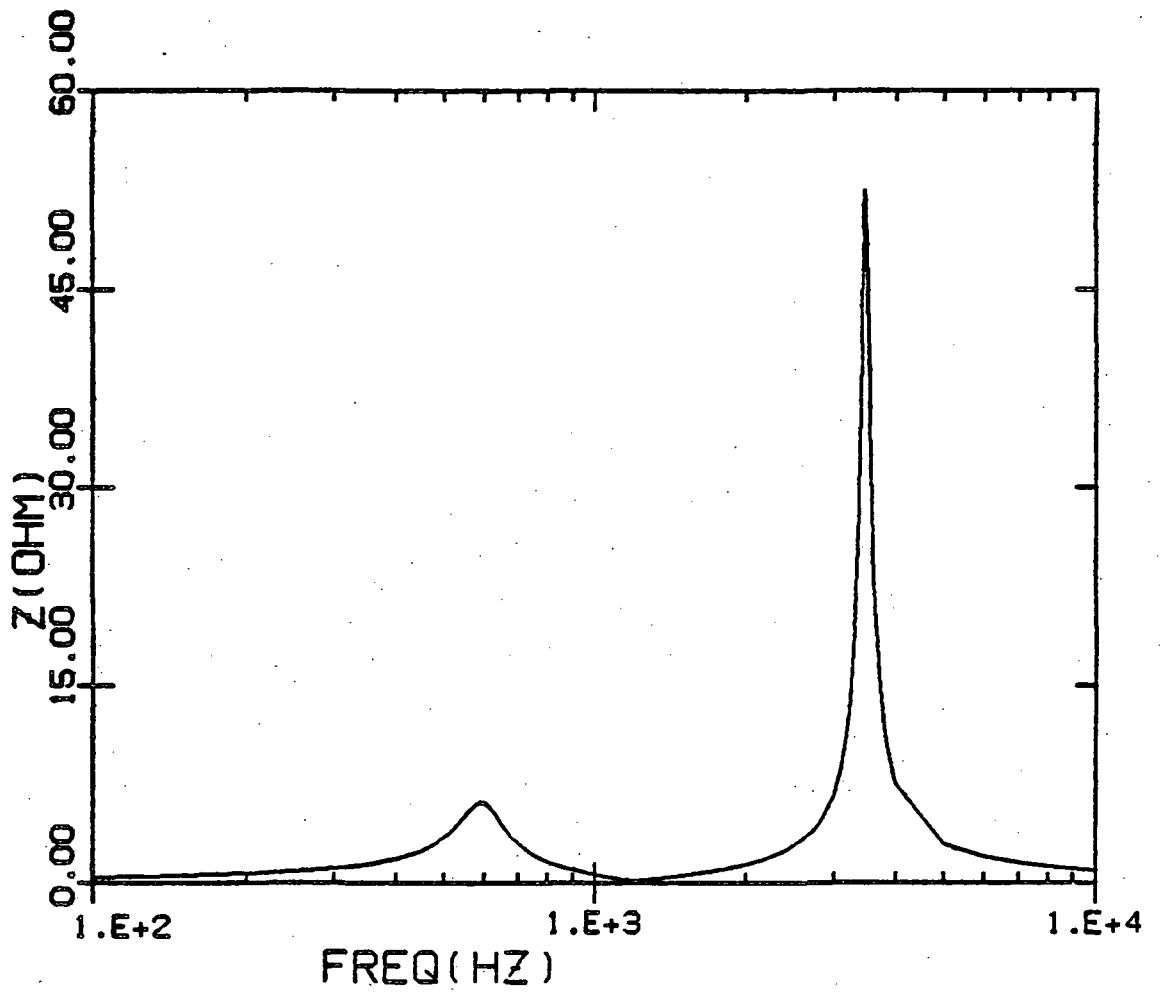


Figure 54:  $Z$  of two stage input filter,  $R_3=0.075$  ohm

above, this confirms anew the adaptive nature of the feed-forward circuit.

#### 6.4 MEASUREMENTS OF OUTPUT IMPEDANCE.

The closed-loop output impedance of a switching regulator should be as low as possible in order that the regulator behave as much as an ideal voltage source as possible. However, as pointed out in Chapter 2, the peaking of the output impedance of the input filter increases the closed-loop output impedance of the regulator.

Measurements of the regulator output impedance with and without feedforward were made, using the two-stage input filter of Figure 36 with  $R_3 = 0.075$  ohm (ESR of  $C_2$ ). Measurements were made by injecting a small signal sinusoidal disturbance at the output in parallel with the load of the regulator, and then using a HP network analyser to measure the corresponding voltage and current [8,9]. The feedforward circuit used was the adaptive feedforward circuit of Figure 33. Figures 55 - 58 show the measured values of output impedance with and without feedforward at four values of supply voltage  $V_I = 25v, 30v, 35v$  and  $40v$  using the same feedforward circuit in all cases.

It can be seen clearly from the figures that the output impedance is increased at the two resonant frequencies of

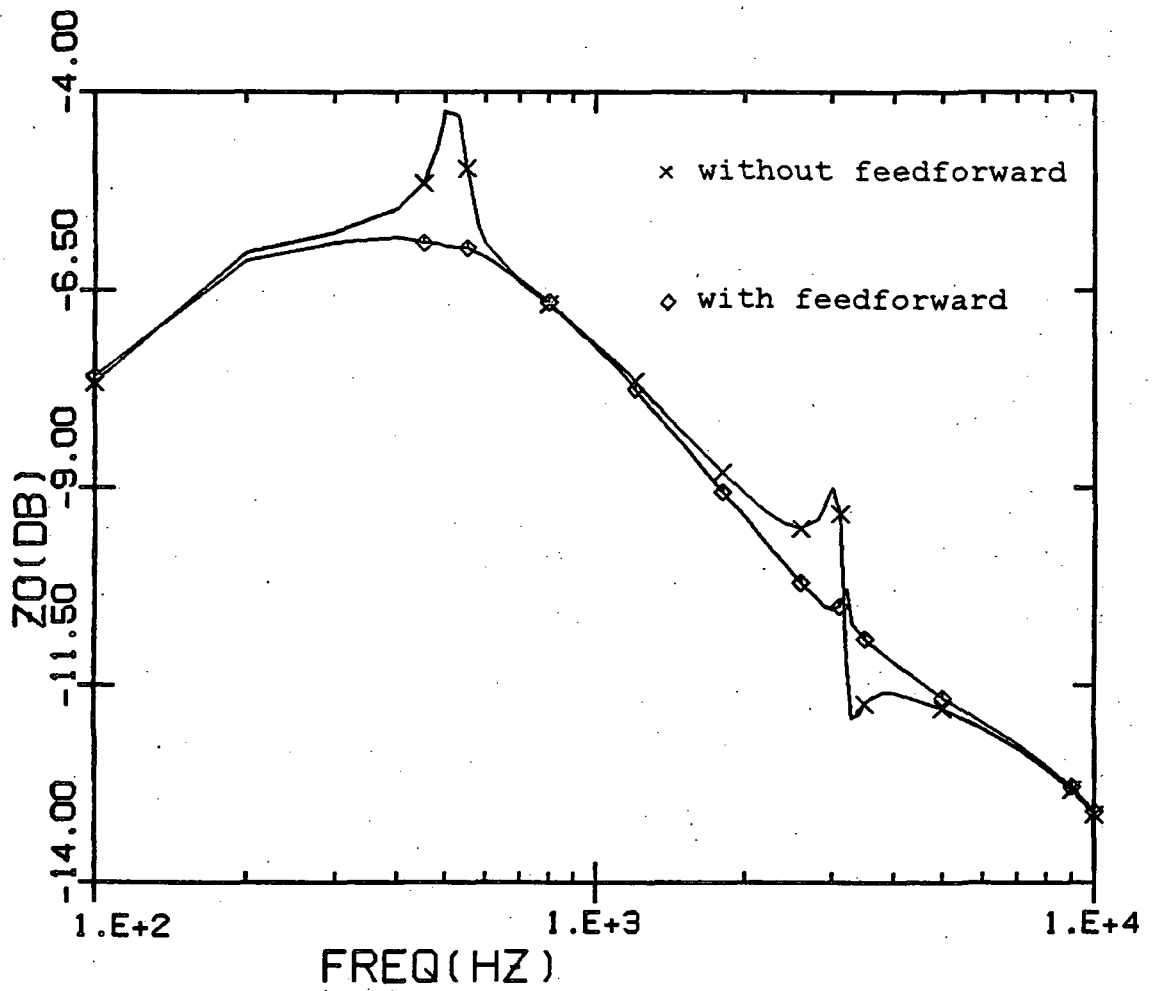


Figure 55: Output impedance with and without feedforward (x) at  $V_I=25v$

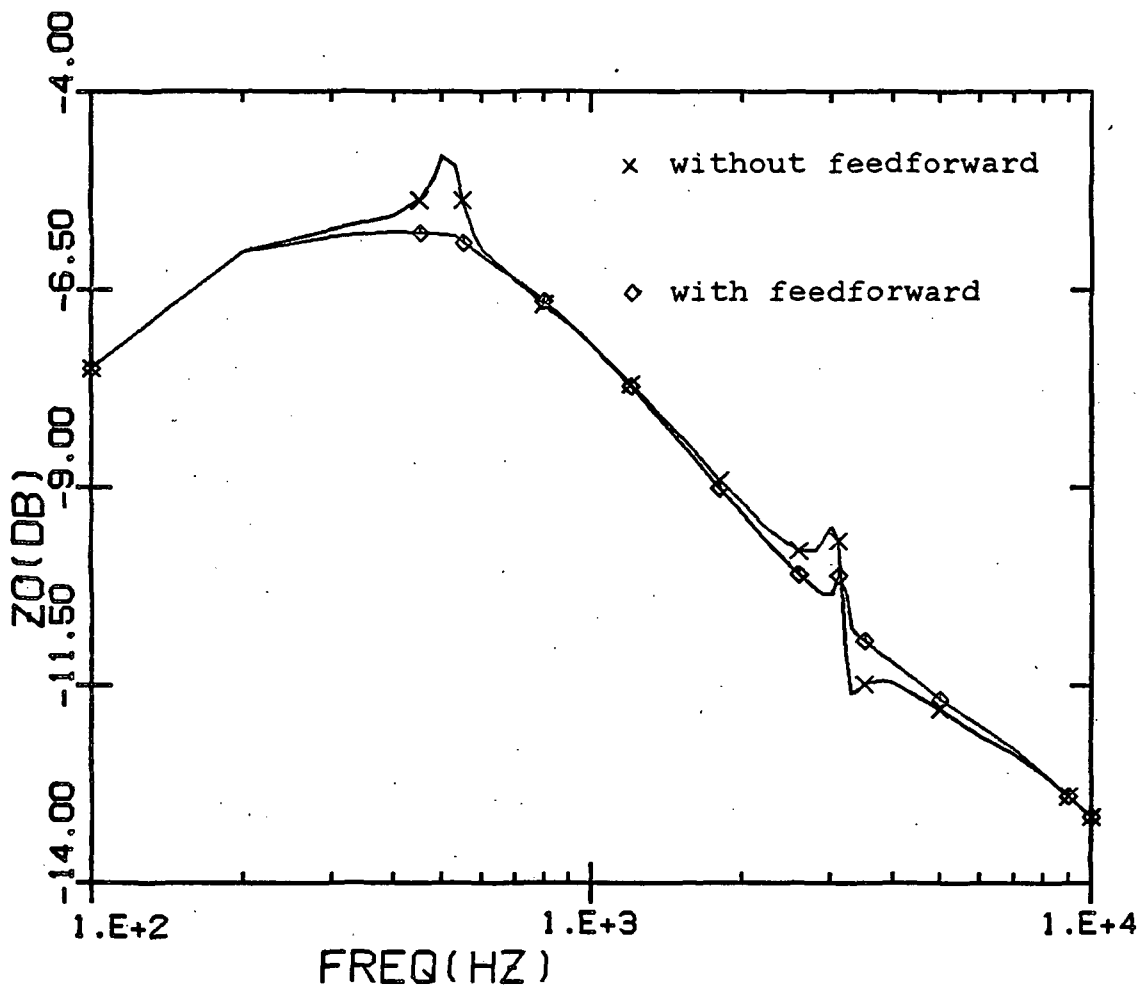


Figure 56: Output impedance with and without feedforward (X) at  $V_I=30v$

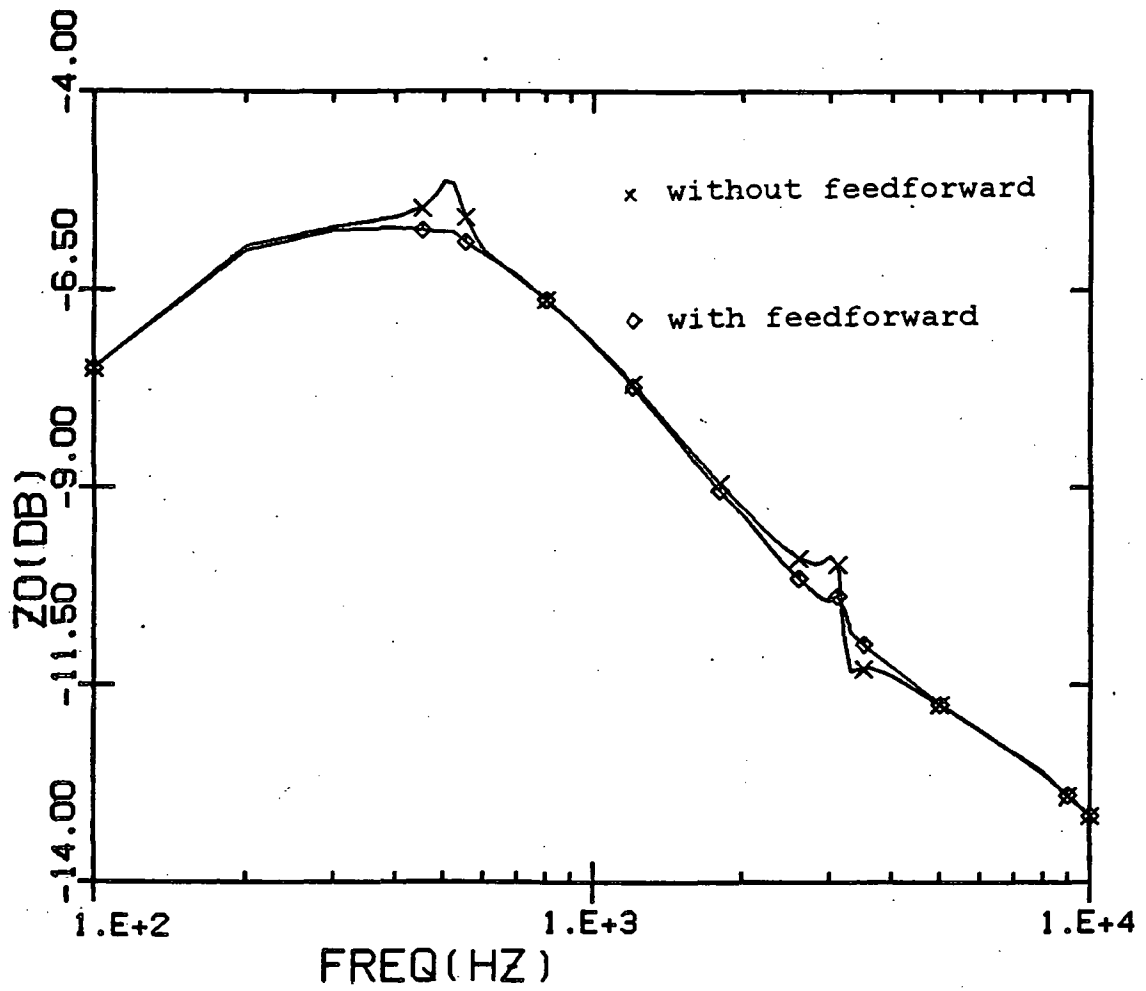


Figure 57: Output impedance with and without feedforward (x) at  $V_I=35v$

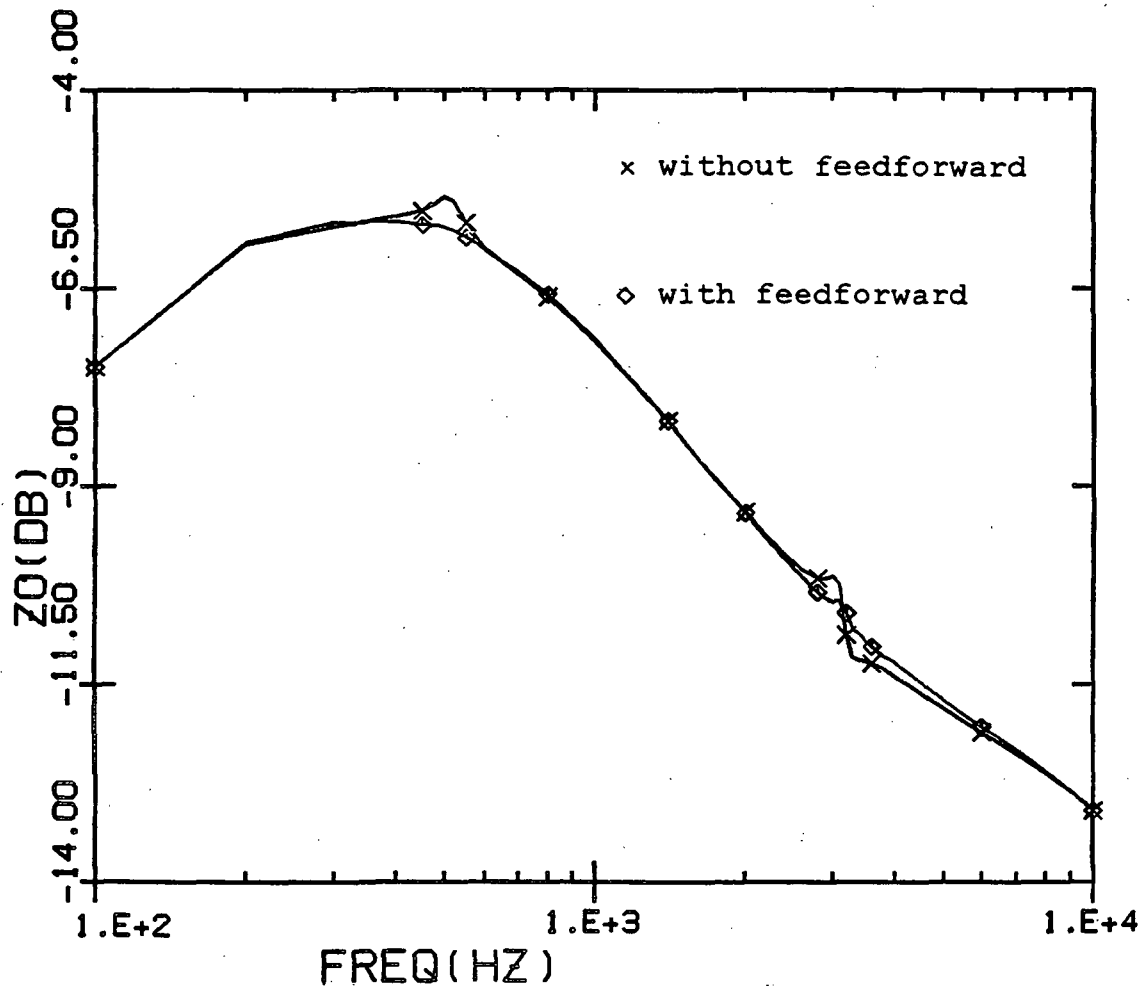


Figure 58: Output impedance with and without feedforward (X) at  $V_I = 40v$

the two-stage input filter. This is a consequence of the disturbances in the loop gain produced at those frequencies by the peaking of the input filter output impedance  $Z(s)$ . As was seen earlier in sections 6.1 and 6.2 the effect of  $Z(s)$  on the open loop gain depends on the duty cycle  $D$ , at higher values of  $D$  i.e. lower supply voltages, the effect of  $Z(s)$  on the open loop gain is higher. Thus the effect of  $Z(s)$  on the output impedance would be greater at lower supply voltages, and this is experimentally confirmed as can be seen from Figures 55 - 58 .

The addition of feedforward almost totally eliminates the undesirable perturbations in the output impedance characteristic at all supply voltages.

## 6.5 MEASUREMENT OF TRANSIENT RESPONSE AND STARTING OF THE REGULATOR.

In this section measurements of output voltage and other parameters for a step change in input voltage or load are presented with and without feedforward.

### 6.5.1 Small Amplitude Transient Response Measurements.

Photographs of the output voltage ripple and other parameters are presented with and without feedforward for two cases:

- (1) Step change in supply voltage.

(2) Step change in load.

The step changes mentioned above are small enough so that the output voltage remains in regulation throughout the transient response period.

6.5.1.1 Step Change in Input Voltage.

The buck regulator used is shown in Figure 34 with the parameters as specified in section 6.1. The input filter used was a single-stage input filter with the following parameters:

$$R_{L1} = 0.2 \text{ ohm} \quad L1 = 325 \text{ micro H} \quad C1 = 220 \text{ micro F}$$

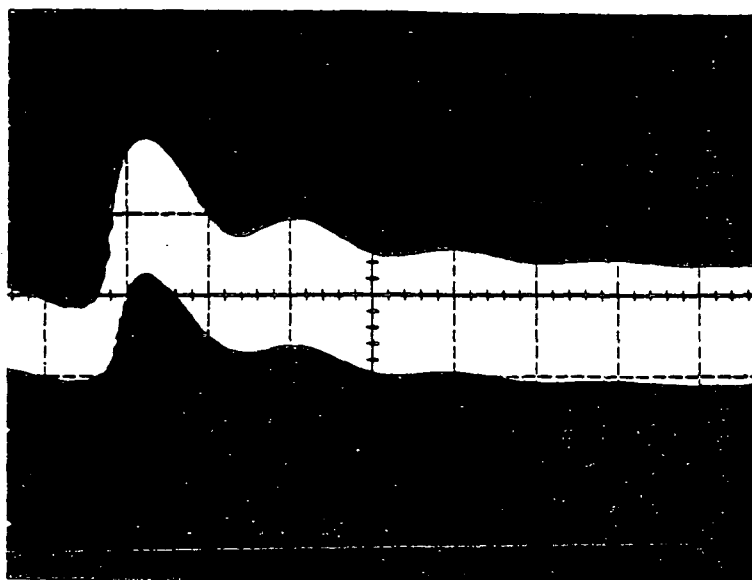
The adaptive feedforward circuit of Figure 33 was used in making the measurements.

The input voltage was abruptly switched from  $V_I = 30\text{v}$  to  $40\text{v}$  and photographs of output voltage ac ripple, input filter capacitor voltage, output filter inductor current and control voltage without using a feedforward loop were taken as shown in Figures 59 (a) and (b) , 60 (a) and (b), respectively. The control voltage is the input to the pulse modulator; without feedforward it is the output at the integrator in the feedback loop while with feedforward it is the sum of the above signal and the feedforward signal. Figures 61 (a) and (b) , 62 (a) and (b) show the photographs of the same variables with feedforward control. Comparing, for ex-

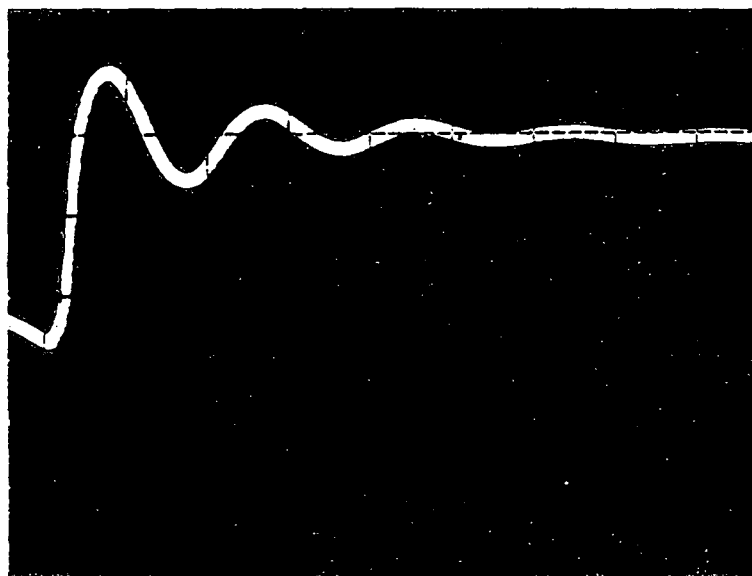
ample, the photographs of the output voltage ripple with and without feedforward, Figures 59 (a) and 61 (a), it can be clearly seen that the transient response is improved with the addition of feedforward. The amount of overshoot is less with feedforward. The magnitude of the oscillations in the output voltage caused by the interaction between the input filter and the regulator control are also lessened with the addition of feedforward.

Comparison of the photographs of input filter capacitor voltage, output filter inductor current and control voltage do not reveal much difference between the two cases (with and without feedforward). This may be explained by noting that the gain of the feedforward loop is fairly small ( 0.03 for  $V_I = 30v$  ) and thus the feedforward signal would be fairly small in amplitude. The addition of such a small amplitude signal to the fairly large amplitude waveforms recorded on the photographs will not show very clearly. The output voltage ripple, however, is small in magnitude and the effect of adding feedforward shows clearly. A computer program was written to simulate the step change in voltage; results from the program are presented in the next chapter and show close agreement with the measurements.

Thus it is concluded that feedforward improves transient response for the case where the supply voltage is subjected to a step change.



(a)

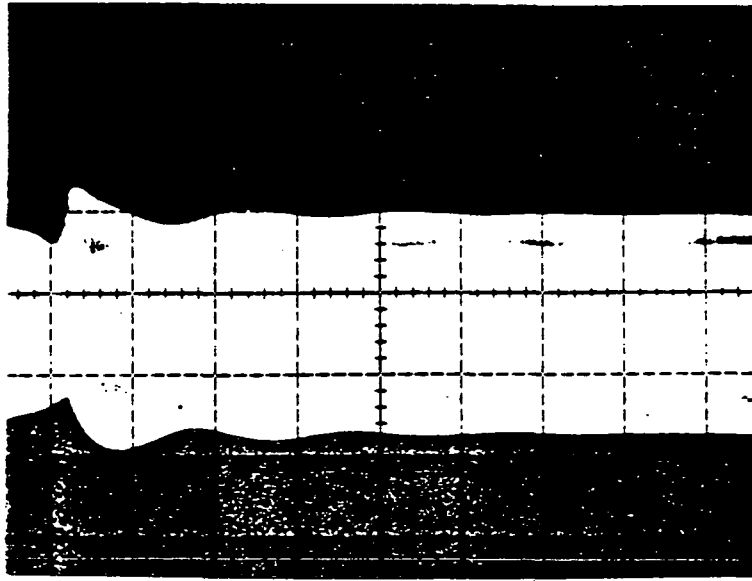


(b)

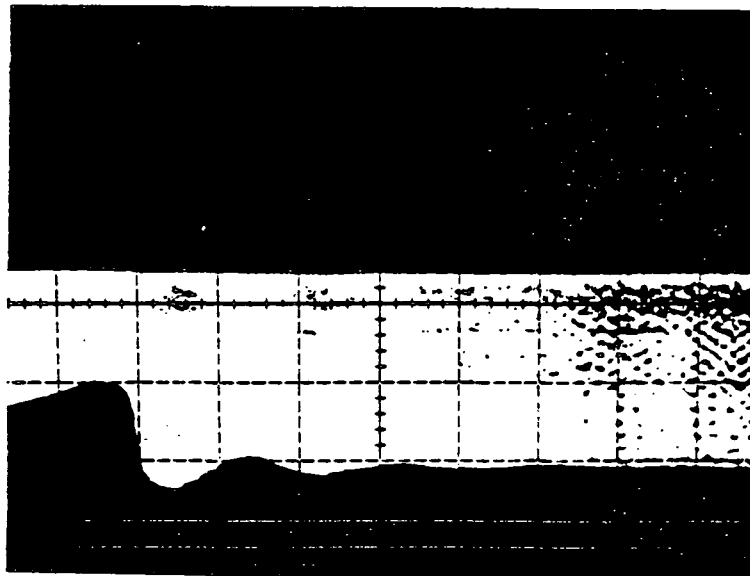
Figure 59: Output voltage ripple (a) and input filter capacitor voltage (b) without feedforward

(a) Y—0.1v/div X—1 msec/div

(b) Y—5v/div X—1 msec/div



(a)

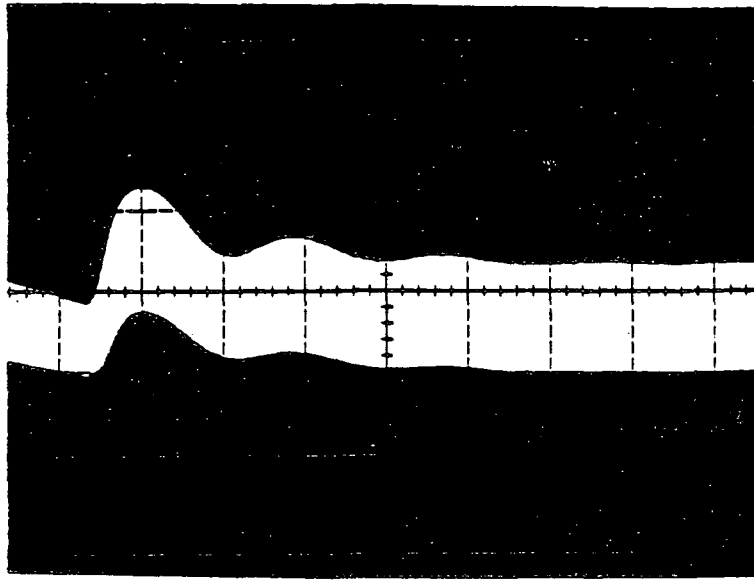


(b)

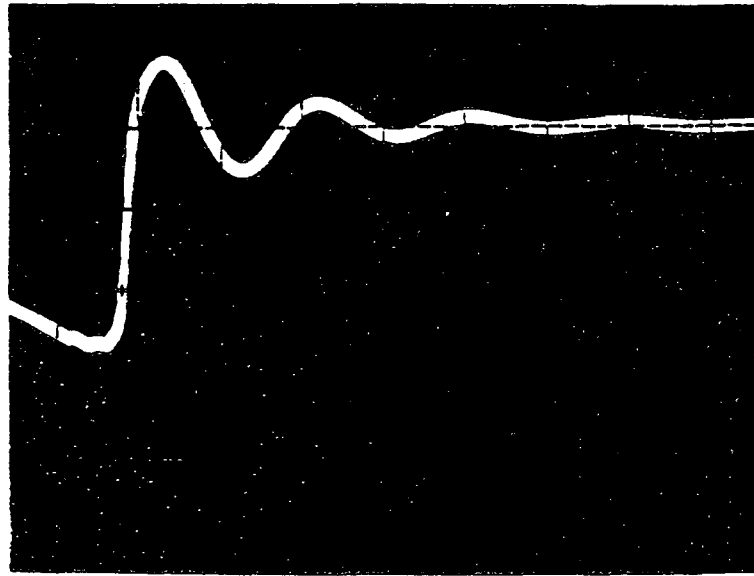
Figure 60: Output filter inductor current (a) and control voltage (b) without feedforward

(a) Y—0.5 A/div X—1 msec/div

(b) Y—0.5v/div X—1 msec/div



(a)

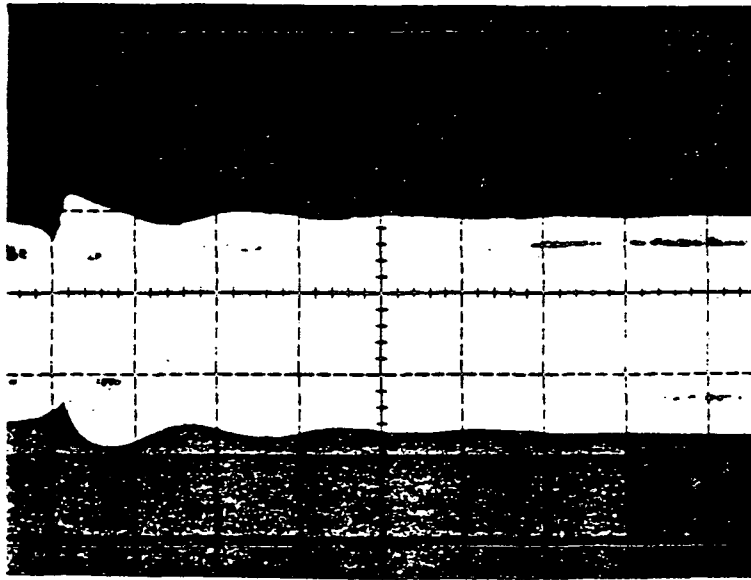


(b)

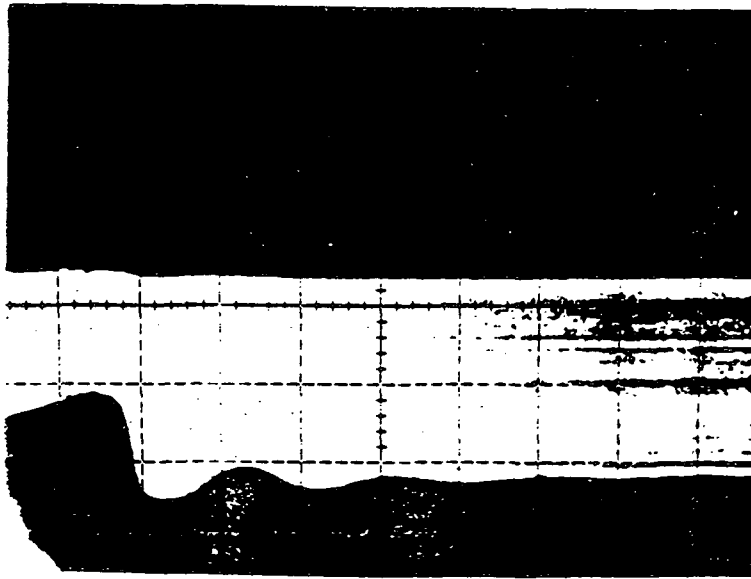
Figure 61: Output voltage ripple (a) and input filter capacitor voltage (b) with feedforward

(a) Y—0.1v/div X—1 msec/div

(b) Y—5v/div X—1 msec/div



(a)



(b)

Figure 62: Output filter inductor current (a) and control voltage (b) with feedforward

(a) Y—0.5 A/div X—1 msec/div

(b) Y—0.5v/div X—1 msec/div

### 6.5.1.2 Step Change in Load.

The buck regulator used is shown in Figure 34 , with the parameters as specified in section 6.1 with the following changes:

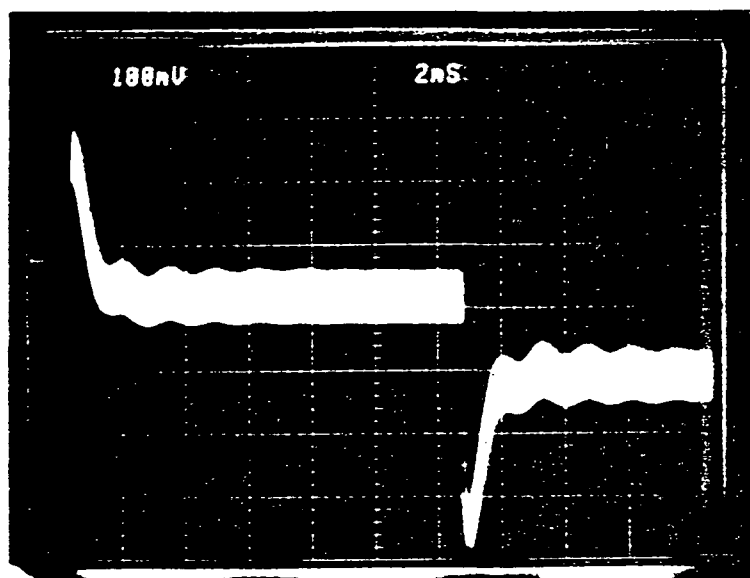
$$V_I = 25v \quad R_{14} = 3.69 \text{ Kilo ohm}$$

A single stage input filter was used with the following parameters:

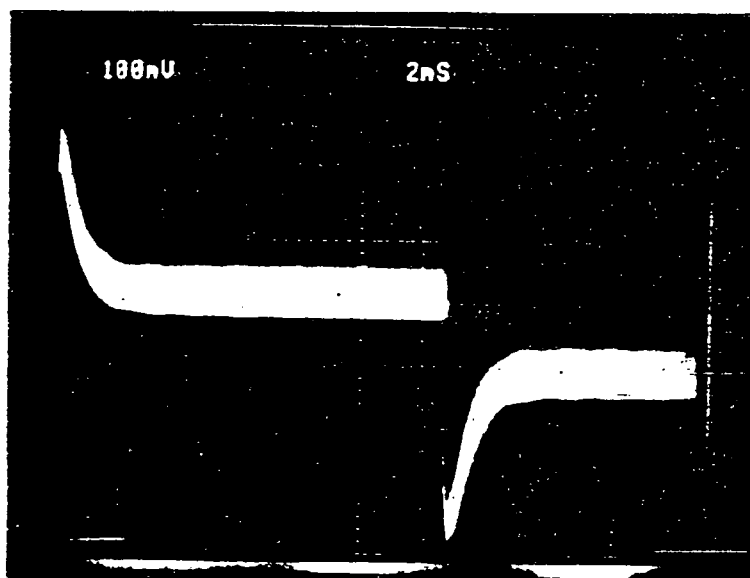
$$R_{L1} = 0.2 \text{ ohm} \quad L1 = 325 \text{ micro H} \quad C1 = 100 \text{ micro F}$$

The adaptive feedforward circuit of Figure 33 was used in making the measurements.

The load was switched repetitively between  $R_L = 10$  ohms and  $R_L = 20$  ohms using a transistor switch. Figures 63 (a) and (b) show the photographs of the output voltage ripple without and with feedforward, respectively, as the load is switched. The output voltage ripple without feedforward, Figure 63 , shows distinct oscillations caused by the interaction between the input filter and the regulator control loop. The oscillation frequency coincides with the input filter resonant frequency. These oscillations are eliminated with the addition of feedforward, as is evident from Figure 63 (b).



(a)



(b)

Figure 63: Output voltage without feedforward (a) and with feedforward (b)

### 6.5.2 Large Amplitude Transient Response Measurements.

Photographs of the output voltage ripple and other parameters are presented with and without feedforward for two cases:

- (1) Large step change in supply voltage.
- (2) Starting of the converter.

The cases mentioned above are large signal changes so that the voltage regulation is momentarily lost for part of the transient response period.

#### 6.5.2.1 Large Step Change in Supply Voltage.

The buck regulator used is shown in Figure 34 with the parameters as specified in section 6.1. The input filter used was the single-stage input filter of section 6.5.1.1. The adaptive feedforward circuit of Figure 33 was used in making the measurements with feedforward.

The input voltage was abruptly switched from  $V_I = 40\text{v}$  to 25v and photographs of the output voltage were made with and without feedforward; Figures 64 (a) and (b) show the photographs.

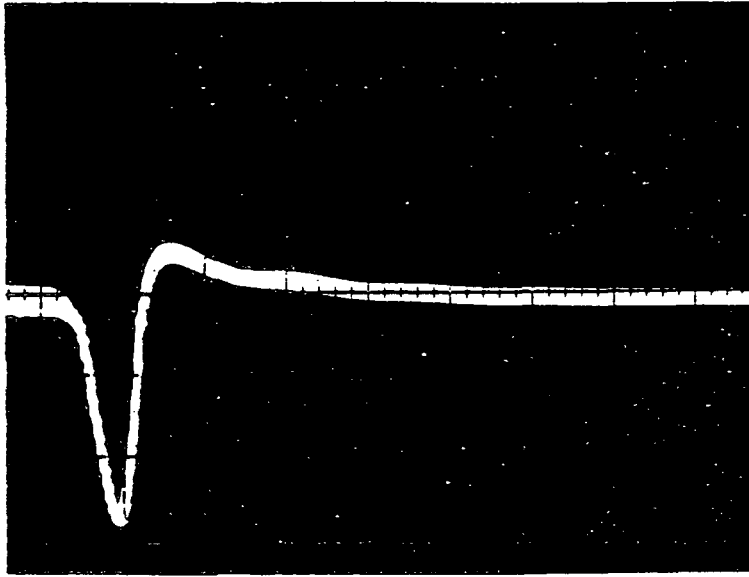
The step change in supply voltage is large enough to cause the regulator to lose regulation -- the output voltage drops by about 1.5v before the regulator recovers. This may be explained by noting that for such a large change in sup-

ply voltage the input filter capacitor voltage drops down close to 20v, and since this value is lower than the design range of 25v - 40v for the regulator supply, the regulator loses regulation. Further details are given in the next chapter which presents results from a computer program written to simulate this large step change. The results show close agreement with the measurements presented here.

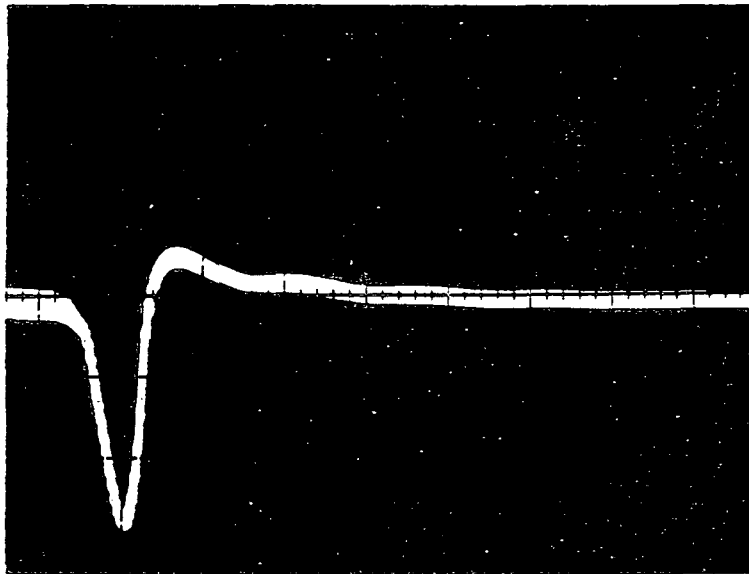
Figures 64 (a) and (b) show that the behavior of the regulator is similar with and without feedforward for such a large step change in supply voltage. This is expected since the regulator control loop momentarily loses its control function during this transient period. Since the feedforward is designed to compensate for the effects of input filter interaction via a duty cycle modulation scheme it is expected that the feedforward does not contribute anything under these conditions. Computer based simulation results presented in the next chapter confirm the measurement results. It is also to be noted that the feedforward does not have any detrimental effect on the transient response.

#### 6.5.2.2 Measurements of the Start Up Behavior of the Regulator

This section investigates the start-up behavior of the switching regulator. The regulator used is shown in Figure



(a)



(b)

Figure 64: Output voltage without feedforward (a) and with feedforward (b)

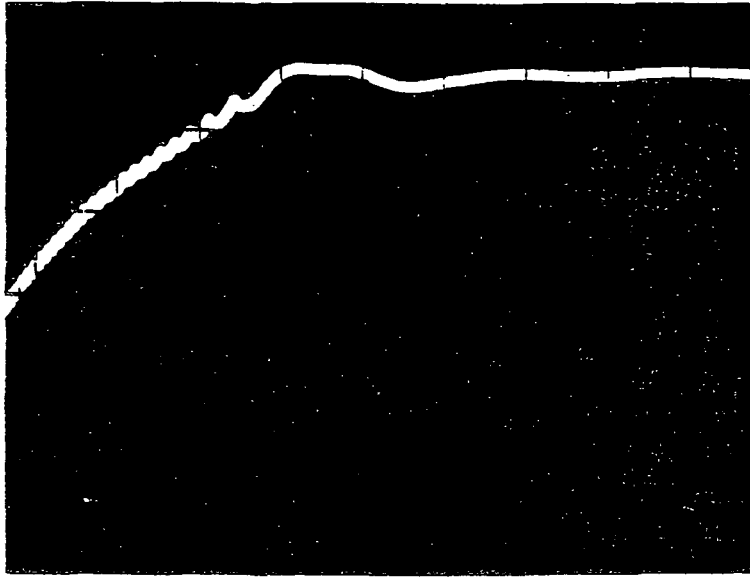
(a) Y—0.5v/div X—0.5 msec/div

(b) Y—0.5v/div X—0.5 msec/div

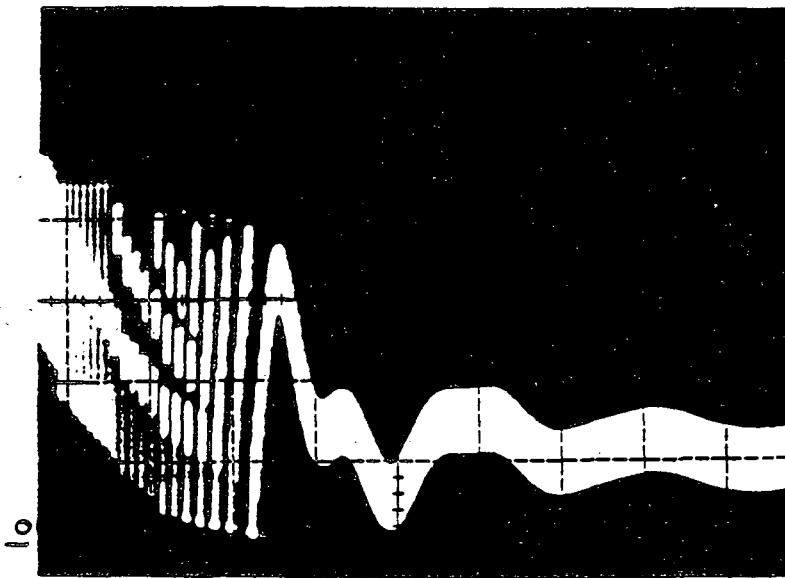
34 with the parameters as specified in section 6.1. The single stage input filter of section 6.5.1.1 was used with the supply voltage set at 30v. The adaptive feedforward circuit of Figure 33 was used in making the measurements with feedforward.

Prior to starting, the output voltage and the output filter inductor current were both zero. Photographs of the output voltage and output filter inductor current were made with and without feedforward and are shown in Figures 65 (a) and (b) 66 (a) and (b). The output voltage without feedforward builds up from zero to 20v (regulated output) in about 3 msec. The inductor current rises sharply at starting but is limited to about 6.0A by the peak current protection circuit built in with the regulator. It settles down to its steady state value in about 4 msec.

The photographs with feedforward show similar behavior - thus the feedforward does not contribute significantly to this transient period nor does it present any detrimental effects.



(a)

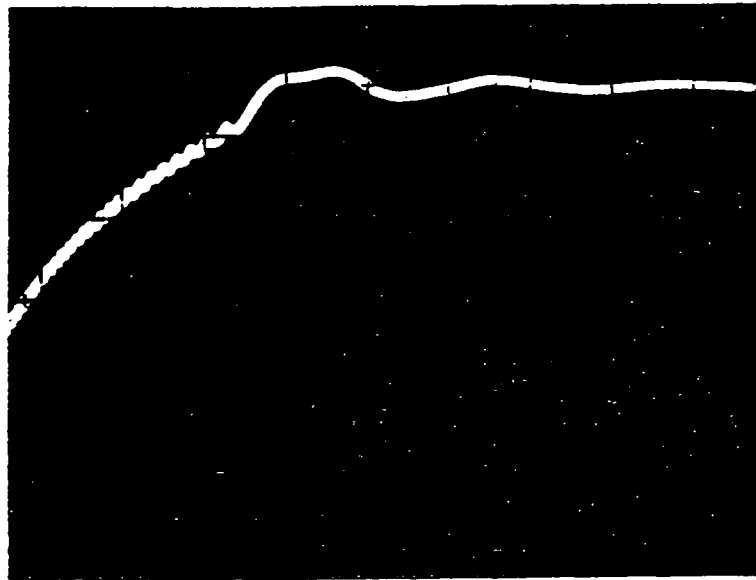


(b)

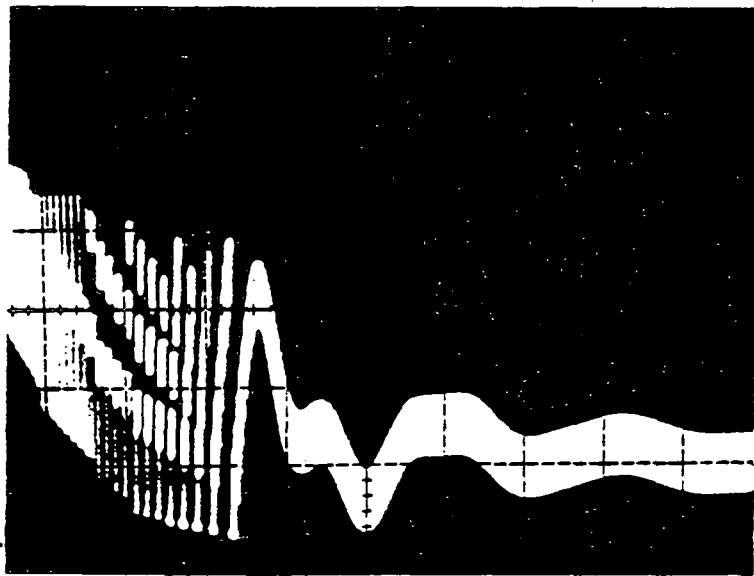
Figure 65: Output voltage (a) and output filter inductor current (b) without feedforward

(a) Y—5v/div X—0.5 msec/div

(b) Y—1 A/div X—0.5 msec/div



(a)



(b)

Figure 66: Output voltage (a) and output filter inductor current (b) with feedforward

(a) Y—5v/div X—0.5 msec/div

(b) Y—1 A/div X—0.5 msec/div

## 6.6 CONCLUSIONS

Extensive measurements made to verify experimentally the feedforward design are presented in this chapter. Measurements of the open loop gain and phase margin, closed loop gain, output impedance and transient response confirm the effectiveness of the feedforward in improving performance, as predicted in the analysis. The following points are noteworthy:

1. The feedforward eliminates the detrimental effect on open loop gain and phase margin of the output impedance of the input filter.
2. The feedforward circuit is shown to be independent of input filter parameters and also independent of input filter configuration.
3. The feedforward effectively eliminates the interaction between an unknown dynamic source impedance and the regulator control loop.
4. The closed loop input-to-output transfer function (audiosusceptibility) and output impedance are both improved significantly by the addition of feedforward.
5. The addition of feedforward improves transient response in those cases where the interaction between the input filter and the control loop degrades the

response. Examples of the above are small step changes in supply voltage and load, and results for these cases are included. For large signal transient behavior the feedforward does not in any way degrade the performance -- examples of these are a large step change in supply voltage and the start up behavior of the regulator.

6. No detrimental effects have been observed due to the use of the proposed feedforward compensation scheme through the course of study and through extensive experiments when the system was subjected to different forms of small and large signal disturbances.

## Chapter VII

### DIGITAL SIMULATION OF BUCK REGULATOR FOR TRANSIENT ANALYSIS

This chapter deals with a program developed to simulate the real time behaviour of the regulator with and without feedforward control under both steady state and transient conditions. Results for a step change in supply voltage are included that are in close agreement with the measurements presented in the last chapter.

#### 7.1 DESCRIPTION OF THE METHOD

The starting point is the definition of the buck regulator in terms of state equations [12,13,14]. The switching regulator used was the one used in Chapter 5 and 6 and is shown in Figure 34. The buck regulator without feedforward is described by a set of state equations. The six state variables used are:

$$x(1) = i_{L1} \text{ (current in input filter inductor)}$$

$$x(2) = v_{C1} \text{ (input filter capacitor voltage)}$$

$$x(3) = e_C \text{ (control voltage, input to pulse modulator)}$$

$$x(4) = i_L \text{ (output filter inductor current)}$$

$$x(5) = v_C \text{ (output filter capacitor voltage)}$$

$$x(6) = e_R \text{ (compensation loop capacitor voltage)}$$

The control voltage is the output of the integrator in the feedback control loop if no feedforward is used and it is the sum of the integrator output and the feedforward signal if feedforward is used. The state variable  $e_R$  is the voltage at the capacitor  $C_2^1$  in the compensation loop. The pulse modulator has as its input the control voltage  $e_C$  and it converts the voltage to a duty cycle signal  $d(t)$ . The transfer function of the pulse modulator is a constant if the supply voltage is a constant, [8], for the constant volt-sec. ( $V_I T_{ON}$ ) control mode that was used. Thus it can be seen that the six state variables defined above completely describe the buck regulator system of Figure 34 .

The state equations for the complete system without feedforward are developed [12,13,14] for the two time periods  $T_{ON}$  and  $T_{OFF}$ .

During  $T_{ON}$  the transistor switch S1 is on while diode S2 is off and the system is characterized by the following state equations:

$$\dot{\underline{x}} = F1 \underline{x} + G1 \underline{u} \quad (7-1)$$

where

$$F1 = \begin{bmatrix} \frac{-R_L}{L} & \frac{-1}{L} & 0 & 0 & 0 & 0 \\ \frac{1}{C} & 0 & 0 & \frac{-1}{C} & 0 & 0 \\ 0 & \frac{-n}{C_1 R_4} & 0 & \frac{-R_L R_C K1}{C_1 (R_L + R_C)} & \frac{R_L K2}{C_1 (R_L + R_C)} & \frac{1}{C_1 R_{13}} \\ 0 & \frac{1}{L} & 0 & -\frac{1}{L} \left( R_L + \frac{R_C R_L}{R_C + R_L} \right) & \frac{-R_L}{L (R_C + R_L)} & 0 \\ 0 & 0 & 0 & \frac{R_L}{C (R_L + R_C)} & \frac{-1}{C (R_L + R_C)} & 0 \\ 0 & 0 & 0 & \frac{R_L R_C}{C_2 R_{13} (R_L + R_C)} & \frac{R_L}{C_2 R_{13} (R_L + R_C)} & \frac{-1}{C_2 R_{13}} \end{bmatrix} \quad (7-2)$$

$$G1 = \begin{bmatrix} \frac{1}{L} & 0 & 0 & 0 \\ 0 & 0 & 0 & 0 \\ 0 & \frac{1}{C_1 R_{14}} & \frac{n}{C_1 R_{14}} & 0 \\ 0 & 0 & \frac{-1}{L} & 0 \\ 0 & 0 & 0 & 0 \\ 0 & 0 & 0 & 0 \end{bmatrix} \quad (7-3)$$

$$K1 = \left[ \frac{R_{12}}{R_{14} (R_{11} + R_{12})} + \frac{1}{R_{13}} - \frac{n}{R_4} + \frac{-n R_L (R_L + R_C)}{R_4 R_L R_C} \right] \quad (7-4)$$

$$K2 = \left[ \frac{n}{R_4} - \frac{1}{R_{13}} - \frac{R_{12}}{R_{14} (R_{11} + R_{12})} \right] \quad (7-5)$$

$$\underline{u} = \begin{bmatrix} V_I \\ E_R \\ E_Q \\ E_D \end{bmatrix} \quad (7-6)$$

In equation (7-6)  $V_I$  is the supply voltage,  $E_R$  is the reference voltage,  $E_Q$  is the saturation voltage drop of the power transistor and  $E_D$  is the conduction voltage drop across the diode.

During  $T_{OFF}$  the transistor S1 is off while diode S2 is conducting and the equations are:

$$\dot{\underline{x}} = F2 \underline{x} + G2 \underline{u} \quad (7-7)$$

where

$$\begin{aligned} F2 &= F1 && \text{except for} \\ F2(2,4) &= 0 \\ F2(3,2) &= 0 && (7-8) \\ F2(4,2) &= 0 \end{aligned}$$

and

$$\begin{aligned} G2 &= 0 && \text{except for} \\ G2(1,1) &= 1/L1 \\ G2(3,2) &= \frac{1}{C_1' R_{14}} \\ G2(3,4) &= \frac{n}{C_1' R_4} && (7-9) \end{aligned}$$

$$G2(4,4) = -\frac{1}{L}$$

Since  $\underline{u}$  is not a function of time the solution to the state equations (7-1) and (7-8) can be written as:

$$\text{During } T_{\text{OFF}} \quad \underline{x}(t + T) = \phi_F * \underline{x}(t) + D_F * \underline{u} \quad (7-10)$$

$$\text{During } T_{\text{ON}} \quad \underline{x}(t + T) = \phi_N * \underline{x}(t) + D_N * \underline{u} \quad (7-11)$$

where  $\phi_N, \phi_F$  are the state transition matrices defined for a small fixed step size  $T$  [12] and

$$D_F = \phi_F * \left[ \int_0^T e^{-F2 \cdot s} ds \right] G2 \quad (7-12)$$

$$D_N = \phi_N * \left[ \int_0^T e^{-F1 \cdot s} ds \right] G1$$

Equations (7-11) and (7-12) are used to simulate the behavior of the regulator without feedforward. Starting at the beginning of the ON time period equation (7-12) is used to propagate the state. The step size  $T$  is defined as half the ON and OFF times and this determines the matrices  $\phi_N, D_N,$

$\phi_F$  and  $D_F$ . Substitution into equation (7-11) along with the initial values at the beginning of the ON period propagates the state through time  $T$ . Similar substitution propagates the state through the ON period [12,13,14]. For the type of duty cycle control used, constant  $V_I T_{ON}$  control, the ON time is fixed whenever  $V_I$  is fixed.

At the end of the ON period, equation (7-10) is used to propagate the state during the OFF period, with the initial condition being the state at the end of the ON interval. The end of the OFF interval is determined as the point when the control voltage  $e_C$  equals the comparator voltage  $E_T$  which was 7.0v in this case. Newton's iteration is performed to find the exact point in time when  $e_C$  equals  $E_T$  [12,13,14].

The equations describing the system with feedforward are very similar to those without feedforward. The nonadaptive feedforward circuit of Chapter 5 was used in the simulation program and it is shown in Figure 67. The output of the capacitor  $C_f$  is included as a state variable. The state variables are thus defined as:

$$\begin{aligned}
 x(1) &= i_{L1} \\
 x(2) &= v_{C1} \\
 x(3) &= v_f \text{ (output of } C_f \text{)} \\
 x(4) &= e_C \\
 x(5) &= i_L
 \end{aligned}
 \tag{7-13}$$

$$x(6) = v_C$$

$$x(7) = e_R$$

The equations during  $T_{ON}$  and  $T_{OFF}$  are the same as equations (7-1) and (7-8) with the following definitions:

$$F1 = \begin{bmatrix} -\frac{R_{L1}}{L1} & -\frac{1}{L1} & 0 & 0 & 0 & 0 & 0 \\ \frac{1}{C1} & 0 & \frac{-1}{C1(R_{f1}+R_{f2})} & 0 & -\frac{1}{C1} & 0 & 0 \\ \frac{1}{C1} & 0 & \frac{-(C_f+C1)}{C_f \cdot C1(R_{f1}+R_{f2})} & 0 & -\frac{1}{C1} & 0 & 0 \\ -\frac{K3}{C1} & \frac{-n}{C1 \cdot R4} & \frac{K3 \cdot (C_f+C1)}{C_f \cdot C1(R_{f1}+R_{f2})} & 0 & \frac{K3}{C1} - \frac{R_C \cdot K1}{C1} & \frac{R_L \cdot K2}{C1(R_L+R_C)} & \frac{1}{C1 \cdot R_{13}} \\ 0 & \frac{1}{L} & 0 & 0 & -\frac{1}{L}(R_L+R_C) & \frac{-R_L}{L(R_L+R_C)} & 0 \\ 0 & 0 & 0 & 0 & \frac{R_L}{C(R_L+R_C)} & \frac{-1}{C(R_L+R_C)} & 0 \\ 0 & 0 & 0 & 0 & \frac{R_C}{C_2 \cdot R_{13}} & \frac{R_L}{C_2 \cdot R_{13}(R_L+R_C)} & \frac{-1}{C_2 \cdot R_{13}} \end{bmatrix}$$

(7-14)

$$G1 = \begin{bmatrix} \frac{1}{L1} & 0 & 0 & 0 \\ 0 & 0 & 0 & 0 \\ 0 & 0 & 0 & 0 \\ 0 & \frac{1}{C1 \cdot R_{14}} & \frac{n}{C1 \cdot R_{14}} & 0 \\ 0 & 0 & -\frac{1}{L} & 0 \\ 0 & 0 & 0 & 0 \\ 0 & 0 & 0 & 0 \end{bmatrix}$$

(7-15)

$$K3 = \frac{R_{f2}}{R_{f1} + R_{f2}} \quad (7-16)$$

In equation (7-15)  $k_1$ ,  $k_2$  and  $\underline{u}$  are as defined earlier.

F2= F1 except for

$$F2(2,5) = 0$$

$$F2(3,5) = 0$$

$$F2(4,2) = 0$$

$$F2(4,5) = -R_C \cdot k_1 / C_1' \quad (7-17)$$

$$F2(5,2) = 0$$

and

G2= 0 except for

$$G2(1,1) = 1/L_1$$

$$G2(4,2) = 1/C_1' \cdot R_{14} \quad (7-18)$$

$$G2(4,4) = n/C_1' \cdot R_4$$

$$G2(5,4) = -1/L$$

The solutions of the state equations and the procedure for propagation of the state from cycle to cycle is identical to the procedure for the case without feedforward.

The discrete simulation technique outlined [12,13,14] lends itself easily to simulation of transient response for

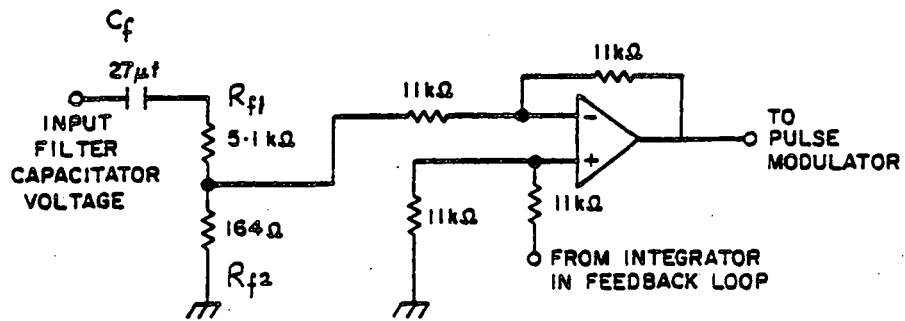


Figure 67: Nonadaptive feedforward circuit

a step change in supply voltage. The change in supply voltage is made to occur at the start of a new ON period; thus all that is necessary to do is to change the value of  $T_{ON}$  before the start of a new cycle.

## 7.2 DESCRIPTION OF THE PROGRAM

A flowchart of the program [12,13,14] is shown in Figure 68 while a listing of the programs is included in the Appendix. The flowchart is for the simulation without feedforward, the simulation with feedforward proceeds in an identical fashion.

A minimum off time duty cycle control is implemented in the program. The regulator also has peak current protection and this capability is also programmed. During the ON period the current in the switch may rise above the set value of the peak current. Newton's iteration [12,13,14] is performed to find the exact point in time where this occurs and the program will automatically terminate the ON time calculation when the current exceeds the set value.

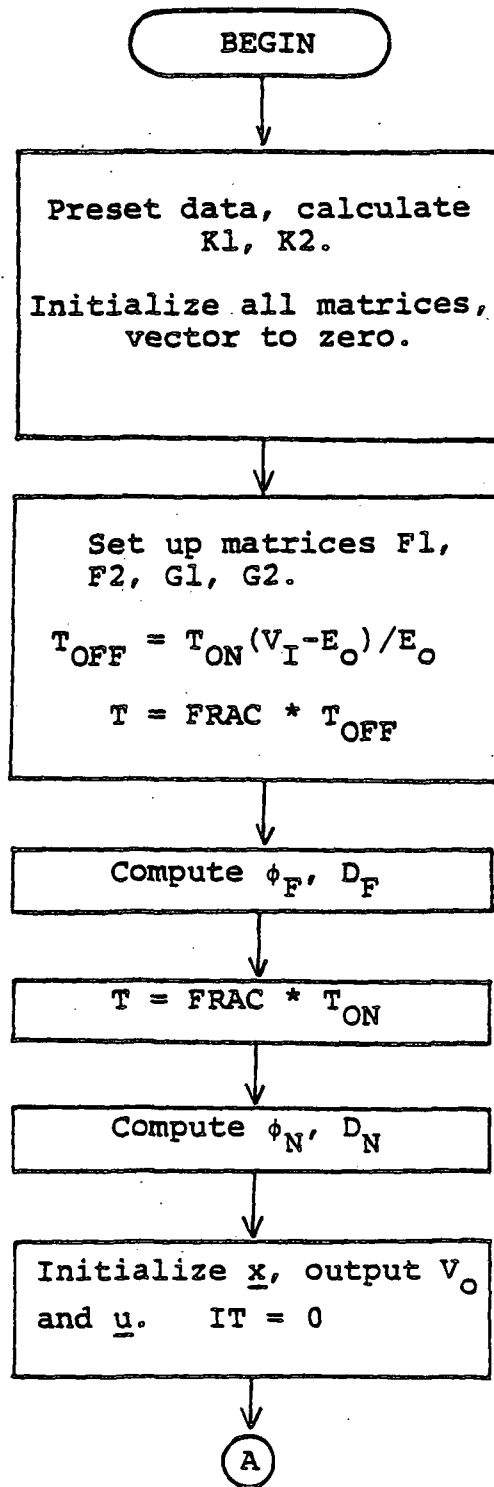
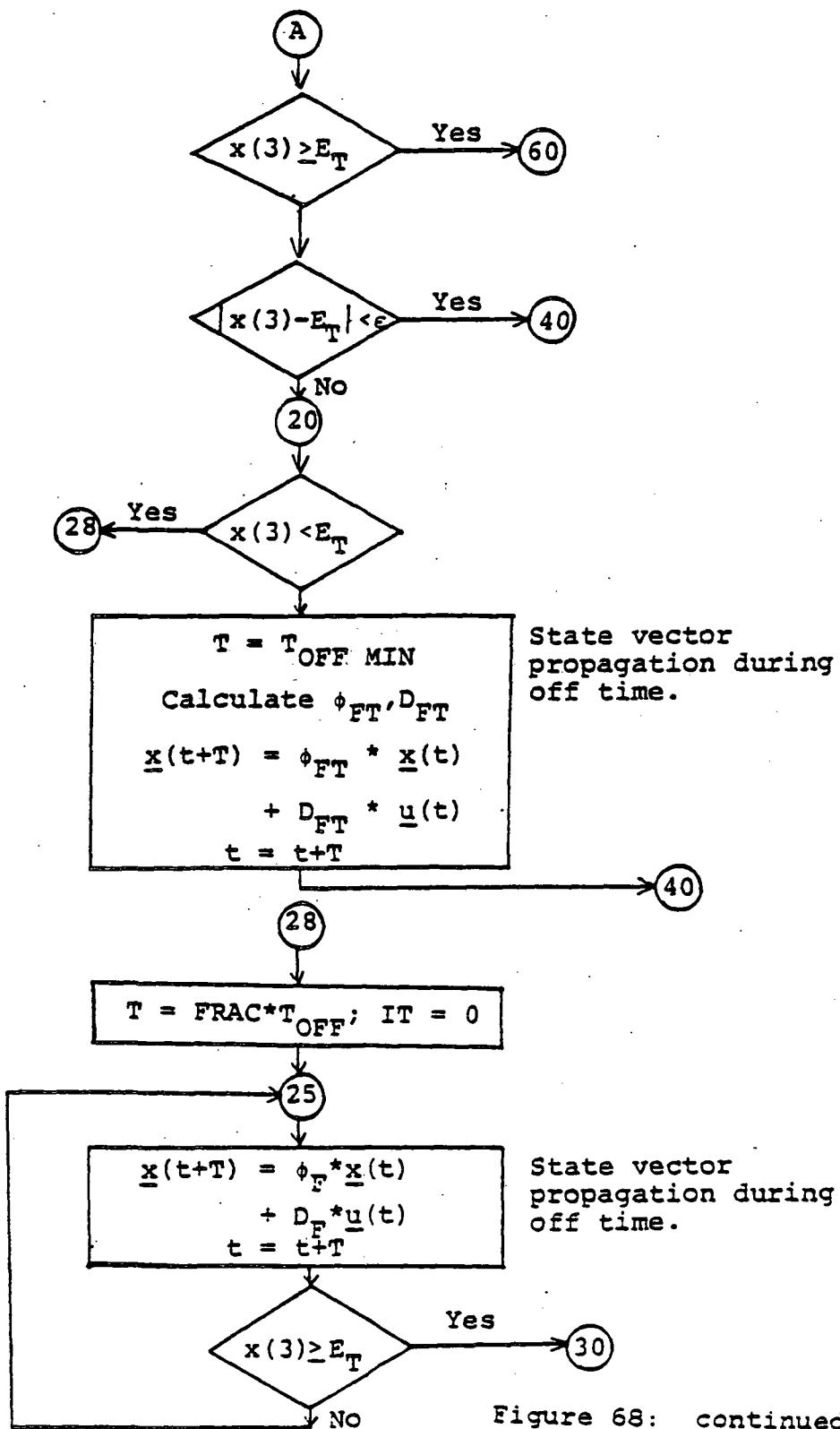


Figure 68: Flow chart for discrete simulation



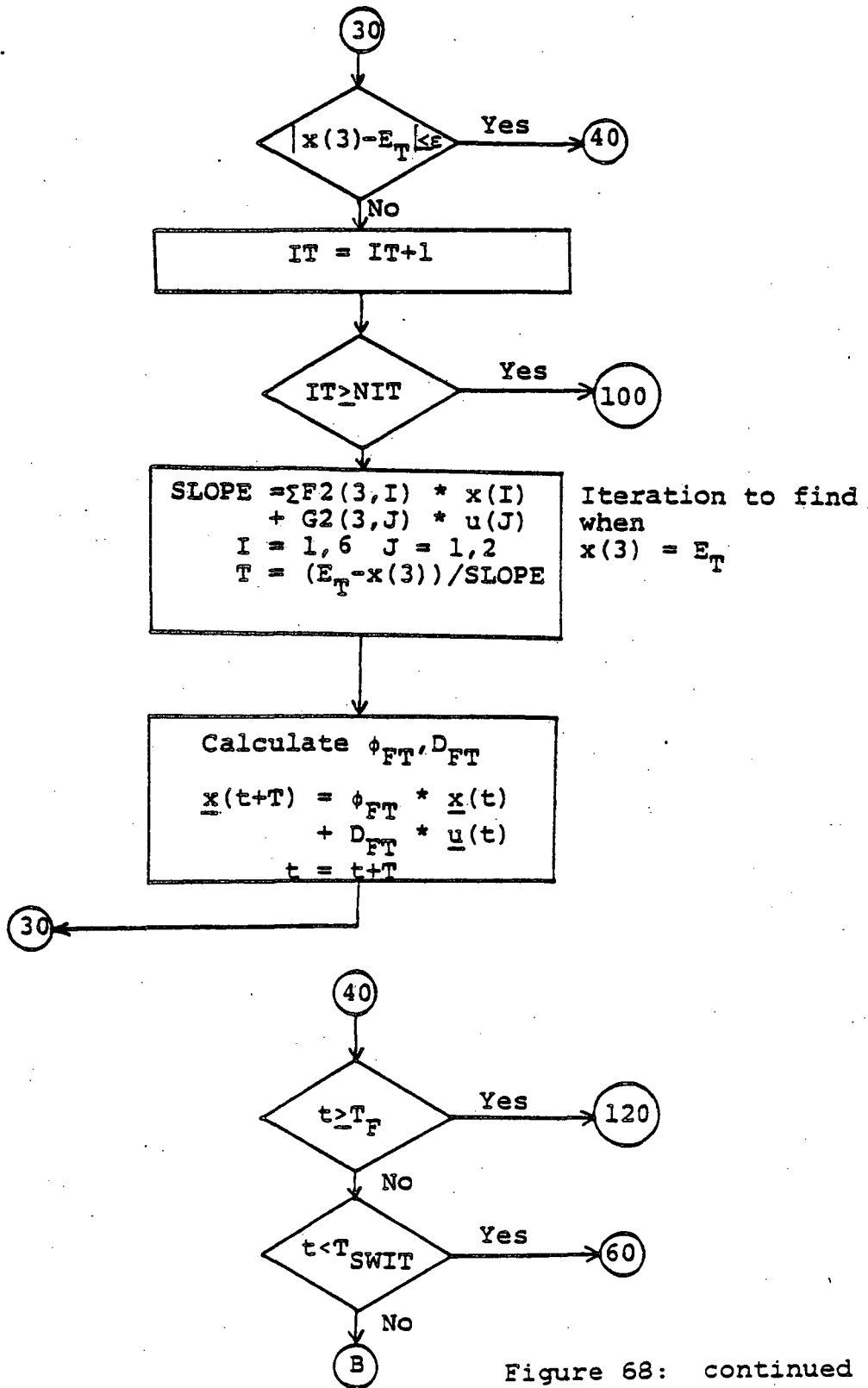


Figure 68: continued

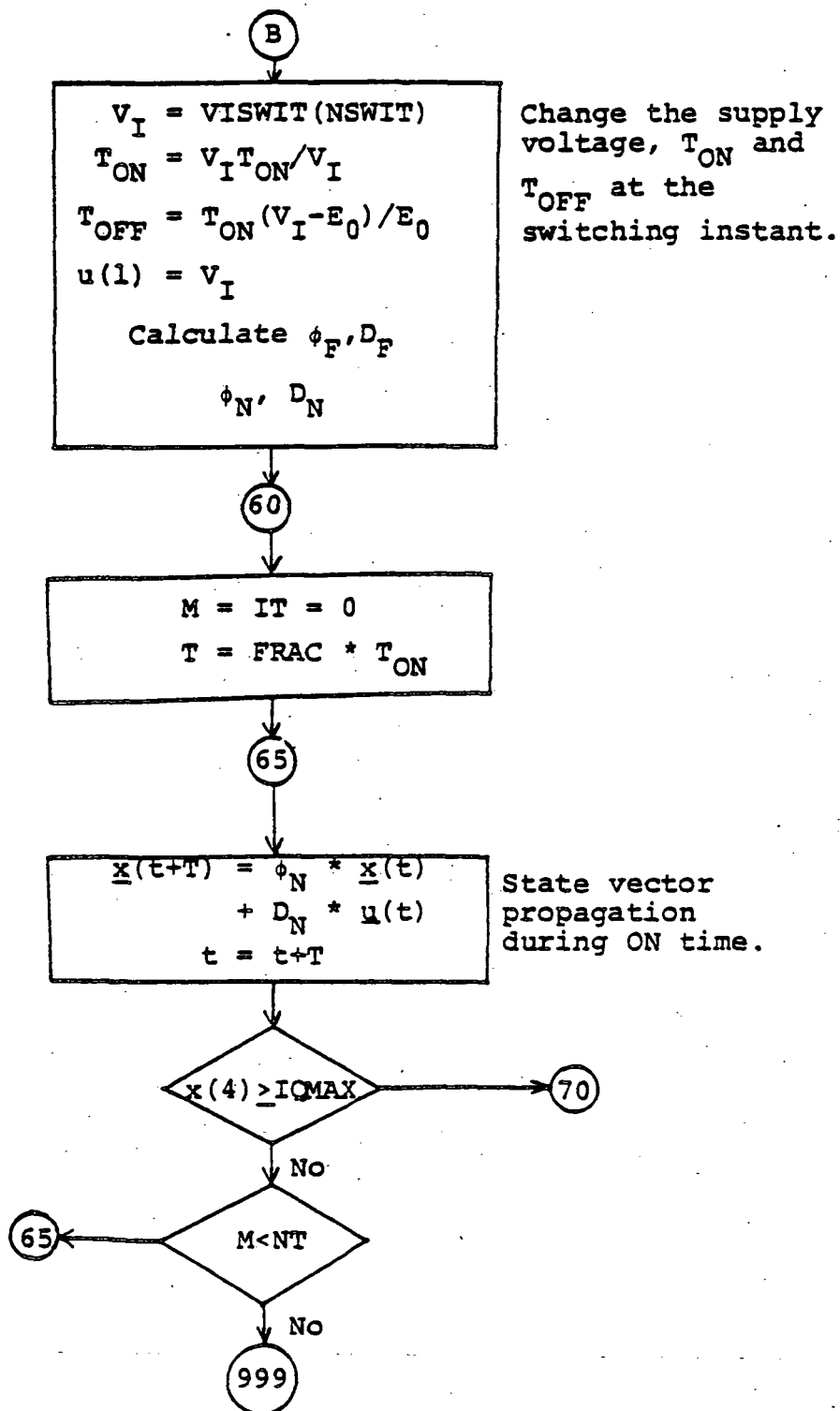


Figure 68: continued

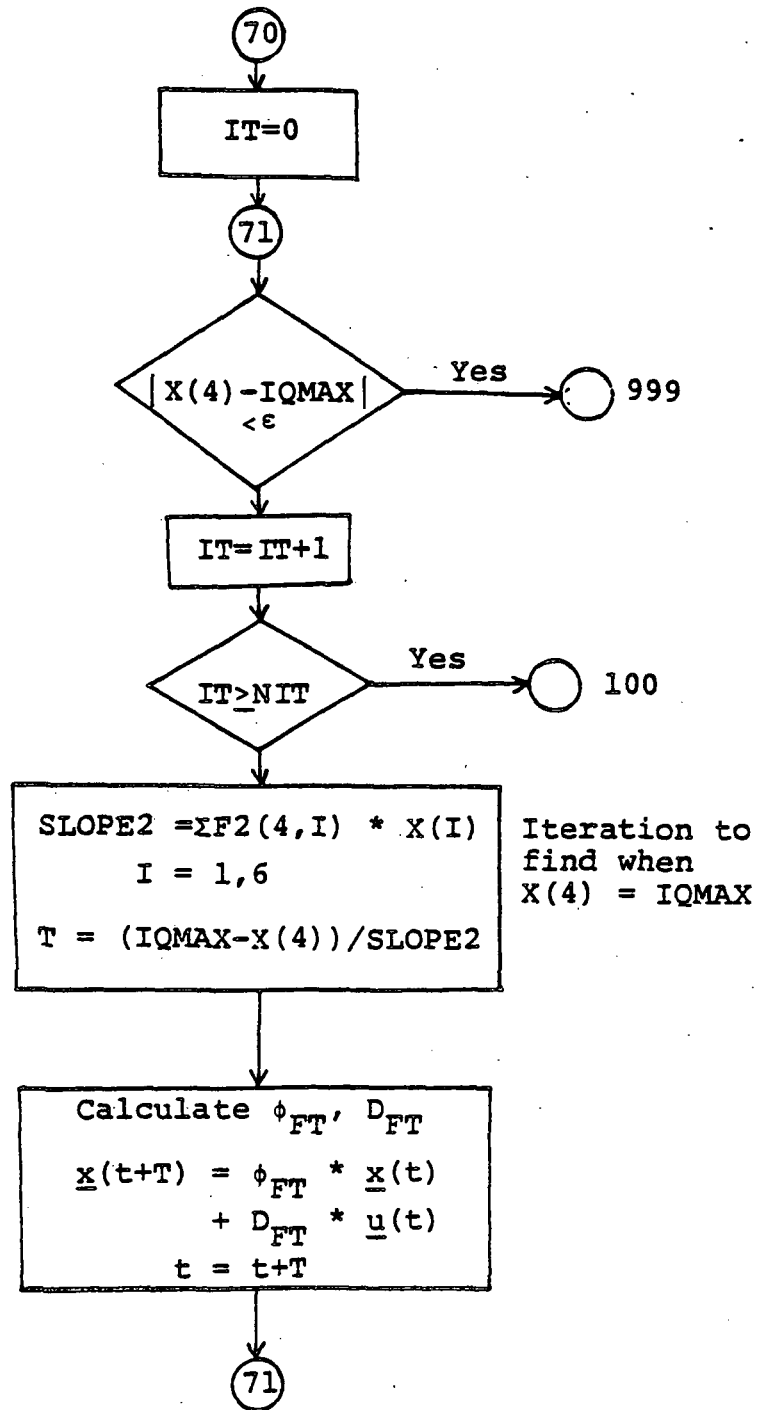


Figure 68: continued

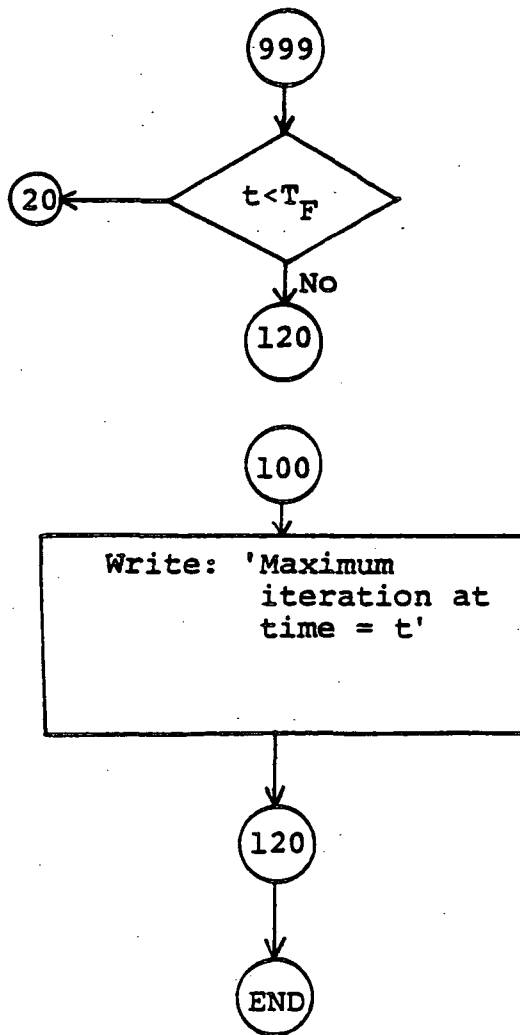


Figure 68: continued

### 7.3 SIMULATION RESULTS

The simulation program was used to simulate the behavior of the system with and without feedforward for a small step change in supply voltage from 30v to 40v and also for a large step change from 40v to 25v. Simulation results presented are in close agreement with the experimental results presented in Chapter 6.

#### 7.3.1 Simulation of steady state operation

The computer program discussed can be used to simulate the steady state operation of the regulator system [12,13,14]. An accurate picture of the behavior of the system is obtained since the simulation method used is an exact method.

The buck regulator of Figure 34 with feedforward was simulated with the following single-stage input filter parameters:

$$R_{L1} = 0.2 \text{ ohm} \quad L1 = 325 \text{ microH} \quad C1 = 220 \text{ microF}$$

The supply voltage  $V_I$  was set equal to 30v and the other parameters were as presented in section 6.1. Figures 69 (a) - (g) show the plots of the output voltage, input filter inductor current, input filter capacitor voltage, output filter inductor current, the feedforward voltage  $v_f$ , the control voltage and the voltage  $e_r$ . It is noticed that the switching period is around 50 microsecs and that the output

voltage ripple is around 60 millivolts. The input filter inductor current has a small magnitude ripple component at the switching frequency, as does the input filter capacitor voltage. The voltage fed forward  $v_f$  consists of the switching frequency component, however its magnitude is around 50 millivolts. The switching frequency component of the control voltage is seen to be around 800 millivolts and thus the effect of adding the switching frequency component from the input filter capacitor voltage to the control voltage would be negligible as discussed in Chapter 5 ; since the magnitude added would be around 1.5 millivolts ( $v_f$  multiplied by the feedforward gain).

### 7.3.2. Simulation for a small step change in supply voltage

The same buck regulator was used with its parameters as specified in section 7.3.1. A value of 0.6 ohm for  $R_{L1}$  was used. The supply voltage  $V_I$  was abruptly switched from  $V_I = 30V$  to 40V. Experimental results for this step change are given in Chapter 6 where a value of 0.2 ohm was specified for  $R_{L1}$ . A value of 0.6 ohm was used in the simulation as this represents the combined winding resistance and source impedance. The values of the other parameters used are:

$$T_{OFF}(\text{minimum}) = 5 \text{ microseconds}$$

$$I_Q(\text{maximum}) = 6 \text{ amps. (set value of peak current)}$$

$$E_Q = 0.2 \text{ volt}$$

$$E_D = 0.7 \text{ volt}$$

(7-19)

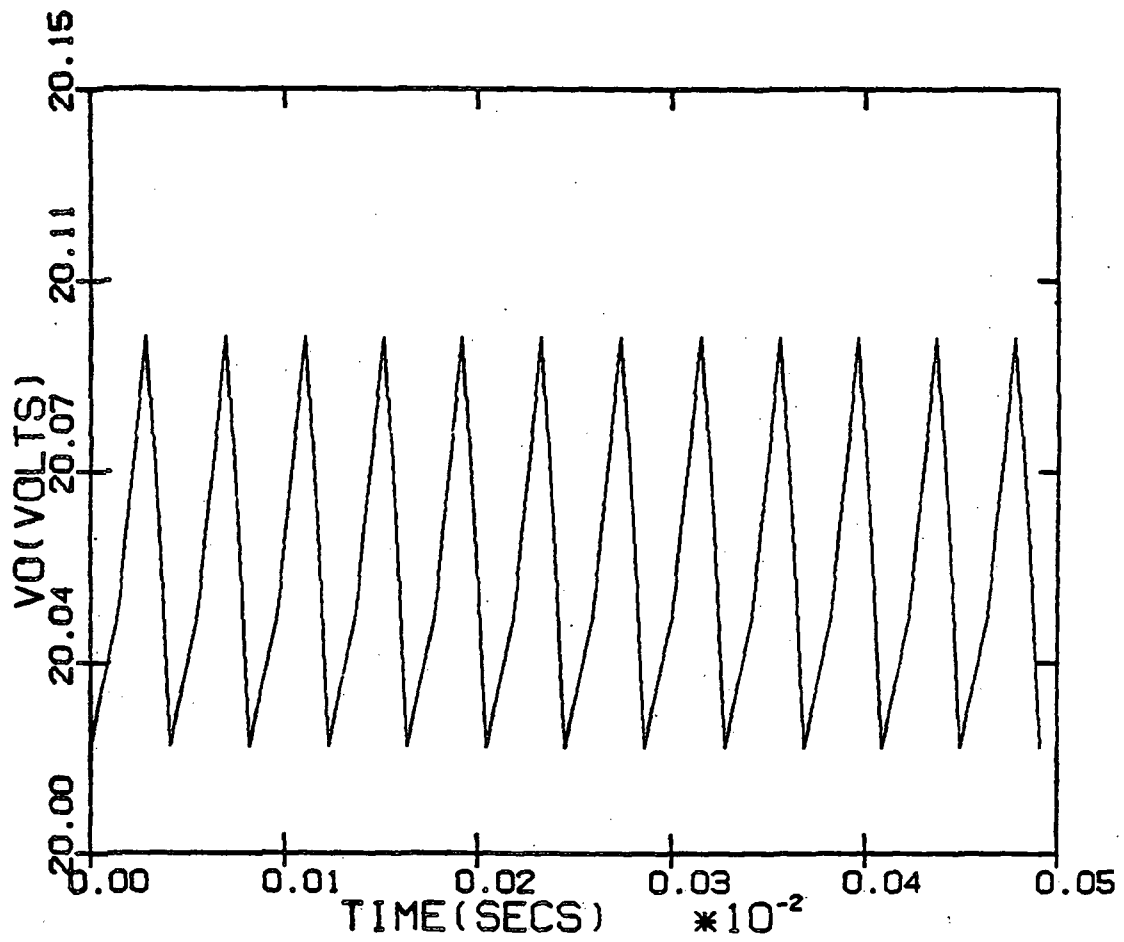


Figure 69: (a) Output voltage during steady state operation.

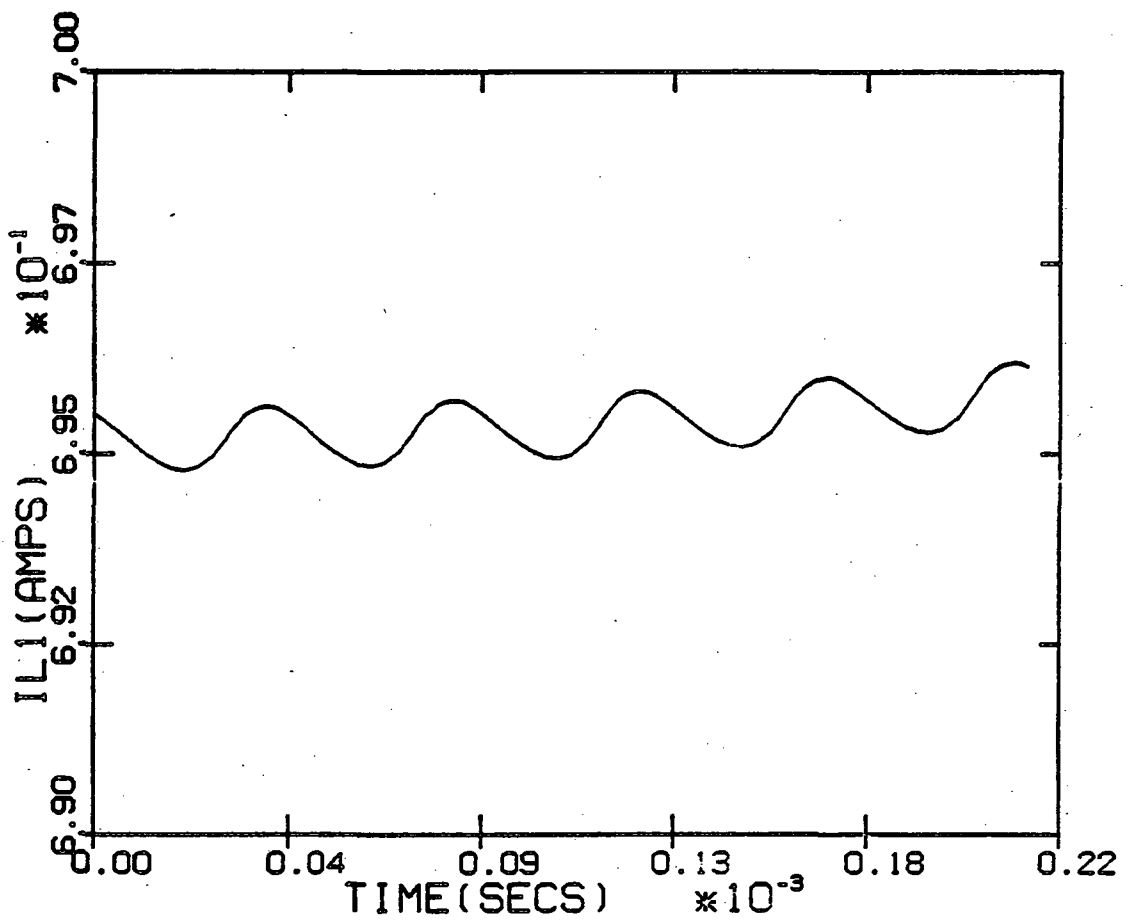


Figure 69: (b) Input filter inductor current during steady state operation

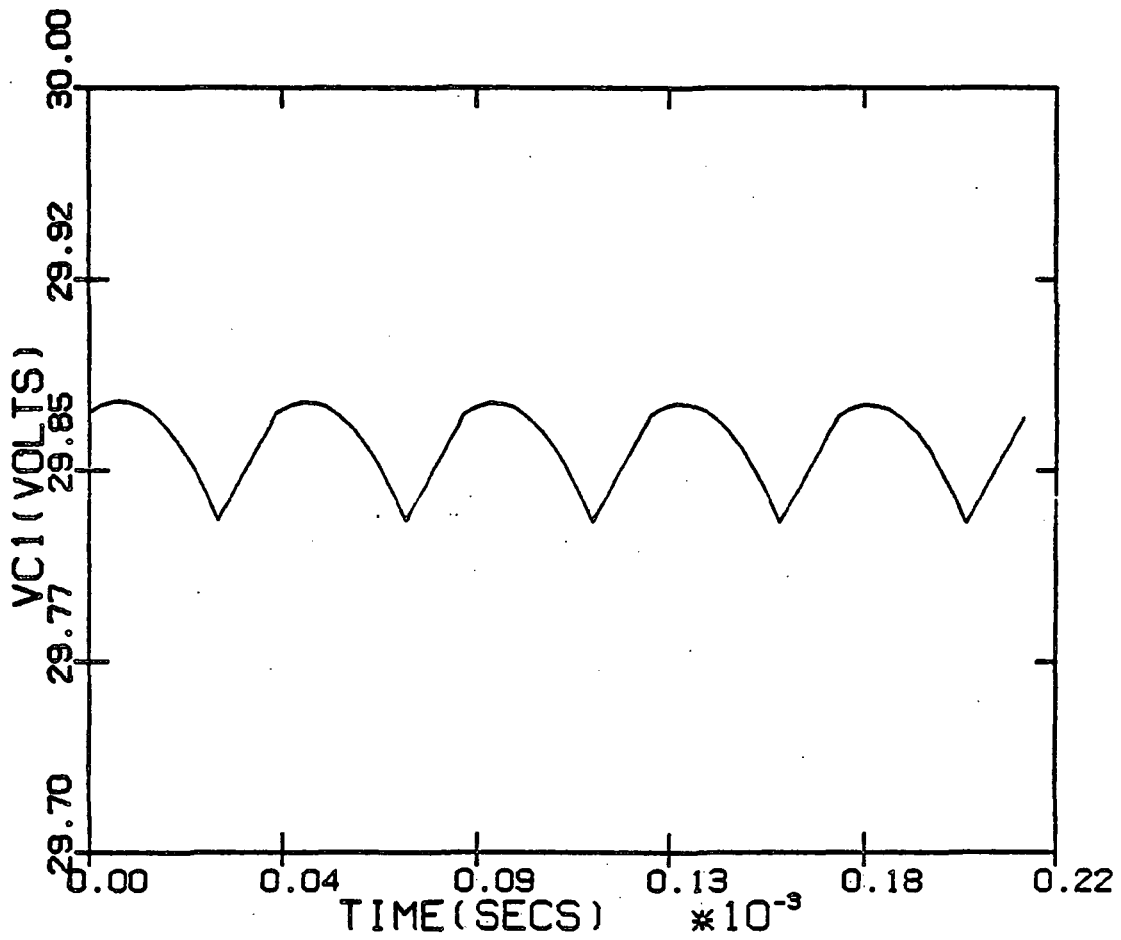


Figure 69: (c) Input filter capacitor voltage during steady state operation

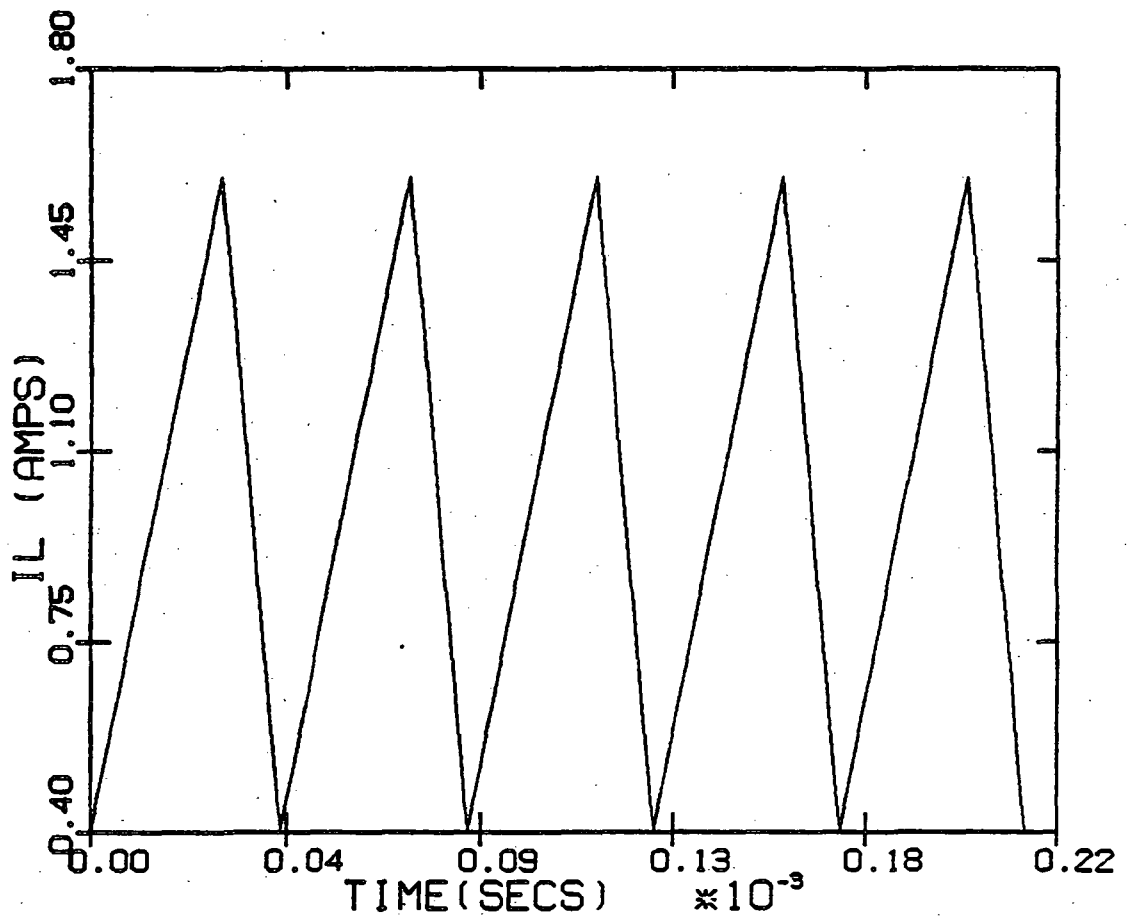


Figure 69: (d) Output filter inductor current during steady state operation

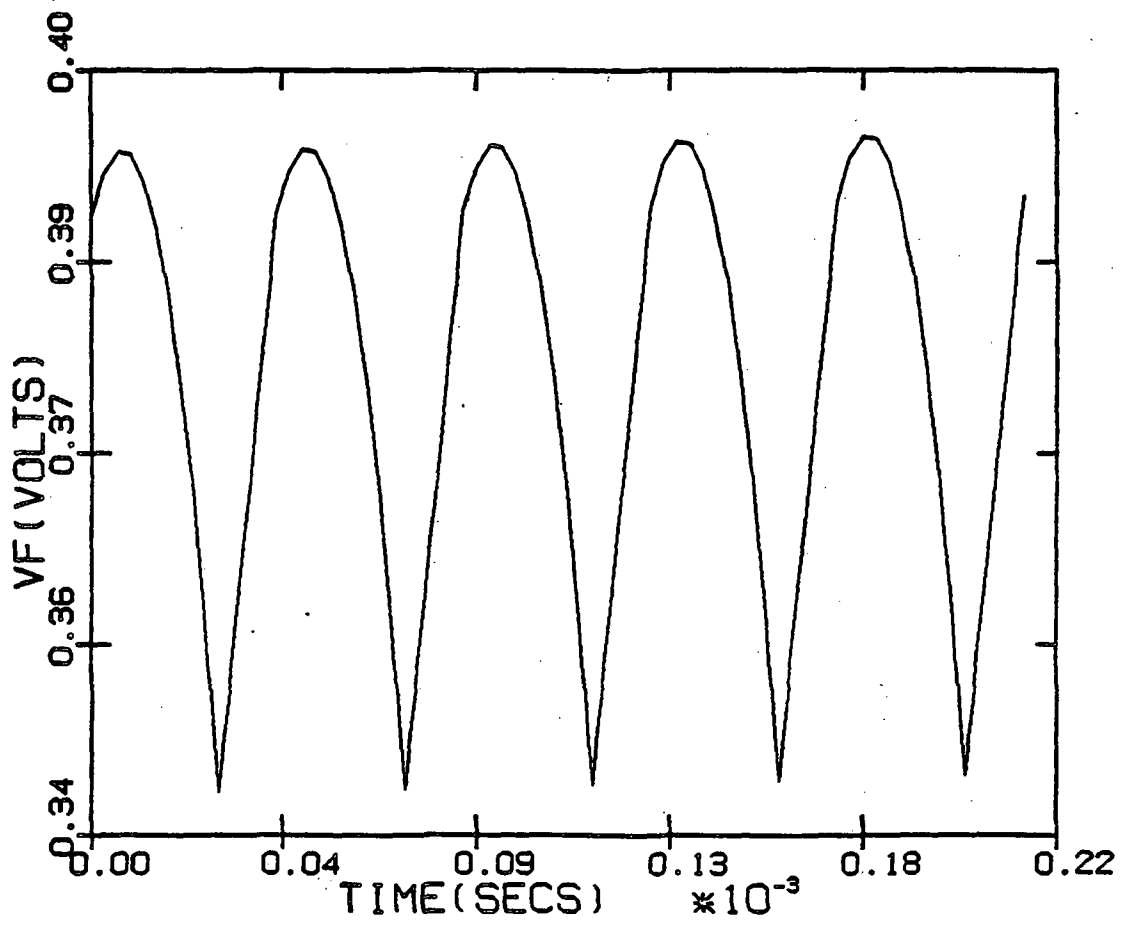


Figure 69: (e) Feedforward voltage during steady state operation

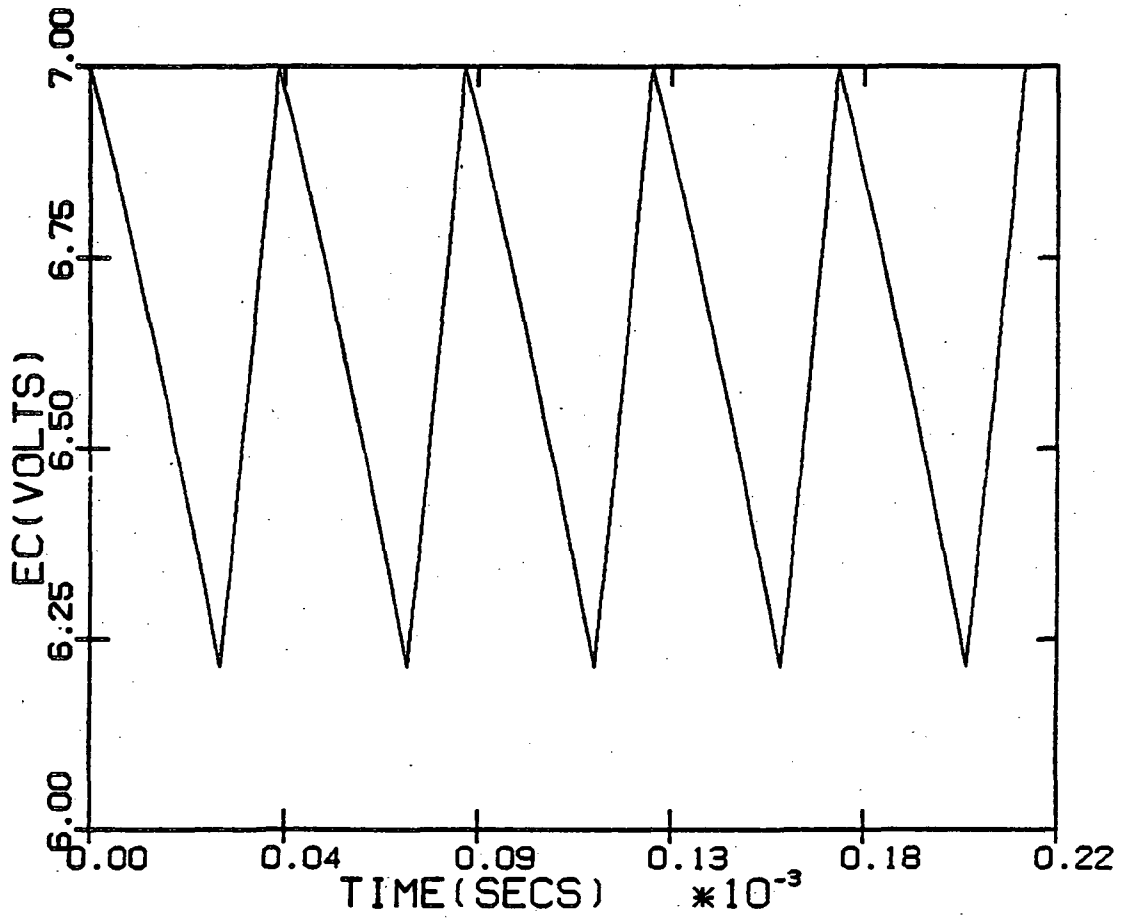


Figure 69: (f) Control voltage during steady state operation

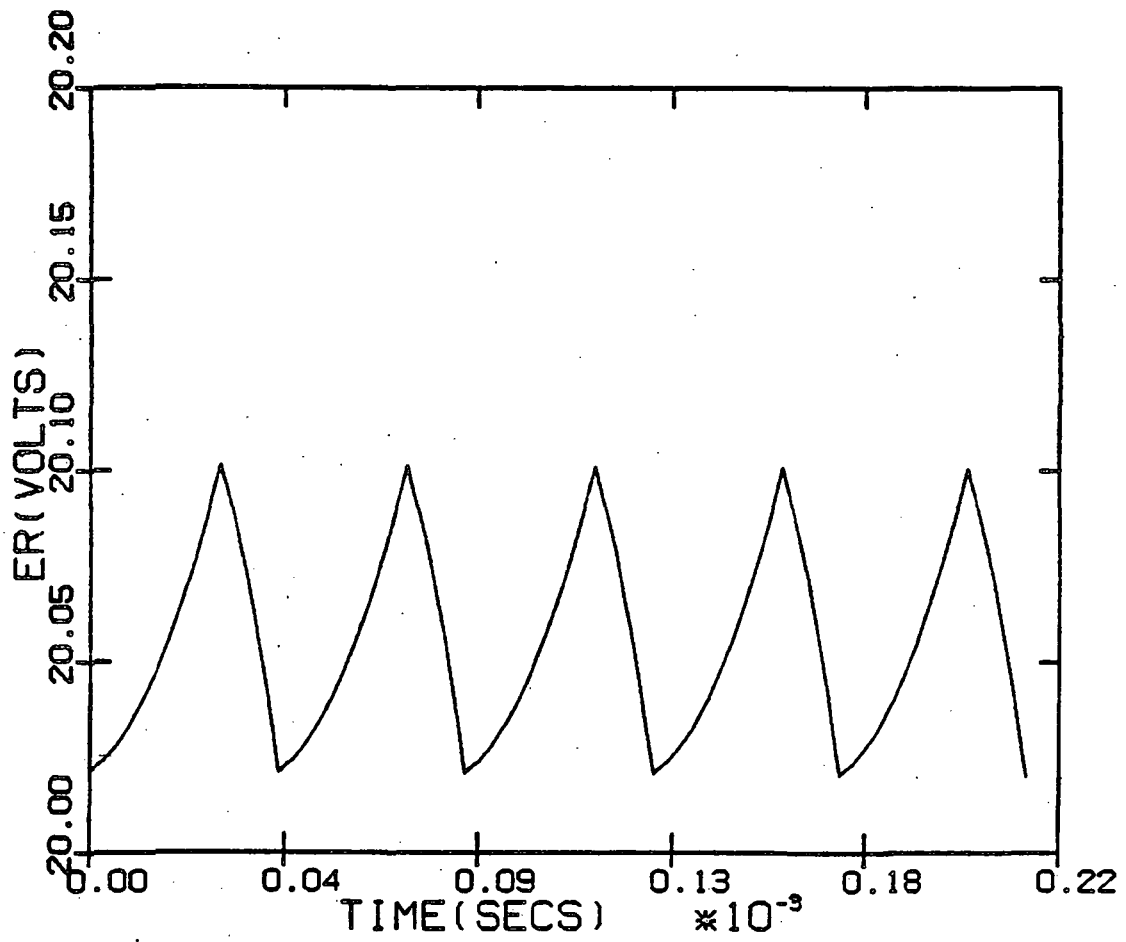


Figure 69: (g) Voltage  $e_R$  during steady state operation

Figures 70 (a) - (d) are plots of the computed values of output voltage, input filter capacitor voltage, output filter inductor current and the control voltage, all without feedforward.

The nonadaptive feedforward design of Figure 67 was used in the simulation of transient response with feedforward. The feedforward circuit parameters used at  $V_I = 30V$  were:

$$C_f = 27 \text{ microF} \quad R_{f1} = 5.1 \text{ Kohm} \quad R_{f2} = 164 \text{ ohm}$$

when the supply voltage is switched to 40V the value of  $R_{f2}$  in the program is changed to 90.97 ohm at the switching instant thus changing the feedforward circuit gain in accordance with the feedforward design.

Figures 71 (a)-(d) are plots of the computed values of the same variables with feedforward. Experimental measurements for the same step change in supply voltage were presented in Chapter 6 and are repeated here for convenience; Figures 72 (a)-(d) are the measurement waveforms without feedforward loop while Figures 73 (a)-(d) are for the case with feedforward loop.

Comparing the plots of the computed values with and without feedforward it is clearly seen that the analytical

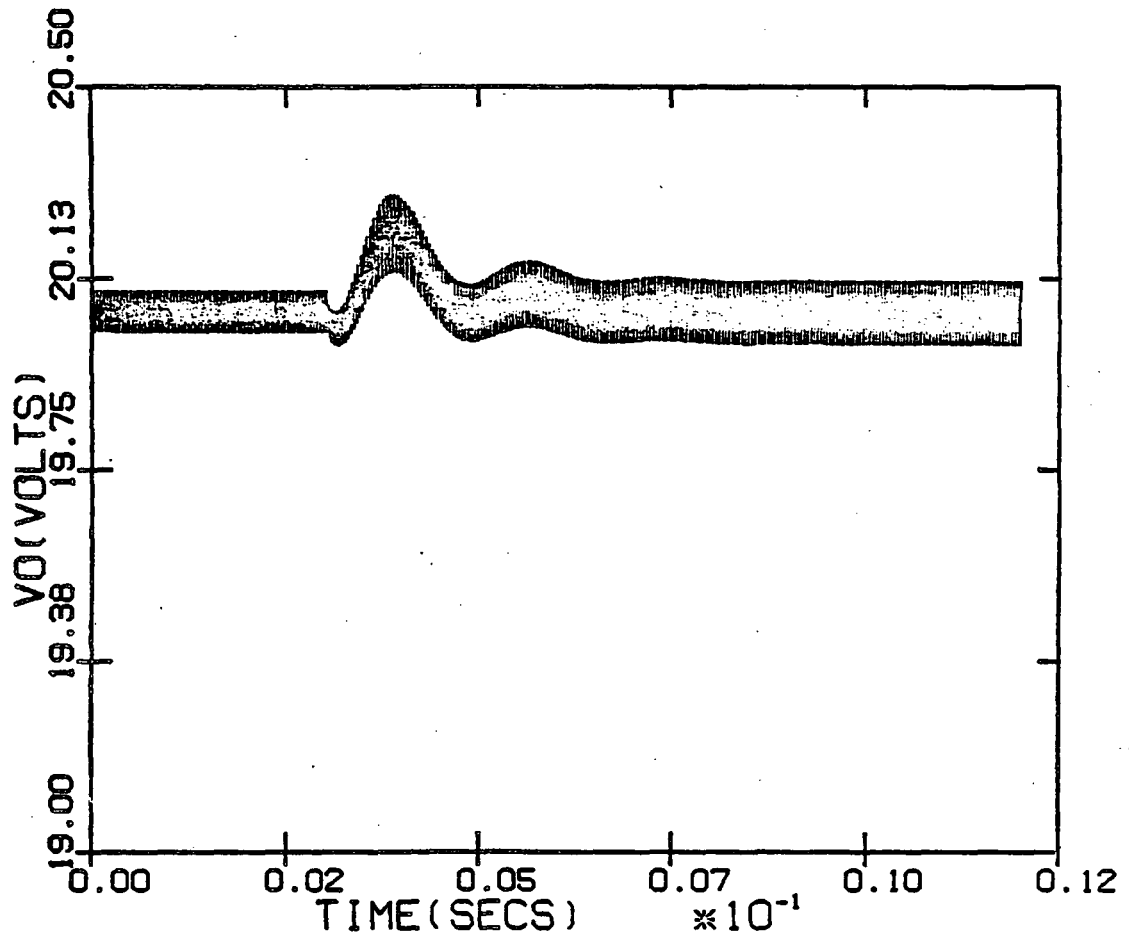


Figure 70: (a) Output voltage simulation without feedforward

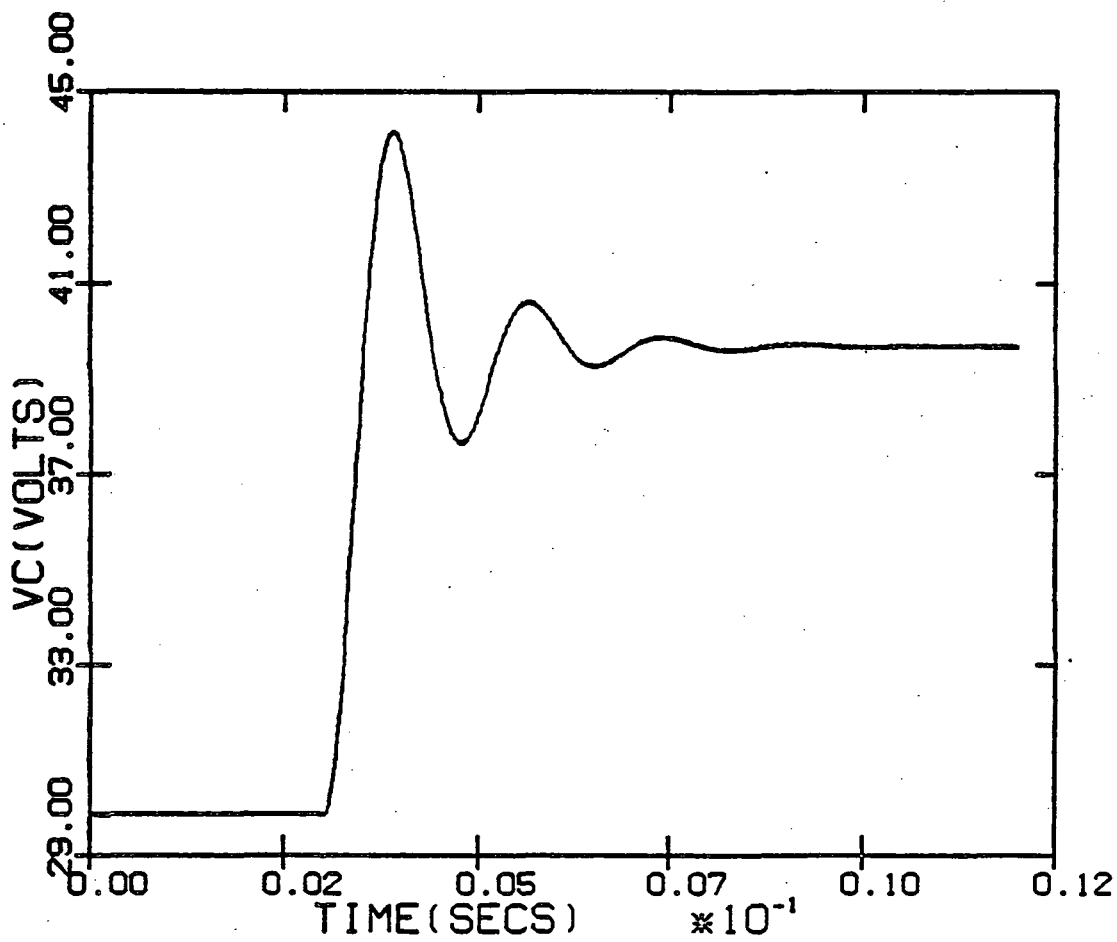


Figure 70: (b) Input filter capacitor voltage simulation without feedforward

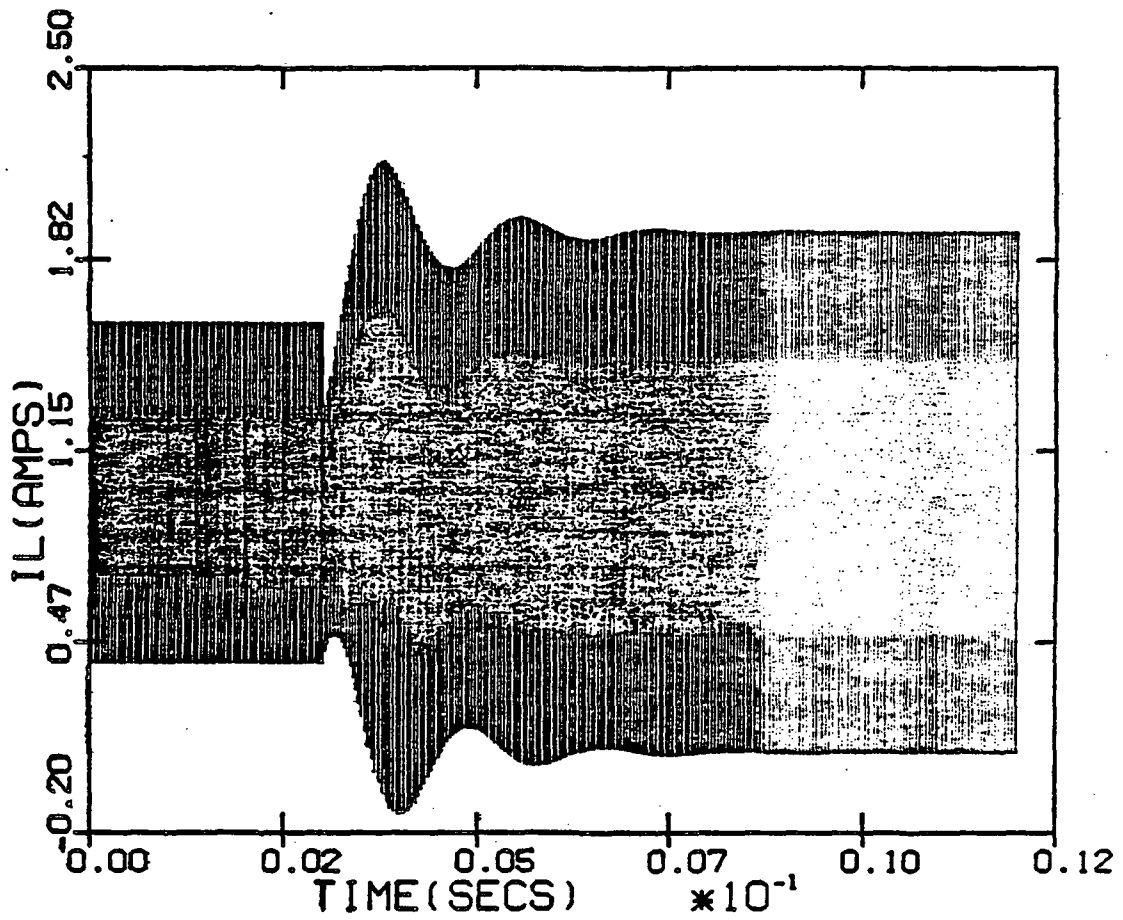


Figure 70: (c) Output filter inductor current simulation without feedforward

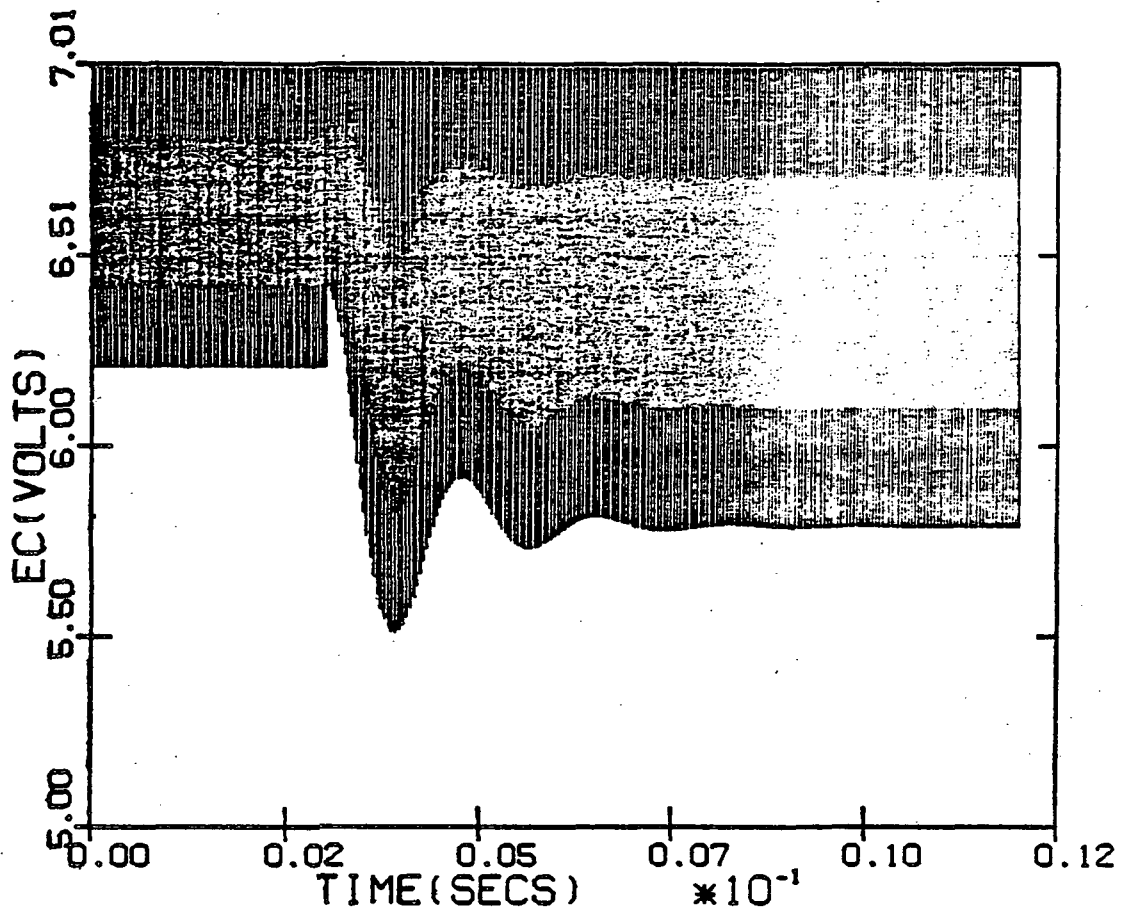


Figure 70: (d) Control voltage simulation without feedforward

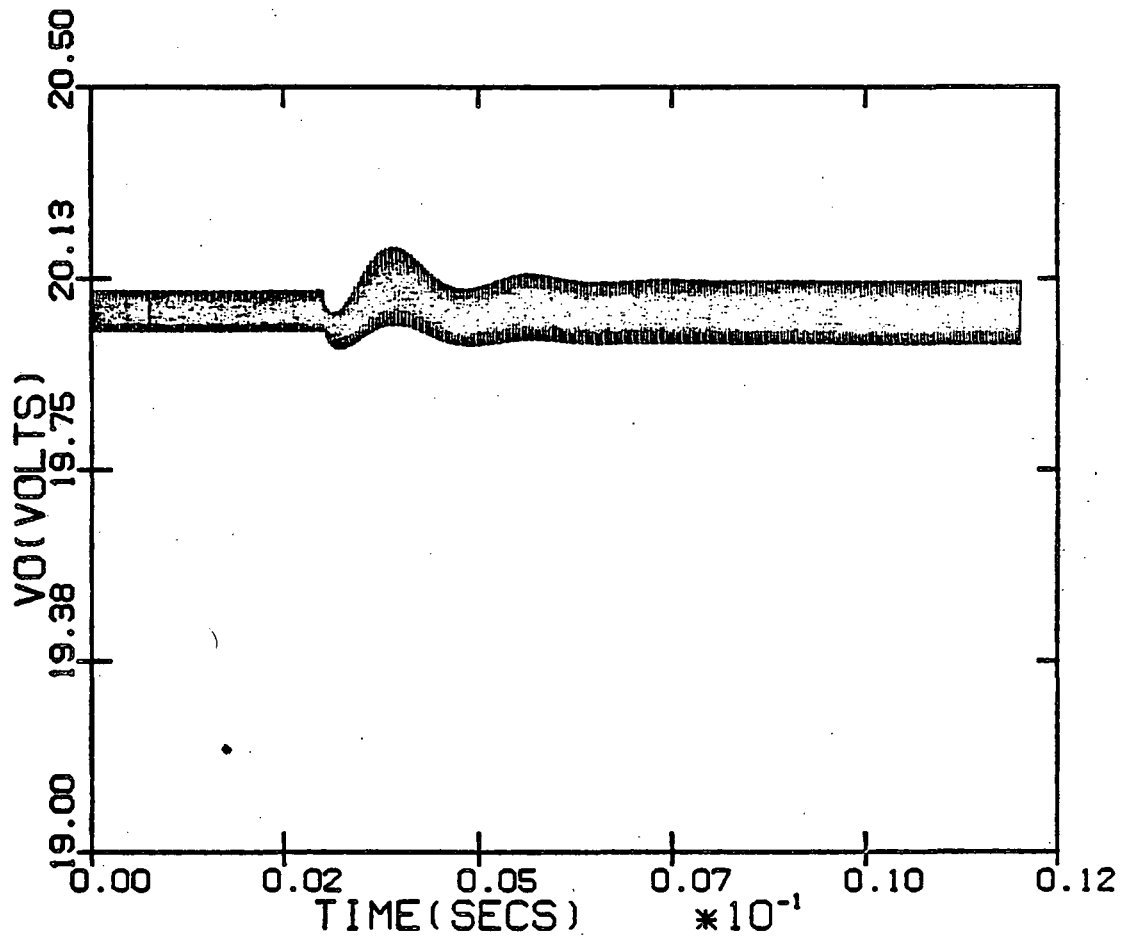


Figure 71: (a) Output voltage simulation with feedforward

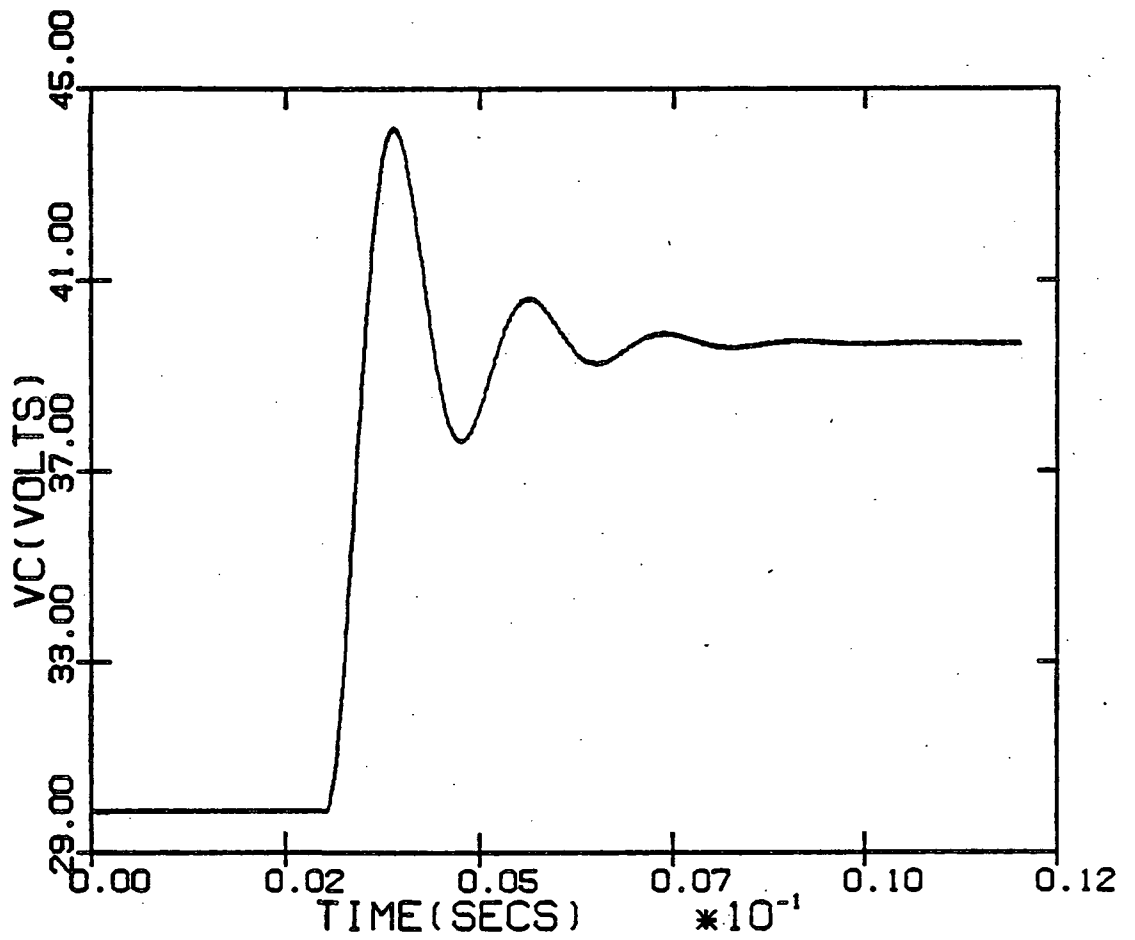


Figure 71: (b) Input filter capacitor voltage simulation with feedforward

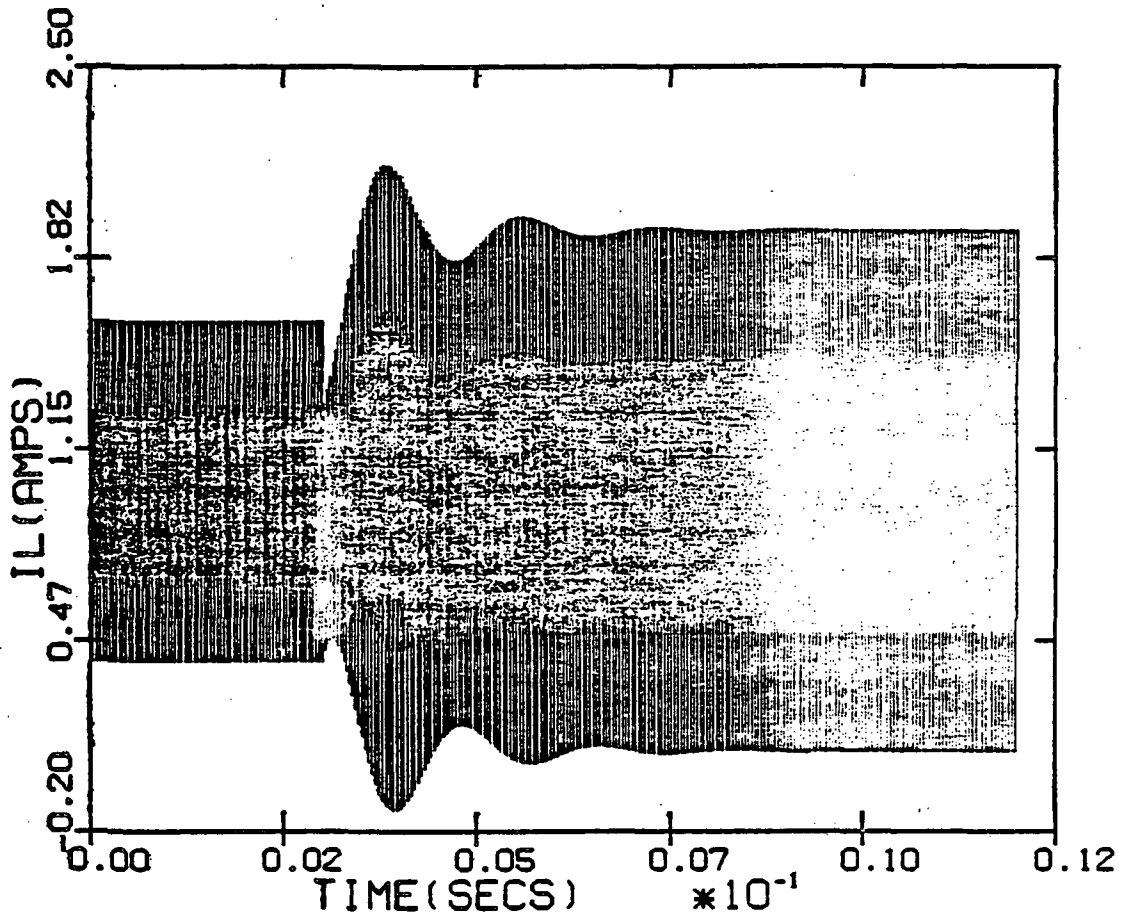


Figure 71: (c) Output filter inductor current simulation with feedforward

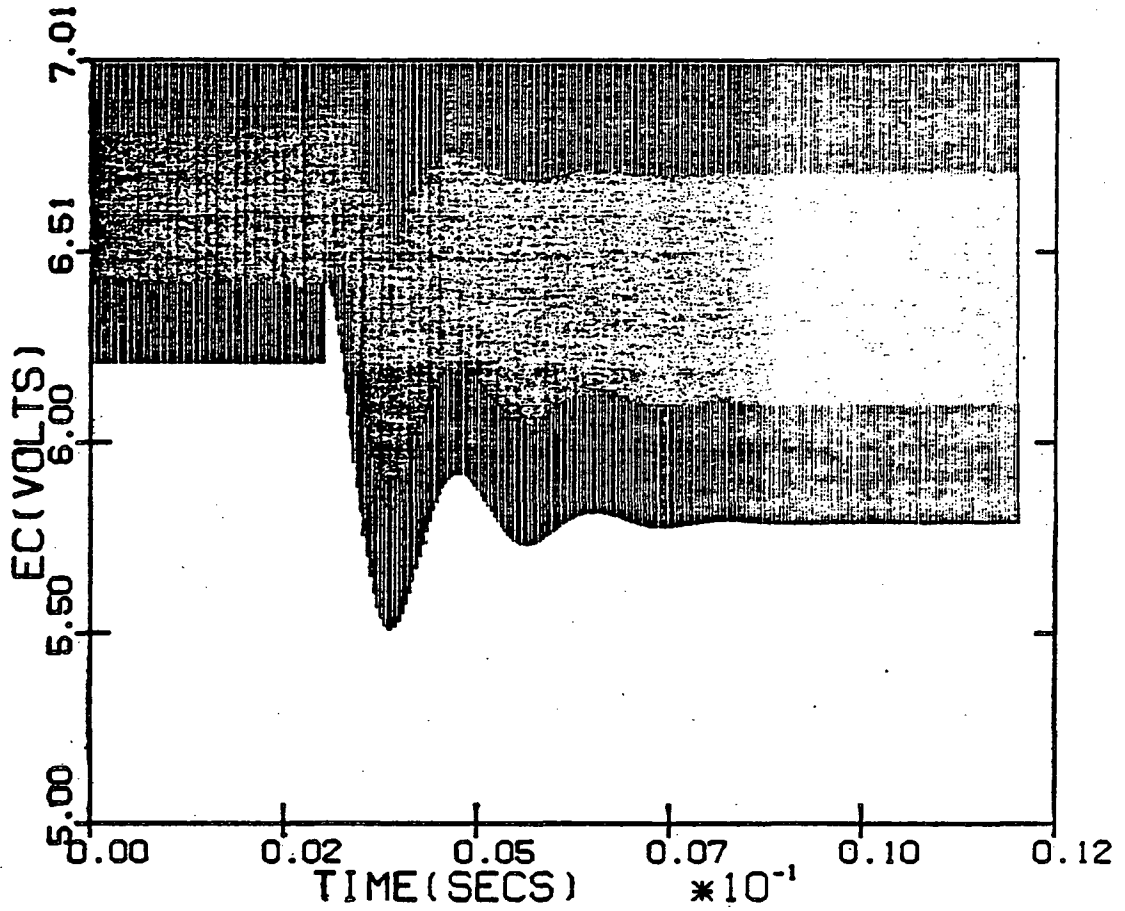
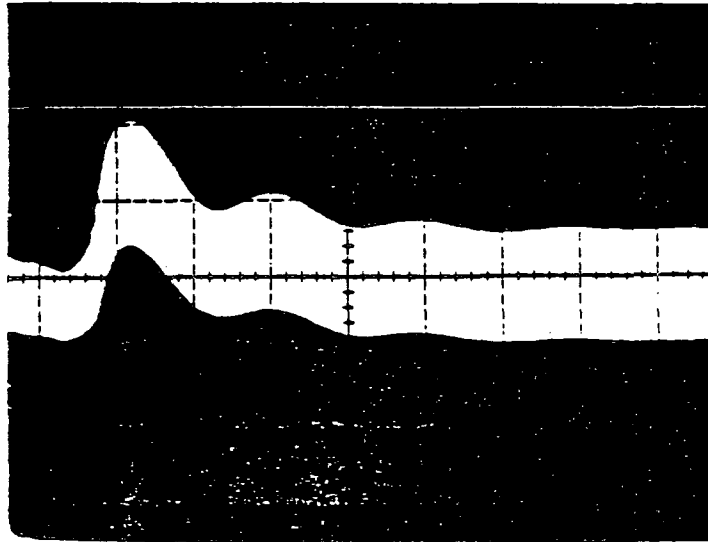
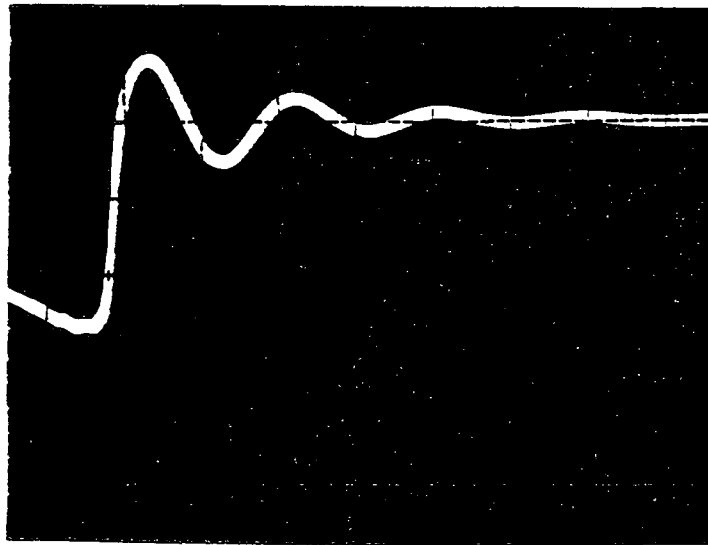


Figure 71: (d) Control voltage simulation with feedforward

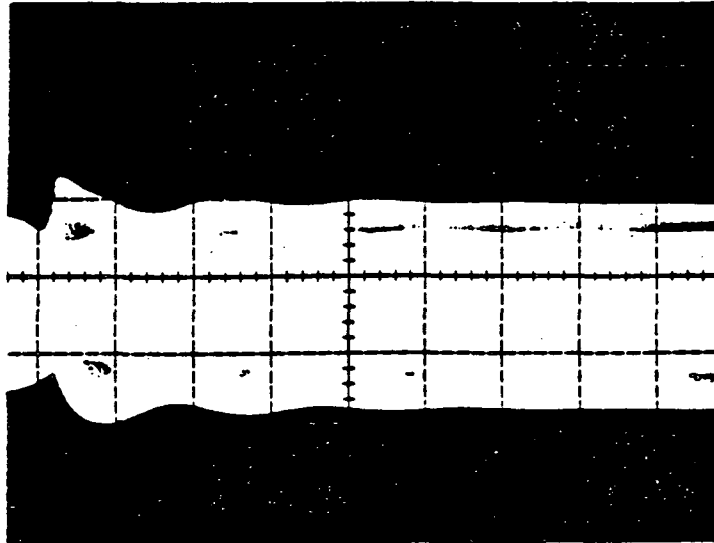


(a)

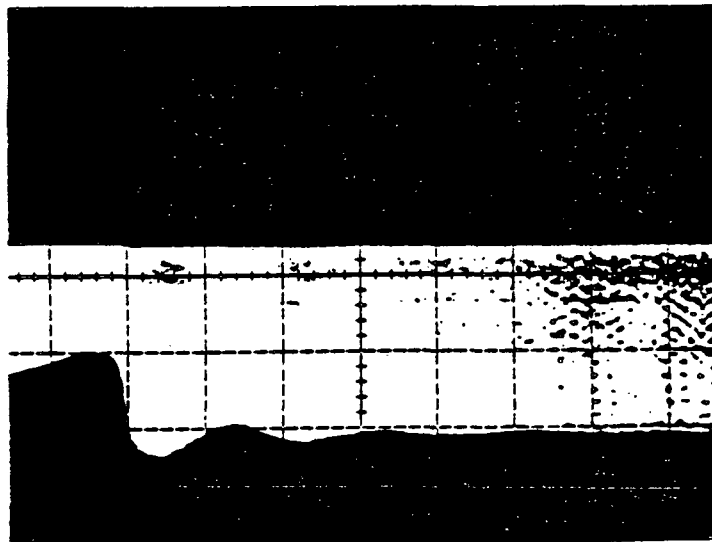


(b)

Figure 72: Measurement without feedforward: output voltage  
 (a) and input filter capacitor voltage (b)  
 (a) Y—0.1v/div X—1 msec/div  
 (b) Y—5v/div X—1 msec/div



(c)

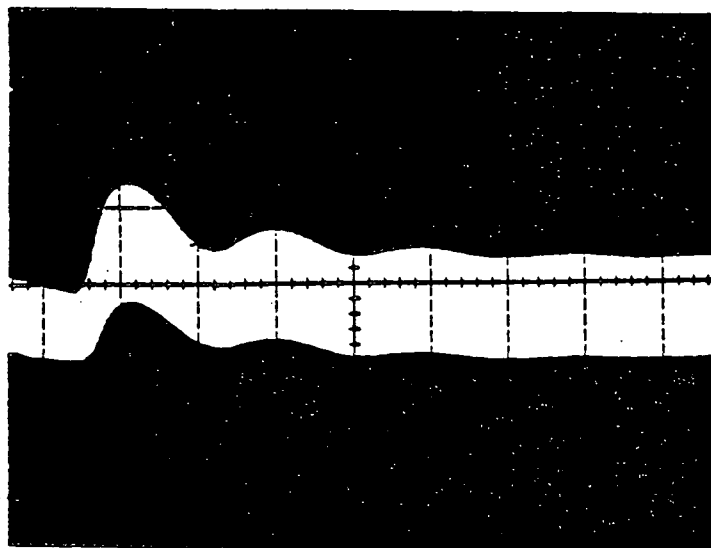


(d)

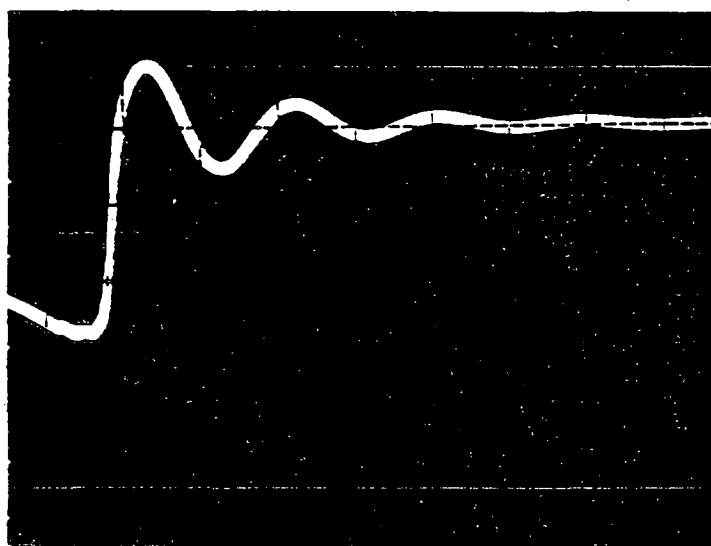
Figure 72: Measurement without feedforward: output filter inductor current (c) and control voltage (d)

(a) Y—0.5 A/div X—1 msec/div

(b) Y—0.5v/div X—1 msec/div

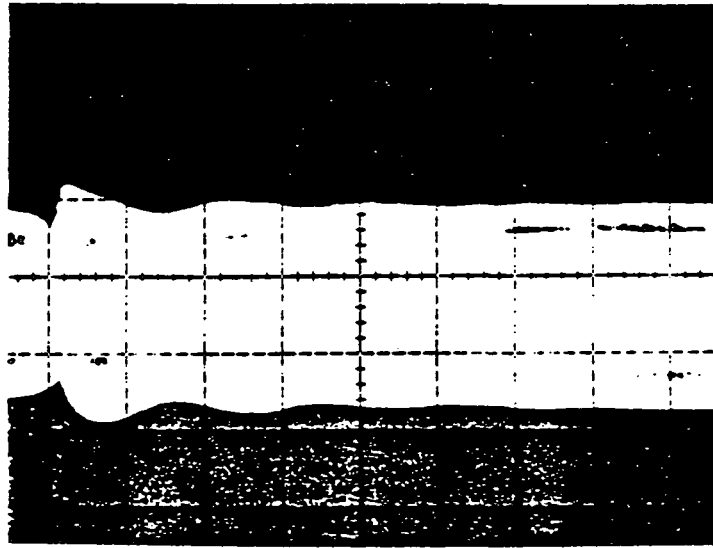


(a)

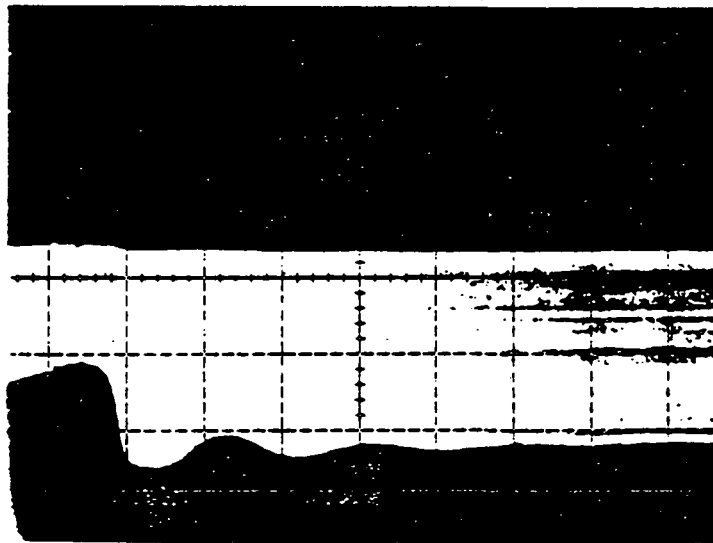


(b)

Figure 73: Measurement with feedforward: output voltage (a)  
and input filter capacitor voltage (b)  
(a) Y—0.1v/div X—1 msec/div  
(b) Y—5v/div X—1 msec/div



(c)



(d)

Figure 73: Measurement with feedforward: output filter inductor current (c) and control voltage (d)

(a) Y—0.5 A/div X—1 msec/div

(b) Y—0.5v/div X—1 msec/div

results agree fairly closely with the experimental data. The analytical results show that the feedforward is effective in reducing the output voltage oscillations -- the amplitude of the oscillation is reduced (Figures 70 (a) and 71 (a)); this is confirmed by the experimental results (Figures 72 (a) and 73 (a)). The plots of the input filter capacitor voltage, output filter inductor current and the control voltage are also in excellent agreement with the experimental data. Also in excellent agreement with the measured data is the observation that the plots of filter capacitor voltage, inductor current and control voltage do not show any noticeable difference between the two cases (with and without feedforward). An explanation for this observation was provided in Chapter 6.

It can thus be concluded that the addition of feedforward improves the transient response for the step change in  $V_I$ , as demonstrated both from the analytical result as well as experimental data.

### 7.3.3 Simulation for a Large Step Change in Supply Voltage

The regulator used was the one used in Section 7.3.1 with the same parameters. The single stage input filter parameters used were:

$$R_{L1} = 1 \text{ ohm} \quad L1 = 325 \text{ microH} \quad C1 = 220 \text{ microF}$$

The supply voltage was abruptly switched from  $V_I = 40V$  to 25V. Experimental results for this step change are given in Chapter 6 where a value of 0.2 ohm was specified for  $R_{L1}$ . A value of 1 ohm was used in the simulation as this represents the combined winding resistance and source impedance. The other parameters are as specified in Section 7.3.1.

Figures 74 (a-d) are plots of the computed values of output voltage, input filter capacitor voltage, output filter inductor current and the control voltage, all without feedforward.

The nonadaptive feedforward design of Figure 67 was used also in the simulation of transient response. When the voltage is switched from 40V to 25V the value of  $R_{f2}$  is changed from 90.97 ohm to 230.27 ohm in order to change the gain of the feedforward circuit in accordance with the feedforward design. Figures 75 (a-d) are plots of the computed values of the same variables with feedforward. Experimental measurements for the same step change in supply voltage were presented in Chapter 6 and are repeated here for convenience; Figure 76 shows the measured output voltage ripple without and with feedforward.

Comparing the plots of the output voltage ripple with the measured data it is clearly seen that the analytical results agree closely with the experimental data. It can be

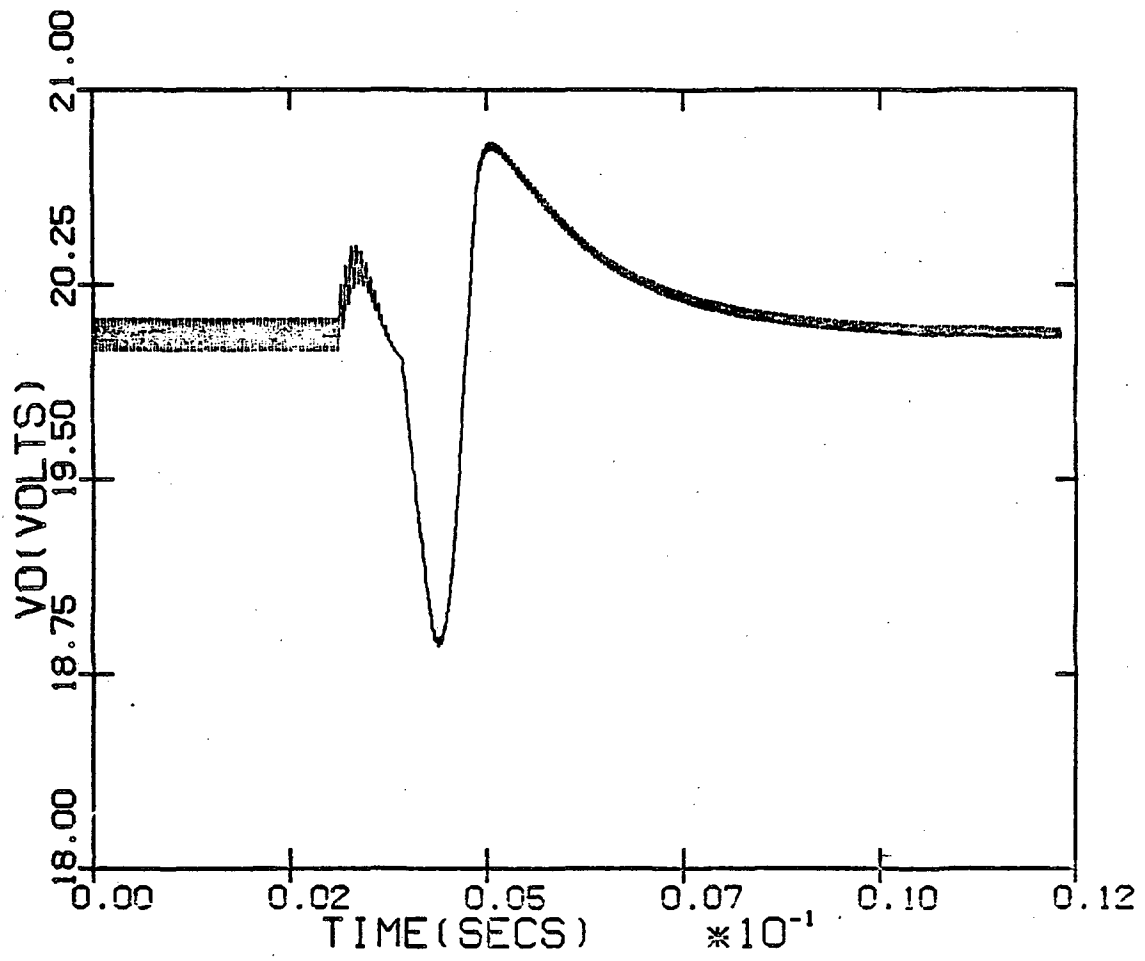


Figure 74: (a) Output voltage simulation without feedforward

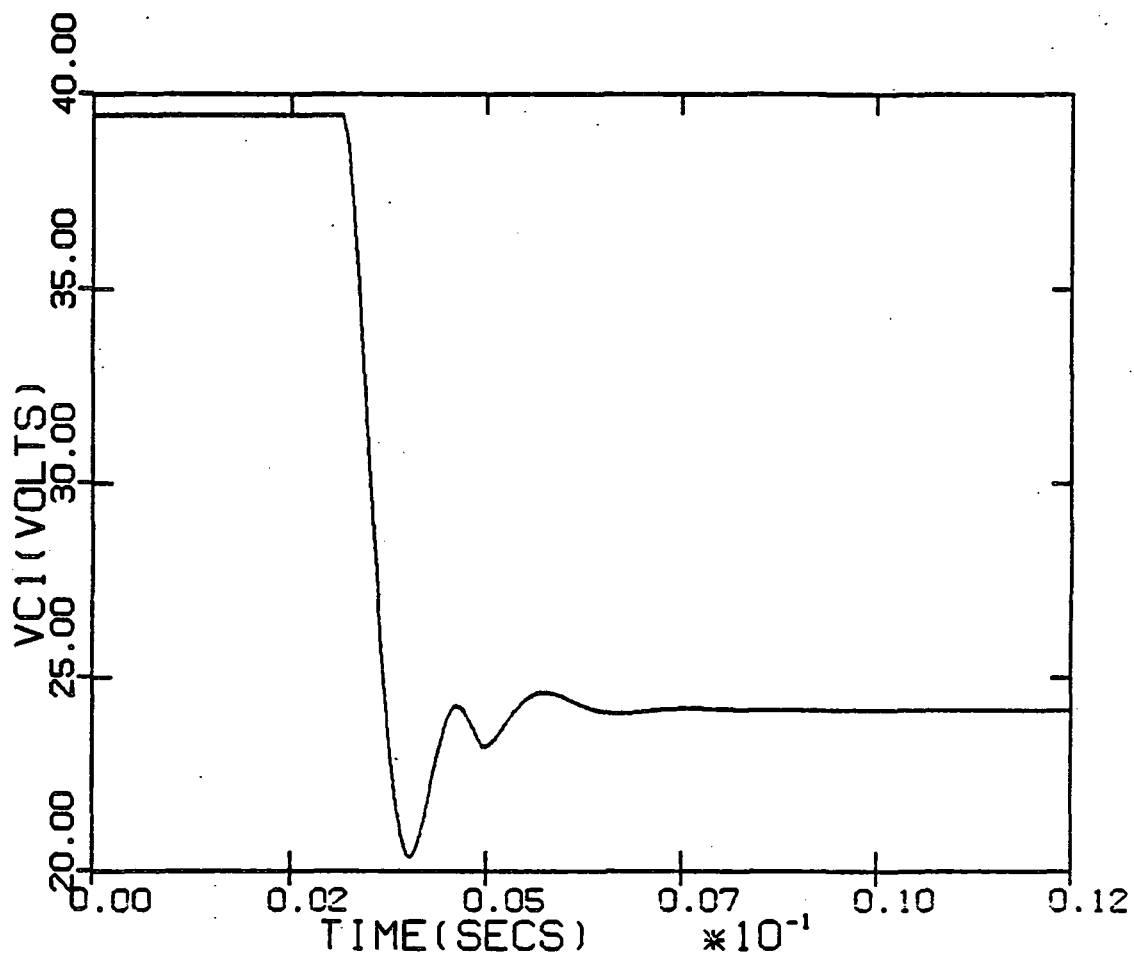


Figure 74: (b) Input filter capacitor voltage simulation without feedforward

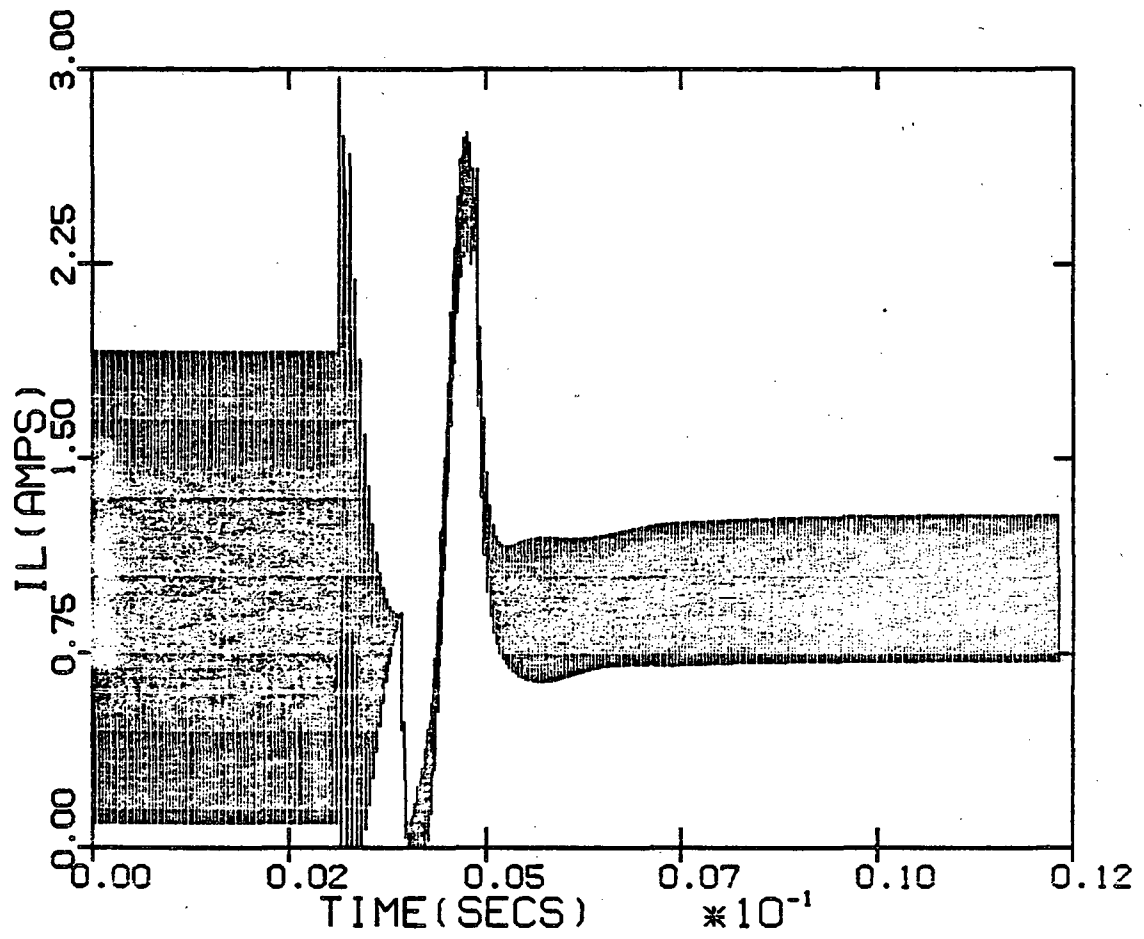


Figure 74: (c) Output filter inductor current simulation without feedforward

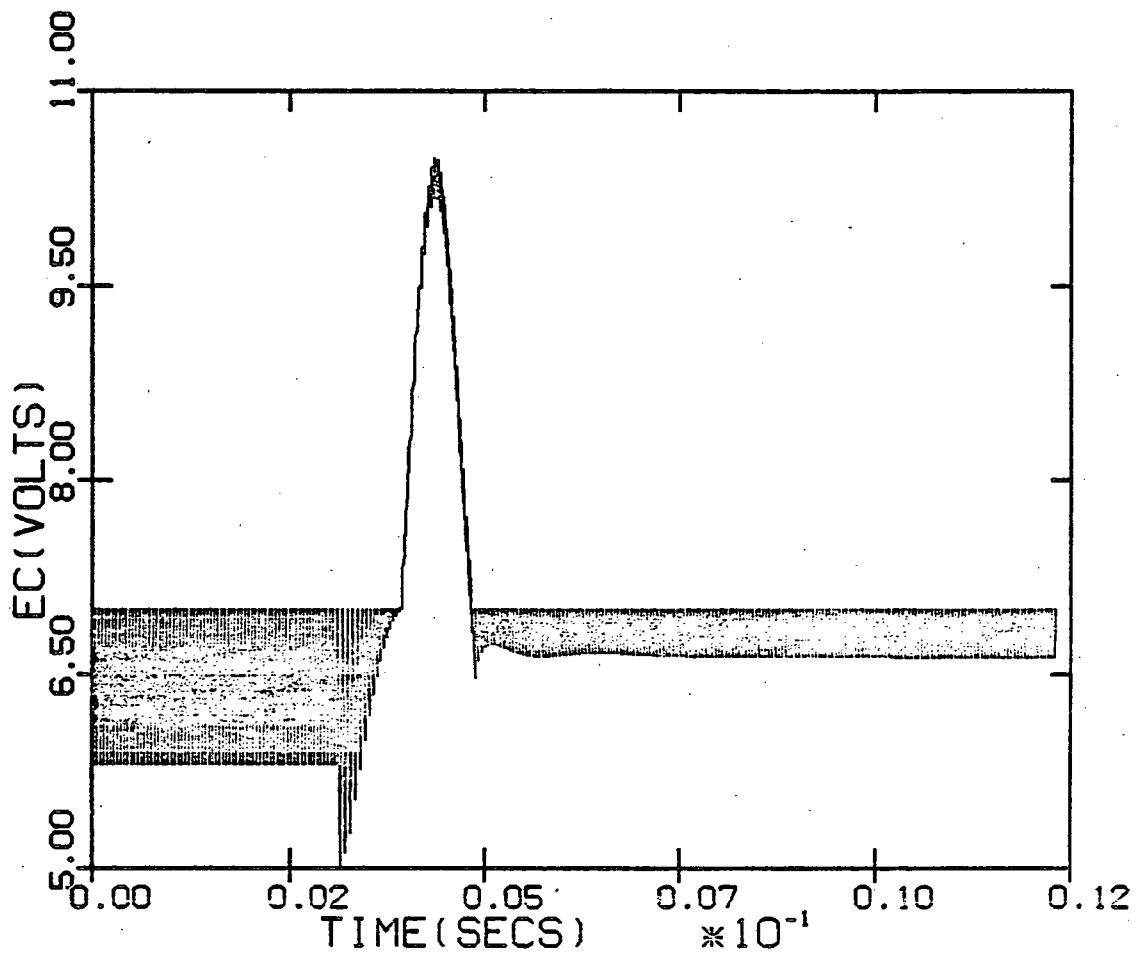


Figure 74: (d) Control voltage simulation without feedforward

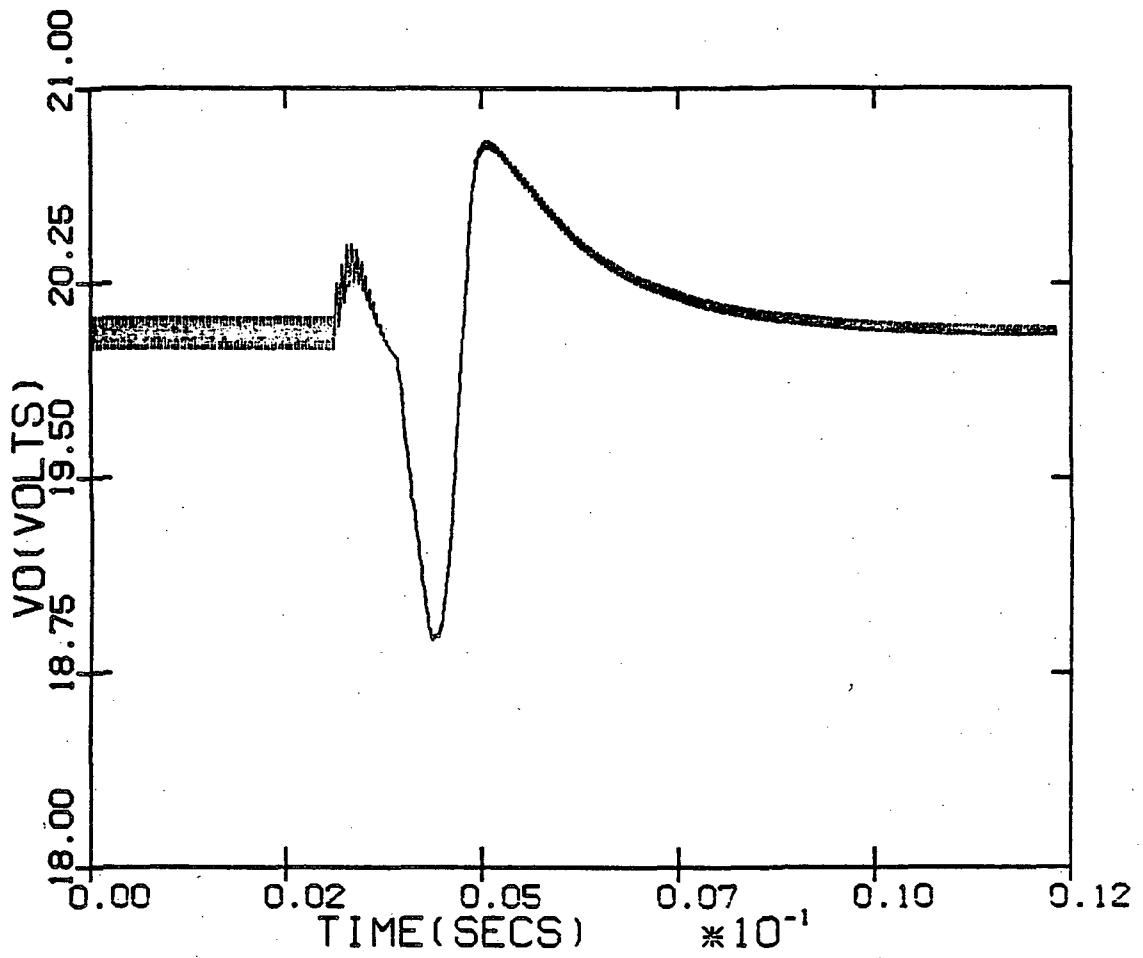


Figure 75: (a) Output voltage simulation with feedforward

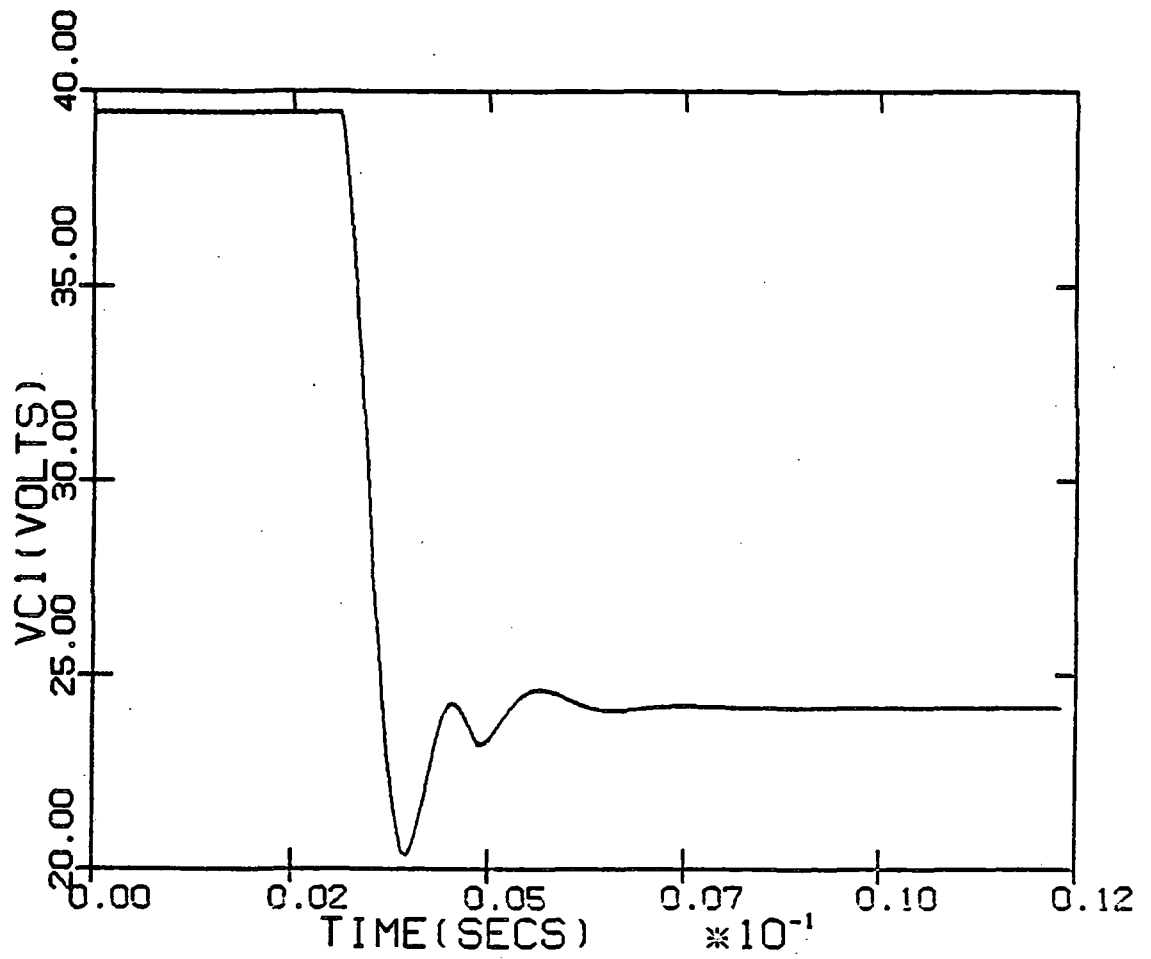


Figure 75: (b) Input filter capacitor voltage simulation with feedforward

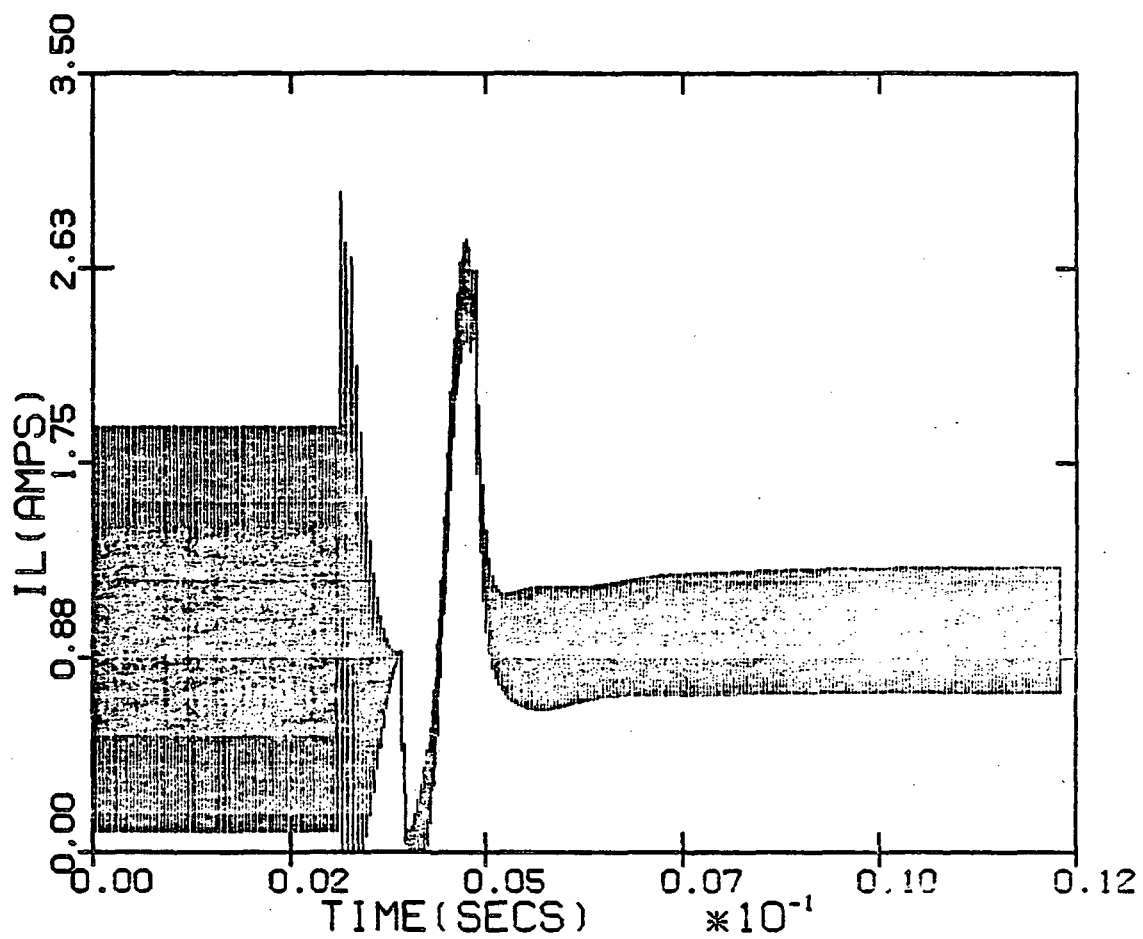


Figure 75: (c) Output filter inductor current simulation with feedforward

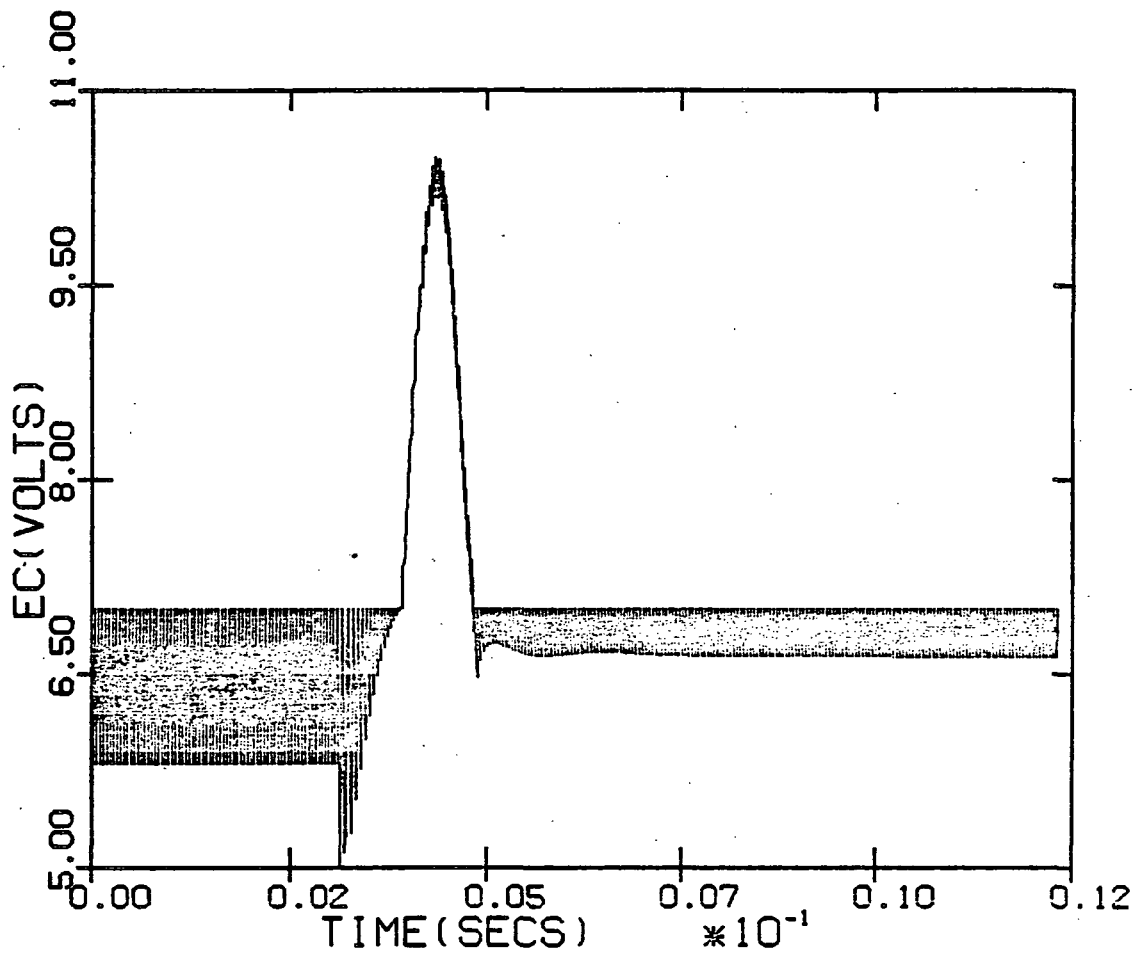
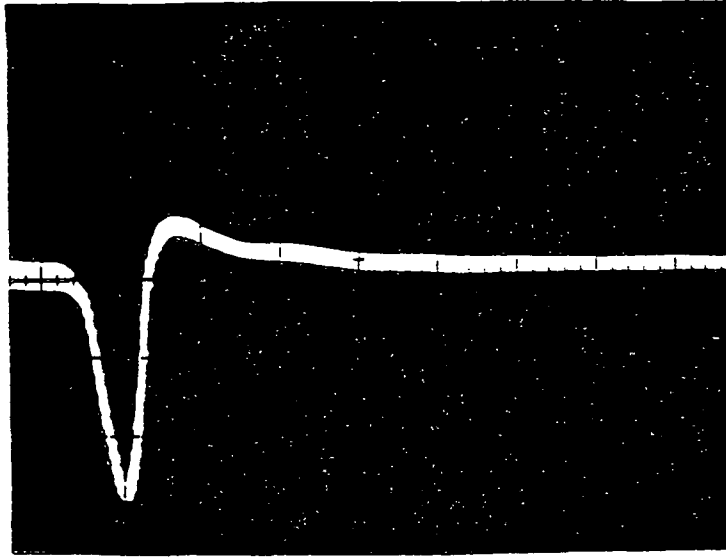
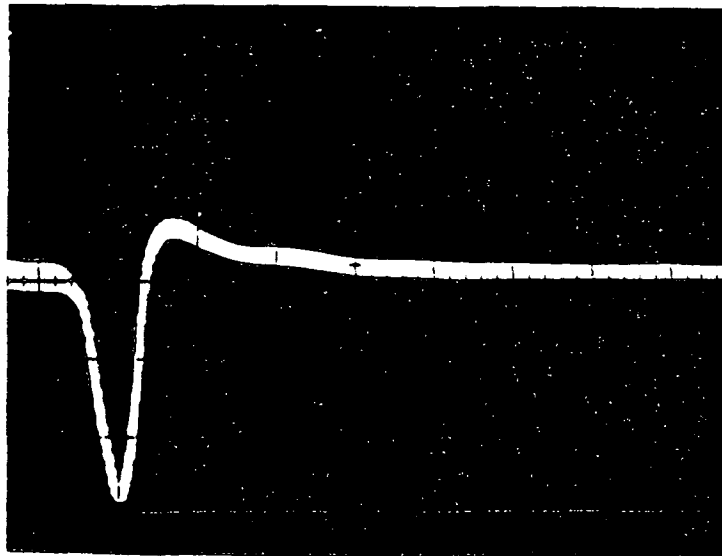


Figure 75: (d) Control voltage simulation with feedforward



(a)



(b)

Figure 76: Measured output voltage ripple without (a) and with (b) feedforward

(a) Y—0.5v/div X—0.5 msec/div

(b) Y—0.5v/div X—0.5 msec/div

seen that the regulator loses regulation momentarily and the output voltage drops down to around 18.3V before regulation is regained. It should be noted when comparing the analytical plots without feedforward (Figures 74) with those with feedforward (Figures 75), the transient waveforms are almost identical. This is expected, since during this large signal transient the regulator has momentarily lost its voltage regulation. Therefore the ability of feedforward compensation via duty cycle modulation is also lost momentarily. The regulator is operating in an open loop fashion (under minimum off time control). This can be verified by observing the voltage waveform input to the regulator.

The input filter capacitor voltage in Figures 73 (b) and 75 (b), which is also the input voltage to the regulator goes down close to 20V in both cases. For such a low input voltage to the regulator the duty cycle would have to be close to unity to maintain regulation, which is only possible if the off time is decreased sharply. However a minimum  $T_{OFF}$  time of 5 microseconds is implemented for various magnetic reset purposes and thus the regulator loses regulation till the input filter capacitor voltage rises.

The analytical plots of the control voltage without and with feedforward both show the large disturbance in control voltage as a result of the loss of regulation. The plot with

feedforward does show a somewhat smaller peak value of the overshoot than the one without feedforward but this difference is about 9%. Negligible difference is noticed between the analytical plots of the inductor current without and with feedforward. The large drop in current as a result of loss of regulation is noticed in both plots, as is the overshoot when regulation is regained.

The analytical results thus strongly support the experimental data and show that the regulator momentarily loses its control function. It is also confirmed through simulation and testing that the feedforward does not have any detrimental effect under large transient conditions.

## Chapter VIII

### DISCRETE TIME DOMAIN STABILITY ANALYSIS OF BUCK REGULATOR

An important concern is the interaction of an input filter with a switching regulator which often results in system instability. As described in detail in Chapter 2, the input filter interaction with the regulator control loop causes a reduction in the loop gain which may result in system instability. When a switching regulator is acquired as a 'black box' for use in a system and an input filter is put in externally, the improper choice of filter parameters can cause the system to be unstable [4,5]. Work presented earlier [4,5] showed that the input filter design should be incorporated in the regulator design itself in order to avoid loop instability and other input filter related problems.

In this Chapter the stability of a buck regulator is examined by varying the input filter parameter values. System instability is predicted analytically, and backed up with experimental data. It is then shown that the addition of the feedforward control enables one to stabilize the system. This is verified both analytically and experimentally. One can conclude that the addition of feedforward, in fact, isolates the regulator from the input filter; any input fil-

ter can be used with the buck regulator without causing loop instability.

### 8.1 ANALYTICAL INVESTIGATION OF STABILITY

An exact time domain analysis is performed to calculate the eigenvalues of the system with a single stage input filter; it was used to study how the eigenvalues move with a change in the input filter parameter (inductance). To correlate the 'exact' discrete time domain analysis results with the 'approximate' continuous time average analysis presented in Chapters 2 through 5, a computer program which calculates the closed loop poles of the continuous system was also written. The closed loop poles as calculated using the program track closely the eigenvalues derived from the exact time domain analysis. System instability occurs for some values of filter inductance but the addition of feedforward eliminates the problem.

#### 8.1.1 Calculation of Eigenvalues.

The method used in calculating the eigenvalues has been described earlier [15,16,17]. The state equations of the system are written for the buck regulator of Figure 34. The state variables describing the system without feedforward are:

$$x(1) = i_{L1} \text{ (input filter inductor current)}$$

$$\begin{aligned}
 x(2) &= v_{C_1} \text{ (input filter capacitor voltage)} \\
 x(3) &= i_L \text{ (output filter inductor current)} \\
 x(4) &= v_C \text{ (output filter capacitor voltage)} \\
 x(5) &= e_R \\
 x(6) &= e_C
 \end{aligned}$$

As discussed in Chapter 7  $e_R$  is the voltage at the capacitor  $C_2$  in the feedback loop while  $e_C$  is the control voltage (input to pulse modulator). Except for the order in which they appear, these are the same state variables as used in Chapter 7, where it is noted that the system is completely described by the above six state variables.

The state equations without feedforward are written as in Chapter 7:

$$\text{During } T_{ON} \text{ (S1 on S2 off)} \tag{8-1}$$

$$\dot{\underline{x}} = F1 \cdot \underline{x} + G1 \cdot \underline{u}$$

$$\text{During } T_{OFF} \text{ (S1 off S2 on)} \tag{8-2}$$

$$\dot{\underline{x}} = F2 \cdot \underline{x} + G2 \cdot \underline{u}$$

The matrices  $F1$  and  $F2$  are identical to the ones in Chapter 7 except for the following reordering; the third rows of equations (7-2) and (7-8) are moved to the sixth place with the other rows being moved up one place to get  $F1$ ,  $F2$  of equations (8-1) and (8-2), while the third columns of equa-

tions (7-2) and (7-8) are moved into sixth place with the other columns being moved up one place in a manner similar to the rows. Matrices G1 and G2 of equations (8-1) and (8-2) are identical to the ones in Chapter 7 except that the third row of Chapter 7 is moved into sixth place with the other rows being moved up one place. The vector  $\underline{u}$  of equations (8-1) and (8-2) is defined exactly as in Chapter 7.

Figure 77 serves to establish notation regarding time instance  $t_K$  etc. and the solutions to the state equations are written as in Chapter 7:

During  $T_{OFF}$

$$\underline{x}(t_K + T) = \phi_F \cdot \underline{x}(t_K) + D_F \cdot \underline{u}$$

During  $T_{ON}$

$$\begin{aligned} \underline{x}(t_K + T_{OFF}^K + T) &= \phi_N \cdot \underline{x}(t_K + T_{OFF}^K) \\ &+ D_N \cdot \underline{u} \end{aligned} \tag{8-3}$$

The matrices  $\phi_N$ ,  $\phi_F$ ,  $D_F$  and  $D_N$  are defined, as is time step  $T$ , exactly as in Chapter 7.

From (8-3) the following is derived [15,16,17] :

$$\begin{aligned} \underline{x}(t_{K+1}) &= \phi_N \cdot \phi_F \cdot \underline{x}(t_K) + \phi_N \cdot D_F \cdot \underline{u} \\ &+ D_N \cdot \underline{u} \end{aligned} \tag{8-4}$$

For the constant volt-sec. ( $V_I T_{ON}$ ) duty-cycle control mode used in the stability investigation, the  $T_{ON}$  is fixed if  $V_I$

is fixed and  $T_{OFF}^K$  is determined by the point at which  $e_c$  intersects the threshold voltage  $E_T$  :

$$E_T = \sum_{I=1}^6 \phi_F(6,I) \cdot x(I) + \sum_{J=1}^4 D_F(6,J) \cdot u(J) \quad (8-5)$$

$T_{OFF}^K$  is thus a function of  $\underline{x}(t_K)$  and (8-4) is a nonlinear equation [15,16,17]. Equations (8-1) - (8-5) thus represent exactly the nonlinear buck regulator system without feedforward.

For the purpose of stability analysis the steady state or equilibrium state is necessary [15,16] and this is derived as

$$\underline{x}(t_{K+1}) = \underline{x}(t_K) = \underline{x}^* \quad (8-6)$$

$$\underline{x}^* = \phi_N \cdot \phi_F \cdot \underline{x}^* + (\phi_N \cdot D_F + D_N) \underline{u}$$

The nonlinear system is linearized for a small perturbation, around the steady state operating point [15,16,17]:

$$\delta \underline{x}(t_K) = \underline{x}(t_K) - \underline{x}^* \quad (8-7)$$

and

$$\delta \underline{x}(t_{K+1}) = \left\{ \phi_N \cdot \frac{\partial}{\partial \underline{x}} \left[ \phi_F \cdot \underline{x}(t_K) + D_F \cdot \underline{u} \right] \right\} \delta \underline{x}(t_K) \quad (8-8)$$

$\underline{x}^*$

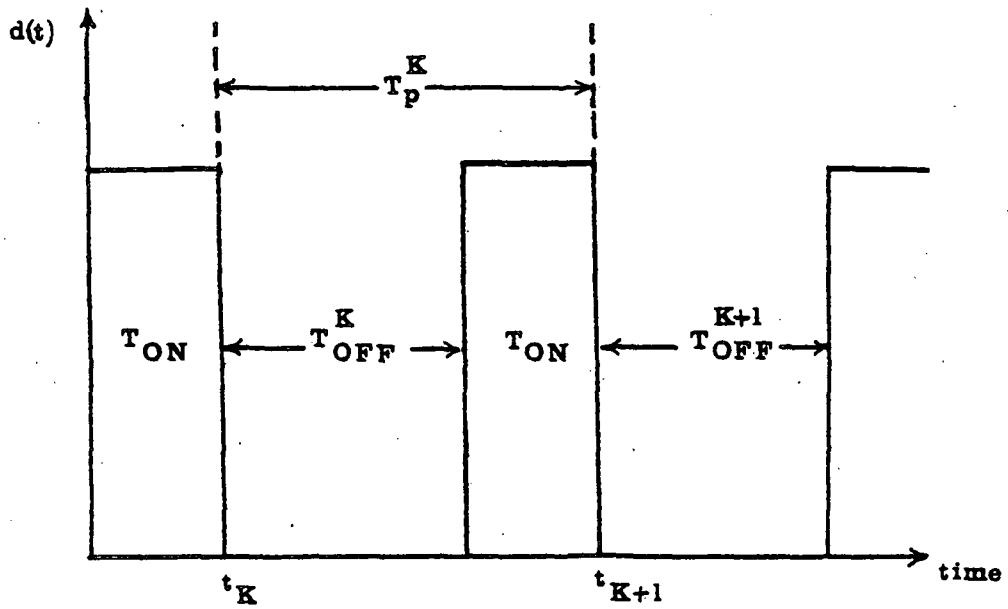


Figure 77: Notation regarding time  $t_K$

Equation (8-8) is derived assuming that the small perturbation in the state does not change the value of  $T_{OFF}^K$  [15,16]. The expression in the curly brackets of equation (8-8) is used to investigate stability:

$$\delta \underline{x}(t_{K+1}) = \psi \cdot \delta \underline{x}(t_K) \quad (8-9)$$

Equation (8-9) thus describes a linear system which will be stable if and only if all the eigenvalues of  $\psi$  are absolutely less than unity --

$$|\lambda_i(\psi)| < 1 \quad i = 1, 2, 3, \dots \quad (8-10)$$

or in other words if all the eigenvalues  $\lambda_i$  lie inside the unit circle [15,16].

The buck regulator system with feedforward is described by a set of seven state variables as in Chapter 7. The nonadaptive feedforward circuit of Figure 67 was used in the analysis and the state variables then are:

$$\begin{aligned} x(1) &= i_{L1} \\ x(2) &= v_{C1} \\ x(3) &= v_f \quad (\text{voltage at capacitor } C_f) \\ x(4) &= i_L \\ x(5) &= v_C \\ x(6) &= e_R \end{aligned} \quad (8-11)$$

$$x(7) = e_c$$

The state equations during  $T_{ON}$  and  $T_{OFF}$  are written as:

During  $T_{ON}$

$$\dot{\underline{x}} = F1.\underline{x} + G1.\underline{u} \quad (8-12)$$

During  $T_{OFF}$

$$\dot{\underline{x}} = F2.\underline{x} + G2.\underline{u} \quad (8-13)$$

Matrices  $F1$ ,  $F2$ ,  $G1$  and  $G2$  of equations (8-12) and (8-13) are similar to the ones in Chapter 7 and are defined exactly as the ones in equations (8-1) and (8-2). The solution of the state equations, the definition of the equilibrium state and the matrix  $\psi$  are identical to the case without feedforward.

A computer program was written to calculate the matrix  $\psi$  and its eigenvalues both without and with feedforward. It can be easily seen that by changing the single stage input filter parameters a set of eigenvalues can be calculated from which inferences regarding system stability can be drawn.

### 8.1.2 Description of the Program Used in Calculating Eigenvalues

A flow chart for the program is given in Figure 78 and a computer listing of both programs is included in the appendix.

There are essentially three steps involved in the calculation of eigenvalues.

First the approximate steady state values are computed [15,16,17], using an approximate value of the off time  $T_{OFF}$ :

$$T_{OFF} = T_{ON} \cdot (V_I - E_O)/E_O \quad (8-14)$$

Equation (8-6) is used to calculate the approximate steady state values  $\underline{x}^*$ , with ISML routine LEQT2F being used to solve the system of linear equations. It is to be noted that equation (8-6) is not valid for the last state variable  $e_C$  since both  $\phi_N(6,6)$  and  $\phi_F(6,6)$  equal unity, and equation (8-5) is used to calculate  $e_C$ .

The approximate steady state calculated is used to find the exact steady state values [15,16]. The best way of determining the exact steady state is to determine the exact off time by iterative linearization (Newton's method) on the cycle-to-cycle matching condition for  $e_C$  [15,16,17]. The vector  $ZT$  is defined :

$$\begin{aligned} \underline{ZT} &= \underline{x}(t_K + T_{OFF}^K) \\ \underline{ZT} &= \phi_F \cdot \underline{x}(t_K) + D_F \cdot \underline{u} \end{aligned} \quad (8-15)$$

with  $ZT(6) = E_T$

The cycle-to-cycle matching condition is expressed as:

$$\begin{aligned}
 \text{SMAT} = x(6) - & \left[ \sum_{I=1}^5 \phi_N(6,I) \cdot ZT(I) + E_T \right. \\
 & \left. + \sum_{J=1}^4 D_N(6,J) \cdot u(J) \right] \quad (8-16)
 \end{aligned}$$

The value of SMAT is calculated using the available value of  $T_{\text{OFF}}$ ; if SMAT is smaller than a certain error tolerance then the value of  $T_{\text{OFF}}$  used is accurate. If SMAT exceeds the tolerance then Newton's method is applied to calculate a better estimate of  $T_{\text{OFF}}$ . The steps involved in the calculation are:

1. Calculate ZT and SMAT.
2. If SMAT is not less than specified tolerance, then perturb  $T_{\text{OFF}}$  by the amount  $DT_{\text{OFF}}$ .
3. Calculate values of state variables corresponding to the perturbed value of off time, using equations (8-5) and (8-6).
4. Calculate SMATN.
5. Calculate a better estimate of  $T_{\text{OFF}}$  using Newton's iteration [15,16,17].
6. Calculate a better estimate of the state variables.
7. Calculate SMAT and go to step 2.

The last step is to calculate the matrix  $\psi$  and its eigenvalues using the exact steady state values computed

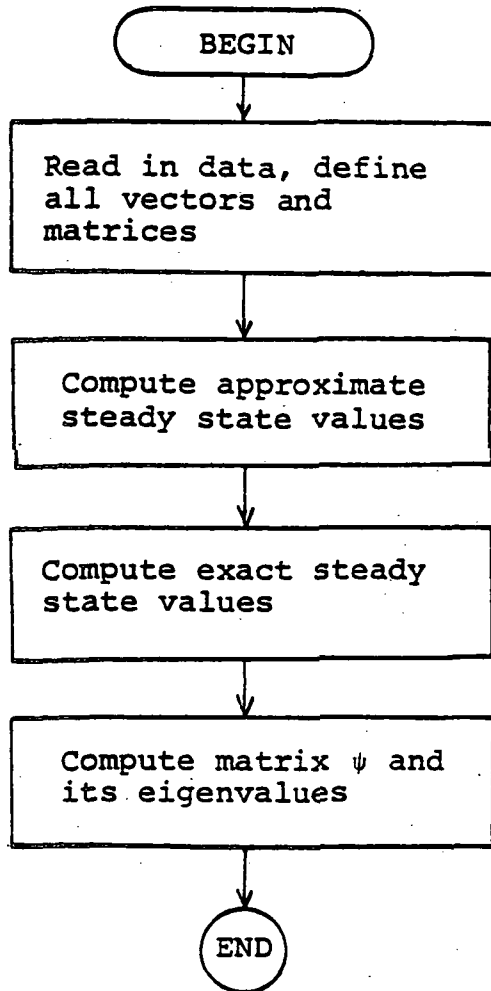


Figure 78: Flowchart for stability analysis.

above; Figure 79 is a flowchart for the calculation. The following are defined:

$$\underline{\text{FUN1}}(\underline{x}^* + \text{Dx}(\text{I})) = \left[ \phi_{\text{F}} \cdot \underline{x} + \text{D}_{\text{F}} \cdot \underline{u} \right]_{\underline{x}^* + \text{Dx}(\text{I})} \quad (8-17)$$

$$\underline{\text{FUN2}}(\underline{x}^* - \text{Dx}(\text{I})) = \left[ \phi_{\text{F}} \cdot \underline{x} + \text{D}_{\text{F}} \cdot \underline{u} \right]_{\underline{x}^* - \text{Dx}(\text{I})} \quad (8-18)$$

$$\underline{\text{TEMP2}} = \left[ \frac{(\underline{\text{FUN1}} - \underline{\text{FUN2}})}{2 \cdot \text{Dx}(1)} \cdot \cdot \cdot \cdot \frac{(\underline{\text{FUN1}} - \underline{\text{FUN2}})}{2 \cdot \text{Dx}(6)} \right]_{6 \times 6} \quad (8-19)$$

$$\underline{\text{PSI}} = \phi_{\text{N}} \cdot \underline{\text{TEMP2}} \quad (8-20)$$

TEMP2 is thus the matrix of partial differentials used in equation (8-8).

The matrix TEMP2 is evaluated one column at a time. For the I'th column a perturbation DX(I) is made in X(I). Two new sets of steady state values XA and XB are defined, as is shown in the flowchart. For the new set of values XA it is necessary to calculate an exact value of off time TFFC1 in order to obtain  $\phi_{\text{F}}$ ,  $\text{D}_{\text{F}}$ . The error function ZETA is defined:

$$\text{ZETA} = \sum_{\text{I}=1}^6 \phi_{\text{F}}(6, \text{I}) \cdot \text{XA}(\text{I}) + \sum_{\text{J}=1}^4 \text{D}_{\text{F}}(6, \text{J}) \text{u}(\text{J}) - \text{E}_{\text{T}} \quad (8-21)$$

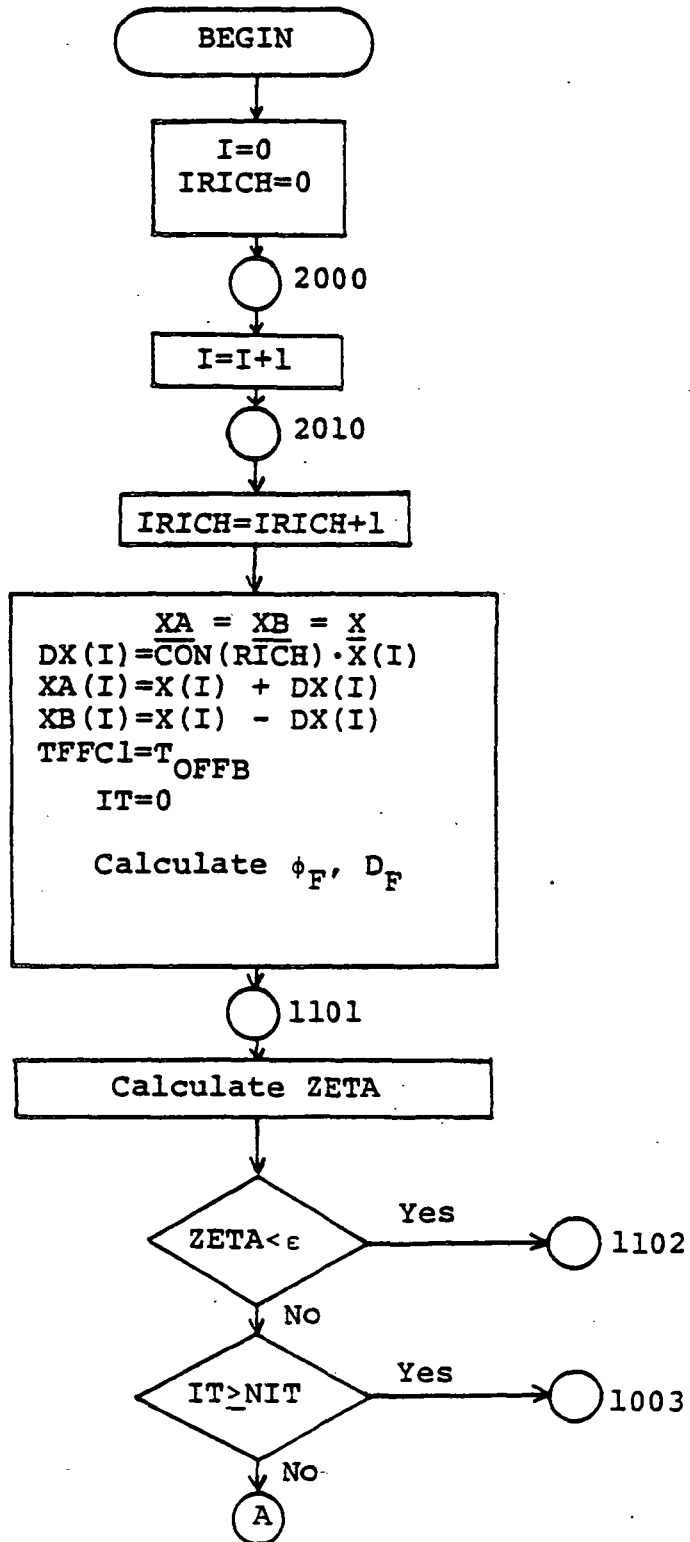


Figure 79: Flowchart for calculating matrix  $\psi$

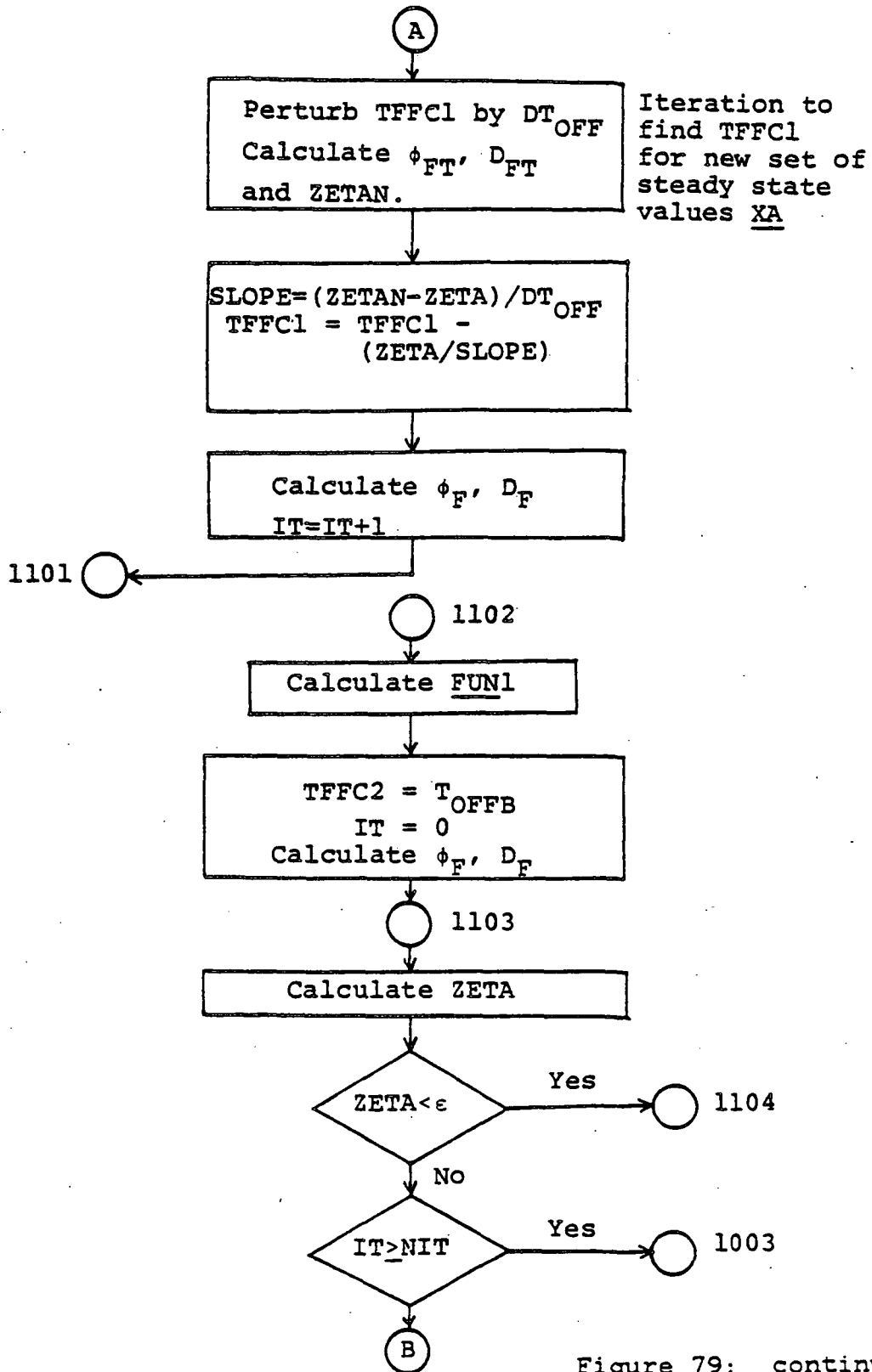


Figure 79: continued

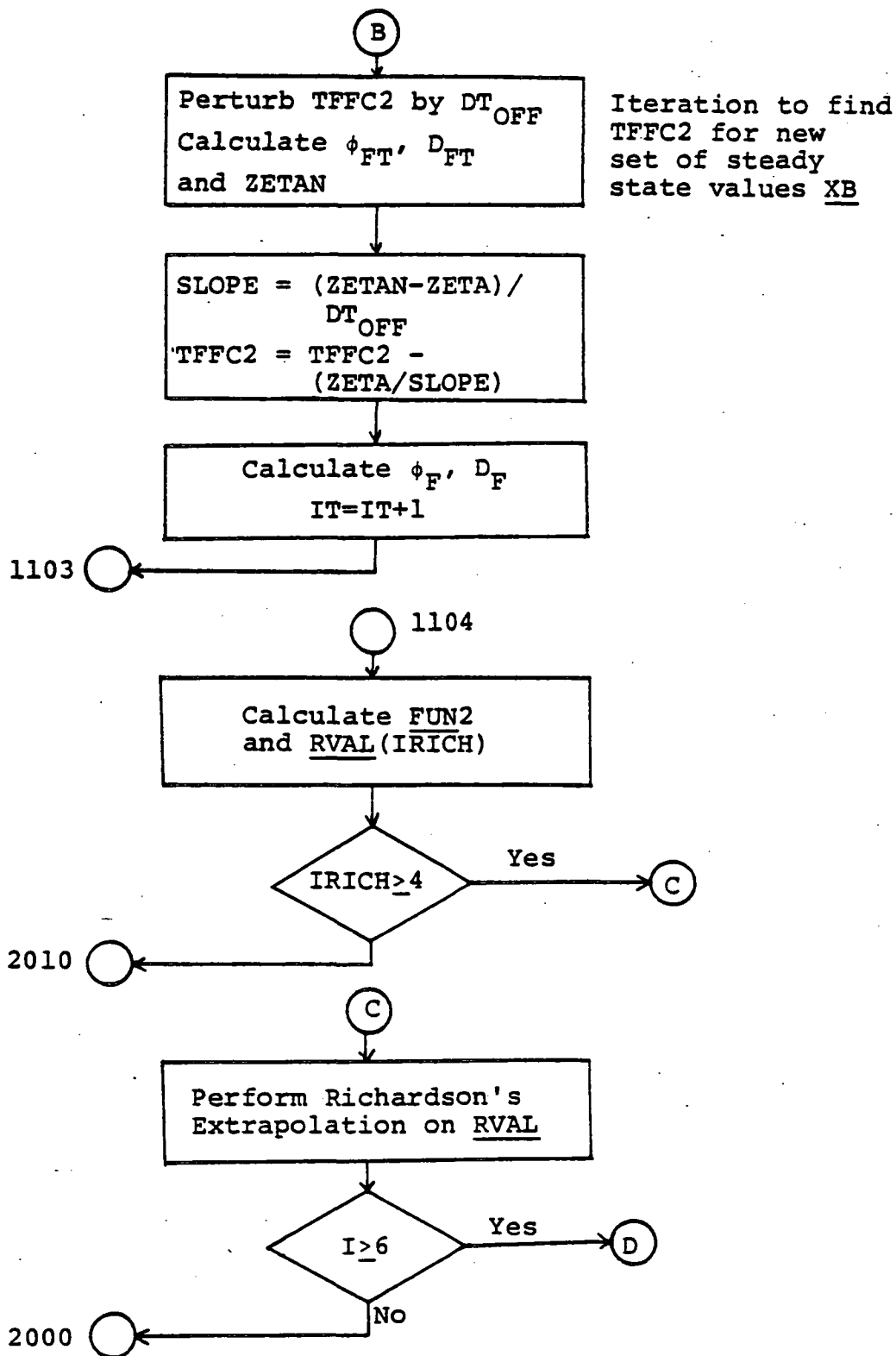


Figure 79: continued

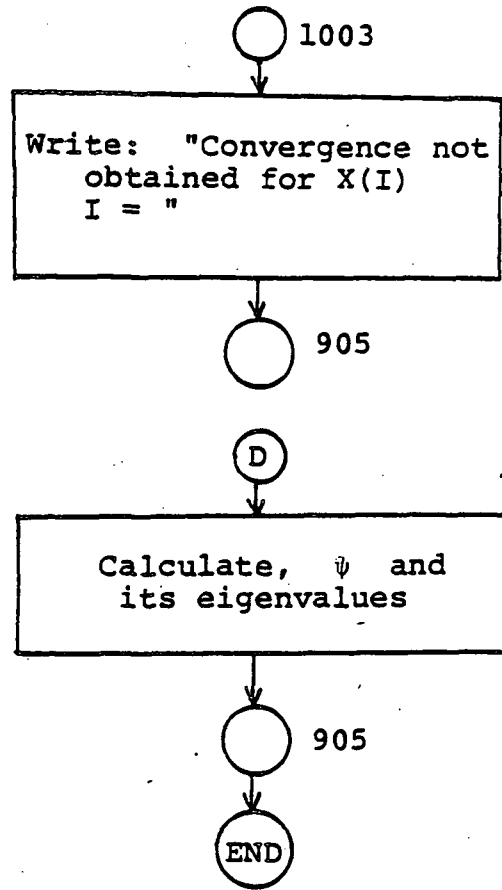


Figure 79: continued

The value of ZETA is calculated using the available value of TFFC1, if it is within the specified tolerance then the value of TFFC1 is the value needed. If ZETA is not within tolerance then Newton's iteration [15,16] is used to obtain a better estimate of TFFC1, as is evident from the flowchart. The values of  $\phi_F$ ,  $D_F$  are obtained and then the vector FUN1 is evaluated.

A similar procedure is used to obtain the exact off time TFFC2 for the other set of values XB. After calculation of FUN2 an estimate for the I'th column of TEMP2 is obtained.

In the calculation of the partial derivatives it was observed that a better estimate of the derivatives can be obtained using the Richardson's extrapolation method [18]. The derivative  $f'(a)$  is sometimes approximated as:

$$A(h) = \frac{f(a+h) - f(a-h)}{2h} \quad (8-22)$$

where h is the step size.

A better estimate may be obtained by evaluating A(h) and A(rh):

$$A(rh) = \frac{f(a+rh) - f(a-rh)}{2rh} \quad (8-23)$$

where  $r$  is usually 0.5 [18].

Combining  $A(h)$  and  $A(rh)$  thus:

$$B(h) = \frac{A(rh) - r^2 A(h)}{1 - r^2} \quad (8-24)$$

gives a better estimate,  $B(h)$ , of the derivative  $f'(a)$  [18]. Thus by combining the value of  $A(h)$  obtained from equation (8-22) with two values for the step size  $h$ , it is possible to get a more accurate estimate of the derivative.

In the program four values of step size were used. The perturbation  $DX(I)$  is assigned four values and for each value the vectors FUN1 and FUN2 are calculated. This results in four estimates for the derivatives in the  $I$ 'th column of TEMP2. Combining these four estimates as in the program [18] gives an accurate estimate of the  $I$ 'th column.

The whole procedure is then repeated for the next column, thus an accurate set of values for the derivatives is obtained. Multiplying TEMP2 by  $\phi_N$  results in the matrix  $\psi$  [15,16,17]. Finally the eigenvalues  $\lambda$  of the matrix  $\psi$  are obtained using the IMSL routine EIGRF.

The eigenvalues with feedforward are calculated in an identical fashion, the only real difference being the change in the order of the system from six state variables to seven.

### 8.1.3 Calculation of the Closed Loop Poles of the System

The closed loop poles of the system of Figure 34 can be calculated. The expression for the closed loop gain  $\hat{v}_O/\hat{v}_I$  can be easily written using Figure 33 for the case without feed-forward:

$$\frac{\hat{v}_O}{\hat{v}_I} = \frac{H \cdot F_{11} / \Delta}{1 + \frac{F_{DC} \cdot F_M \cdot F_{12}}{\Delta} + \frac{F_3 \cdot F_{AC} \cdot F_M \cdot F_{22}}{\Delta}} \quad (8-25)$$

with  $F_{11}$ ,  $\Delta$  etc. as defined in Chapter 5.

Equation (8-25) can also be used to calculate the closed loop poles of the system without input filter; all that is necessary to do is to set  $H = 1$  and  $Z = 0$ , as discussed earlier.

Expressions for  $F_{12}$ ,  $\Delta$  etc. are substituted into equation (8-28) for the case without input filter. The resulting expression in the denominator is then a polynomial of the fourth degree:

$$\begin{aligned} P_1(s) = & S^4 (K_7 K_6 LC) + \\ & S^3 (K_7 K_6 K_8 + K_7 C_1' LC + K_5 K_4 C R_L) + \\ & S^2 (K_7 C_1' K_8 + K_7 K_6 + K_3 K_2 C R_C + K_5 K_4 \\ & \quad + K_5 nL C R_L) + \\ & S (K_7 C_1' + K_3 K_2 + K_3 K_1 C R_C + nL K_5) \\ & + K_3 K_1 \end{aligned} \quad (8-26)$$

The constants  $k_7$ ,  $k_8$  etc. are defined as functions of the regulator parameters like inductance  $L$  etc. The appendix contains a listing of the program used and the constants are defined there. An IMSL routine ZPOLR is used to calculate the roots of  $P_1$  which are the closed loop poles of the system without input filter.

For the case with input filter the same equation, (8-25), is used and substitution leads to a sixth degree polynomial in the denominator:

$$\begin{aligned}
 P_2(s) = & s^6 (K_7 K_6 Y_8) + \\
 & s^5 (K_7 C_1' Y_8 + K_7 K_6 Y_9 + K_5 K_4 Y_5) + \\
 & s^4 (K_7 C_1' Y_9 + K_7 K_6 Y_{10} + K_3 K_2 Y_1 + K_5 n L Y_5 \\
 & \quad + K_4 K_5 Y_6) + \\
 & s^3 (K_7 C_1' Y_{10} + K_7 K_6 Y_{11} + K_3 K_2 Y_2 + K_3 K_1 Y_1 + \\
 & \quad K_5 n L Y_6 + K_5 K_4 Y_7) + \\
 & s^2 (K_7 C_1' Y_{11} + K_7 K_6 Y_{12} + K_3 K_1 Y_2 + K_3 K_2 Y_3 \\
 & \quad + K_5 n L Y_7 + K_5 K_4 Y_4) + \\
 & s (C_1' K_7 Y_{12} + K_3 K_1 Y_3 + K_3 K_2 Y_4 + n L K_5 Y_4) \\
 & \quad + K_3 K_1 Y_4
 \end{aligned} \tag{8-27}$$

The constants  $Y_1$  etc. used in equation (8-27) are again defined in the program. The same routine ZPOLR is used to obtain the six closed loop poles.

#### 8.1.4 Location of Eigenvalues and Poles as a Function of Input Filter Parameters.

The computer programs written were used to locate closed loop poles and eigenvalues as a function of input filter inductance. The buck regulator of Figure 34 was used and the parameters of the regulator were as defined in section 6.1 except for the following changes:

$$\begin{array}{ll} V_I = 25 \text{ v} & R_{13} = 200 \text{ Kohms} \\ C_2 = 100 \text{ pf} & R_L = 10 \text{ ohm} \end{array}$$

The values of  $R_{13}$  and  $C_2$  were changed so that the compensation loop is largely ineffective, [7,8]. This was done in order to facilitate making the measurements discussed in section 8.2. It was found difficult to achieve instability in the high loop gain system used in making the measurements. Making the compensation loop largely ineffective reduced the loop gain so that with a large input filter the system was made unstable.

A single stage input filter with the following parameters was used:

$$R_{L1} = 0.2 \text{ ohm} \quad L1 \text{ variable} \quad C1 = 220 \text{ microF}$$

First the eigenvalues and closed loop poles without input filter and feedforward were calculated using the eigenvalue and the closed loop programs. Figures 80 and 81 are the plots of the eigenvalues and closed loop poles respectively. It is noticed that there are four poles and four eigenvalues since without input filter the system is of the fourth order.

The eigenvalues and poles are:

$$\begin{array}{ll} z_1 = 0.844 * 10^{-7} & s_1 = -55,000 + j0 \\ z_2 = 0.12 & s_2 = -50,000 + j0 \\ z_3 = 0.98 + j0.103 & s_3 = -346 + j2240 \\ z_4 = 0.98 - j0.103 & s_4 = -346 - j2240 \end{array}$$

The eigenvalues and the closed loop poles are related [15]:

$$\begin{array}{l} z = e^{sT} \\ s = \sigma + j\omega \end{array} \quad (8-28)$$

Thus

$$\begin{array}{l} |z| = e^{\sigma T} \\ \angle z = \omega T \end{array} \quad (8-29)$$

Knowing the location of the closed loop poles it is thus possible to locate the eigenvalues if a value of T is known. In this case T is the switching period and its value was

found to be 41.85 microsec.; thus equations (8-28) and (8-29) could be used to crosscheck the results from the eigenvalue program once the closed loop poles are known. Equation (8-29) was used to calculate the eigenvalues and the calculated values were found to be very close to the values from the eigenvalue program. The two poles on the real axis correspond to the two eigenvalues close to the origin while the two complex poles result in the two complex eigenvalues.

Next the single stage input filter was put in and the eigenvalues and closed loop poles calculated using the respective programs. Figures 82 and 83 are the plots of the eigenvalues and the closed loop poles respectively. The values of the filter inductance  $L_1$  used were --

50, 150, 325, 450, 650, 800, 1000, 1425 and 1800 microH

Table 1 lists the eigenvalues and closed loop poles, for different values of  $L_1$ . Starting at 50 microH it is seen that the complex eigenvalues move to the right, closer to the unit circle as inductance is increased. The two eigenvalues on the real axis  $z_1$  and  $z_2$ , which correspond to  $z_1$  and  $z_2$  on Figure 80, do not move with change in inductance. The complex eigenvalues with a real part of 0.98  $z_5$  and  $z_6$ , which correspond to  $z_3$  and  $z_4$  on Figure 80, are pushed out of the unit circle for a value of  $L_1 = 800$  microH. For values above 800 microH the eigenvalues do not move much; the

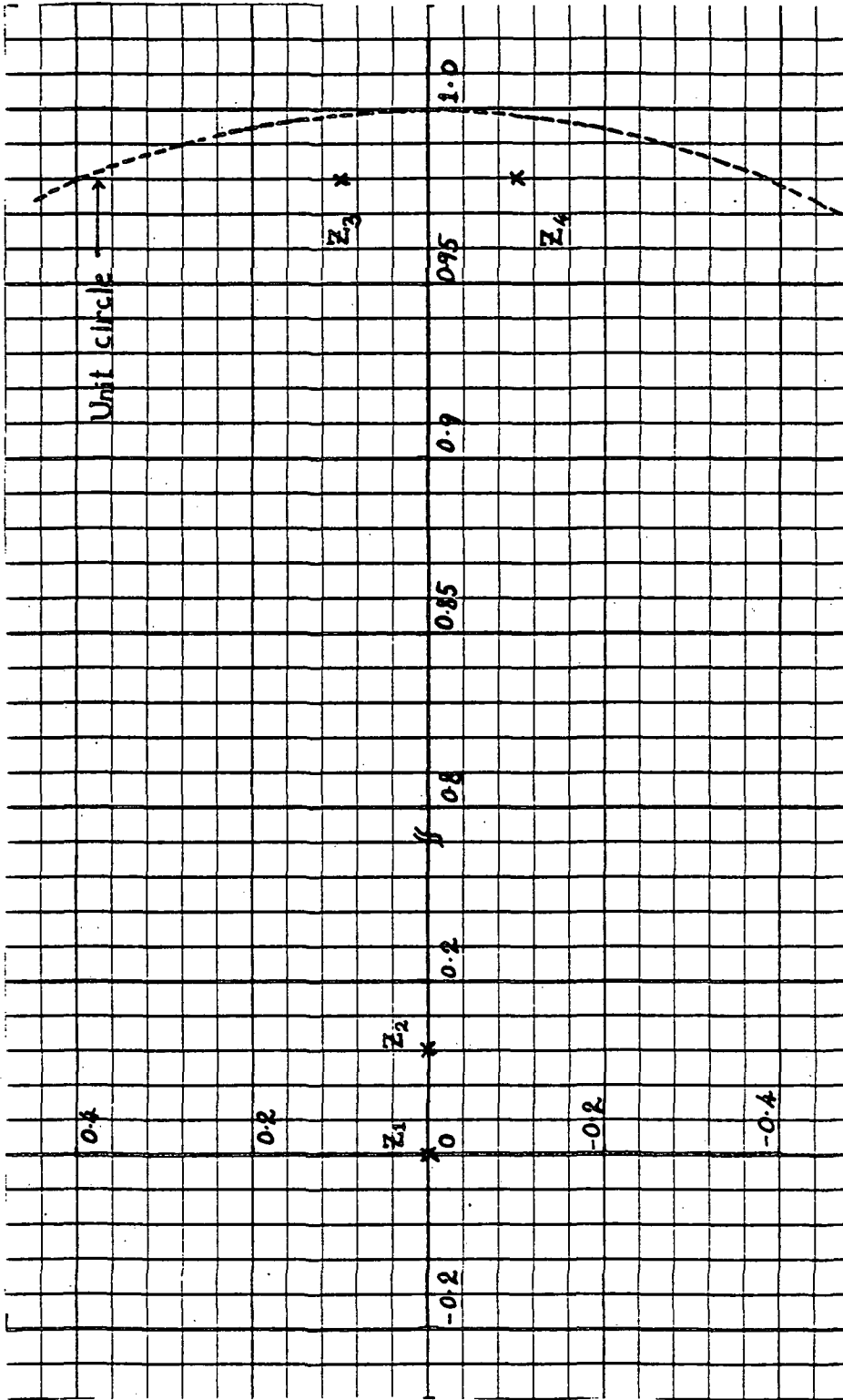


Figure 80: Eigenvalues without input filter

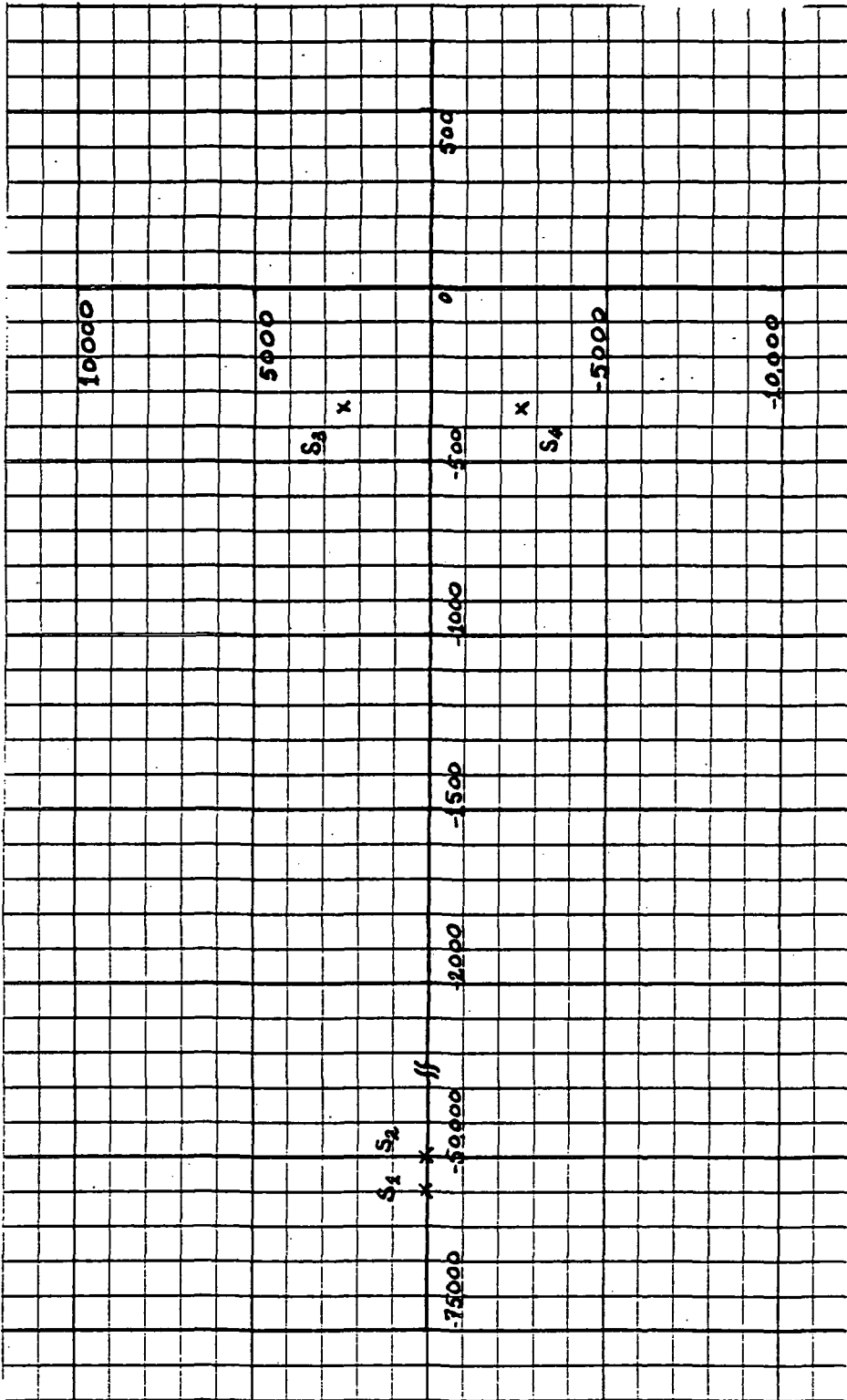


Figure 81: Closed loop poles without input filter

real part stays at around 1.003 for the ones outside the unit circle and around 0.97 for the ones inside. This may be used to explain the bunching up of the eigenvalues for large values of inductance. Thus the eigenvalue plot of Figure 82 predicts that the system will be unstable for values of filter inductance above 800 microH.

The plot of the closed loop poles, Figure 83, shows similar behavior. The two poles on the real axis  $s_1$  and  $s_2$  are not changed as inductance increases, however two complex poles  $s_5$  and  $s_6$  move into the right half plane, indicating instability. The poles move across the origin at 800 microH which checks well with the eigenvalue plot. Equation (8-29) was used to calculate the eigenvalues from the closed loop poles and the calculated eigenvalues agreed closely with the results from the eigenvalue program for all the values of  $L_1$  that were used, thus providing a crosscheck.

The other pair of complex poles  $s_3$  and  $s_4$  in Figure 83 initially move closer to the right half plane, then move away from it for values of  $L_1$  greater than 450 microH. This behavior should be reflected in the eigenvalue plot for eigenvalues  $z_3$  and  $z_4$ , however it is noticed that in equation (8-29) the value of  $T$  is so small that for a change in the real part from -300 to -500 the change in the eigenvalues will be about 1%, which is too small a change to show up in

TABLE 1

Eigenvalues and Closed Loop Poles for various values of L1.

	Eigenvalues	Closed Loop Poles
L1 = 50 $\mu$ H	-0.00274 + j0 0.1234 + j0 0.851 $\pm$ j 0.348 0.9806 $\pm$ j 0.1025	-55,045 + j0 -50,005 + j0 -1978 $\pm$ j 9314 -339 $\pm$ j 2227
L1 = 150 $\mu$ H	-0.0028 + j0 0.1233 + j0 0.9457 $\pm$ j 0.2194 0.9819 $\pm$ j 0.1026	-55,045 + j0 -50,005 + j0 -662 $\pm$ j 5462 -319 $\pm$ j 2227
L1 = 325 $\mu$ H	-0.003 + j0 0.1233 + j0 0.9706 $\pm$ j 0.1539 0.9851 $\pm$ j 0.103	-55,045 + j0 -50,005 + j0 -351 $\pm$ j 3725 -271 $\pm$ j 2232

TABLE 1  
continued

	Eigenvalues	Closed Loop Poles
$L = 450 \mu H$	-0.003 + j0 0.1233 + j0 0.971 ± j 0.132 0.9897 ± j 0.1026	-55,045 + j0 -50,005 + j0 -323 ± j 3165 -214 ± j 2237
$L = 650 \mu H$	-0.003 + j0 0.1233 + j0 0.97 ± j 0.1162 0.9975 ± j 0.0954	-55,045 + j0 -50,005 + j0 -419 ± j 2684 -49.8 ± j 2189
$L = 800 \mu H$	-0.003 + j0 0.1232 + j0 0.97 ± j 0.111 0.9996 ± j 0.089	-55,045 + j0 -50,005 + j0 -483 ± j 2546 43.6 ± j 2069

TABLE 1  
continued

	Eigenvalues	Closed Loop Poles
$L1 = 1000 \mu H$	-0.003 + j0 0.1233 + j0 0.971 ± j 0.1078 1.0002 ± j 0.082	-55,046 + j0 -50,005 + j0 -513 ± j 2455 98.3 ± j 1909
$L1 = 1425 \mu H$	-0.003 + j0 0.1233 + j0 0.972 ± j 0.1052 1.003 ± j 0.071	-55,046 + j0 -50,005 + j0 -517 ± j 2371 133 ± j 1650
$L1 = 1800 \mu H$	-0.003 + j0 0.1233 + j0 0.972 ± j 0.1055 1.004 ± j 0.063	-55,046 + j0 -50,005 + j0 -511 ± j 2339 141 ± j 1487

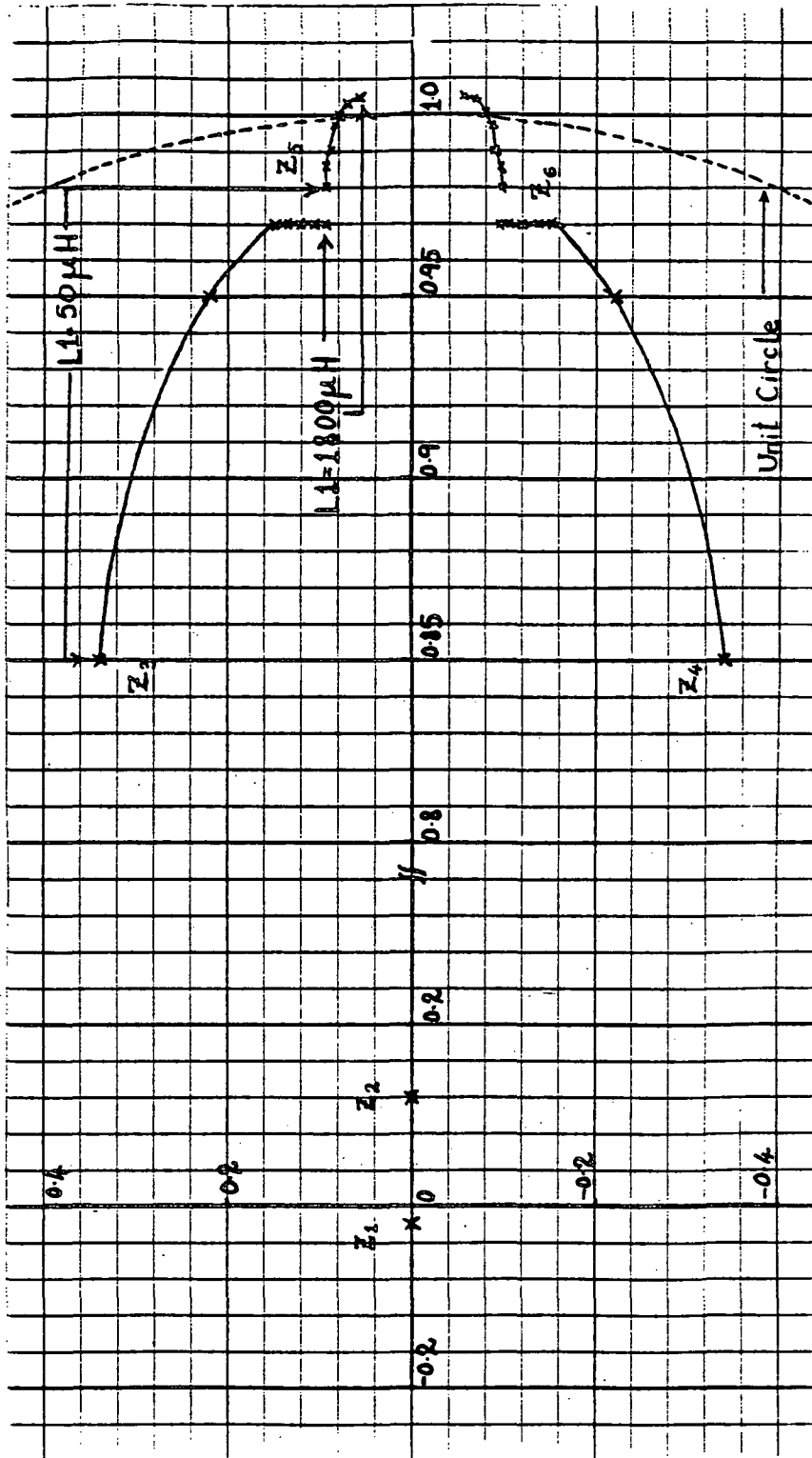


Figure 82: Eigenvalues with input filter, without feedforward

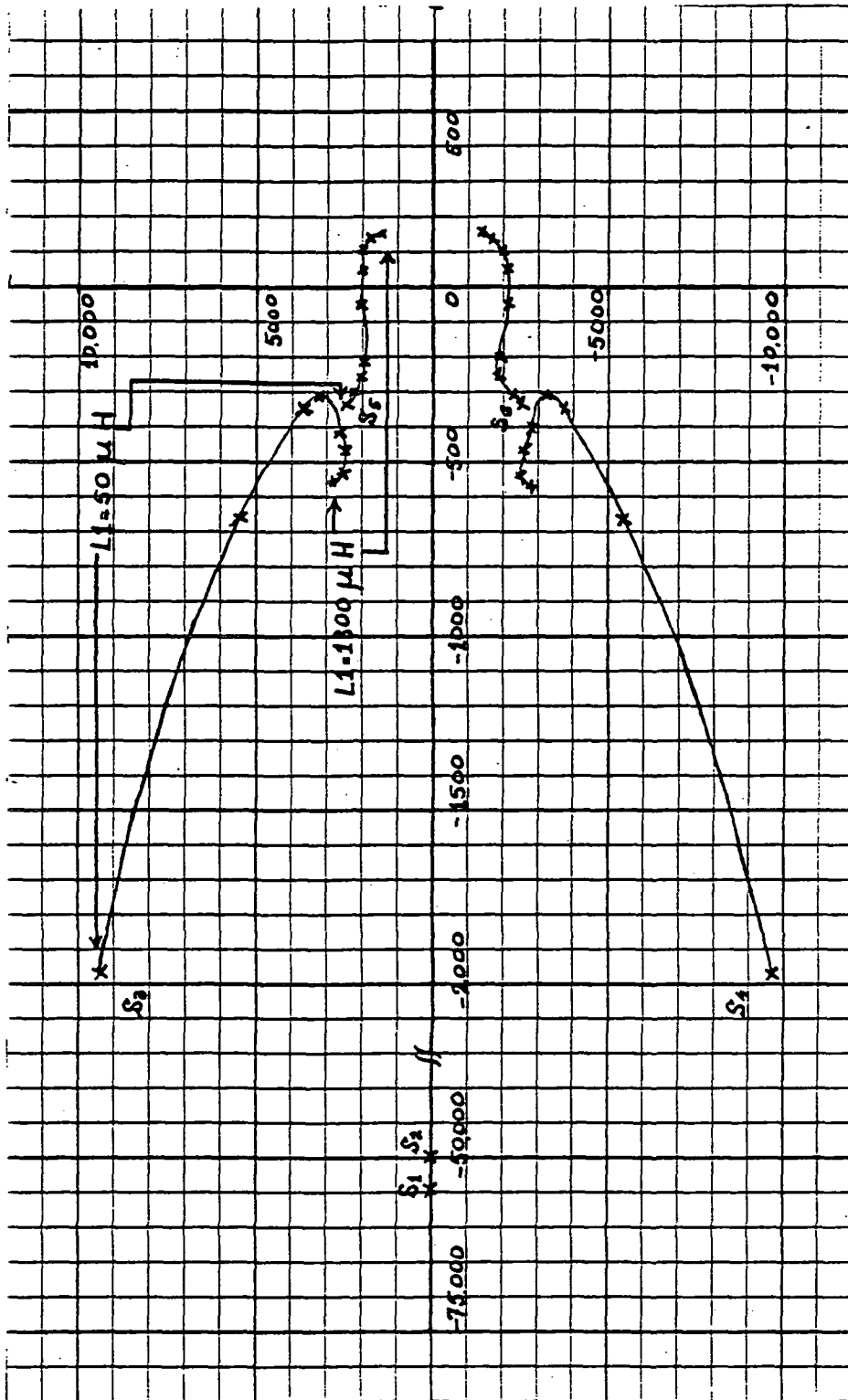


Figure 83: Closed loop poles with input filter, without feedforward

the eigenvalue plot. The bunching up of the closed loop poles for higher values of  $L_1$  is also noticed; this provides another crosscheck with the eigenvalue plot.

Thus it is seen that the eigenvalues and the closed loop poles match both qualitatively, as examination of Figures 82 and 83 show, and quantitatively through the use of equation (8-29) to crosscheck the eigenvalues. It is also noticed that system instability is predicted for values of  $L_1$  above 800 microH.

Lastly the eigenvalues were calculated for the case with feedforward using the program. The nonadaptive feedforward circuit of Figure 67 was used with the following parameters:

$$C_f = 27 \text{ microF} \qquad R_{f1} = 5100 \text{ ohms}$$

$$R_{f2} \text{ variable from } 210 \text{ ohm to } 300 \text{ ohm.}$$

Figure 84 shows the plot of the eigenvalues with feedforward for the following values of  $R_{f2}$ , with the value of  $L_1$  kept fixed at 1425 microH:

$$R_{f2} = 210, 220, 230, 235, 240, 260, 270 \text{ and } 300 \text{ ohms}$$

The value of  $R_{f2}$  was changed to see the effect of feedforward on the eigenvalues. Table 2 lists the eigenvalues for different values of  $R_{f2}$ . It is noticed from Figure 84 that there are seven eigenvalues and that the three on the real axis  $z_1$ ,  $z_2$  and  $z_3$  do not change as  $R_{f2}$  changes in value.

As  $R_{f2}$  is increased one pair of complex eigenvalues  $z_4$  and  $z_5$  move outside the unit circle while the other pair  $z_6$  and  $z_7$  move inside. For the value of  $L1$  used the closed loop poles and eigenvalues without feedforward clearly predict instability, whereas with feedforward it is seen that the system will be stable for some values of  $R_{f2}$ . For the regulator under consideration the value of  $R_{f2}$  is calculated to be 220 ohm from the feedforward design as obtained in Chapter 5. A value less than the design value causes the eigenvalues  $z_6$  and  $z_7$  to be outside the unit circle while it is noticed that a value higher than the design value also causes instability in the system. For the design value of 220 ohms all the eigenvalues are inside the unit circle thus clearly indicating that the addition of feedforward stabilizes a system that was unstable due to the interaction between the input filter and the regulator control loop.

As  $R_{f2}$  is increased further the real parts of the complex eigenvalues do not change much but eigenvalues  $z_4$  and  $z_5$  do move outside the unit circle. For  $R_{f2}$  between 220 and 260 ohm all the eigenvalues are inside the unit circle, with the optimum value being around 230 ohm.

In order to see clearly the effect of changing the feedforward loop gain the open loop gain and phase margin were calculated for various values of  $R_{f2}$ . The parameters of

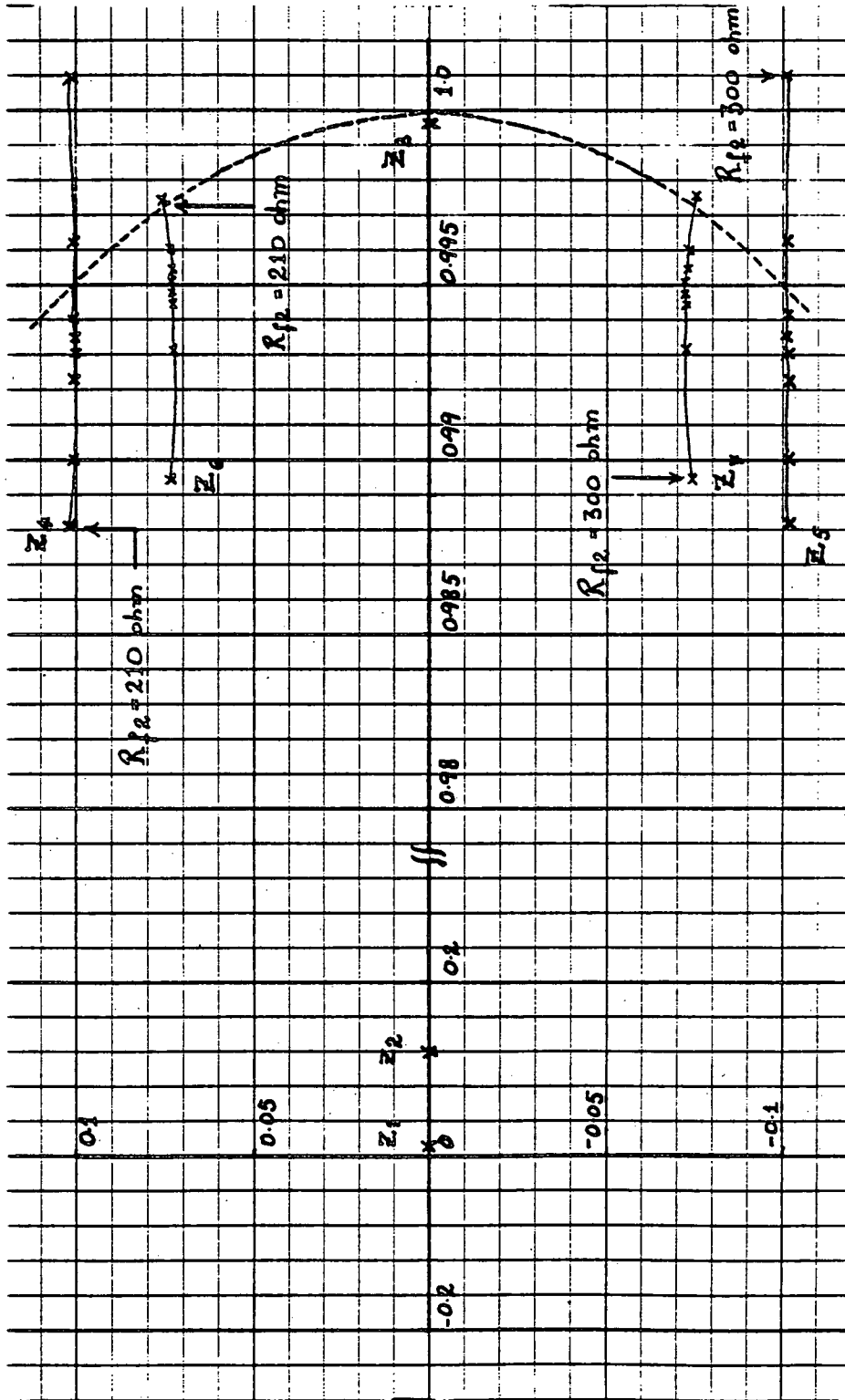


Figure 84: Eigenvalues with feedforward

the buck converter used in the calculation were the same as used in the eigenvalue calculation, with  $L_1 = 1425$  microH. Figure 85 (a) - (f) shows the plots of the open loop gain and phase margin for three values of  $R_{f2}$ . The solid lines on the figures are the plots without feedforward and with feedforward ( $R_{f2} = 220$  ohms), whereas the triangles represent values with  $R_{f2}$  either lower than or higher than the design value of 220 ohm. Exact compensation of the input filter interaction is achieved with  $R_{f2} = 220$  ohm, with any value other than 220 ohm the compensation is not complete. Decreasing the feedforward loop gain (210 ohm) results in a loss of open loop gain at the filter resonant frequency. Increasing the feedforward loop gain results in a loss of phase margin at the resonant frequency. For a value of 240 ohm the open loop gain obtained is close to the gain with 220 ohm but the phase margin is decreased. Increasing the feedforward gain further (300 ohm) makes the situation worse as Figure 85 (f) shows. The open loop gain in Figure 85 (e) is decreased to around 8 db at a frequency of about 300 Hz while at that frequency the phase margin is almost zero, indicating that the system is close to instability. This is confirmed on examination of Figure 84 which shows that the system is unstable for  $R_{f2} = 300$  ohm. It should be noted that the open loop gain with an input filter and  $R_{f2} = 220$  ohm is identical to that without input filter.

It is thus concluded that exact compensation is obtained at the design value of the feedforward loop gain. Increasing or decreasing the feedforward gain from the design value results in incomplete compensation. There may be no compensation achieved at all if the feedforward gain is far different from the design value.

It is noticed in Figure 84 as in the other eigenvalue plot that the eigenvalues do not seem to move very much, for example in Figure 84 the real part of the pair  $z_4$  and  $z_5$  changes from about 0.9885 to 0.9975 while from Figure 82 it changes from about 0.98 to 1.004. It is noted however that from Figure 83 the above change in real part corresponds to a change in the real part of the poles from about -323 to +140. This may be explained by noting as before that  $T$  in equation (8-29) is fairly small so this change in real part will correspond to a very small change in the real and imaginary parts of the eigenvalues.

From the results presented in this section it is seen that the eigenvalue program is a powerful tool for the analysis of stability. It is also seen that for the regulator used, a high value of input filter inductance will cause instability, but the addition of feedforward restores stability. Experimental data that strongly support this analytical prediction are presented next.

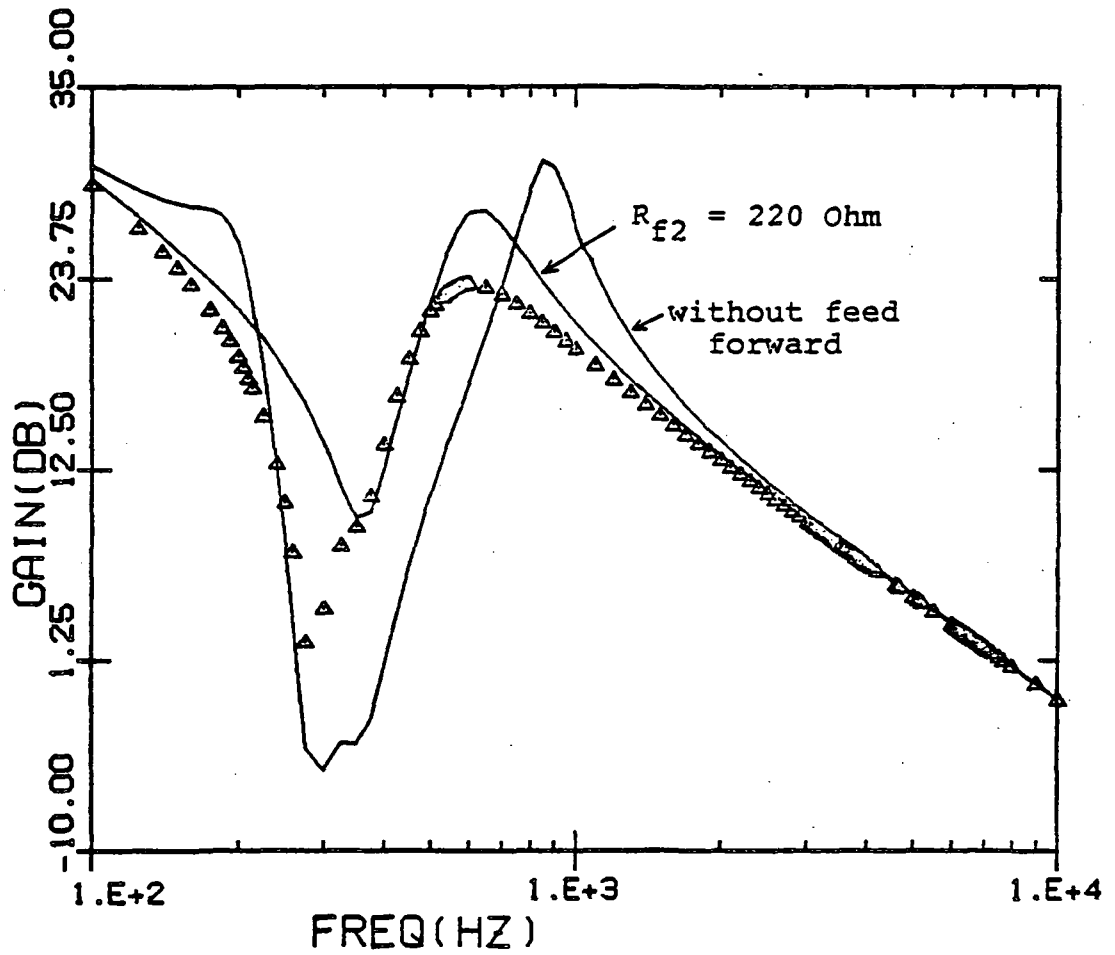


Figure 85: (a) Open loop gain: calculated values without feedforward, with  $R_{f2} = 220 \text{ ohm}$  and  $R_{f2} = 210 \text{ ohm}$

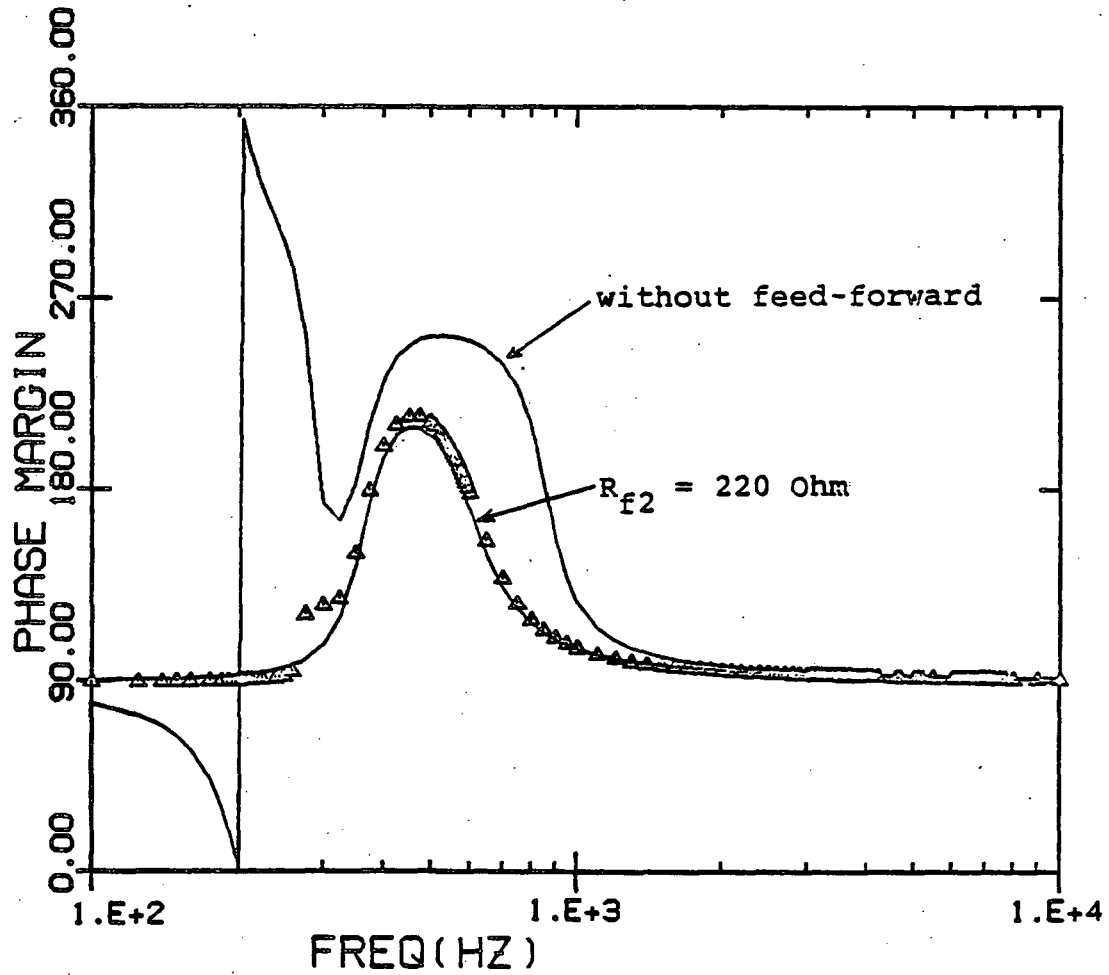


Figure 85: (b) Open loop phase margin: calculated values without feedforward, with  $R_{f2}=220$  ohm and  $R_{f2}=210$  ohm

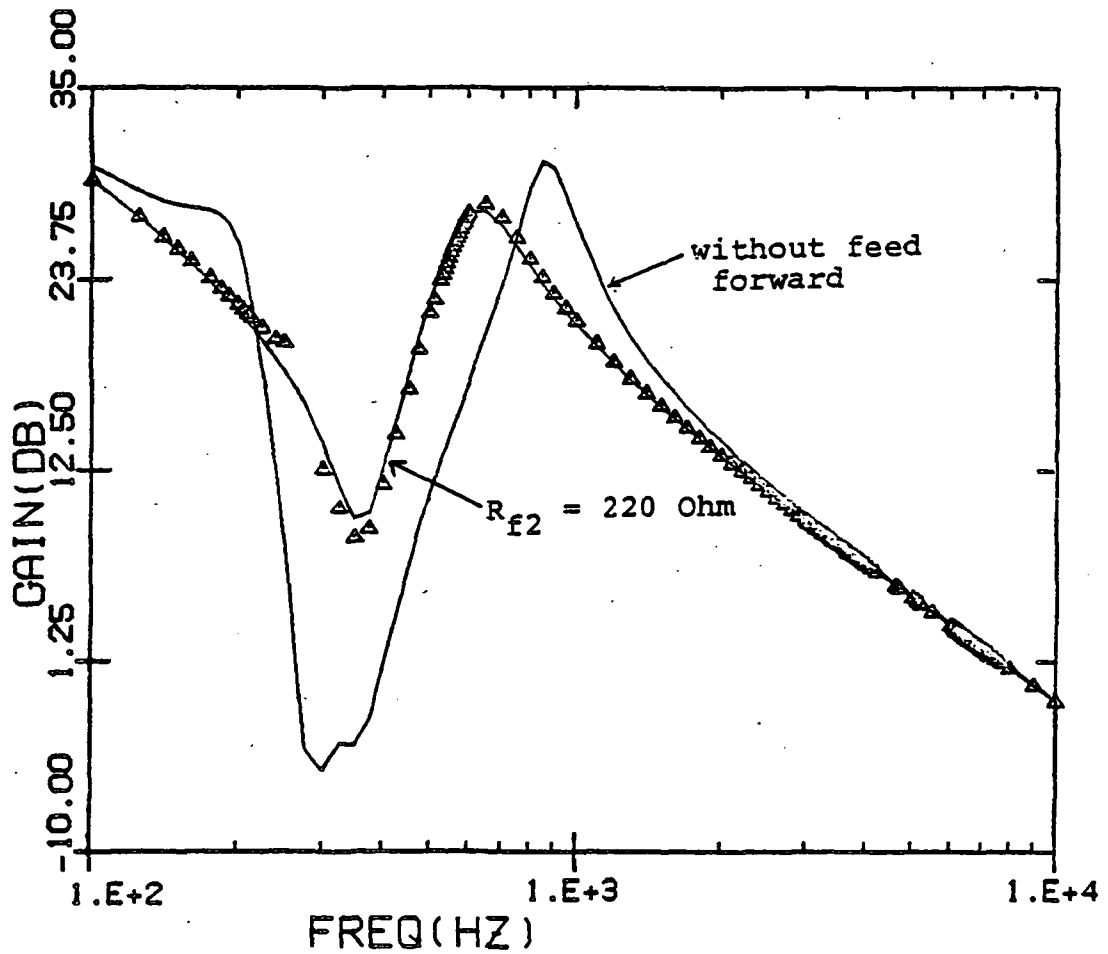


Figure 85: (c) Open loop gain: calculated values without feedforward, with  $R_{f2}=220$  ohm and  $R_{f2}=240$  ohm

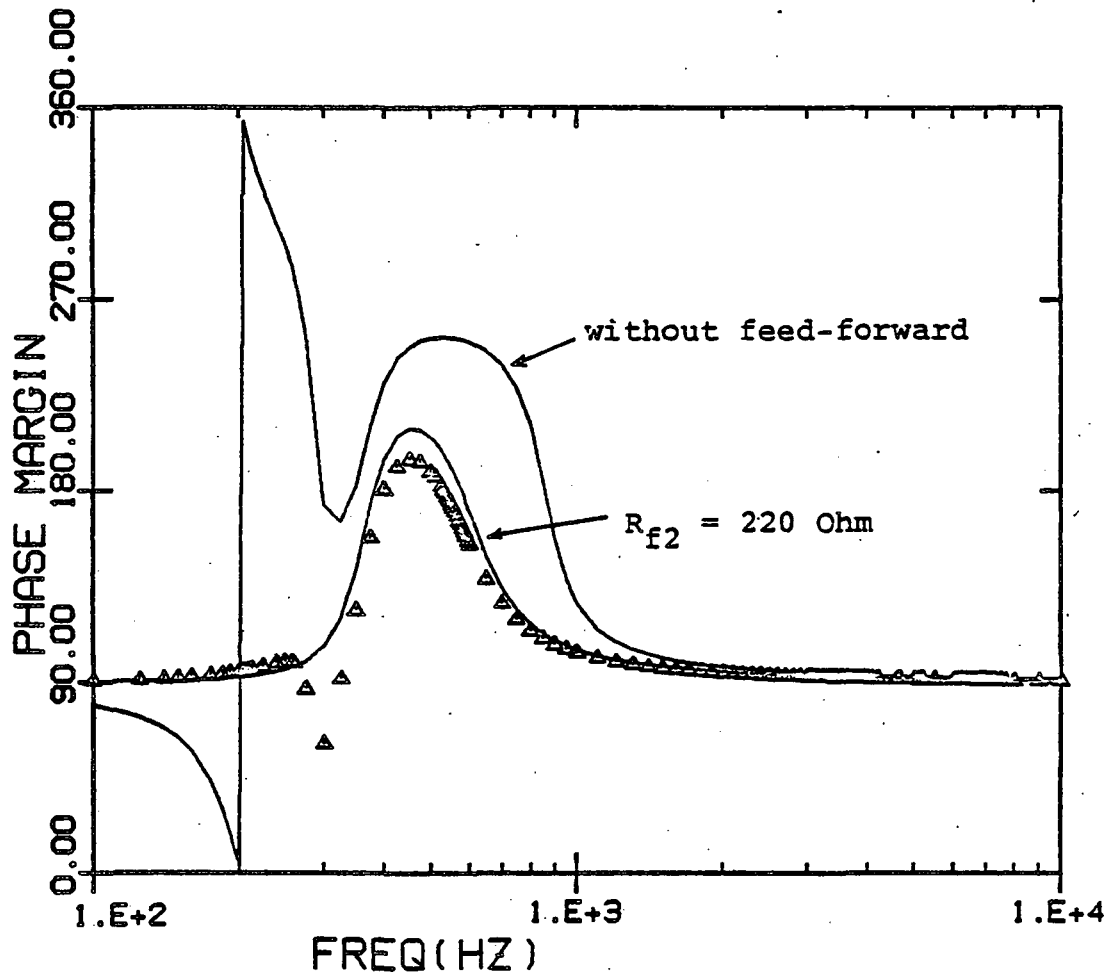


Figure 85: (d) Open loop phase margin: calculated values without feedforward, with  $R_{f2}=220$  ohm and  $R_{f2}=240$  ohm

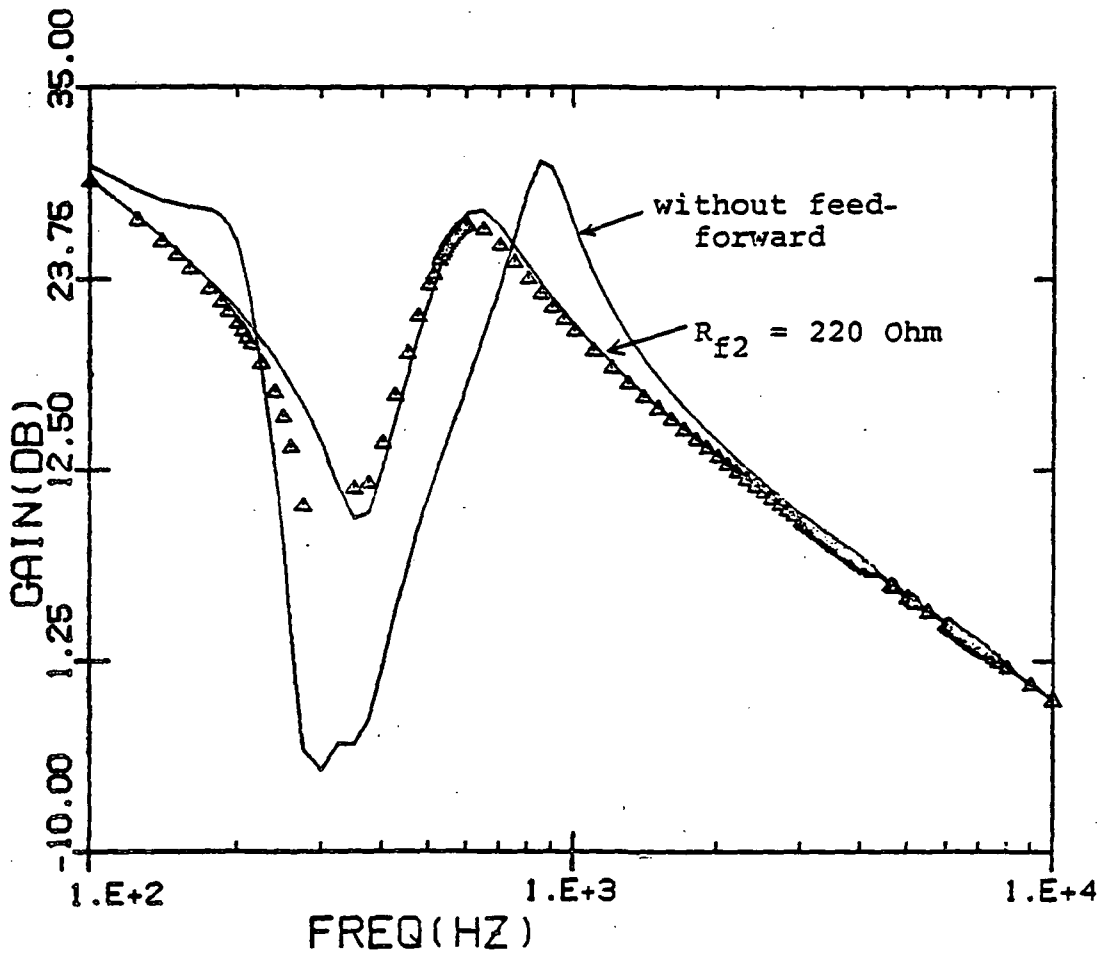


Figure 85: (e) Open loop gain: calculated values without feedforward, with  $R_{f2} = 220$  ohm and  $R_{f2} = 300$  ohm

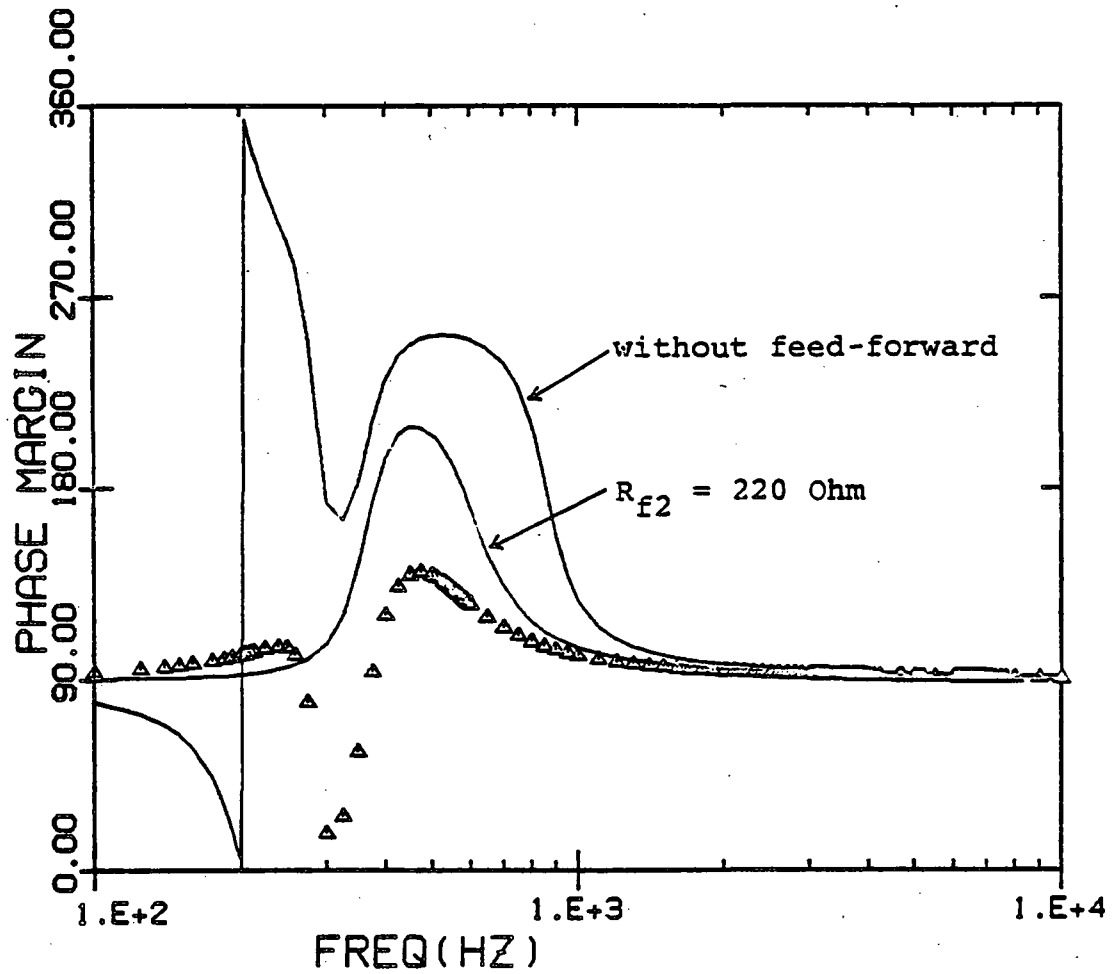


Figure 85: (f) Open loop phase margin: calculated values without feedforward, with  $R_{f2} = 220 \text{ ohm}$  and  $R_{f2} = 300 \text{ ohm}$

TABLE 2

Eigenvalues for different values of  $R_{f2}$ .

	Eigenvalues
$R_{f2} = 210 \text{ ohm}$	$0.00116 + j0$ $0.1282 + j0$ $0.9998 + j0$ $0.9974 \pm j 0.0738$ $0.9883 \pm j 0.101$
$R_{f2} = 220 \text{ ohm}$	$0.00017 + j0$ $0.1282 + j0$ $0.9998 + j0$ $0.9963 \pm j 0.0742$ $0.9907 \pm j 0.1006$
$R_{f2} = 230 \text{ ohm}$	$0.00122 + j0$ $0.1282 + j0$ $0.9998 + j0$ $0.9955 \pm j 0.0743$ $0.9922 \pm j 0.10121$

TABLE 2  
continued

	Eigenvalues
$R_{f2} = 235 \text{ ohm}$	$-0.00025 + j0$ $0.1282 + j0$ $0.9998 + j0$ $0.9952 \pm j 0.0742$ $0.9931 \pm j 0.1006$
$R_{f2} = 240 \text{ ohm}$	$-0.00011 + j0$ $0.1282 + j0$ $0.9998 + j0$ $0.9948 \pm j 0.0743$ $0.9936 \pm j 0.10049$
$R_{f2} = 260 \text{ ohm}$	$0.00039 + j0$ $0.1283 + j0$ $0.9998 + j0$ $0.9946 \pm j 0.0744$ $0.9941 \pm j 0.1011$

TABLE 2  
continued

	Eigenvalues
$R_{f2} = 270 \text{ ohm}$	0.00023 + j0 0.1283 + j0 0.9998 + j0 0.9933 ± j 0.0742 0.9964 ± j 0.1008
$R_{f2} = 300 \text{ ohm}$	0.00029 + j0 0.1285 + j0 0.9998 + j0 0.98952 ± j 0.0724 1.0054 ± j 0.1036

## 8.2 EXPERIMENTAL VERIFICATION OF STABILITY ANALYSIS.

In this section experimental data pertaining to the stability of the system are presented. The buck regulator of Figure 34 was used with the parameters as defined in section 8.1.4 with the exception that the input filter inductance  $L_1$  had a constant value of 1.425 mH. The adaptive feedforward circuit of Chapter 5 was used, however it is noted that if the input voltage is kept constant, as it was in the following measurements, the nonadaptive and the adaptive feedforward circuits provide the same gain.

The regulator was set up with the HP network analyser to measure open loop gain exactly like in Chapter 6 [7,8]. The open loop gain and phase margin were measured without input filter, with and without feedforward. Figure 86 shows the measured values of the open loop gain and phase margin. It can be seen that without the input filter the gain dips down around 320 Hz -- this may be explained by noting that the values of  $R_{13}$  and  $C_2$  are such that the compensation loop [7,8] is largely ineffective. Thus the open loop gain and phase margin correspond to a value of  $\alpha = 0.355$  as shown in the literature [7,8].

The addition of the input filter causes the gain to fall below 0 db and when the gain is close to 0 db the phase margin is only about 10 degrees at a frequency of about 250

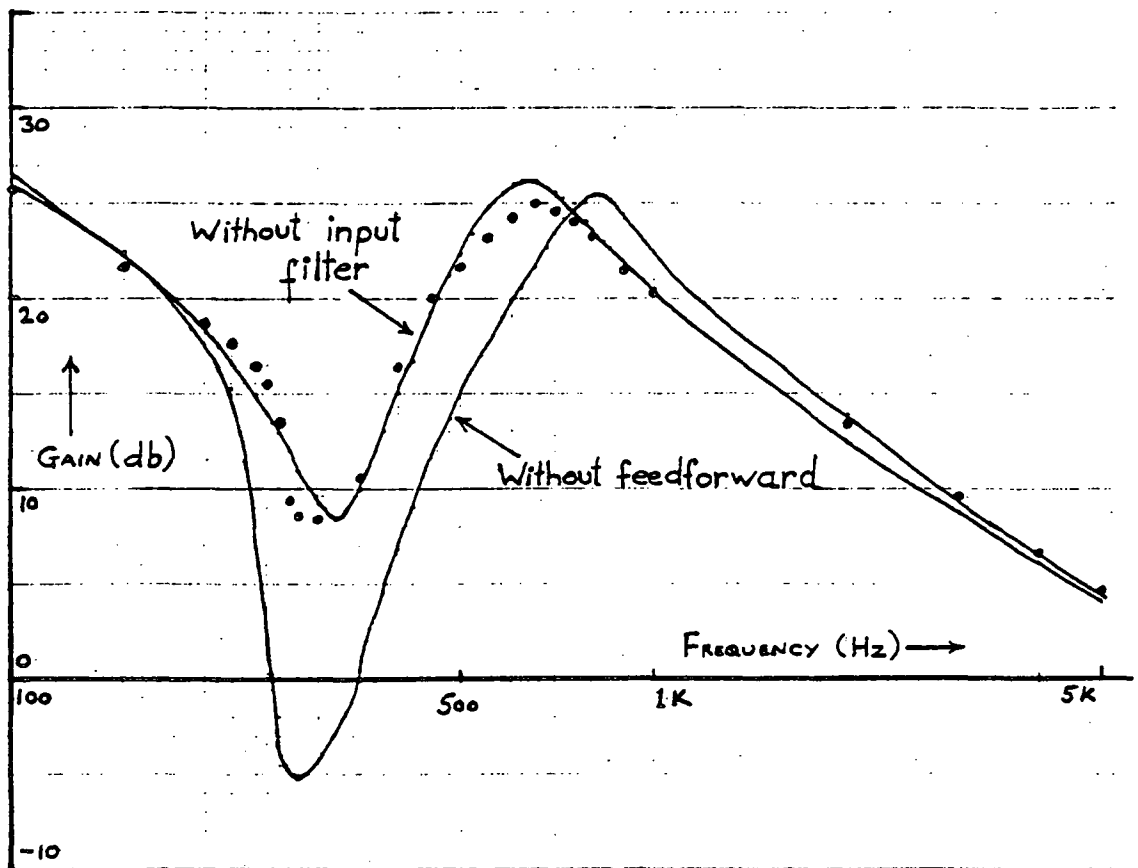


Figure 86: (a) Open loop gain: measured values without input filter, with (•) and without feedforward.

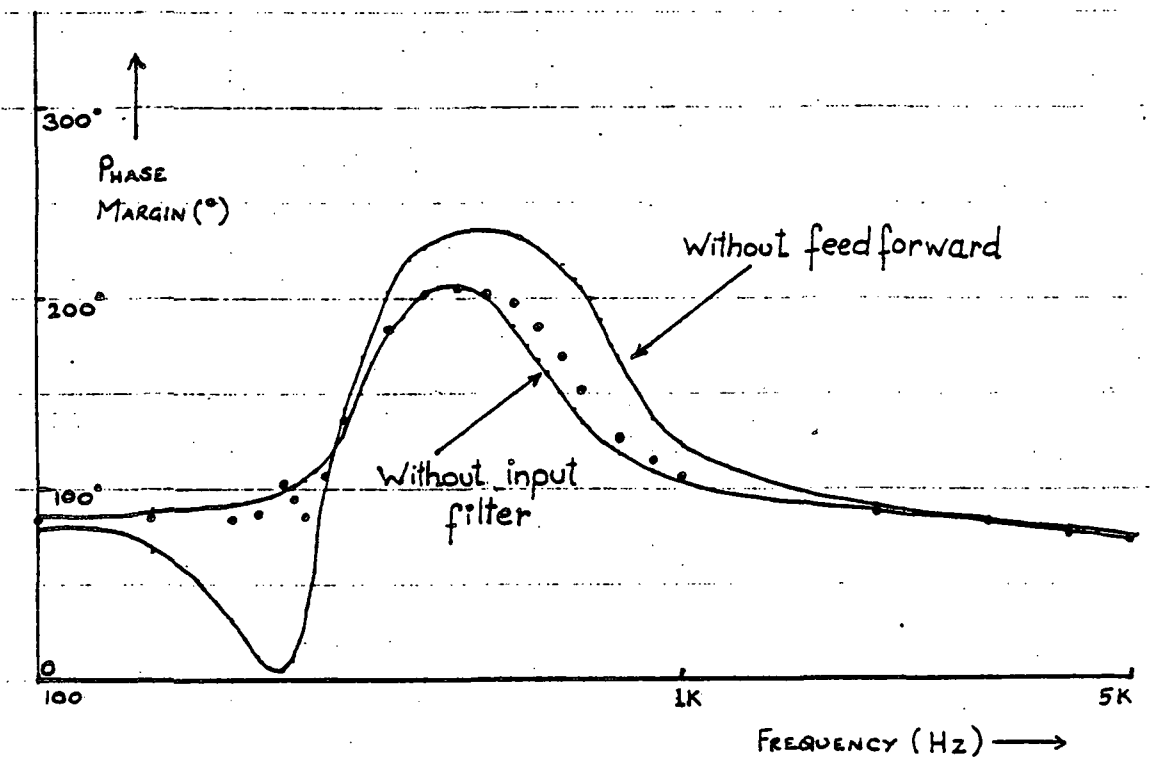
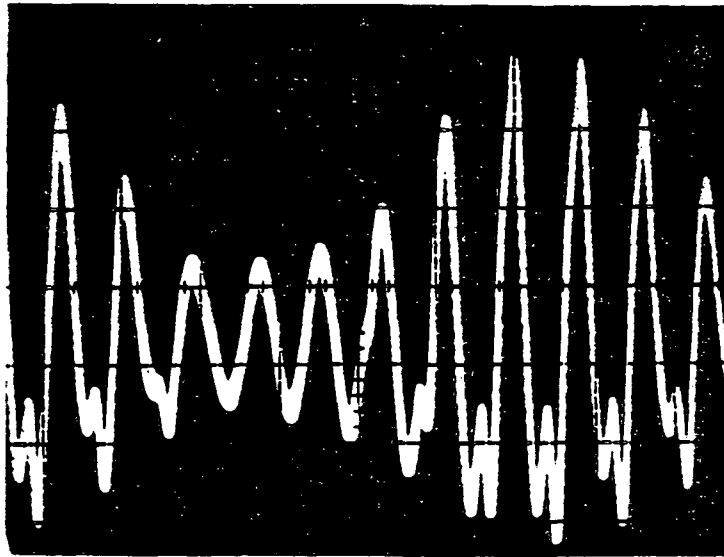


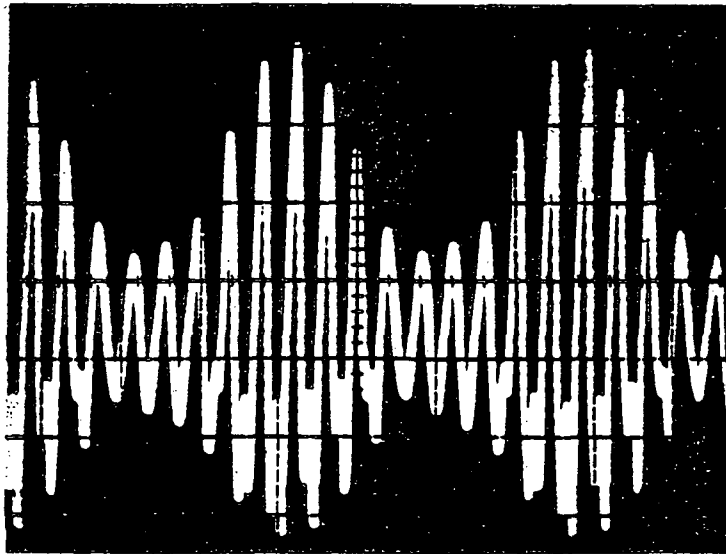
Figure 86: (b) Open loop phase margin: measured values without input filter, with (•) and without feedforward

Hz. The system is thus marginally stable and a small signal 250 Hz sinusoidal disturbance is injected into the loop to induce unstable operation and it was observed that the output voltage has oscillations. Figure 87 shows the output voltage ripple -- it is clearly seen that the oscillations are around 1.2 v in magnitude. It is concluded that the system is clearly unstable. Analysis presented earlier showed that the system would be unstable for  $L_1 = 1425$  microH while experimental results show a marginally stable system, thus lending support to the analysis.

Feedforward was added to the circuit and measurements of the open loop gain and phase margin were made. It is seen clearly from Figure 85 that the addition of feedforward removes the instability -- this is confirmed by recording the output voltage ripple. Figure 88 shows the output voltage ripple and it can clearly be seen that the oscillations that were present earlier without feedforward have been eliminated, making the system stable. The 250 Hz oscillation in Figure 88 is the injected disturbance. The analytical prediction that feedforward eliminates instability caused by input filter interaction is thus strongly supported by experimental data.

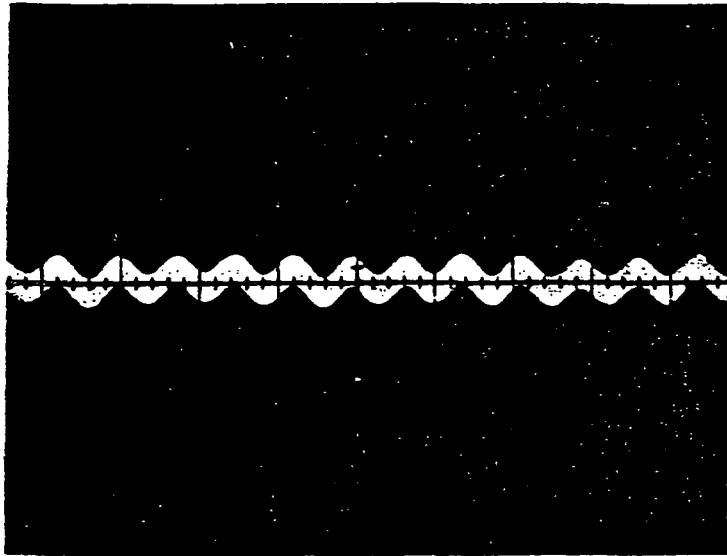


(a)

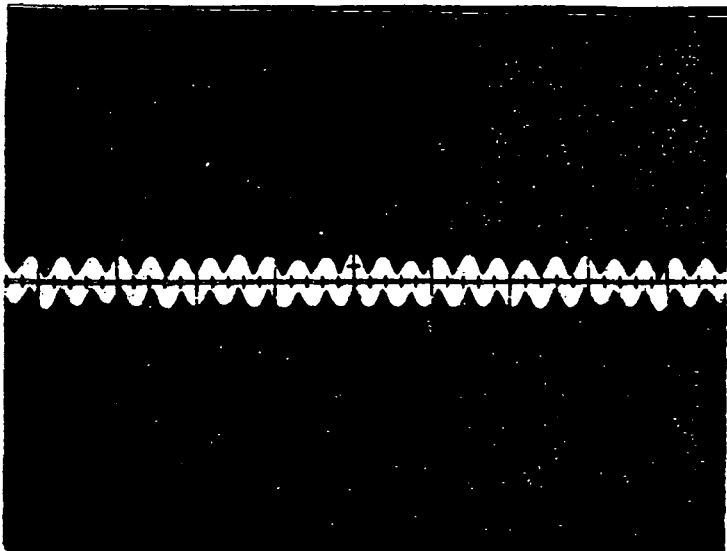


(b)

Figure 87: Output voltage ripple without feedforward: (a) Y:0.2v/div X:5 msec/div. (b) Y:0.2v/div X:10 msec/div.



(a)



(b)

Figure 88: Output voltage ripple with feedforward: (a) Y:0.2v/div X:5 msec/div. (b) Y:0.2v/div X:10 msec/div.

### 8.3 CONCLUSIONS

It is seen that the eigenvalue analysis program is a powerful tool for the analysis of stability. Using a buck regulator system a stability analysis was performed for various values of input filter inductance and it was observed that system instability was predicted for large values of inductance. A valuable crosscheck was provided by a program that calculated the closed loop poles and it was observed that the closed loop poles and the eigenvalues track very closely for all the values of inductance used, including those values for which system instability is predicted.

The addition of feedforward removes the instability at large values of inductance as the eigenvalue analysis presented shows. It is noticed that complete compensation of the input filter interaction is obtained for the design value of feedforward gain; any other value of feedforward gain results in incomplete compensation. It was demonstrated both from the eigenvalue analysis and the open loop gain and phase margin plots that a too large or too small value of feedforward gain would not be able to remove the instability caused by the input filter interaction.

Experimental measurements were made to confirm the analytical results presented. It was noticed that without feedforward the output voltage has large magnitude oscillations

indicating system instability. These oscillations occur at a value of input filter inductance for which the eigenvalue analysis also predicts instability thus tying in the analysis with experimental measurements. The addition of feedforward (with the gain set to its design value) completely removes these oscillations as measurement data show. Since the eigenvalue analysis also predicted stability with the addition of feedforward, it is thus concluded that the addition of feedforward does result in removing the system instability caused by input filter interaction with the regulator control loop.

## Chapter IX

### EXTENSIONS OF THE CONCEPT OF INPUT FILTER COMPENSATION TO OTHER CONVERTER TYPES

The concept of feedforward loop compensation to mitigate converter--input filter interaction is extended to several other cases, three of which are discussed in this chapter.

#### 9.1 EXTENSION TO OTHER TYPES OF REGULATOR CONTROL

The concept of feedforward compensation for the input filter has been developed with reference to a buck regulator. Extensive experimental data, together with analysis, confirm the validity of the concept. This was done exclusively on a buck converter with multiple-loop control and constant volt-sec duty cycle modulation. Use of other types of control are discussed in this section.

##### 9.1.1 Feedforward compensation for multiple-loop control using other types of duty-cycle control

The feedforward design was presented in Chapter 5 where it was noted that the gain of the feedforward loop depends on the transfer function of the pulse modulator,  $F_M$ . The transfer function  $F_M$  is dependent on the type of duty-cycle control used [2,8]. In this dissertation the constant volt-sec. type of duty-cycle control was used. However, it is

easy to see that for other types of duty-cycle control, for example for constant frequency control or constant off time control, the feedforward design procedure outlined in Chapter 5 is still valid. The feedforward design process presented earlier is general since it treated the pulse modulator in terms of its transfer gain only. Thus other types of duty-cycle control can be easily incorporated in the feedforward compensation after the transfer gain of the duty-cycle control is identified.

As an example for multi-loop constant frequency control the following pulse modulator gain is identified [8]:

$$F_M = \frac{2R_4 C_1'}{nM}$$

where

(9-1)

$$M = V_I(1-2D)T_p$$

In equation (9-1)  $T_p$  is the constant switching period. Substitution into the feedforward loop gain expression from Chapter 5 results in:

$$c_2 = \frac{-D^2 nM}{V_o \cdot 2R_4 C_1'} \quad (9-2)$$

For a constant supply voltage  $D$  and  $M$  would be constants and thus the feedforward gain would be a constant. An adaptive

feedforward circuit that tracks the supply voltage can be realized using equation (9-2).

For multi-loop constant off time control  $F_M$  is identified as [8]:

$$F_M = \frac{2R_4C_1'}{nM} \quad (9-3)$$

$$M = V_{I}T_{OFF}$$

where  $T_{OFF}$  is the constant off time. Substitution into the feedforward loop gain expression results in:

$$c_2 = \frac{-D^2 n V_{I} T_{OFF}}{V_O 2R_4 C_1'} \quad (9-4)$$

For a constant supply voltage  $D$  would be a constant and thus the gain would be a constant. An adaptive feedforward circuit that tracks the supply voltage variations can be realized from equation (9-4).

### 9.1.2 Feedforward compensation for single-loop control

A multi-loop feedback controlled buck regulator was used in the feedforward design discussed in Chapter 5. However, it is noted that in the design procedure the feedback loop transfer functions played no part in the feedforward design. This is evident since the feedforward gain is independent of the feedback loop transfer functions.

For single loop feedback control the regulator can be represented by a generalized block diagram as shown in Figure 89 . The feedback loop has as its input the output voltage ripple and it can be represented as  $F_E$ , as shown in Figure 89. Expressions for  $F_E$  and  $F_M$  are given in the literature [8], and it is noted that the transfer function  $F_E$  essentially processes the small signal variation in the output voltage and feeds it to the pulse modulator exactly like  $F_{DC}$  of Figure 28 . A feedforward loop that will sense the input filter state variables, process this information and feed it to the pulse modulator can thus be designed in a manner exactly as presented in Chapter 5. The transfer function  $F_M$  would be a constant [6] and would be a part of the feedforward gain, exactly as it is in the design presented.

As an example the following is identified for single loop constant frequency control [6]:

$$F_M = (1/A_0 T_p) \quad (9-5)$$

where  $A_0$ ,  $T_p$  are constants.

The error processor consists of an amplifier and a lead-lag compensation network and its transfer function  $F_E$  is available in the literature [6]. Since  $F_M$  is a constant the design of feedforward loop is relatively simpler as substitu-

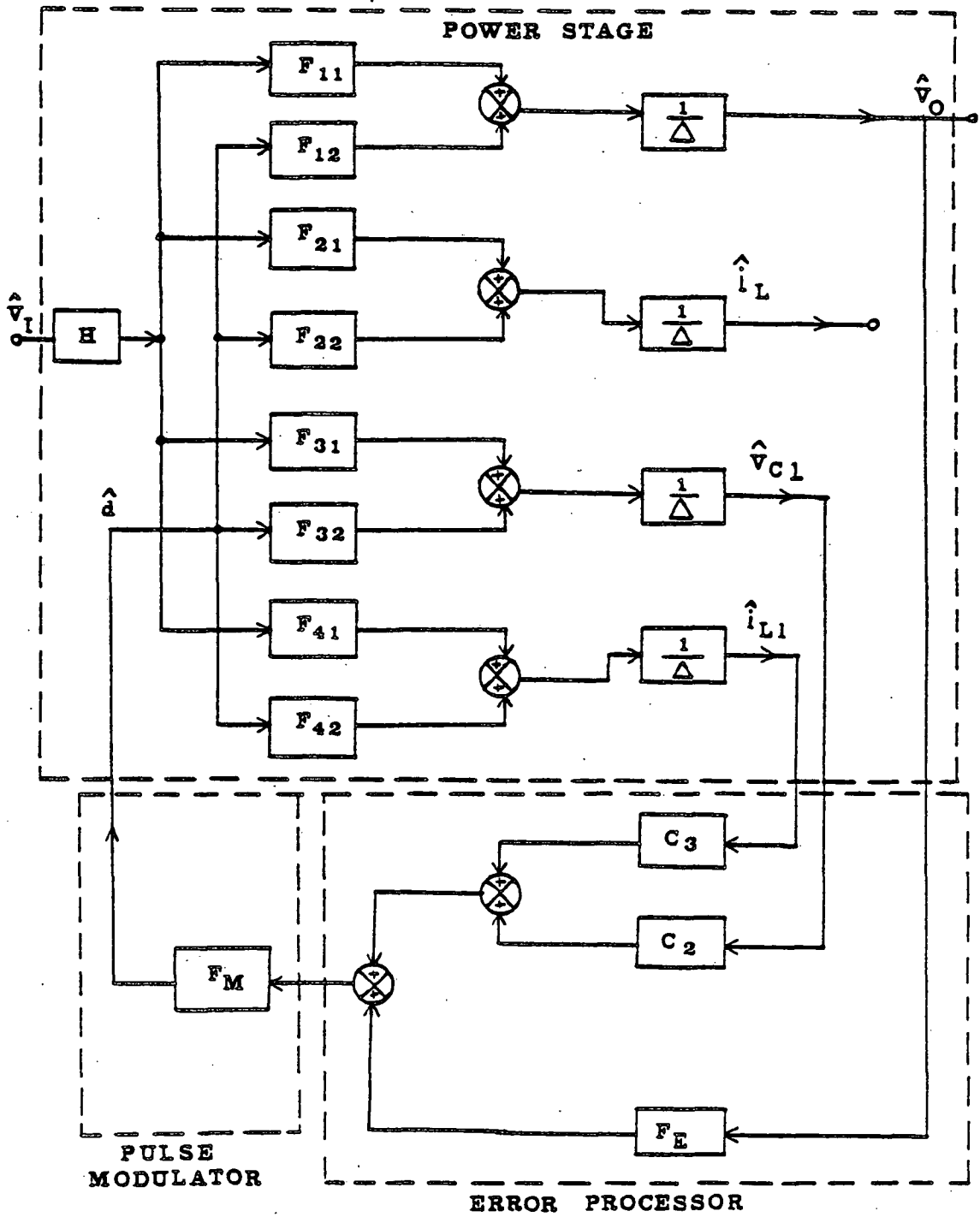


Figure 89: Generalized small signal model for single loop control

tion into the feedforward gain expression of Chapter 5 shows:

$$c_2 = \frac{-V_o A_o^T p}{V_I^2} \quad (9-6)$$

For constant supply voltage the gain  $c_2$  is a constant. An adaptive feedforward circuit that tracks the supply voltage variations could be developed exactly as shown in Chapter 5.

It is thus seen that an extension of the feedforward concept to single loop control is easily affected.

## 9.2 FEEDFORWARD COMPENSATION FOR THE BUCK-BOOST AND BOOST REGULATORS

Extension of the feedforward concept to the two other types of regulators-- boost and buck-boost can be obtained following the outline presented in Chapter 5. A feedforward design for the buck-boost regulator is presented.

The state space model of the buck-boost regulator is shown in Figure 90. In the figure the feedforward loop has as its input the input filter state variables (inductor current and capacitor voltage). These two are multiplied by the transfer functions  $c_2$  and  $c_3$  whose properties have yet to be determined. This state space model is based on the model for the buck-boost power stage developed in Chapter 4. The

feedback loops form the standardized control module (SCM) developed earlier [2,7,8] and discussed in Chapter 5. The pulse modulator has as its transfer function  $F_M$  [8] and has as its input information regarding the state variables of both the input filter and the output filter. The total state feedforward/feedback error signal is thus used to modulate the duty cycle of the switch for loop gain correction.

The generalized small signal model for the buck-boost regulator is developed next and used to write the transfer function  $\hat{v}_o/\hat{v}_x$ .

### 9.2.1 Generalized small signal model for the buck-boost regulator

The generalized small signal model is shown in Figure 91. The regulator is modeled according to the three basic functional blocks : power stage, error processor and duty cycle pulse modulator, as in Chapter 5. It is noticed that in this case the flux is a state variable, because it is continuous unlike the inductor current. The transfer functions  $F_3$ ,  $F_{AC}$  and  $F_{DC}$  play no part in the feedforward design process, as earlier in Chapter 5.

The power stage transfer functions  $F_{11}$  etc. are written as in Chapter 5, using the following equations:

$$T_{11}\hat{v}_I + T_{12}\hat{d} = \hat{v}_o$$

$$T_{21}\hat{v}_I + T_{22}\hat{d} = \hat{\phi}$$

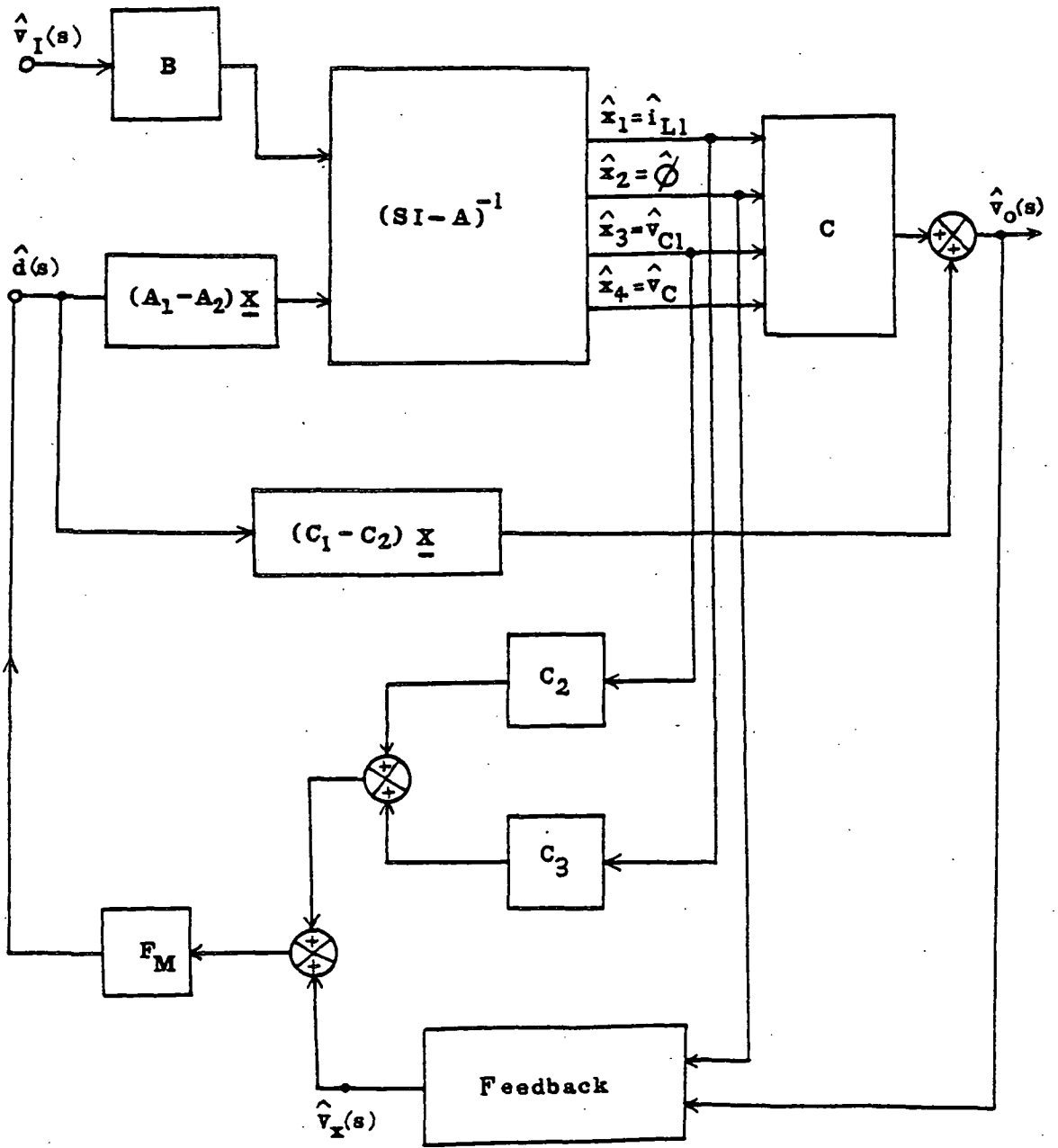


Figure 90: State space model of the buck-boost regulator

$$T_{31}\hat{v}_I + T_{32}\hat{d} = \hat{v}_{C1} \quad (9-7)$$

$$T_{41}\hat{v}_I + T_{42}\hat{d} = \hat{i}_{L1}$$

Thus it is seen that

$$T_{11} = \left. \frac{\hat{v}_O}{\hat{v}_I} \right|_{\hat{d} = 0} \quad (9-8)$$

and

$$T_{11} = \frac{HF_{11}}{\Delta} \quad (9-9)$$

$$T_{12} = \frac{F_{12}}{\Delta}$$

The transfer functions  $T_{11}$ ,  $T_{21}$ ,  $T_{31}$  and  $T_{41}$  are developed with  $\hat{d}=0$  and the others with  $\hat{v}_I = 0$ . The starting point for the derivation is again the small signal equivalent circuit model for the buck-boost regulator developed in Chapter 4.

Evaluation of transfer functions with  $\hat{d} = 0$ .

The equivalent circuit model with  $\hat{d} = 0$  is shown in Figure 92. In Figure 92 the input filter has been replaced by its forward transfer function  $H(s)$  and its output impedance  $Z(s)$ , the expressions for  $H$  and  $Z$  being the same as in Chapter 5. From the equivalent circuit of Figure 92 the following are derived, assuming that  $R_{C1} \cong 0$  :

$$T_{11} = \frac{H \cdot D_1 \cdot D' \cdot R_L (1 + sCR_c)}{\Delta} \quad (9-10)$$

$$T_{21} = \frac{H \cdot L_s \cdot D_1 (1 + sCR_L)}{N_s \Delta}$$

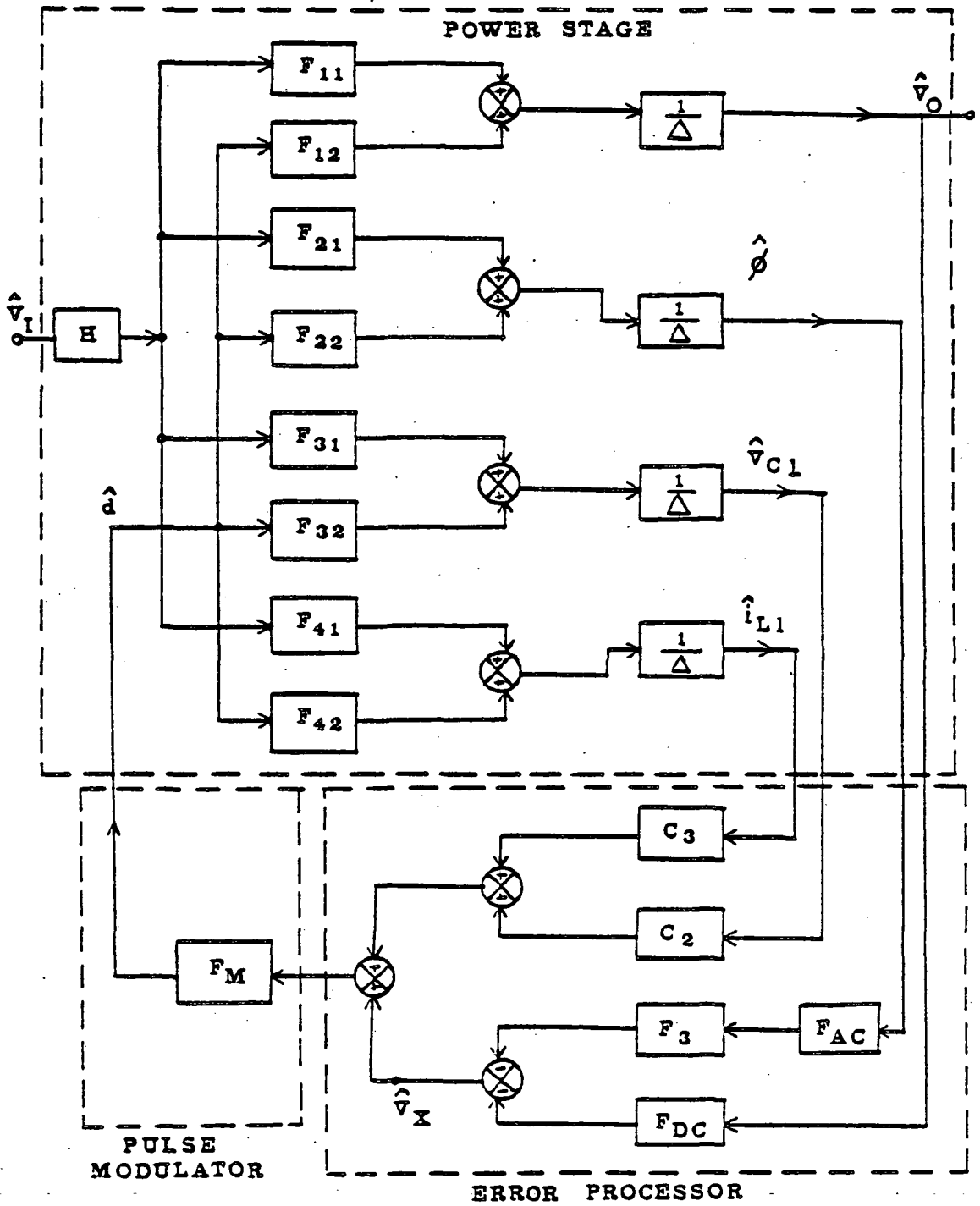


Figure 91: Generalized small signal model

$$T_{31} = \frac{H \cdot a_1}{\Delta}$$

$$T_{41} = \frac{\Delta - a_1 H}{(R_{L1} + sL1) \Delta}$$

where

$$a_1 = s^2 L_s C R_L + s C R_L (R_s + D' R_C + \frac{L_s}{C R_L}) + R_s D D' R_C + D'^2 R_L$$

$$\Delta = a_1 + D_1^2 Z (1 + s C R_L) \quad (9-11)$$

$$D_1 = \frac{D N_s}{N_p}, \text{ where } D \text{ is the duty cycle.}$$

$$R_L + R_C = R_L$$

Using the above equations the following can be derived:

$$F_{11} = D_1 D' R_L (1 + s C R_C)$$

$$F_{21} = \frac{L_s D_1 (1 + s C R_L)}{N_s} \quad (9-12)$$

$$F_{31} = a_1$$

$$F_{41} = \frac{\Delta/H - a_1}{(R_{L1} + sL1)}$$

The ESR of the capacitor  $R_{C1}$  has been neglected in the derivation for the same reasons as outlined in Chapter 5, while equation (5-9) is used in the derivation of  $T_{41}$ .

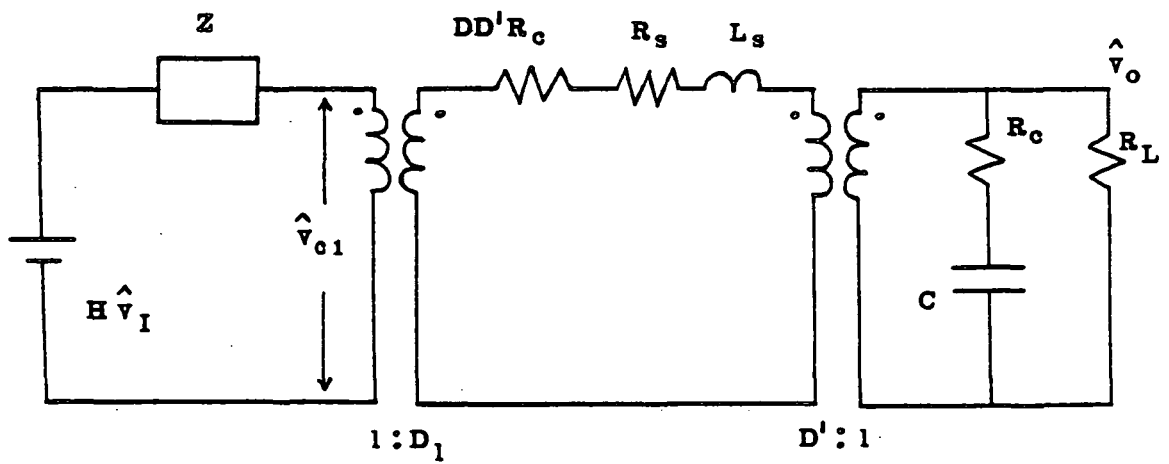


Figure 92: Small signal equivalent circuit with  $\hat{d}=0$

Evaluation of the transfer functions with  $\hat{v}_I = 0$ .

The small signal equivalent circuit with  $\hat{v}_I = 0$  is shown in Figure 93. The following are derived from the equivalent circuit:

$$\begin{aligned}
 T_{12} &= \frac{V_o(1 + sCR_c) \{-D_1^2 Z + D'^2 R_L - DsL_s\}}{DD'\Delta} \\
 T_{22} &= \frac{L_s \{V_o(1 + sCR_L) (-D'D_1^2 Z + D'^2 R_L - DsL_s) + DV_o a_1\}}{N_s DD'^2 R_L \Delta} \\
 T_{32} &= \frac{V_o(1 + sCR_L) D_1^2 Z (DR + DsL_s - D'^2 R_L) + V_o a_1 (DR - D_1^2 Z)}{DD_1 D'^2 R_L \Delta} \\
 T_{42} &= -T_{32} / (R_{L1} + sL1)
 \end{aligned} \tag{9-13}$$

where  $\Delta$  and  $a_1$  are as defined earlier and

$$\begin{aligned}
 I &= \frac{V_o}{R_L D'} \\
 V_1 &= \frac{V_o}{D}
 \end{aligned} \tag{9-14}$$

Using the above equations the following are derived:

$$\begin{aligned}
 F_{12} &= \frac{V_o(1 + sCR_c) \{-D_1^2 Z + D'^2 R_L - DsL_s\}}{DD'} \\
 F_{22} &= \frac{L_s \{V_o(1 + sCR_L) (-D'D_1^2 Z + D'^2 R_L - DsL_s) + DV_o a_1\}}{N_s DD'^2 R_L}
 \end{aligned}$$

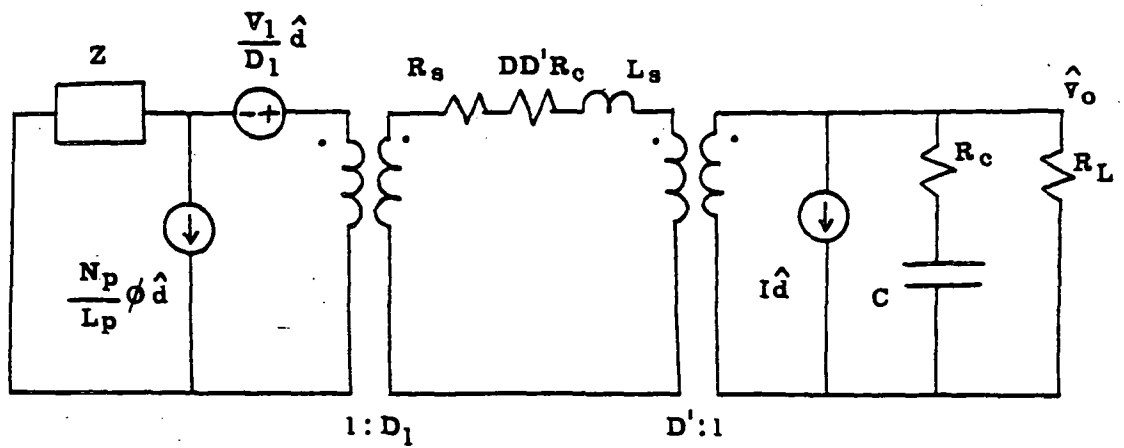


Figure 93: Small signal equivalent circuit with  $\hat{v}_I = 0$

$$F_{32} = \frac{V_o(1 + sCR_L)D_1^2 Z(DR + DsL_s - D'^2 R_L) + V_o a_1(DR - D_1^2 Z)}{DD'^2 D_1 R_L}$$

$$F_{42} = -F_{32}/(R_{L1} + sL1)$$

(9-15)

$$\text{where } R = R_s + DD' R_c$$

(9-16)

The feedback transfer functions  $F_3$ ,  $F_{AC}$  and  $F_{DC}$  constitute the two loop SCM feedback control scheme reported earlier [2,8]. The transfer functions are defined in the literature [2,7,8], and it is noted that they do not play any part in the design process, as in Chapter 5. The pulse modulator transfer function  $F_M$  depends on the type of duty cycle control used [7,8] and it will be seen that the feedforward loop gain depends on  $F_M$ , as earlier in Chapter 5.

### 9.2.2 Design of the Feedforward Loop

With  $\hat{v}_I = 0$  the following equations are derived from Figure 91 :

$$[\hat{v}_x + c_2 \hat{v}_{C1} + c_3 \hat{i}_{L1}] F_M = \hat{d} \quad (9-17)$$

and after substitution

$$\frac{\hat{v}_o}{\hat{v}_x} = \frac{\left(\frac{F_{12}}{\Delta}\right) F_M}{1 - c_2 \left(\frac{F_{32}}{\Delta}\right) F_M - c_3 \left(\frac{F_{42}}{\Delta}\right) F_M} \quad (9-18)$$

In the absence of feedforward i.e. with  $c_2 = 0 = c_3$  it can be seen that

$$\frac{\hat{v}_o}{\hat{v}_x} = \frac{V_o (1 + sCR_c) \{-D_1^2 Z + D'^2 R_L - DsL_S\} F_M}{DD'\Delta} \quad (9-19)$$

The effect of peaking of  $Z$  is to cause a reduction in the gain of the transfer function and thus also in the open loop gain. It is also noticed that equation (9-18) shows the positive zero term in the transfer function.

With the addition of feedforward the effect of peaking of  $Z$  could be avoided by a proper choice of feedforward loop gains  $c_2$  and  $c_3$ . Two approximations are made to facilitate the design:

1. The effect of the positive zero is assumed to be negligible at the frequency at which  $Z$  peaks. Thus it is assumed that:

$$D'^2 R_L - DsL_S = D'^2 R_L \quad (9-20)$$

This is not an unrealistic assumption since  $Z$  peaks at a much lower frequency.

2. It is also assumed that

$$DR - D_1^2 Z = -D_1^2 Z \quad (9-21)$$

at the frequency at which Z peaks. Again this is not an unrealistic assumption given the low value of R.

Using the above assumptions, the following choice is made:

$$\begin{aligned} c_3 &= 0 \\ c_2 &= \frac{-DD_1}{V_O F_M} \end{aligned} \quad (9-22)$$

Substitution into equation (9-18) leads to:

$$\frac{\hat{v}_O}{\hat{v}_X} = \frac{V_O (1 + sCR_L) \{-D_1^2 Z + D'^2 R_L\} F_M}{DD' \Delta} \frac{DD'^2 R_L D_1 \Delta}{a_1 DD_1 \{-D_1^2 Z + D'^2 R_L\}} \quad (9-23)$$

which leads to

$$\frac{\hat{v}_O}{\hat{v}_X} = \frac{V_O (1 + sCR_L) D' R_L F_M}{Da_1} \quad (9-24)$$

It is seen from equation (9-24) that the transfer function is now independent of the peaking effect of Z. It is also noted that equation (9-24) is valid only at low frequencies where the two assumptions made earlier hold. The feedforward loop gains are very similar to the gains developed for the buck regulator, and are identical if  $N_S = N_P$ . It is also noted from equations (9-15) and (9-18) that the gain of  $F_{32}$

would be fairly small at frequencies other than the resonant frequencies at which Z peaks. Thus the addition of feedforward would not affect, in any noticeable manner, the open loop gain and phase margin at any frequency other than those at which Z peaks. Thus the feedforward compensation is effective for most input filter designs because the filter resonant frequencies are relatively low in comparison to the positive zero.

### 9.2.3 Analytical and Experimental Verification

The buck-boost regulator shown in Figure 94 was used to obtain verification of the feedforward design. A multi-loop standardized control module (SCM) type feedback control was used [2,7,8]. The parameters of the converter are as follows:

#### Power Stage Parameters:

$$\begin{array}{llll}
 V_I = 20 \text{ v} & V_O = 28 \text{ v} & D = 0.5833 & P_O = 28 \text{ watts} \\
 L_S = 220 \text{ microH} & & C = 300 \text{ microF} & \\
 R_C = 0.05 \text{ ohm} & & R_L = 28 \text{ ohm (load)} & \\
 N_S = N_P = 33 & & R_S = 0.087 \text{ ohm} &
 \end{array}$$

#### Pulse Modulator Parameters:

$$M = V_I T_{ON} = 0.5 \times 10^{-3} \text{ v-sec.}$$

Control Circuit Parameters:

$$\begin{array}{lll}
 E_R = 7\text{v} & R_{11} = 43.2 \text{ Kohm} & R_2' = 15 \text{ Kohm} \\
 R_3 = 47.5 \text{ Kohm} & R_4 = 40 \text{ Kohm} & R_5 = 1.1 \text{ Kohm} \\
 n = 0.667 & C_1' = 5600 \text{ pf} & C_2' = 32000 \text{ pf}
 \end{array}$$

Input Filter Parameters

$$\begin{array}{lll}
 R_1 = 0.2 \text{ ohm} & L_1 = 325 \text{ microH} & C_1 = 200 \text{ microF} \\
 R_2 = 0.02 \text{ ohm} & L_2 = 116 \text{ microH} & C_2 = 20 \text{ microF} \\
 R_3 = 0.075 \text{ ohm} & (\text{ESR of } C_1) &
 \end{array}$$

The regulator was operated in a predetermined duty cycle control mode (constant  $V_I T_{ON}$  control) [2,7,8].

The open loop gain can be written from Figure 91 as

$$G_T(s) = \frac{\left\{ F_{DC} \left( \frac{F_{12}}{\Delta} \right) + F_3 F_{AC} \left( \frac{F_{22}}{\Delta} \right) \right\} F_M}{1 - c_2 \left( \frac{F_{32}}{\Delta} \right) F_M} \quad (9-25)$$

It is noted that in deriving the above equation  $c_3$  is set equal to zero since that is the design value. Equation (9-25) was used to plot the open loop gain and phase margin without input filter, with and without feedforward. The transfer functions  $F_{DC}$ ,  $F_3$ ,  $F_{AC}$  and  $F_M$  constitute the feedback and are defined in the literature [2,7,8], while  $F_{12}$ ,  $F_{22}$  and  $F_{32}$  were defined earlier in this chapter. Equation (9-25) is also valid for the case without input filter, all

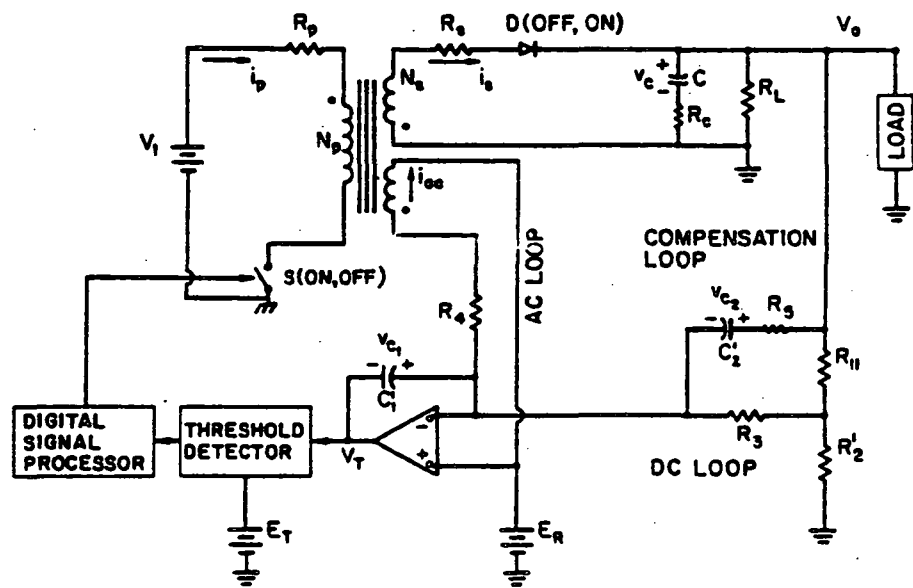


Figure 94: Schematic of a buck-boost regulator

that is necessary to do is to set  $Z = 0$ , while for the case without feedforward  $c_2$  is set equal to zero. Figure 95 shows the calculated values of open loop gain and phase margin. It is important to note at this point that equation (9-25) is an exact equation and that the assumptions made earlier in the feedforward design process are not made in deriving this equation.

It is seen from Figure 95 (a) and (b) that the two stage input filter causes disturbances in the open loop gain and phase at the two resonant frequencies, but the addition of feedforward removes these disturbances. The feedforward loop is seen to be effective at both the resonant frequencies though at the higher frequency there is a drop in phase margin. The two assumptions made in the feedforward design process have not been used in calculating the open loop gain with feedforward, and thus it is seen that Figure 95 indicates that the feedforward is effective in eliminating input filter interaction with the regulator control loop.

The same regulator circuit was used to obtain experimental results using a single stage input filter:

$$R_{L1} = 0.2 \text{ ohm} \quad L = 116 \text{ microH} \quad C1 = 20 \text{ microF}$$

The regulator was set up to measure the open loop gain and phase margin [8]. The nonadaptive feedforward circuit of Figure 67 was used in making the measurements. The feedfor-

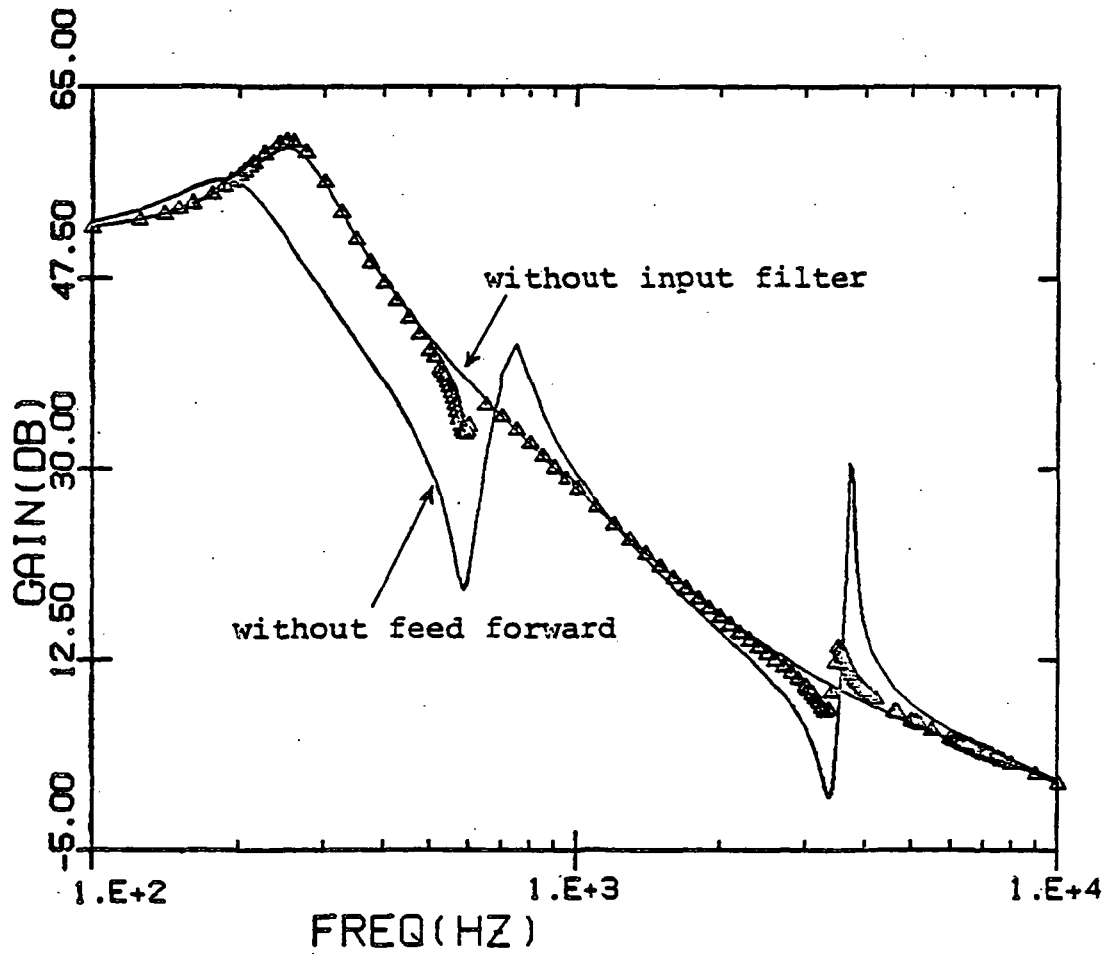


Figure 95: (a) Open loop gain: Calculated values without input filter, with ( $\Delta$ ) and without feedforward

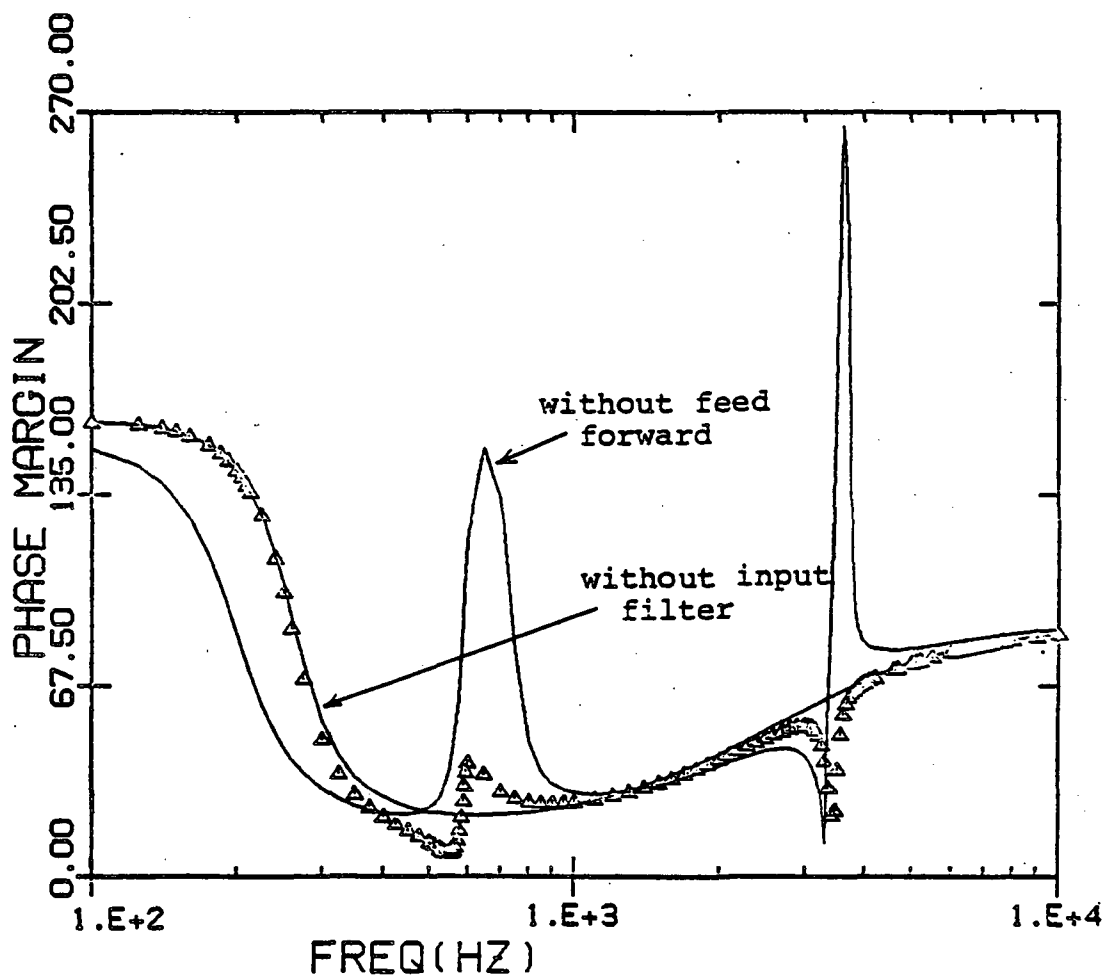


Figure 95: (b) Open loop phase margin: Calculated values without input filter, and ( $\Delta$ ) and without feedforward

ward gain was calculated from equation (9-22) as -0.009 and this led to the following choice of feedforward circuit parameters:

$$C_f = 27 \text{ microF} \quad R_{f1} = 5.6 \text{ Kohm} \quad R_{f2} = 50 \text{ ohm}$$

The input of the feedforward circuit is the input filter capacitor voltage, and the output is subtracted from the output at the integrater in the feedback loop, as was done earlier.

Figure 96 shows some preliminary measurements obtained. It is noticed that the input filter causes a disturbance in open loop gain and phase margin at the resonant frequency but the feedforward compensates for the input filter interaction to some extent. The approximation of equation (9-20) is valid at low frequencies, thus if the input filter resonates at high frequencies the feedforward as designed may not be effective in completely compensating for input filter interaction. Measurements of Figure 96 were obtained using an input filter with a somewhat high resonant frequency which can be used to explain the fact that the feedforward is effective to a somewhat lesser degree in compensating for the input filter interaction. Due to lack of time extensive experimental verification of the feedforward design was not possible; more measurement data is necessary to check the effect of feedforward on open loop gain and phase, and other performance specifications.

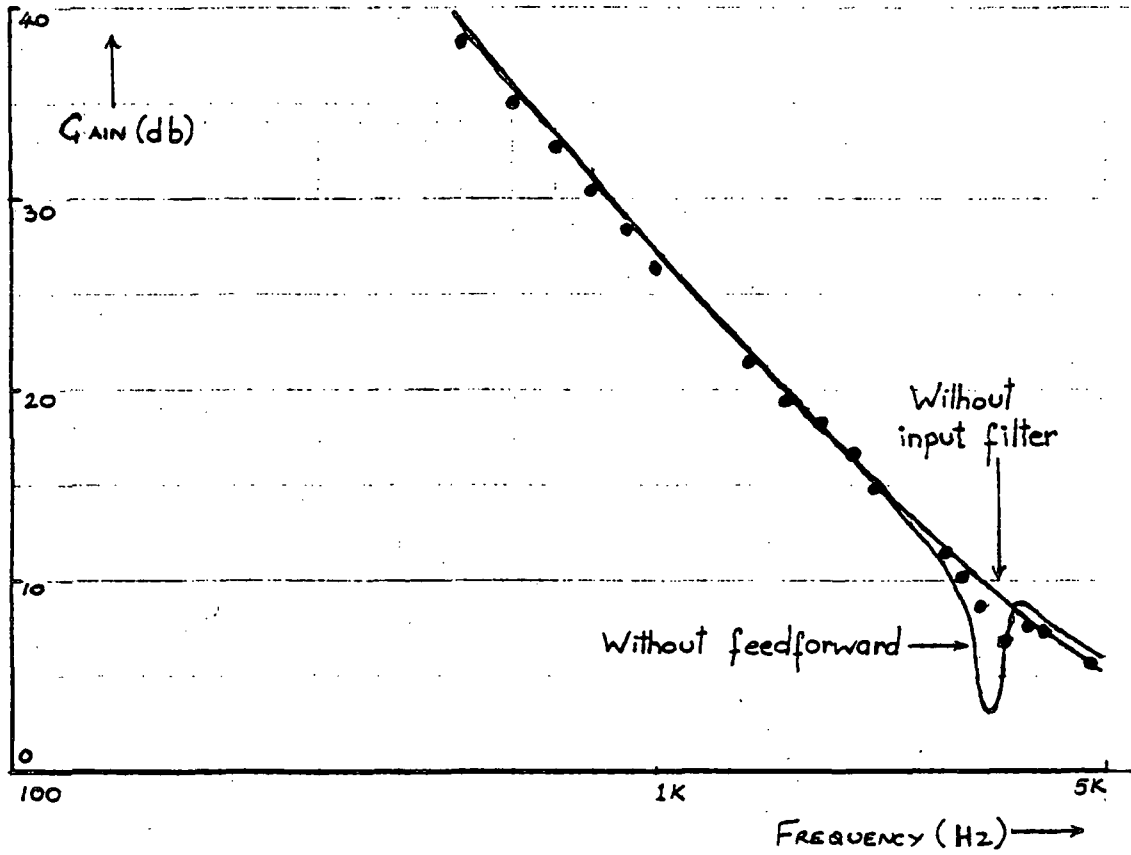


Figure 96: (a) Open loop gain: Measured values without input filter, with (•) and without feedforward

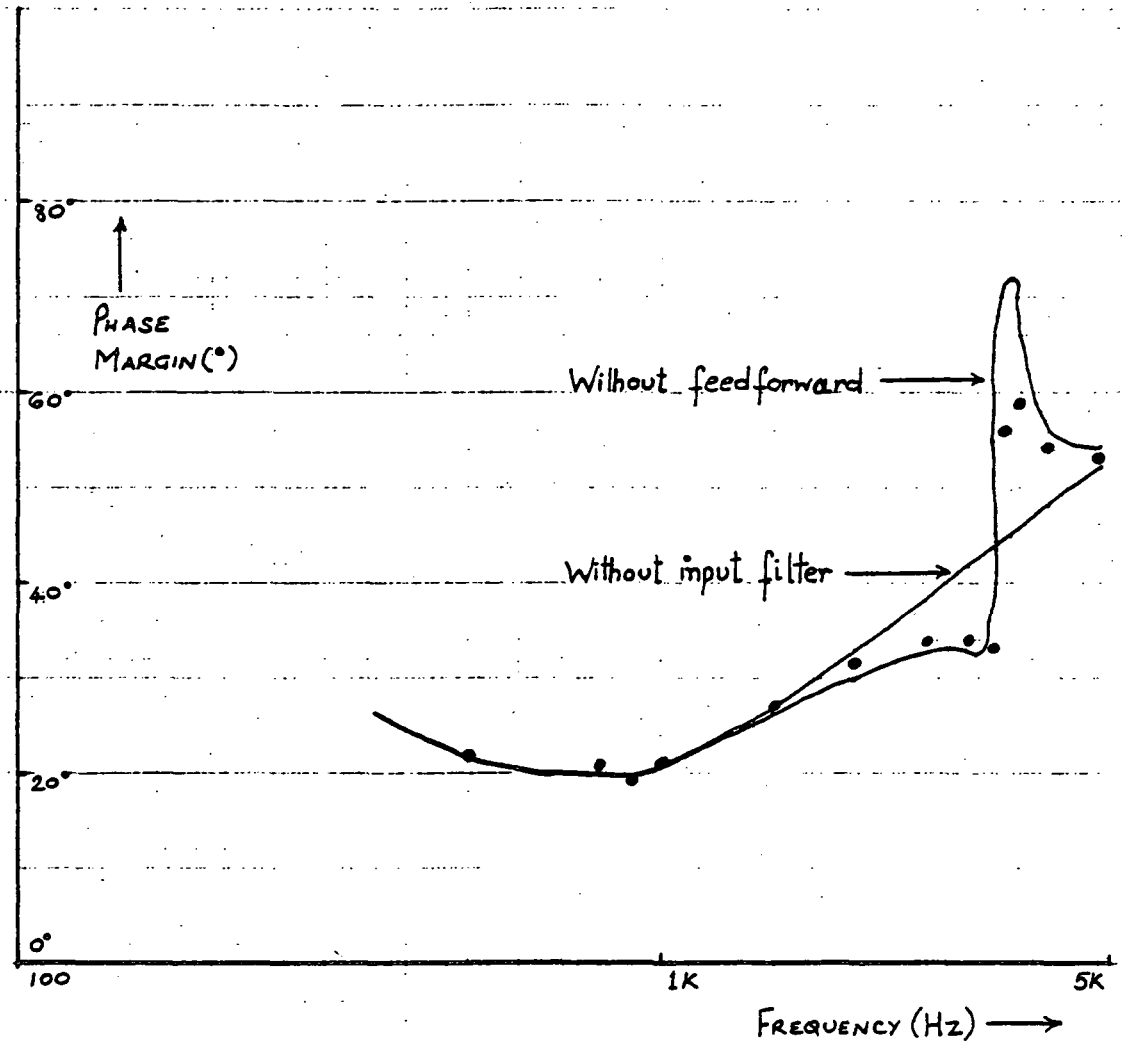


Figure 96: (b) Open loop phase margin: Measured values without input filter, with (•) and without feedforward

The feedforward design process for the boost regulator would be identical to the one presented above; similar assumptions may be necessary to accommodate the positive zero in the boost regulator transfer function.

### 9.3 REMARKS

The following observations are made:

1. The feedforward design process presented in Chapter 5 is general; it can be used for any type of duty cycle control and for single loop or multi-loop feedback control schemes.
2. The problem of input filter interaction with the regulator control loop is present in the buck-boost regulator also and the concept of feedforward compensation can be extended to design a feedforward loop that eliminates the interaction.

## Chapter X

### CONCLUSIONS AND FUTURE WORK

#### 10.1 CONCLUSIONS

A novel scheme for input filter compensation is presented in this dissertation. The input filter, while a necessary component of a switching regulator, interacts with the regulator control loop and this interaction can cause serious performance degradation such as loop instability, degradation of transient response, audiosusceptibility and the output impedance characteristics [3,4,5,6,10]. These problems are caused mainly by the peaking of the output impedance of the input filter and its interaction with the control loop.

Conventional input filter design techniques for single stage and two stage input filters [3,5,6] minimize the peaking effect but this often results in a penalty of weight or loss increase in the input filter. A novel feedforward compensation scheme is developed for buck regulators that eliminates the undesirable interaction between the input filter and the regulator control loop. The compensation scheme is implemented by a feedforward loop that senses the input filter state variables. Extensive analytical and experimental data confirm that the regulator is made immune to the peaking of the input filter output impedance.

The following points regarding the feedforward compensation scheme presented are noteworthy:

1. The feedforward design process is straightforward and it is seen that the feedforward loop gain is independent of the type of feedback control used and of the feedback loop transfer functions.
2. An important characteristic of the feedforward control scheme presented is its ease in implementation.
3. Extensive experimental data supported by analytical results show that significant improvement in performance is achieved with the use of feedforward in the following categories--
  - (a) open loop gain and phase margin;
  - (b) audiosusceptibility;
  - (c) output impedance; and
  - (d) transient response.

The data shows clearly that the peaking effect of the input filter output impedance is eliminated with the use of feedforward.

4. It is shown that the feedforward loop is independent of the input filter parameters and also independent of the input filter configuration.
5. Examination of the extensive experimental data confirm that the use of the feedforward compensation

scheme does not have any detrimental effect on regulator performance.

6. If a switching regulator is acquired as a 'black box' for use in a system, providing an inadequate input filter could lead to system instability [4,5]. This is shown analytically using a program that calculates the eigenvalues of the system, and confirmed experimentally. It is then shown that the use of the feedforward compensation scheme can stabilize a system that was made unstable due to input filter interaction with the regulator control loop. Experimental verification of the stabilizing action of the feedforward loop is presented and this shows that an arbitrary input filter may be used with the feedforward-loop controlled regulator.
7. From the results presented it is logical to conclude that the feedforward loop can provide effective compensation for an unknown source impedance. For example, a preregulator which often has an unknown, dynamic output impedance can interact with a switching regulator downstream and result in system instability. The feedforward circuit effectively isolates the switching regulator from its source thus preventing interaction between the switching converter and equipment upstream.

8. The use of the feedforward compensation scheme removes some of the input filter design constraints thus making the input filter design process simpler and allows the input filter to be optimized. A high performance regulator system with an optimum input filter can thus be realized with the use of the feedforward compensation scheme.
9. The feedforward design concept presented can be easily extended to types of control other than those used in this dissertation.
10. Extension of the concept of feedforward compensation to other types of switching regulators is possible. Such a scheme for a buck-boost regulator is presented and preliminary results indicate the validity of the compensation scheme.

#### 10.2 SUGGESTIONS FOR FUTURE WORK

The following suggestions for future work are made:

1. The concept of feedforward compensation for buck-boost switching regulators needs to be verified experimentally. Data indicating the effect of using the feedforward scheme on performance categories like audiosusceptibility, output impedance, transient response and stability is also needed.

2. An investigation into the use of the feedforward compensation scheme for the boost converter should be made.
3. The use of the feedforward loop is shown to isolate the regulator from its source, and this could be used to advantage in situations where regulators are put in series/parallel for load sharing.
4. Current injected control is an important mode of control and an investigation of the feasibility of using feedforward compensation for this type of control could be made.
5. Single loop control using the constant frequency duty cycle type control is very widely used and test results using feedforward compensation for this type of control are needed.
6. It may be possible to simplify the adaptive feedforward circuit by using the dc component of the input filter capacitor voltage instead of the supply voltage. This may have an effect on the transient response for a step change in supply voltage since then the duty cycle would change in accordance with changes in input filter capacitor voltage.

Appendix A

SOFTWARE FOR  
DISCRETE TIME SIMULATION OF A BUCK REGULATOR

```

C *****
C * DISCRETE TIME SIMULATION OF A BUCK CONVERTER. *
C *****
C THIS PROGRAM SIMULATES THE STEADY-STATE BEHAVIOR AS WELL AS
C THE TRANSIENT PERFORMANCE FOR A BUCK REGULATOR
C WITH INPUT FILTER, WITHOUT FEEDFORWARD.
C
C DIMENSION X(6,9000), F1(6,6), F2(6,6), G1(6,4), G2(6,4), TIME(9000),
1U(4), PHIF(6,6), PHIN(6,6), DF(6,4), DN(6,4), TVEC1(6), TSWIT(2),
2VISWIT(2), VO(9000), PHIFT(6,6), DFT(6,4), TVEC2(9000)
C DIMENSION F3(6,6), G3(6,4), TVEC3(6), PHIFT3(6,6), DFT3(6,4),
1PHIF3(6,6), DF3(6,4)
C
C REAL L1, L, K1, K2, IQMAX
C
C DATA RL1, L1, C1, L, RO, RN, RC, C/1.0, 325.E-6, 20.E-5, 230.E-6, 0.2, 0.65,
20.067, 300.E-6/
C DATA RL, R11, R12, R13, R14, C2, R4, CP1/20.0, 33.3E3, 16.7E3, 2.E3,
147.E3, 0.01E-6, 40.7E3, 5600.E-12/
C DATA ER, ET, VI, EO/6.7, 7.0, 40., 20./
C DATA TON, TOFMIN, TSWIT, VISWIT, VITON/2.20E-5, 5.E-6, 0.003, 10.,
125.0, 50., 0.88E-3/
C DATA NIT, FRAC, EPS, TF/10, 0.5, 5.E-6, 0.012/
C DATA IQMAX, EQ, ED/8.0, 0.2, 0.7/
C CL1S=0.5291665
C VC1S=39.48866
C ECS=7.0
C CLS=0.09291243
C VCS=20.05715
C ERS=20.05712
C VOS=19.99638
C
C TON=VITON/VI
C K1=(R12/(R14*(R11+R12)))+(1./R13)-(RN/R4)
C K1=K1-(RN*RO*(RL+RC))/(R4*RL*RC)
C K2=(RN/R4)-(1./R13)-(R12/(R14*(R11+R12)))
C DO 1 I=1,6
C DO 80 J=1,4
C G1(I,J)=0.
C G2(I,J)=0.
C DF(I,J)=0.
C DN(I,J)=0.

```

```

80 DFT(1,J)=0.
DO 1 J=1,6
F1(1,J)=0.
1 F2(1,J)=0.
C
DO 2 I=1,6
DO 2 J=1,6
PHIFT(1,J)=0.
PHIF(1,J)=0.
2 PHIN(1,J)=0.
C
F1(1,1)=(-1.*RL1)/L1
F1(1,2)=-1./L1
F1(2,1)=1./C1
F1(2,4)=-1./C1
F1(3,2)=(-1.*RN)/(CP1*R4)
F1(3,4)=(-1.*RL*RC*K1)/(CP1*(RL+RC))
F1(3,5)=(RL*K2)/(CP1*(RL+RC))
F1(3,6)=1./(CP1*R13)
F1(4,2)=1./L
F1(4,4)=(-1.*R0)/L+(-1.*RC*RL)/(L*(RC+RL))
F1(4,5)=(-1.*RL)/(L*(RC+RL))
F1(5,4)=RL/(C*(RL+RC))
F1(5,5)=-1./(C*(RL+RC))
F1(6,4)=(RL*RC)/(C2*R13*(RL+RC))
F1(6,5)=RL/(C2*R13*(RL+RC))
F1(6,6)=-1./(C2*R13)
G1(1,1)=1./L1
G1(3,2)=1./(CP1*R14)
G1(3,3)=RN/(CP1*R4)
G1(4,3)=-1./L
DO 3 I=1,6
DO 3 J=1,6
3 F2(I,J)=F1(I,J)
F2(2,4)=0.
F2(3,2)=0.
F2(4,2)=0.
G2(1,1)=G1(1,1)
G2(3,2)=G1(3,2)
G2(3,4)=RN/(CP1*R4)
G2(4,4)=-1./L
DO 530 I=1,6
DO 531 J=1,6

```

```
531 F3(1,J)=F2(1,J)
      DO 532 J=1,4
532 G3(1,J)=G2(1,J)
530 CONTINUE
      DO 535 I=1,6
      F3(4,I)=0.0
535 F3(1,4)=0.0
      DO 536 I=1,4
536 G3(4,I)=0.0
```

```
C
      NSWIT=0
      ITEMP=NSWIT+1
      TXX=TSWIT(I TEMP)
      NT=0.1+1./FRAC
      TOFF=TON*(V1-EO)/EO
      TIME(1)=0.0
      ND=1
      M=0
      IT=0
      T=FRAC*TOFF
```

```
C
      CALL STRAN(T,PHIF,DF,F2,G2,6,4,6,4,1,0,EPS,DIFMAX,ITER,I FLAG)
```

```
C
      T=FRAC*TON
      CALL STRAN(T,PHIN,DN,F1,G1,6,4,6,4,1,0,EPS,DIFMAX,ITER,I FLAG)
      WRITE(6,704)
704 FORMAT('/', ' VALUES OF X ON THE NEXT PAGE')
```

```
C
      X(1,1)=CL1S
      X(2,1)=VC1S
      X(3,1)=ECS
      X(4,1)=CLS
      X(5,1)=VCS
      X(6,1)=ERS
      VO(1)=VOS
      U(1)=V1
      U(2)=ER
      U(3)=EQ
      U(4)=ED
```

```
C
C
      IF(X(3,ND).GE.ET) GO TO 60
      TEMPA=ABS(X(3,ND)-ET)
```

```

20 IF(TEMPA.LT.EPS) GO TO 40
   CONTINUE
   IF(X(3,ND).LT.ET) GO TO 28
C
C *****
C MINIMUM OFF TIME CALCULATION *
C *****
C
T=TOFMIN
CALL STRAN(T,PHIFT,DFT,F2,G2,6,4,6,4,1,0,EPS,DIFMAX,ITER,I FLAG)
DO 6 I=1,6
6 TVEC1(I)=X(I,ND)
CALL FUTURE(TVEC1,U,PHIFT,DFT,6,6,6,4,6,6,6,4,1)
TEMP=TIME(ND)
ND=ND+1
TIME(ND)=TEMP+T
DO 7 I=1,6
7 X(I,ND)=TVEC1(I)
VO(ND)=(RL*RC)*X(4,ND)/(RL+RC)+RL*X(5,ND)/(RL+RC)
IF(X(4,ND).GT.0.0) GO TO 570
IT1=0
571 IF(ABS(X(4,ND)).LT.EPS) GO TO 579
IT1=IT1+1
IF(NIT.GE.NIT) GO TO 100
SLOPE3=F2(4,4)*X(4,ND)+F2(4,5)*X(5,ND)+G2(4,4)*U(4)
T3=-X(4,ND)/SLOPE3
CALL STRAN(T3,PHIFT3,DFT3,F2,G2,6,4,6,4,1,0,EPS,DIFMAX,ITER,I FLAG)
DO 572 I=1,6
572 TVEC3(I)=X(I,ND)
CALL FUTURE(TVEC3,U,PHIFT3,DFT3,6,6,6,4,6,6,6,4,1)
TIME(ND)=TIME(ND)+T3
DO 573 I=1,6
573 X(I,ND)=TVEC3(I)
VO(ND)=RL*RC*X(4,ND)+RL*X(5,ND)
VO(ND)=VO(ND)/(RL+RC)
GO TO 571
579 CONTINUE
CALL STRAN(T3,PHIF3,DF3,F3,G3,6,4,6,4,1,0,EPS,DIFMAX,ITER,I FLAG)
DO 574 I=1,6
574 TVEC3(I)=X(I,ND)
X(4,ND)=0.0
CALL FUTURE(TVEC3,U,PHIF3,DF3,6,6,6,4,6,6,6,4,1)
TEMP=TIME(ND)

```

```

ND=ND+1
TIME(ND)=TEMP+T3
DO 575 I=1,6
575 X(I,ND)=TVEC3(I)
VO(ND)=(RL*X(5,ND))/(RL+RC)
570 CONTINUE
GO TO 40
C
C *****
C OFF TIME CALCULATION *
C *****
C
28 T=FRAC*TOFF
IT=0
25 CONTINUE
DO 8 I=1,6
8 TVEC1(I)=X(I,ND)
IF(ND.LT.300) GO TO 5000
WRITE(6,706)
706 FORMAT(/, ' STATE VECTOR IN OFF TIME')
WRITE(6,9004)(TVEC1(I),I=1,6)
9004 FORMAT(6F15.11)
WRITE(6,*) VO(ND)
5000 CONTINUE
IF(X(4,ND).LE.0) GO TO 502
C
CALL FUTURE(TVEC1,U,PHIF,DF,6,6,6,4,6,6,6,4,1)
C
TEMP=TIME(ND)
ND=ND+1
TIME(ND)=TEMP+T
DO 9 I=1,6
9 X(I,ND)=TVEC1(I)
VO(ND)=RL*RC*X(4,ND)+RL*X(5,ND)
VO(ND)=VO(ND)/(RL+RC)
GO TO 520
502 CONTINUE
C
C *****
C * CALCULATION TO FIND WHEN X(4)=0 *
C *****
C
IT1=0

```

```

503 IF(ABS(X(4,ND)).LT.EPS) GO TO 509
    IT1=IT1+1
    IF(IT1.GE.NIT) GO TO 100
    SLOPE3=F2(4,4)*X(4,ND)+F2(4,5)*X(5,ND)+G2(4,4)*U(4)
    T3=-X(4,ND)/SLOPE3
    CALL STRAN(T3,PHIFT3,DFT3,F2,G2,6,4,6,4,1,0,EPS,DIFMAX,ITER,IFLAG)
    DO 504 I=1,6
504 TVEC3(I)=X(I,ND)
    CALL FUTURE(TVEC3,U,PHIFT3,DFT3,6,6,6,4,6,6,6,4,1)
    TIME(ND)=TIME(ND)+T3
    DO 505 I=1,6
505 X(I,ND)=TVEC3(I)
    VO(ND)=RL*RC*X(4,ND)+RL*X(5,ND)
    VO(ND)=VO(ND)/(RL+RC)
    GO TO 503
509 CONTINUE
    CALL STRAN(T,PHIF3,DF3,F3,G3,6,4,6,4,1,0,EPS,DIFMAX,ITER,IFLAG)
    DO 540 I=1,6
540 TVEC3(I)=X(I,ND)
    X(4,ND)=0.0
    CALL FUTURE(TVEC3,U,PHIF3,DF3,6,6,6,4,6,6,6,4,1)
    TEMP=TIME(ND)
    ND=ND+1
    TIME(ND)=TEMP+T
    DO 511 I=1,6
511 X(I,ND)=TVEC3(I)
    VO(ND)=(RL*X(5,ND))/(RL+RC)
520 CONTINUE
    IF(X(3,ND).GE.ET) GO TO 30
    GO TO 25
C
C *****
C CALCULATION TO HIT THRESHOLD WHEN *
C X(3)=ET. *
C *****
C
30 IF(ABS(X(3,ND)-ET).LT.EPS) GO TO 40
    IT=IT+1
    IF(IT.GE.NIT) GO TO 100
    SLOPE=F2(3,4)*X(4,ND)+F2(3,5)*X(5,ND)+F2(3,6)*X(6,ND)
    SLOPE=SLOPE+G2(3,2)*U(2)
    T=(ET-X(3,ND))/SLOPE
C

```

```

CALL STRAN(T,PHIFT,DFT,F2,G2,6,4,6,4,1,0,EPS,DIFMAX,ITER,I FLAG)
C
DO 10 I=1,6
10 TVEC1(I)=X(I,ND)
CALL FUTURE(TVEC1,U,PHIFT,DFT,6,6,6,4,6,6,6,4,1)
TIME(ND)=TIME(ND)+T
DO 11 I=1,6
11 X(I,ND)=TVEC1(I)
VO(ND)=RL*RC*X(4,ND)+RL*X(5,ND)
VO(ND)=VO(ND)/(RL+RC)
GO TO 30
40 CONTINUE
IF(ND.LT.300) GO TO 5001
WRITE(6,440) TIME(ND)
440 FORMAT(/,'SWITCH ON TIME=',F15.11)
5001 CONTINUE
IF(TIME(ND).GE.TF) GO TO 120
C
C *****
C CHANGE VI,TON,TOFF AT THE SWITCHING *
C INSTANT. ALSO CHANGE PHIF,DF, IF *
C NECESSARY. *
C *****
C
IF(TIME(ND).LT.TXX) GO TO 60
NSWIT=NSWIT+1
ITEMP=NSWIT+1
TXX=TSWIT(ITEMP)
VI=VISWIT(NSWIT)
TON=VI*TON/VI
TOFF=TON*(VI-EO)/EO
U(1)=VI
T=FRAC*TOFF
C
CALL STRAN(T,PHIF,DF,F2,G2,6,4,6,4,1,0,EPS,DIFMAX,ITER,I FLAG)
C
T=FRAC*TON
C
CALL STRAN(T,PHIN,DN,F1,G1,6,4,6,4,1,0,EPS,DIFMAX,ITER,I FLAG)
C
60 CONTINUE
M=0
T=FRAC*TON
C

```

```

C *****
C ON TIME CALCULATION *
C *****
C
65 CONTINUE
DO 12 I=1,6
12 TVEC1(I)=X(I,ND)
IF(ND.LT.300) GO TO 5002
WRITE(6,709)
709 FORMAT(//,' STATE VECTOR IN ON TIME' )
WRITE(6,9005)(TVEC1(I),I=1,6)
9005 FORMAT(6F15.11)
WRITE(6,*) VO(ND)
5002 CONTINUE
C
CALL FUTURE(TVEC1,U,PHIN,DN,6,6,6,4,6,6,6,4,1)
C
TEMP=TIME(ND)
ND=ND+1
TIME(ND)=TEMP+T
DO 13 I=1,6
13 X(I,ND)=TVEC1(I)
VO(ND)=RL*RC*X(4,ND)+RL*X(5,ND)
VO(ND)=VO(ND)/(RL+RC)
M=M+1
IF(X(4,ND).GE.IQMAX) GO TO 70
IF(M.LT.NT) GO TO 65
C
GO TO 999
C
C *****
C CALCULATION TO FIND WHEN INDUCTOR *
C CURRENT HITS THE THRESHOLD VALUE. *
C *****
C
70 CONTINUE
IT=0
71 IF(ABS(X(4,ND)-IQMAX).LE.EPS) GO TO 999
IT=IT+1
IF(IT.GE.NIT) GO TO 100
SLOPE2=X(2,ND)*F1(4,2)+X(4,ND)*F1(4,4)+X(5,ND)*F1(4,5)
T=(IQMAX-X(4,ND))/SLOPE2
CALL STRAN(T,PHIFT,DFT,F1,G1,6,4,6,4,1,0,EPS,DIFMAX,ITER,IFLAG)

```

```

15 DO 15 I=1,6
   TVEC1(I)=X(I,ND)
   CALL FUTURE(TVEC1,U,PHIFT,DFT,6,6,6,4,6,6,6,4,1)
   TIME(ND)=TIME(ND)+T
16 DO 16 I=1,6
   X(I,ND)=TVEC1(I)
   VO(ND)=RL*RC*X(4,ND)+RL*X(5,ND)
   VO(ND)=VO(ND)/(RL+RC)
   GO TO 71
999 CONTINUE

```

```

C
   IF(ND.LT.300) GO TO 5003
   WRITE(6,442) TIME(ND)
442  FORMAT(/,'SWITCH OFF TIME=',F15.11)
5003 CONTINUE
   IF(TIME(ND).LT.TF) GO TO 20
   GO TO 120
100  CONTINUE
   WRITE(6,204) TIME(ND)
204  FORMAT(/,'MAXIMUM ITERATION AT TIME=',F15.11)
120  CONTINUE
   DO 104 I=1,ND
   WRITE(8,103) TIME(I),X(3,I)
103  FORMAT(2E20.10)
104  CONTINUE
   DO 105 I=1,ND
   WRITE(8,103) TIME(I),X(4,I)
105  CONTINUE
   DO 106 I=1,ND
   WRITE(8,103) TIME(I),VO(I)
106  CONTINUE
   DO 107 I=1,ND
   WRITE(8,103) TIME(I),X(2,I)
107  CONTINUE
   DO 14 I=1,ND
14   TVEC2(I)=VO(I)
   CALL ABPLOT(ND,TIME,TVEC2)
   STOP
   END

```

C  
C

```

1 SUBROUTINE STRAN(TAU,PHI,THETA,A,B,NA,NB,MA,MB,MODE,NTERMS,
1 TOL,DIFMAX,ITER,I FLAG)

```

```

REAL          PHI(NA,NA), THETA(NA,NB), A(NA,NA), B(NA,NB),
1 WORK1(10,10), WORK2(10,10), DUMMY(1,1), FAC1, CON1, FAC2, CON2
  C1=1
  TS=TAU
  DO 4 I=1, MA
  DO 2 J=1, MA
  WORK1(I,J)=0
  WORK2(I,J)=0
  PHI(I,J)=0
2 CONTINUE
  WORK1(I,I)=1
  WORK2(I,I)=TAU
  PHI(I,I)=1
4 CONTINUE
  DO 6 I=1, MA
  DO 6 J=1, MB
6 THETA(I,J)=0
  DIFMAX=1.E8
  NDO=50
  IF(NTERMS.GT.0) NDO=NTERMS
  FAC1=1
  IFLAG=0
  DO 1000 I=1, NDO
  CALL MXMUL(DUMMY, WORK1, A, TS, 1, 1, 10, 10, NA, NA, MA, MA, MA, MA, 1)
  FAC1=FAC1*I
  CON1=1./FAC1
  IF(NTERMS.EQ.0.AND.I.GE.4) CALL SERROR(PHI, WORK1, CON1, NA, NA,
1 10, 10, MA, MA, DIFMAX)
  CALL MXADD(DUMMY, PHI, WORK1, C1, CON1, 1, 1, NA, NA, 10, 10, MA, MA, 1)
  IF(MODE.EQ.2) GO TO 500
  FAC2=FAC1*(I+1)
  CON2=TAU/FAC2
  CALL MXADD(DUMMY, WORK2, WORK1, C1, CON2, 1, 1, 10, 10, 10, 10, MA, MA, 1)
500 CONTINUE
  ITER=1
  IF(NTERMS.GT.0.OR.I.LT.4) GO TO 1000
  IF(DIFMAX.LE.TOL) GO TO 1100
1000 CONTINUE
1100 CONTINUE
  IF(MODE.EQ.1) CALL MXMUL(THETA, WORK2, B, C1, NA, NB, 10, 10, NA, NB,
1 MA, MA, MA, MB, 2)
  IF(ITER.EQ.NDO.AND.NTERMS.EQ.0) IFLAG=1
  RETURN

```

END

C  
C

```
1 SUBROUTINE SERROR(AMX, BMX, CCC, IA, JA, IB, JB, IDO, JDO, DIFMAX)
  DIMENSION      AMX( IA, JA), BMX( IB, JB)
  DIFMAX=1.E-30
  DO 100 I=1, IDO
  DO 50 J=1, JDO
  IF(AMX(I, J).EQ.0.0 ) GO TO 50
  CHANGE= ABS(BMX(I, J)*CCC/AMX(I, J))
  IF(CHANGE.GT.DIFMAX) DIFMAX=CHANGE
50 CONTINUE
100 CONTINUE
  RETURN
  END
```

C  
C

```
1 SUBROUTINE FUTURE(X, V, PHI, THETA, LP, MP, LT, MT, IP, JP, IT, JT, MODE)
  DIMENSION      X(MP), V(MT), PHI(LP, MP), THETA(LT, MT), TEMP(20)
  DO 20 I=1, IP
  SUM=0
  DO 10 J=1, JP
 10 SUM=SUM+PHI(I, J)*X(J)
 20 TEMP(I)=SUM
  DO 30 I=1, IP
 30 X(I)=TEMP(I)
  IF(MODE.EQ.2) RETURN
  DO 60 I=1, IT
  SUM=0
  DO 50 J=1, JT
 50 SUM=SUM+THETA(I, J)*V(J)
  X(I)=X(I)+SUM
 60 CONTINUE
  RETURN
  END
```

C  
C

```
1 SUBROUTINE MXADD(RMX, AMX, BMX, ACC, BCC, IR, JR, IA, JA, IB, JB, IDO, JDO,
1 MODE)
  DIMENSION      AMX( IA, JA), BMX( IB, JB), RMX( IR, JR)
  IF(IA.LT.IDO.OR.JA.LT.JDO) GO TO 999
  IF(IB.LT.IDO.OR.JB.LT.JDO) GO TO 999
  GO TO (10, 100), MODE
```

```

10 CONTINUE
DO 50 I=1,IDO
DO 50 J=1,JDO
50 AMX(I,J)=AMX(I,J)*ACC+BMX(I,J)*BCC
GO TO 300
100 CONTINUE
IF(IR.LT.IDO.OR.JR.LT.JDO) GO TO 999
DO 200 I=1,IDO
DO 200 J=1,JDO
200 RMX(I,J)=AMX(I,J)*ACC+BMX(I,J)*BCC
300 RETURN
999 CONTINUE
RETURN
END

```

C  
C

```

1 SUBROUTINE MXMUL(RMX,AMX,BMX,CCC,IR,JR,IA,JA,IB,JB,IDA,JDA,IDB,JDB
1,MODE)
DIMENSION AMX(IA,JA),BMX(IB,JB),RMX(IR,JR),TEMP(20)
IF(IDA>IDB>JDA>JDB.GT.IA>IB>JA>JB) GO TO 999
IF(JDB.GT.JDA) GO TO 999
GO TO (10,210),MODE
10 DO 100 I=1,IDA
DO 20 L=1,JDA
20 TEMP(L)=AMX(I,L)
DO 80 J=1,JDB
SUM=0
DO 40 K=1,JDA
40 SUM=SUM+TEMP(K)*BMX(K,J)
AMX(I,J)=SUM*CCC
80 CONTINUE
100 CONTINUE
GO TO 600
210 CONTINUE
IF(IR.LT.IDA.OR.JR.LT.JDB) GO TO 999
DO 400 I=1,IDA
DO 380 J=1,JDB
SUM=0
DO 340 K=1,JDA
340 SUM=SUM+AMX(I,K)*BMX(K,J)
RMX(I,J)=SUM*CCC
380 CONTINUE
400 CONTINUE

```

600 RETURN  
999 CONTINUE  
RETURN  
END

```

C *****
C DISCRETE TIME SIMULATION OF A BUCK CONVERTER *
C *****
C THIS PROGRAM SIMULATES THE STEADY-STATE BEHAVIOR AS WELL AS
C THE TRANSIENT PERFORMANCE FOR A BUCK REGULATOR
C WITH INPUT FILTER AND WITH FEEDFORWARD.
C
C DIMENSION X(7,9000), F1(7,7), F2(7,7), G1(7,4), G2(7,4), TIME(9000),
1U(4), PHIF(7,7), PHIN(7,7), DF(7,4), DN(7,4), TVEC1(7), TSWIT(2),
2VISWIT(2), VO(9000), PHIFT(7,7), DFT(7,4), TVEC2(9000)
C DIMENSION F3(7,7), G3(7,4), TVEC3(7), PHIFT3(7,7), DFT3(7,4),
1PHIF3(7,7), DF3(7,7)
C
C REAL L1, L, K1, K2, IQMAX, K3
C
C DATA RL1, L1, C1, L, RO, RN, RC, C/1.0, 325.E-6, 22.E-5, 230.E-6, 0.2, 0.65,
20.067, 300.E-6/
C DATA RL, R11, R12, R13, R14, C2, R4, CP1/20.0, 33.3E3, 16.7E3, 2.E3,
147.E3, 0.01E-6, 40.7E3, 5600.E-12/
C DATA ER, ET, V1, EO/6.7, 7.0, 40., 20./
C DATA TON, TOFMIN, TSWIT, VISWIT, VITON/2.20E-5, 5.E-6, 0.003, 10.0,
125., 50., 0.88E-3/
C DATA NIT, FRAC, EPS, TF/10, 0.1, 10.E-6, 0.0120/
C DATA IQMAX, EQ, ED/6.0, 0.2, 0.7/
C DATA RF1, RF2, CF, VFS/5.1E3, 90.970, 27.E-6, 0.0507E-1/
C CL1S=0.69552390
C VC1S=39.87245
C ECS=7.0
C CLS=0.40158130
C VCS=20.06141
C ERS=20.06143
C VOS=20.02125
C VFS=+0.38948170
C
C TON=VITON/V1
C K1=(R12/(R14*(R11+R12)))+(1./R13)-(RN/R4)
C K1=K1-(RN*RO*(RL+RC))/(R4*RL*RC)
C K2=(RN/R4)-(1./R13)-(R12/(R14*(R11+R12)))
C K3=RF2/(RF1+RF2)
C DO 1 I=1,7
C DO 80 J=1,4
C G1(I,J)=0.
C G2(I,J)=0.

```

```

80 DF(1,J)=0.
   DN(1,J)=0.
   DFT(1,J)=0.
   DO 1 J=1,7
   F1(1,J)=0.
1   F2(1,J)=0.
C
   DO 2 I=1,7
   DO 2 J=1,7
   PHIFT(I,J)=0.
   PHIF(I,J)=0.
2   PHIN(I,J)=0.
C
   F1(1,1)=(-1.*RL1)/L1
   F1(1,2)=-1./L1
   F1(2,1)=1./C1
   F1(2,3)=-1./(C1*(RF1+RF2))
   F1(2,5)=-1./C1
   F1(3,1)=1./C1
   F1(3,3)=(-1.*(CF+C1))/(CF*C1*(RF1+RF2))
   F1(3,3)=0
   F1(3,5)=-1./C1
   F1(4,1)=(-1.*K3)/C1
   F1(4,2)=(-1.*RN)/(CP1*R4)
   F1(4,3)=(K3*(CF+C1))/(CF*C1*(RF1+RF2))
   F1(4,5)=(K3/C1)-((RL*RC*K1)/(CP1*(RL+RC)))
   F1(4,6)=(RL*K2)/(CP1*(RL+RC))
   F1(4,7)=1./(CP1*R13)
   F1(5,2)=1./L
   F1(5,5)=((-1.*RO)/L)+((-1.*RC*RL)/(L*(RC+RL)))
   F1(5,6)=(-1.*RL)/(L*(RC+RL))
   F1(6,5)=RL/(C*(RL+RC))
   F1(6,6)=-1./(C*(RL+RC))
   F1(7,5)=(RL*RC)/(C2*R13*(RL+RC))
   F1(7,6)=RL/(C2*R13*(RL+RC))
   F1(7,7)=-1./(C2*R13)
   G1(1,1)=1./L1
   G1(4,2)=1./(CP1*R14)
   G1(4,3)=RN/(CP1*R4)
   G1(5,3)=-1./L
   DO 3 I=1,7
   DO 3 J=1,7
3   F2(I,J)=F1(I,J)

```

```

F2(2,5)=0.
F2(3,5)=0.
F2(3,3)=0
F2(4,2)=0.
F2(4,5)=(-1.*RL*RC*K1)/(CP1*(RL+RC))
F2(5,2)=0.
G2(1,1)=G1(1,1)
G2(4,2)=G1(4,2)
G2(4,4)=RN/(CP1*R4)
G2(5,4)=-1./L
DO 530 I=1,7
DO 531 J=1,7
531 F3(I,J)=F2(I,J)
DO 532 J=1,4
532 G3(I,J)=G2(I,J)
530 CONTINUE
DO 535 I=1,7
F3(5,I)=0.0
535 F3(I,5)=0.0
DO 536 I=1,4
536 G3(5,I)=0.0
C
NSWIT=0
TEMP=NSWIT+1
TXX=TSWIT(TEMP)
NT=0.1+1./FRAC
TOFF=TON*(V1-E0)/E0
TIME(1)=0.0
ND=1
M=0
IT=0
T=FRAC*TOFF
C
CALL STRAN(T,PHIF,DF,F2,G2,7,4,7,4,1,0,EPS,DIFMAX,ITER,IFLAG)
C
T=FRAC*TON
CALL STRAN(T,PHIN,DN,F1,G1,7,4,7,4,1,0,EPS,DIFMAX,ITER,IFLAG)
704 WRITE(6,704)
C
FORMAT(//,' VALUES OF X ON THE NEXT PAGE')
X(1,1)=CL1S
X(2,1)=VC1S
X(3,1)=VFS

```

```
X(4,1)=ECS
X(5,1)=CLS
X(6,1)=VCS
X(7,1)=ERS
VO(1)=VOS
U(1)=VI
U(2)=ER
U(3)=EQ
U(4)=ED
```

```
C
C
```

```
IF(X(4,ND).GE.ET) GO TO 60
TEMPA=ABS(X(4,ND)-ET)
IF(TEMPA.LT.EPS) GO TO 40
CONTINUE
```

```
20
```

```
C
```

```
IF(X(4,ND).LT.ET) GO TO 28
```

```
C
```

```
*****
MINIMUM OFF TIME CALCULATION *
*****
```

```
T=TOFMIN
CALL STRAN(T,PHIFT,DFT,F2,G2,7,4,7,4,1,0,EPS,DIFMAX,ITER,I FLAG)
DO 6 I=1,7
6 TVEC1(I)=X(I,ND)
CALL FUTURE(TVEC1,U,PHIFT,DFT,7,7,7,4,7,7,7,4,1)
TEMP=TIME(ND)
ND=ND+1
```

```
6
```

```
TIME(ND)=TEMP+T
DO 7 I=1,7
7 X(I,ND)=TVEC1(I)
VO(ND)=(RL*RC)*X(5,ND)/(RL+RC)+RL*X(6,ND)/(RL+RC)
IF(X(5,ND).GT.0.0) GO TO 570
ITI=0
```

```
571
```

```
IF(ABS(X(5,ND)).LT.EPS) GO TO 579
ITI=ITI+1
IF(ITI.GE.NIT) GO TO 579
SLOPE3=F2(5,5)*X(5,ND)+F2(5,6)*X(6,ND)+G2(5,4)*U(4)
T3=-X(5,ND)/SLOPE3
CALL STRAN(T3,PHIFT3,DFT3,F2,G2,7,4,7,4,1,0,EPS,DIFMAX,ITER,I FLAG)
DO 572 I=1,7
```

```
572
```

```
TVEC3(I)=X(I,ND)
```

```

CALL FUTURE(TVEC3,U,PHIFT3,DFT3,7,7,7,4,7,7,7,4,1)
TIME(ND)=TIME(ND)+T3
DO 573 I=1,7
573 X(I,ND)=TVEC3(I)
VO(ND)=RL*RC*X(5,ND)+RL*X(6,ND)
VO(ND)=VO(ND)/(RL+RC)
GO TO 571
579 CONTINUE
CALL STRAN(T3,PHIF3,DF3,F3,G3,7,4,7,4,1,0,EPS,DIFMAX,ITER,IFLAG)
DO 574 I=1,7
574 TVEC3(I)=X(I,ND)
X(5,ND)=0.0
CALL FUTURE(TVEC3,U,PHIF3,DF3,7,7,7,4,7,7,7,4,1)
TEMP=TIME(ND)
ND=ND+1
TIME(ND)=TEMP+T3
DO 575 I=1,7
575 X(I,ND)=TVEC3(I)
VO(ND)=(RL*X(6,ND))/(RL+RC)
570 CONTINUE
GO TO 40

```

```

C
C *****
C OFF TIME CALCULATION *
C *****
C

```

```

28 T=FRAC*TOFF
IT=0
25 CONTINUE
DO 8 I=1,7
8 TVEC1(I)=X(I,ND)
IF(ND.LT.300) GO TO 5000
WRITE(6,706)
706 FORMAT('/', ' STATE VECTOR IN OFF TIME')
WRITE(6,9004)(TVEC1(I),I=1,7)
9004 FORMAT(7F15.11)
WRITE(6,*) VO(ND)
5000 CONTINUE
IF(X(5,ND).LE.0.0) GO TO 502
C
CALL FUTURE(TVEC1,U,PHIF,DF,7,7,7,4,7,7,7,4,1)
C
TEMP=TIME(ND)

```

```

          ND=ND+1
          TIME(ND)=TEMP+T
          DO 9 I=1,7
9          X(I,ND)=TVEC1(I)
          VO(ND)=RL*RC*X(5,ND)+RL*X(6,ND)
          VO(ND)=VO(ND)/(RL+RC)
          GO TO 520
502        CONTINUE
C
C          *****
C          * CALCULATION TO FIND WHEN X(5)=0 *
C          *****
C
          ITI=0
503        IF(ABS(X(5,ND)).LT.EPS) GO TO 509
          ITI=ITI+1
          IF(ITI.GE.NIT) GO TO 100
          SLOPE3=F2(5,5)*X(5,ND)+F2(5,6)*X(6,ND)+G2(5,4)*U(4)
          T3=-X(5,ND)/SLOPE3
          CALL STRAN(T3,PHIFT3,DFT3,F2,G2,7,4,7,4,1,0,EPS,DIFMAX,ITER,IFLAG)
          DO 504 I=1,7
504          TVEC3(I)=X(I,ND)
          CALL FUTURE(TVEC3,U,PHIFT3,DFT3,7,7,7,4,7,7,4,1)
          TIME(ND)=TIME(ND)+T3
          DO 505 I=1,7
505          X(I,ND)=TVEC3(I)
          VO(ND)=RL*RC*X(5,ND)+RL*X(6,ND)
          VO(ND)=VO(ND)/(RL+RC)
          GO TO 503
509        CONTINUE
          CALL STRAN(T,PHIF3,DF3,F3,G3,7,4,7,4,1,0,EPS,DIFMAX,ITER,IFLAG)
          DO 540 I=1,7
540          TVEC3(I)=X(I,ND)
          X(5,ND)=0.0
          CALL FUTURE(TVEC3,U,PHIF3,DF3,7,7,7,4,7,7,4,1)
          TEMP=TIME(ND)
          ND=ND+1
          TIME(ND)=TEMP+T
          DO 511 I=1,7
511          X(I,ND)=TVEC3(I)
          VO(ND)=(RL*X(6,ND))/(RL+RC)
520        CONTINUE
          IF(X(4,ND).GE.ET) GO TO 30

```

```

GO TO 25
C
C *****
C CALCULATION TO HIT THRESHOLD WHEN *
C X(3)=ET. *
C *****
C
30 IF (ABS(X(4,ND)-ET).LT.EPS) GO TO 40
IT=IT+1
IF (IT.GE.NIT) GO TO 100
SLOPE=F2(4,1)*X(1,ND)+F2(4,3)*X(3,ND)+F2(4,5)*X(5,ND)+
1F2(4,6)*X(6,ND)+F2(4,7)*X(7,ND)
SLOPE=SLOPE+G2(4,2)*U(2)+G2(4,4)*U(4)
T=(ET-X(4,ND))/SLOPE
C
CALL STRAN(T,PHIFT,DFT,F2,G2,7,4,7,4,1,0,EPS,DIFMAX,ITER,IFLAG)
C
DO 10 I=1,7
10 TVEC1(I)=X(I,ND)
CALL FUTURE(TVEC1,U,PHIFT,DFT,7,7,7,4,7,7,4,1)
TIME(ND)=TIME(ND)+T
DO 11 I=1,7
11 X(I,ND)=TVEC1(I)
VO(ND)=RL*RC*X(5,ND)+RL*X(6,ND)
VO(ND)=VO(ND)/(RL+RC)
GO TO 30
40 CONTINUE
IF(ND.LT.1000) GO TO 5001
WRITE(6,440) TIME(ND)
440 FORMAT(/,'SWITCH ON TIME=',F15.11)
5001 CONTINUE
IF(TIME(ND).GE.TF) GO TO 120
C
C *****
C CHANGE VI,TON,TOFF AT THE SWITCHING *
C INSTANT. ALSO CHANGE PHIF,DF IF *
C NECESSARY. *
C *****
C
IF(TIME(ND).LT.TXX) GO TO 60
NSWIT=NSWIT+1
TEMP=NSWIT+1
TXX=TSWIT(TEMP)

```

```

VI=VISWIT(NSWIT)
TON=VI*TON/VI
TOFF=TON*(VI-EO)/EO
U(1)=VI
RF2=230.27
K3=RF2/(RF1+RF2)
F1(2,3)=-1./(C1*(RF1+RF2))
F1(3,3)=(-1.*(CF+C1))/(CF*C1*(RF1+RF2))
F1(4,1)=(-1.*K3)/C1
F1(4,3)=(K3*(CF+C1))/(CF*C1*(RF1+RF2))
F1(4,5)=(K3/C1)-((RL*RC*K1)/(CP1*(RL+RC)))
F2(2,3)=F1(2,3)
F2(3,3)=F1(3,3)
F2(4,1)=F1(4,1)
F2(4,3)=F1(4,3)
T=FRAC*TOFF

```

```

C CALL STRAN(T,PHIF,DF,F2,G2,7,4,7,4,1,0,EPS,DIFMAX,ITER,I FLAG)
C T=FRAC*TON
C CALL STRAN(T,PHIN,DN,F1,G1,7,4,7,4,1,0,EPS,DIFMAX,ITER,I FLAG)
C 60 CONTINUE
M=0
T=FRAC*TON
C *****
C ON TIME CALCULATION *
C *****
C 65 CONTINUE
DO 12 I=1,7
12 TVEC1(I)=X(I,ND)
IF(ND.LT.1000) GO TO 5002
WRITE(6,709)
709 FORMAT(//,' STATE VECTOR IN ON TIME')
WRITE(6,9005)(TVEC1(I),I=1,7)
9005 FORMAT(7F15.11)
WRITE(6,*) VO(ND)
5002 CONTINUE
C CALL FUTURE(TVEC1,U,PHIN,DN,7,7,7,4,7,7,7,4,1)
C

```

```

TEMP=TIME(ND)
ND=ND+1
TIME(ND)=TEMP+T
DO 13 I=1,7
13 X(I,ND)=TVEC1(I)
VO(ND)=RL*RC*X(5,ND)+RL*X(6,ND)
VO(ND)=VO(ND)/(RL+RC)
M=M+1
IF(X(5,ND).GE.IQMAX) GO TO 70
IF(M.LT.NT) GO TO 65
C
GO TO 999
C
*****
C
CALCULATION TO FIND WHEN INDUCTOR *
C
CURRENT HITS THE THRESHOLD VALUE. *
C
*****
C
70 CONTINUE
IT=0
71 IF(ABS(X(5,ND)-IQMAX).LE.EPS) GO TO 999
IT=IT+1
IF(IT.GE.NIT) GO TO 100
SLOPE2=F1(5,2)*X(2,ND)+F1(5,5)*X(5,ND)+F1(5,6)*X(6,ND)+
IG1(5,3)*U(3)
T=(IQMAX-X(5,ND))/SLOPE2
CALL STRAN(T,PHIFT,DFT,F1,G1,7,4,7,4,1,0,EPS,DIFMAX,ITER,IFLAG)
DO 15 I=1,7
15 TVEC1(I)=X(I,ND)
CALL FUTURE(TVEC1,U,PHIFT,DFT,7,7,7,4,7,7,4,1)
TIME(ND)=TIME(ND)+T
DO 16 I=1,7
16 X(I,ND)=TVEC1(I)
VO(ND)=RL*RC*X(5,ND)+RL*X(6,ND)
VO(ND)=VO(ND)/(RL+RC)
GO TO 71
999 CONTINUE
C
IF(ND.LT.1000) GO TO 5003
WRITE(6,442) TIME(ND)
442 FORMAT(/,'SWITCH OFF TIME=',F15.11)
5003 CONTINUE
IF(TIME(ND).LT.TF) GO TO 20

```

```

GO TO 120
100 CONTINUE
WRITE(6,204) TIME(ND)
204 FORMAT(/,'MAXIMUM ITERATION AT TIME=',F15.11)
120 CONTINUE
111 DO 105 I=1,ND
WRITE(8,103) TIME(I),X(1,I)
105 CONTINUE
DO 106 I=1,ND
WRITE(8,103) TIME(I),X(2,I)
106 CONTINUE
DO 104 I=1,ND
WRITE(8,103) TIME(I),X(3,I)
103 FORMAT(2E20.10)
104 CONTINUE
DO 107 I=1,ND
WRITE(8,103) TIME(I),X(4,I)
107 CONTINUE
DO 122 I=1,ND
WRITE(8,103) TIME(I),X(5,I)
122 CONTINUE
DO 123 I=1,ND
WRITE(8,103) TIME(I),VO(I)
123 CONTINUE
DO 124 I=1,ND
WRITE(8,103) TIME(I),X(7,I)
124 CONTINUE
109 CONTINUE
DO 14 I=1,ND
14 TVEC2(I)=VO(I)
STOP
END

```

C  
C

```

SUBROUTINE STRAN(TAU,PHI,THETA,A,B,NA,NB,MA,MB,MODE,NTERMS,
1 TOL,DIFMAX,ITER,IFLAG)
REAL PHI(NA,NA),THETA(NA,NB),A(NA,NA),B(NA,NB),
1 WORK1(10,10),WORK2(10,10),DUMMY(1,1),FAC1,CON1,FAC2,CON2
C1=1
TS=TAU
DO 4 I=1,MA
DO 2 J=1,MA
WORK1(I,J)=0

```

```

WORK2(I,J)=0
PHI(I,J)=0
2 CONTINUE
WORK1(I,I)=1
WORK2(I,I)=TAU
PHI(I,I)=1
4 CONTINUE
DO 6 I=1,MA
DO 6 J=1,MB
6 THETA(I,J)=0
DIFMAX=1.E8
NDO=50
IF(NTERMS.GT.0) NDO=NTERMS
FAC1=1
IFLAG=0
DO 1000 I=1,NDO
CALL MXMUL(DUMMY,WORK1,A,TS,1,1,10,10,NA,NA,MA,MA,MA,MA,1)
FAC1=FAC1*I
CON1=1./FAC1
IF(NTERMS.EQ.0.AND.I.GE.4) CALL SERROR(PHI,WORK1,CON1,NA,NA,
1 10,10,MA,MA,DIFMAX)
CALL MXADD(DUMMY,PHI,WORK1,C1,CON1,1,1,NA,NA,10,10,MA,MA,1)
IF(MODE.EQ.2) GO TO 500
FAC2=FAC1*(I+1)
CON2=TAU/FAC2
CALL MXADD(DUMMY,WORK2,WORK1,C1,CON2,1,1,10,10,10,10,MA,MA,1)
500 CONTINUE
ITER=I
IF(NTERMS.GT.0.OR.I.LT.4) GO TO 1000
IF(DIFMAX.LE.TOL) GO TO 1100
1000 CONTINUE
1100 CONTINUE
IF(MODE.EQ.1) CALL MXMUL(THETA,WORK2,B,C1,NA,NB,10,10,NA,NB,
1 MA,MA,MA,MB,2)
IF(ITER.EQ.NDO.AND.NTERMS.EQ.0) IFLAG=1
RETURN
END

```

C  
C

```

SUBROUTINE SERROR(AMX,BMX,CCC,IA,JA,IB,JB,IDO,JDO,DIFMAX)
DIMENSION AMX(IA,JA),BMX(IB,JB)
DIFMAX=1.E-30
DO 100 I=1,IDO

```

```

DO 50 J=1,JDO
IF(AMX(I,J).EQ.0.0 ) GO TO 50
CHANGE= ABS(BMX(I,J)*CCC/AMX(I,J))
IF(CHANGE.GT.DIFMAX) DIFMAX=CHANGE
50 CONTINUE
100 CONTINUE
RETURN
END

```

C  
C

```

SUBROUTINE FUTURE(X,V,PHI,THETA,LP,MP,LT,MT,IP,JP,IT,JT,MODE)
DIMENSION X(MP),V(MT),PHI(LP,MP),THETA(LT,MT),TEMP(20)
DO 20 I=1,IP
SUM=0
DO 10 J=1,JP
10 SUM=SUM+PHI(I,J)*X(J)
20 TEMP(I)=SUM
DO 30 I=1,IP
30 X(I)=TEMP(I)
IF(MODE.EQ.2) RETURN
DO 60 I=1,IT
SUM=0
DO 50 J=1,JT
50 SUM=SUM+THETA(I,J)*V(J)
X(I)=X(I)+SUM
60 CONTINUE
RETURN
END

```

C  
C

```

SUBROUTINE MXADD(RMX,AMX,BMX,ACC,BCC,IR,JR,IA,JA,IB,JB,IDO,JDO,
1 MODE)
DIMENSION AMX(IA,JA),BMX(IB,JB),RMX(IR,JR)
IF(IA.LT.IDO.OR.JA.LT.JDO) GO TO 999
IF(IB.LT.IDO.OR.JB.LT.JDO) GO TO 999
GO TO (10,100),MODE
10 CONTINUE
DO 50 I=1,IDO
DO 50 J=1,JDO
50 AMX(I,J)=AMX(I,J)*ACC+BMX(I,J)*BCC
GO TO 300
100 CONTINUE
IF(IR.LT.IDO.OR.JR.LT.JDO) GO TO 999

```

```
DO 200 I=1,IDO
DO 200 J=1,JDO
200 RMX(I,J)=AMX(I,J)*ACC+BMX(I,J)*BCC
300 RETURN
999 CONTINUE
RETURN
END
```

C  
C

```
SUBROUTINE MXMUL(RMX,AMX,BMX,CCC,IR,JR,IA,JA,IB,JB,IDA,JDA,IDB,JDB
1,MODE)
  DIMENSION AMX(IA,JA),BMX(IB,JB),RMX(IR,JR),TEMP(20)
  IF(IDA*IDB*JDA*JDB.GT.IA*IB*JA*JB) GO TO 999
  IF(JDB.GT.JDA) GO TO 999
  GO TO (10,210),MODE
10 DO 100 I=1,IDA
  DO 20 L=1,JDA
20 TEMP(L)=AMX(I,L)
  DO 80 J=1,JDB
  SUM=0
  DO 40 K=1,JDA
40 SUM=SUM+TEMP(K)*BMX(K,J)
  AMX(I,J)=SUM*CCC
80 CONTINUE
100 CONTINUE
  GO TO 600
210 CONTINUE
  IF(IR.LT.IDA.OR.JR.LT.JDB) GO TO 999
  DO 400 I=1,IDA
  DO 380 J=1,JDB
  SUM=0
  DO 340 K=1,JDA
340 SUM=SUM+AMX(I,K)*BMX(K,J)
  RMX(I,J)=SUM*CCC
380 CONTINUE
400 CONTINUE
600 RETURN
999 CONTINUE
RETURN
END
```

Appendix B

SOFTWARE FOR  
STABILITY ANALYSIS OF A BUCK REGULATOR

```

C *****
C * THIS PROGRAM COMPUTES THE CLOSED-LOOP POLES OF A BUCK CONVERTER *
C * WITH A SINGLE-STAGE INPUT FILTER, AS A FUNCTION OF THE INPUT *
C * FILTER PARAMETERS. *
C *****
C
C DIMENSION A(7),B(6),CC1(7),CC2(5)
C REAL NXEG,IXR,M,K1,K2,K3,K4,K5,K6,K7,L,L1,K8
C INTEGER NDEG,IER
C COMPLEX Z(6),Z1(5),Z2(6),Z3(4)
C DATA VI,L,RO,RC,C,RL,VO/25.0,230.0E-6,0.2,0.067,300.0E-6,10.0,20.0
C 1/
C DATA RN,R11,R12,R13,R14,R4,C2,CP1,M/0.65,33.3E3,16.7E3,2.0E5,
C 147.0E3,40.7E3,1.0E-10,5600.0E-12,0.88E-3/
C
C DO 2000 I=1,1000
C READ(5,*) RL1,L1,C1
C IF(RL1.LT.0.) GO TO 2001
C D=0.8388579
C
C Y1=RL*L1*C1*C*RC
C Y2=RL*L1*C1+C*RC*(C1*RL1*RL-(D**2)*L1)
C Y3=C1*RL1*RL-(D**2)*L1+C*RC*(RL-(D**2)*RL1)
C Y4=RL-(D**2)*RL1
C Y5=RL*L1*C1*C*RL
C Y6=RL*L1*C1+C*RL*(C1*RL1*RL-(D**2)*L1)
C Y7=C1*RL1*RL-(D**2)*L1+C*RL*(RL-(D**2)*RL1)
C Y8=L*C*RL*L1*C1
C Y9=(L*C*RL*C1*RL1)+(C*RL*L1*C1*(RO+RC+(L/(C*RL))))
C Y10=L*C*RL+C*RL*C1*RL1*(RO+RC+(L/(C*RL)))+L1*C1*RL+(D**2)*C*RL*L1
C Y11=C*RL*(RO+RC+(L/(C*RL)))+C1*RL1*RL+(D**2)*(L1+C*RL*RL1)
C Y12=RL+(D**2)*RL1
C RX=(R11*R12)/(R11+R12)
C G=RX/R11
C K1=G/(R14+RX)
C K2=C2*(1.0+K1*R13)
C FM=(2.0*R4*CP1)/(RN*M)
C K3=VO*RL*R4*FM
C K4=RN*L*C2*R13
C K5=VO*FM
C K6=CP1*C2*R13
C K7=D*RL*R4

```

```

      K8=C*(RO+RC+(L/(C*RL)))
C
C *****
C * THIS CALCULATION IS FOR THE CLOSED LOOP POLES WITH *
C * INPUT FILTER. *
C *****
C
      A(1)=K7*K6*Y8
      A(2)=K7*CP1*Y8+K7*K6*Y9+K5*K4*Y5
      A(3)=K7*CP1*Y9+K7*K6*Y10+K3*K2*Y1+K5*RN*L*Y5+K5*K4*Y6
      A(4)=K7*CP1*Y10+K7*K6*Y11+K3*K2*Y2+K3*K1*Y1+K5*RN*L*Y6+K5*K4*Y7
      A(5)=K7*CP1*Y11+K7*K6*Y12+K3*K1*Y2+K3*K2*Y3+K5*RN*L*Y7+K5*K4*Y4
      A(6)=CP1*K7*Y12+K3*K1*Y3+K3*K2*Y4+RN*L*K5*Y4
      A(7)=K3*K1*Y4
      NDEG=6
      CALL ZPOLR(A,NDEG,Z,IER)
C
      WRITE(6,101) RL1,L1,C1
101  FORMAT(/,10X,' RL1=',F15.10,' L1=',F15.10,' C1=',F15.10)
      WRITE(6,103)
103  FORMAT(/,20X,' THE CLOSED LOOP POLES WITH I.FILTER ARE-')
      WRITE(6,102)(Z(IX),IX=1,6)
102  FORMAT(/,20X,2E15.8)
C
      B(1)=K5*K4*Y5
      B(2)=K5*RN*L*Y5+K5*K4*Y6+K3*K2*Y1
      B(3)=K5*RN*L*Y6+K5*K4*Y7+K3*K2*Y2+K3*K1*Y1
      B(4)=K5*RN*L*Y7+K5*K4*Y4+K3*K1*Y2+K3*K2*Y3
      B(5)=RN*L*K5*Y4+K3*K1*Y3+K3*K2*Y4
      B(6)=K3*K1*Y4
      NDEG=5
      CALL ZPOLR(B,NDEG,Z1,IER)
      WRITE(6,104)
104  FORMAT(/,20X,' THE OPEN LOOP ZEROES ARE ')
      WRITE(6,102)(Z1(IX),IX=1,5)
C
      CC1(1)=K7*K6*Y8
      CC1(2)=K7*CP1*Y8+K7*K6*Y9
      CC1(3)=K7*CP1*Y9+K7*K6*Y10
      CC1(4)=K7*CP1*Y10+K7*K6*Y11
      CC1(5)=K7*CP1*Y11+K7*K6*Y12
      CC1(6)=CP1*K7*Y12
      CC1(7)=0.0

```

```

      CALL ZPOLR(CC1,6,Z2,IER)
      WRITE(6,105)
105  FORMAT(/,20X,' THE OPEN LOOP POLES ARE ')
      WRITE(6,102){Z2(IX),IX=1,6)
C
C *****
C * THIS CALCULATION IS FOR THE CLOSED LOOP POLES WITHOUT INPUT *
C * FILTER. *
C *****
C
      CC2(1)=K7*K6*L*C
      CC2(2)=K7*K6*K8+K7*CP1*L*C+K5*K4*C*RL
      CC2(3)=K7*CP1*K8+K7*K6+K3*K2*C*RC+K5*K4+K5*RN*L*C*RL
      CC2(4)=K7*CP1+K3*K2+K3*K1*C*RC+RN*L*K5
      CC2(5)=K3*K1
      CALL ZPOLR(CC2,4,Z3,IER)
      WRITE(6,785)
785  FORMAT(/,20X,' THE CLOSED LOOP POLES W/O I.FILTER ARE-')
      WRITE(6,102){Z3(IX),IX=1,4)
2000 CONTINUE
2001 CONTINUE
      STOP
      END

```

C  
C  
C  
C  
C  
C

\*\*\*\*\*  
STABILITY ANALYSIS OF A BUCK CONVERTER WITH INPUT FILTER \*  
\*\*\*\*\*

THIS PROGRAM COMPUTES THE EIGENVALUES OF A BUCK REGULATOR  
SYSTEM WITH INPUT FILTER.

DIMENSION F1(6,6),F2(6,6),G1(6,4),G2(6,4),U(4),PHIF(6,6),  
1PHIN(6,6),DF(6,4),DN(6,4),X(6),ZT(6),AA(6,6),BB(6),TEMP1(6,4),  
2PHIFT(6,6),DFT(6,4),XA(6),ZN1(6),XB(6)  
DIMENSION PSI(6,6),XN1(6),FUN1(6),FUN2(6),CON(4),RVAL(6,9)  
DIMENSION TEMP2(6,6),DX(6)  
DIMENSION WKAREA(70),WK(70)  
REAL L1,L,K1,K2  
COMPLEX W(6),Z(6,6),ZN  
DATA RL1,L1,C1,L,RO,RN,RC,C/0.2000,50.0E-6,220.E-6,230.E-6,0.2E0  
1,0.65E0,0.067E0,300.E-6/  
DATA RL,R11,R12,R13,R14,C2,R4,CP1/10.0E0,33.3E3,16.7E3,2.E5,  
147.E3,0.01E-8,40.7E3,5600.E-12/  
DATA ER,ET,VI,E0/6.7E0,7.E0,25.E0,20.E0/  
DATA VITON,EQ,ED/0.88E-3,0.2E0,0.7E0/  
DATA NIT,EPS/90,10.E-6/  
DATA EPS1,ERROR/2.E-6,0.5E-6/  
DATA CON/0.1E-1,0.05E-1,0.025E-1,0.0125E-1/  
DATA TOLL/0.01/

C

K1=(R12/(R14\*(R11+R12)))+(1./R13)-(RN/R4)  
K1=K1-(RN\*RO\*(RL+RC))/(R4\*RL\*RC)  
K2=(RN/R4)-(1./R13)-(R12/(R14\*(R11+R12)))  
TON=VITON/VI  
TOFFB=TON\*((VI-E0)/E0)  
DO 1 I=1,6  
DO 2 J=1,4  
G1(I,J)=0.  
G2(I,J)=0.  
DF(I,J)=0.  
DN(I,J)=0.  
CONTINUE  
2  
DO 3 K=1,6  
F1(I,K)=0.  
F2(I,K)=0.  
AA(I,K)=0.  
PHIF(I,K)=0.

```

PHIN(1,K)=0.
3 CONTINUE
1 CONTINUE
DO 5 I=1,6
  ZT(I)=0.
  BB(I)=0.
  FUN1(I)=0.
  FUN2(I)=0.
  XA(I)=0.
  XB(I)=0.
  XN1(I)=0.
  ZN1(I)=0.
5 CONTINUE
  F1(1,1)=(-1.*RL1)/L1
  F1(1,2)=-1.00/L1
  F1(2,1)=1.00/C1
  F1(2,3)=-1.00/C1
  F1(3,2)=1.00/L
  F1(3,3)=(-1.00*R0)/L+(-1.00*RC*RL)/(L*(RL+RC))
  F1(3,4)=-1.00*RL/(L*(RL+RC))
  F1(4,3)=RL/(C*(RC+RL))
  F1(4,4)=-1.00/(C*(RC+RL))
  F1(5,3)=(RL*RC)/(C2*R13*(RC+RL))
  F1(5,4)=RL/(C2*R13*(RC+RL))
  F1(5,5)=-1.00/(C2*R13)
  F1(6,2)=(-1.00*RN)/(CP1*R4)
  F1(6,3)=(-1.00*RL*RC*K1)/(CP1*(RC+RL))
  F1(6,4)=(RL*K2)/(CP1*(RL+RC))
  F1(6,5)=1.00/(CP1*R13)
  G1(1,1)=1.00/L1
  G1(3,3)=-1.00/L
  G1(6,2)=1.00/(CP1*R14)
  G1(6,3)=RN/(CP1*R4)
  U(1)=VI
  U(2)=ER
  U(3)=EQ
  U(4)=ED
DO 4 I=1,6
DO 4 J=1,6
4 F2(I,J)=F1(I,J)
  F2(2,3)=0.00
  F2(3,2)=0.00
  F2(6,2)=0.00

```

```

G2(1,1)=G1(1,1)
G2(6,2)=G1(6,2)
G2(3,4)=-1.00/L
G2(6,4)=RN/(CP1*R4)
C
T=TON
CALL STRAN(T, PHIN, DN, F1, G1, 6, 4, 6, 4, 1, 0, ERROR, DIFMAX, ITER, IFLAG)
T=TOFFB
CALL STRAN(T, PHIF, DF, F2, G2, 6, 4, 6, 4, 1, 0, ERROR, DIFMAX, ITER, IFLAG)
C
C *****
C CALCULATION OF THE APPROXIMATE STEADY STATE *
C *****
C
DO 5000 I=1,6
DO 5000 J=1,6
AA(I,J)=0.
DO 5001 K=1,6
5001 AA(I,J)=AA(I,J)+PHIN(I,K)*PHIF(K,J)
AA(I,J)=-1.*AA(I,J)
5000 CONTINUE
DO 5002 I=1,6
5002 AA(I,1)=1.+AA(I,1)
DO 5003 I=1,6
DO 5003 J=1,4
TEMP1(I,J)=0.
DO 5004 K=1,6
5004 TEMP1(I,J)=TEMP1(I,J)+PHIN(I,K)*DF(K,J)
5003 TEMP1(I,J)=TEMP1(I,J)+DN(I,J)
DO 5005 I=1,6
BB(I)=0.
DO 5006 J=1,4
5006 BB(I)=BB(I)+TEMP1(I,J)*U(J)
5005 CONTINUE
MM=1
NN=5
IAA=6
IDGT=0
CALL LEQT2F(AA, MM, NN, IAA, BB, IDGT, WKAREA, IER)
DO 5007 I=1,5
5007 X(I)=BB(I)
X(6)=ET-PHIF(6,1)*X(1)-PHIF(6,2)*X(2)-PHIF(6,3)*X(3)-PHIF(6,4)*X(
14)-PHIF(6,5)*X(5)-DF(6,1)*U(1)-DF(6,2)*U(2)-DF(6,3)*U(3)-DF(6,4)*

```

```

2U(4)
WRITE(6,5008)
5008 FORMAT(1H1,37X,' APPROXIMATE STEADY STATE VALUES,X= ')
WRITE(6,5009)(X(I),I=1,6)
5009 FORMAT(1H ,6F15.10)
WRITE(6,5010) TOFFB
5010 FORMAT(1H0,37X,' APPROXIMATE VALUE OF OFF TIME= ',F15.10)
C
C *****
C CALCULATION OF THE EXACT STEADY STATE VALUES *
C *****
C
IT1=0
900 DO 26 I=1,5
ZT(I)=0.00
DO 27 K=1,6
27 ZT(I)=ZT(I)+PHIF(I,K)*X(K)
DO 28 J=1,4
28 ZT(I)=ZT(I)+DF(I,J)*U(J)
26 CONTINUE
IT1=IT1+1
SMAT=X(6)-PHIN(6,1)*ZT(1)-PHIN(6,2)*ZT(2)-PHIN(6,3)*ZT(3)-PHIN(6,4
1)*ZT(4)-PHIN(6,5)*ZT(5)-PHIN(6,6)*ET-DN(6,1)*U(1)-DN(6,2)*U(2)-
2DN(6,3)*U(3)-DN(6,4)*U(4)
IF(ABS(SMAT).LE.EPS1) GO TO 70
IF(IT1.GT.60) GO TO 70
DTOFF=0.01*TOFFB
T=TOFFB+DTOFF
CALL STRAN(T,PHIFT,DFT,F2,G2,6,4,6,4,1,0,ERROR,DIFMAX,ITER,I FLAG)
DO 29 I=1,6
DO 29 J=1,6
AA(I,J)=0.00
DO 56 K=1,6
56 AA(I,J)=AA(I,J)+PHIN(I,K)*PHIFT(K,J)
AA(I,J)=-1.00*AA(I,J)
29 CONTINUE
DO 31 I=1,6
31 AA(I,1)=1.00+AA(I,1)
DO 32 I=1,6
DO 32 J=1,4
TEMP1(I,J)=0.00
DO 34 K=1,6
34 TEMP1(I,J)=TEMP1(I,J)+PHIN(I,K)*DFT(K,J)

```

```

32  TEMP1(I,J)=TEMP1(I,J)+DN(I,J)
    DO 35 I=1,6
    BB(I)=0.00
    DO 36 J=1,4
36  BB(I)=BB(I)+TEMP1(I,J)*U(J)
35  CONTINUE
    MM=1
    NN=5
    IAA=6
    IDGT=0
    CALL LEQT2F(AA,MM,NN,IAA,BB,IDGT,WKAREA,IER)
    DO 37 I=1,5
37  XN1(I)=BB(I)
    XN1(6)=ET-PHIFT(6,1)*XN1(1)-PHIFT(6,2)*XN1(2)-PHIFT(6,3)*XN1(3)-
1PHIFT(6,4)*XN1(4)-PHIFT(6,5)*XN1(5)-DFT(6,1)*U(1)-DFT(6,2)*U(2)-
2DFT(6,3)*U(3)-DFT(6,4)*U(4)
    DO 38 I=1,5
    ZN1(I)=0.00
    DO 39 K=1,6
39  ZN1(I)=ZN1(I)+PHIFT(I,K)*XN1(K)
    DO 40 J=1,4
40  ZN1(I)=ZN1(I)+DFT(I,J)*U(J)
38  CONTINUE
    SMATN=XN1(6)-PHIN(6,1)*ZN1(1)-PHIN(6,2)*ZN1(2)-PHIN(6,3)*ZN1(3)-
1PHIN(6,4)*ZN1(4)-PHIN(6,5)*ZN1(5)-PHIN(6,6)*ET-DN(6,1)*U(1)-DN(6,2)
2)*U(2)-DN(6,3)*U(3)-DN(6,4)*U(4)
    DSMAT=SMATN-SMAT
    TOFFB=TOFFB+((-1.00*SMAT)/(DSMAT/DTOFF))
    T=TOFFB
    CALL STRAN(T,PHIF,DF,F2,G2,6,4,6,4,1,0,ERROR,DI FMAX,ITER,I FLAG)
    DO 42 I=1,6
    DO 42 J=1,6
    AA(I,J)=0.00
    DO 43 K=1,6
43  AA(I,J)=AA(I,J)+PHIN(I,K)*PHIF(K,J)
    AA(I,J)=-1.00*AA(I,J)
42  CONTINUE
    DO 55 I=1,6
55  AA(I,1)=AA(I,1)+1.
    DO 44 I=1,6
    DO 44 J=1,4
    TEMP1(I,J)=0.00
    DO 46 K=1,6

```

```

46 TEMP1(I,J)=TEMP1(I,J)+PHIN(I,K)*DF(K,J)
44 TEMP1(I,J)=TEMP1(I,J)+DN(I,J)
   DO 47 I=1,6
   BB(I)=0.00
   DO 48 J=1,4
48 BB(I)=BB(I)+TEMP1(I,J)*U(J)
47 CONTINUE
   MM=1
   NN=5
   IAA=6
   IDGT=0
   CALL LEQT2F(AA,MM,NN,IAA,BB,IDGT,WKAREA,IER)
   DO 49 I=1,5
49 X(I)=BB(I)
   X(6)=ET-PHIF(6,1)*X(1)-PHIF(6,2)*X(2)-PHIF(6,3)*X(3)-PHIF(6,4)*
1X(4)-PHIF(6,5)*X(5)-DF(6,1)*U(1)-DF(6,2)*U(2)-DF(6,3)*U(3)-
2DF(6,4)*U(4)
   GO TO 900
70 CONTINUE
   WRITE(6,50)
50 FORMAT(1H0,37X,' EXACT STEADY STATE VALUES,X= ')
   WRITE(6,199)(X(I),I=1,6)
199 FORMAT(1H ,6F15.10)
   WRITE(6,198) TOFFB
198 FORMAT(1H0,37X,' EXACT OFF TIME= ',F15.10)
   DVAL=TON/(TON+TOFFB)
   WRITE(6,624) DVAL
624 FORMAT(1H0,37X,' VALUE OF D=',F15.10)
   WRITE(6,51) IT1
51 FORMAT(1H0,37X,' NO. OF ITERATIONS REQD.= ',I4)
C *****
C * CALCULATION OF THE MATRIX PSI AND ITS EIGENVALUES *
C *****
C
   DO 2000 I=1,6
   DO 2010 IRICH=1,4
   DO 61 IZ=1,6
   XA(IZ)=X(IZ)
61 XB(IZ)=X(IZ)
   DX(I)=CON(IRICH)*ABS(X(I))
   IF(ABS(X(I)).LE.TOLL) DX(I)=0.01
   XA(I)=X(I)+DX(I)

```

```

XB(1)=X(1)-DX(1)
TFFC1=TOFFB
IT=0
T8=TOFFB
CALL STRAN(T8, PHIF, DF, F2, G2, 6, 4, 6, 4, 1, 0, ERROR, DIFMAX, ITER, IFLAG)
1101 ZETA=PHIF(6, 3)*XA(3)+PHIF(6, 4)*
1XA(4)+PHIF(6, 5)*XA(5)+1.0*XA(6)+DF(6, 1)*U(1)+DF(6, 2)*U(2)+
2DF(6, 3)*U(3)+DF(6, 4)*U(4)-ET
IF(ABS(ZETA).LE.EPS) GO TO 1102
IF(IT.GE.NIT) GO TO 1003
DTOFF=CON(IRICH)*TFFC1
T=TFFC1+DTOFF
CALL STRAN(T, PHIFT, DFT, F2, G2, 6, 4, 6, 4, 1, 0, ERROR, DIFMAX, ITER, IFLAG)
ZETAN=PHIFT(6, 3)*XA(3)+PHIFT(6, 4)
1)*XA(4)+PHIFT(6, 5)*XA(5)+1.0*XA(6)+DFT(6, 1)*U(1)+DFT(6, 2)*
2U(2)+DFT(6, 3)*U(3)+DFT(6, 4)*U(4)-ET
DZETA=ZETAN-ZETA
SLOPE=DZETA/DTOFF
TFFC1=TFFC1-(ZETA/SLOPE)
T=TFFC1
CALL STRAN(T, PHIF, DF, F2, G2, 6, 4, 6, 4, 1, 0, ERROR, DIFMAX, ITER, IFLAG)
IT=IT+1
GO TO 1101
1102 DO 13 J=1, 6
TEMP=0.00
DO 14 K=1, 6
DO 81 MENT=1, 5
81 PHIF(MENT, 6)=0.0
PHIF(6, 6)=1.0
14 TEMP=TEMP+PHIF(J, K)*XA(K)
DO 15 K=1, 4
15 TEMP=TEMP+DF(J, K)*U(K)
FUN1(J)=TEMP
13 CONTINUE
TFFC2=TOFFB
IT=0
T=TOFFB
CALL STRAN(T, PHIF, DF, F2, G2, 6, 4, 6, 4, 1, 0, ERROR, DIFMAX, ITER, IFLAG)
1103 ZETA=PHIF(6, 3)*XB(3)+PHIF(6, 4)*
1XB(4)+PHIF(6, 5)*XB(5)+1.0*XB(6)+DF(6, 1)*U(1)+DF(6, 2)*U(2)+
2DF(6, 3)*U(3)+DF(6, 4)*U(4)-ET
IF(ABS(ZETA).LE.EPS) GO TO 1104
IF(IT.GE.NIT) GO TO 1003

```

```

17 CONTINUE
WRITE(6,92)
92 FORMAT(1H0,37X,' MATRIX PSI-- ')
DO 30 I=1,6
30 WRITE(6,93)(PSI(I,J),J=1,6)
93 FORMAT(6F15.10)
GO TO 1004
1003 WRITE(6,100) I
100 FORMAT(/,' CONVERGENCE NOT OBTAINED FOR X(I), I= ',I4)
1004 CONTINUE
CALL EIGRF(PSI,6,6,2,W,Z,6,WK,IER)
WRITE(6,94)
94 FORMAT(1H0,37X,' THE EIGENVALUES ARE-- ')
WRITE(6,103)(W(I),I=1,6)
103 FORMAT(1H ,6F15.10)
WRITE(6,104) WK(1),IER
104 FORMAT(1H0,37X,' CONVERGENCE TOLERANCE=',F15.10,' IER=',I4)
905 CONTINUE
STOP
END

```

C  
C

```

SUBROUTINE STRAN(TAU,PHI,THETA,A,B,NA,NB,MA,MB,MODE,NTERMS,
1 TOL,DIFMAX,ITER,IFLAG)
REAL PHI(NA,NA),THETA(NA,NB),A(NA,NA),B(NA,NB),
1 WORK1(10,10),WORK2(10,10),DUMMY(1,1),FAC1,CON1,FAC2,CON2
C1=1
TS=TAU
DO 4 I=1,MA
DO 2 J=1,MA
WORK1(I,J)=0
WORK2(I,J)=0
PHI(I,J)=0
2 CONTINUE
WORK1(I,I)=1
WORK2(I,I)=TAU
PHI(I,I)=1
4 CONTINUE
DO 6 I=1,MA
DO 6 J=1,MB
6 THETA(I,J)=0
DIFMAX=1.E8
NDO=50

```

```

IF(NTERMS.GT.0) NDO=NTERMS
FAC1=1
IFLAG=0
DO 1000 I=1,NDO
CALL MXMUL(DUMMY,WORK1,A,TS,1,1,10,10,NA,NA,MA,MA,MA,MA,1)
FAC1=FAC1*I
CON1=1./FAC1
IF(NTERMS.EQ.0.AND.I.GE.4) CALL SERROR(PHI,WORK1,CON1,NA,NA,
1 10,10,MA,MA,DIFMAX)
CALL MXADD(DUMMY,PHI,WORK1,C1,CON1,1,1,NA,NA,10,10,MA,MA,1)
IF(MODE.EQ.2) GO TO 500
FAC2=FAC1*(I+1)
CON2=TAU/FAC2
CALL MXADD(DUMMY,WORK2,WORK1,C1,CON2,1,1,10,10,10,10,MA,MA,1)
500 CONTINUE
ITER=I
IF(NTERMS.GT.0.OR.I.LT.4) GO TO 1000
IF(DIFMAX.LE.TOL) GO TO 1100
1000 CONTINUE
1100 CONTINUE
IF(MODE.EQ.1) CALL MXMUL(THETA,WORK2,B,C1,NA,NB,10,10,NA,NB,
1 MA,MA,MA,MB,2)
IF(ITER.EQ.NDO.AND.NTERMS.EQ.0) IFLAG=1
RETURN
END

```

C  
C

```

SUBROUTINE SERROR(AMX,BMX,CCC,IA,JA,IB,JB,IDO,JDO,DIFMAX)
DIMENSION AMX(IA,JA),BMX(IB,JB)
DIFMAX=1.E-30
DO 100 I=1,IDO
DO 50 J=1,JDO
IF(AMX(I,J).EQ.0.0) GO TO 50
CHANGE=ABS(BMX(I,J)*CCC/AMX(I,J))
IF(CHANGE.GT.DIFMAX) DIFMAX=CHANGE
50 CONTINUE
100 CONTINUE
RETURN
END

```

C  
C

```

SUBROUTINE MXADD(RMX,AMX,BMX,ACC,BCC,IR,JR,IA,JA,IB,JB,IDO,JDO,
1 MODE)

```

```

        DIMENSION      AMX( IA, JA), BMX( IB, JB), RMX( IR, JR)
        IF( IA.LT. IDO. OR. JA.LT. JDO) GO TO 999
        IF( IB.LT. IDO. OR. JB.LT. JDO) GO TO 999
        GO TO ( 10, 100), MODE
10    CONTINUE
        DO 50 I=1, IDO
        DO 50 J=1, JDO
50    AMX( I, J)=AMX( I, J)*ACC+BMX( I, J)*BCC
        GO TO 300
100   CONTINUE
        IF( IR.LT. IDO. OR. JR.LT. JDO) GO TO 999
        DO 200 I=1, IDO
        DO 200 J=1, JDO
200   RMX( I, J)=AMX( I, J)*ACC+BMX( I, J)*BCC
300   RETURN
999   CONTINUE
        RETURN
        END

```

C  
C

```

SUBROUTINE MXMUL( RMX, AMX, BMX, CCC, IR, JR, IA, JA, IB, JB, IDA, JDA, IDB, JDB
1, MODE)
        DIMENSION      AMX( IA, JA), BMX( IB, JB), RMX( IR, JR), TEMP( 20)
        IF( IDA*IDB*JDA*JDB.GT. IA*IB*JA*JB) GO TO 999
        IF( JDB.GT. JDA) GO TO 999
        GO TO ( 10, 210), MODE
10    DO 100 I=1, IDA
        DO 20 L=1, JDA
20    TEMP( L)=AMX( I, L)
        DO 80 J=1, JDB
        SUM=0
        DO 40 K=1, JDA
40    SUM=SUM+TEMP( K)*BMX( K, J)
        AMX( I, J)=SUM*CCC
80    CONTINUE
100   CONTINUE
        GO TO 600
210   CONTINUE
        IF( IR.LT. IDA. OR. JR.LT. JDB) GO TO 999
        DO 400 I=1, IDA
        DO 380 J=1, JDB
        SUM=0
        DO 340 K=1, JDA

```

```
340 SUM=SUM+AMX(I,K)*BMX(K,J)
    RMX(I,J)=SUM*CCC
380 CONTINUE
400 CONTINUE
600 RETURN
999 CONTINUE
    RETURN
    END
```

C  
C  
C  
C  
C  
C  
C  
C

```
*****  
* STABILITY ANALYSIS OF A BUCK CONVERTER *  
*****
```

THIS PROGRAM COMPUTES THE EIGENVALUES OF A BUCK  
REGULATOR SYSTEM WITH INPUT FILTER AND  
FEEDFORWARD.

```
    DIMENSION F1(7,7),F2(7,7),G1(7,4),G2(7,4),U(4),PHIF(7,7),  
    1PHIN(7,7),DF(7,4),DN(7,4),X(7),ZT(7),AA(7,7),BB(7),TEMP1(7,4),  
    2PHIFT(7,7),DFT(7,4),XN1(7),ZN1(7)  
    DIMENSION PSI(7,7),XA(7),FUN1(7),FUN2(7),XB(7),CON(4),RVAL(7,9)  
    DIMENSION TEMP2(7,7),DX(7)  
    DIMENSION WKAREA(90),WK(90)  
    REAL L1,L,K1,K2,K3  
    COMPLEX W(7),Z(7,7),ZN  
    DATA RL1,L1,C1,L,RO,RN,RC,C/0.20E0,1.425E-3,220.E-6,230.E-6,0.2E0,  
    10.65E0,0.067E0,300.E-6/  
    DATA RL,R11,R12,R13,R14,C2,R4,CP1/10.0E0,33.3E3,16.7E3,2.E5,  
    147.E3,0.01E-8,40.7E3,5600.E-12/  
    DATA ER,ET,VI,E0/6.7E0,7.E0,25.E0,20.E0/  
    DATA VITON,EQ,ED/0.88E-3,0.7E0,0.2E0/  
    DATA NIT,EPS/150,5.E-6/  
    DATA EPS1/0.5E-6/  
    DATA ERROR/0.5E-6/  
    DATA CON/0.2E-1,0.1E-1,0.05E-1,0.025E-1/  
    DATA CF,RF1,RF2,TOLL/2.7E-5,5.1E3,220.0E0,0.11/
```

C

```
    K1=(R12/(R14*(R11+R12)))+(1./R13)-(RN/R4)  
    K1=K1-(RN*RO*(RL+RC))/(R4*RL*RC)  
    K2=(RN/R4)-(1./R13)-(R12/(R14*(R11+R12)))  
    K3=RF2/(RF1+RF2)  
    TON=VITON/VI  
    TOFFB=TON*((VI-E0)/E0)  
    DO 1 I=1,7  
    DO 2 J=1,4  
    G1(I,J)=0.  
    G2(I,J)=0.  
    DF(I,J)=0.  
    DN(I,J)=0.  
    CONTINUE  
    DO 3 K=1,7
```

2

```

F1(1,K)=0.
F2(1,K)=0.
AA(1,K)=0.
PHIF(1,K)=0.
PHIN(1,K)=0.
3
1
CONTINUE
CONTINUE
DO 5 I=1,7
ZT(I)=0.
BB(I)=0.
FUN1(I)=0.
FUN2(I)=0.
XA(I)=0.
XB(I)=0.
XN1(I)=0.
ZN1(I)=0.
5
CONTINUE
F1(1,1)=(-1.*RL1)/L1
F1(1,2)=-1.00/L1
F1(2,1)=1.00/C1
F1(2,3)=-1./(C1*(RF1+RF2))
F1(2,4)=-1.00/C1
F1(3,1)=1./C1
F1(3,3)=-1.*(C1+CF)/(C1*CF*(RF1+RF2))
F1(3,4)=-1./C1
F1(4,2)=1.00/L
F1(4,4)=(-1.00*RO)/L+(-1.00*RC*RL)/(L*(RL+RC))
F1(4,5)=-1.00*RL/(L*(RL+RC))
F1(5,4)=RL/(C*(RC+RL))
F1(5,5)=-1.00/(C*(RC+RL))
F1(6,4)=(RL*RC)/(C2*R13*(RC+RL))
F1(6,5)=RL/(C2*R13*(RC+RL))
F1(6,6)=-1.00/(C2*R13)
F1(7,1)=-1.*K3/C1
F1(7,2)=(-1.00*RN)/(CP1*R4)
F1(7,3)=K3*(C1+CF)/(C1*CF*(RF1+RF2))
F1(7,4)=(K3/C1)-((RL*RC*K1)/(CP1*(RL+RC)))
F1(7,5)=(RL*K2)/(CP1*(RL+RC))
F1(7,6)=1.00/(CP1*R13)
G1(1,1)=1.00/L1
G1(4,3)=-1.00/L
G1(7,2)=1.00/(CP1*R14)
G1(7,3)=RN/(CP1*R4)

```

```

U(1)=V1
U(2)=ER
U(3)=EQ
U(4)=ED
DO 4 I=1,7
DO 4 J=1,7
4 F2(1,J)=F1(I,J)
F2(2,4)=0.
F2(3,4)=0.
F2(4,2)=0.
F2(7,2)=0.
F2(7,4)=(-1.*RL*RC*K1)/(CP1*(RL+RC))
G2(1,1)=G1(1,1)
G2(7,2)=G1(7,2)
G2(4,4)=-1.00/L
G2(7,4)=RN/(CP1*R4)
C
T=TON
CALL STRAN(T, PHIN, DN, F1, G1, 7, 4, 7, 4, 1, 0, ERROR, DIFMAX, ITER, IFLAG)
T=TOFFB
CALL STRAN(T, PHIF, DF, F2, G2, 7, 4, 7, 4, 1, 0, ERROR, DIFMAX, ITER, IFLAG)
C
C *****
C * CALCULATION OF THE APPROXIMATE STEADY STATE *
C *****
C
DO 5000 I=1,7
DO 5000 J=1,7
AA(I,J)=0.
DO 5001 K=1,7
5001 AA(I,J)=AA(I,J)+PHIN(I,K)*PHIF(K,J)
AA(I,J)=-1.*AA(I,J)
5000 CONTINUE
DO 5002 I=1,7
5002 AA(I,1)=1.+AA(I,1)
DO 5003 I=1,7
DO 5003 J=1,4
TEMP1(I,J)=0.
DO 5004 K=1,7
5004 TEMP1(I,J)=TEMP1(I,J)+PHIN(I,K)*DF(K,J)
5003 TEMP1(I,J)=TEMP1(I,J)+DN(I,J)
DO 5005 I=1,7
BB(I)=0.

```

```

DO 5006 J=1,4
5006 BB(I)=BB(I)+TEMP1(I,J)*U(J)
5005 CONTINUE
MM=1
NN=6
IAA=7
IDGT=0
CALL LEQT2F(AA,MM,NN,IAA,BB,IDGT,WKAREA,IER)
DO 5007 I=1,6
5007 X(I)=BB(I)
X(7)=ET-PHIF(7,1)*X(1)-PHIF(7,2)*X(2)-PHIF(7,3)*X(3)-PHIF(7,4)*X(
14)-PHIF(7,5)*X(5)-DF(7,1)*U(1)-DF(7,2)*U(2)-DF(7,3)*U(3)-DF(7,4)*
2U(4)-PHIF(7,6)*X(6)
WRITE(6,5008)
5008 FORMAT(1H1,37X,' APPROXIMATE STEADY STATE VALUES,X= ')
WRITE(6,5009)(X(I),I=1,7)
5009 FORMAT(1H,7F15.10)
WRITE(6,5010)TOFFB
5010 FORMAT(1H0,37X,' APPROXIMATE VALUE OF OFF TIME=',F15.10)
C
C *****
C * CALCULATION OF THE EXACT STEADY STATE VALUES *
C *****
C
IT1=0
900 DO 26 I=1,6
ZT(I)=0.00
DO 27 K=1,7
27 ZT(I)=ZT(I)+PHIF(I,K)*X(K)
DO 28 J=1,4
28 ZT(I)=ZT(I)+DF(I,J)*U(J)
26 CONTINUE
IT1=IT1+1
SMAT=X(7)-PHIN(7,1)*ZT(1)-PHIN(7,2)*ZT(2)-PHIN(7,3)*ZT(3)-PHIN(7,4
1)*ZT(4)-PHIN(7,5)*ZT(5)-PHIN(7,7)*ET-DN(7,1)*U(1)-DN(7,2)*U(2)-
2DN(7,3)*U(3)-DN(7,4)*U(4)-PHIN(7,6)*ZT(6)
IF(ABS(SMAT).LE.EPS1) GO TO 70
IF(IT1.GT.60) GO TO 70
DTOFF=0.01*TOFFB
T=TOFFB+DTOFF
CALL STRAN(T,PHIFT,DFT,F2,G2,7,4,7,4,1,0,ERROR,DIFMAX,ITER,I FLAG)
DO 29 I=1,7
DO 29 J=1,7

```

```

AA(I,J)=0.00
DO 56 K=1,7
56 AA(I,J)=AA(I,J)+PHIN(I,K)*PHIFT(K,J)
AA(I,J)=-1.00*AA(I,J)
29 CONTINUE
DO 31 I=1,7
31 AA(I,1)=1.00+AA(I,1)
DO 32 I=1,7
DO 32 J=1,4
TEMP1(I,J)=0.00
DO 34 K=1,7
34 TEMP1(I,J)=TEMP1(I,J)+PHIN(I,K)*DFT(K,J)
32 TEMP1(I,J)=TEMP1(I,J)+DN(I,J)
DO 35 I=1,7
BB(I)=0.00
DO 36 J=1,4
36 BB(I)=BB(I)+TEMP1(I,J)*U(J)
35 CONTINUE
MM=1
NN=6
IAA=7
IDGT=0
CALL LEQT2F(AA,MM,NN,IAA,BB,IDGT,WKAREA,IER)
DO 37 I=1,6
37 XN1(I)=BB(I)
XN1(7)=ET-PHIFT(7,1)*XN1(1)-PHIFT(7,2)*XN1(2)-PHIFT(7,3)*XN1(3)-
1PHIFT(7,4)*XN1(4)-PHIFT(7,5)*XN1(5)-DFT(7,1)*U(1)-DFT(7,2)*U(2)-
2DFT(7,3)*U(3)-DFT(7,4)*U(4)-PHIFT(7,6)*XN1(6)
DO 38 I=1,6
ZNI(I)=0.00
DO 39 K=1,7
39 ZNI(I)=ZNI(I)+PHIFT(I,K)*XN1(K)
DO 40 J=1,4
40 ZNI(I)=ZNI(I)+DFT(I,J)*U(J)
38 CONTINUE
SMATN=XN1(7)-PHIN(7,1)*ZNI(1)-PHIN(7,2)*ZNI(2)-PHIN(7,3)*ZNI(3)-
1PHIN(7,4)*ZNI(4)-PHIN(7,5)*ZNI(5)-PHIN(7,7)*ET-DN(7,1)*U(1)-DN(7,2)
2*U(2)-DN(7,3)*U(3)-DN(7,4)*U(4)-PHIN(7,6)*ZNI(6)
DSMAT=SMATN-SMAT
TOFFB=TOFFB+((-1.00*SMAT)/(DSMAT/DTOFF))
C
T=TOFFB
CALL STRAN(T,PHIF,DF,F2,G2,7,4,7,4,1,0,ERROR,DIFMAX,ITER,I FLAG)

```

```

DO 42 I=1,7
DO 42 J=1,7
AA(I,J)=0.00
DO 43 K=1,7
43 AA(I,J)=AA(I,J)+PHIN(I,K)*PHIF(K,J)
AA(I,J)=-1.00*AA(I,J)
42 CONTINUE
DO 55 I=1,7
55 AA(I,I)=AA(I,I)+1.
DO 44 I=1,7
DO 44 J=1,4
TEMP1(I,J)=0.00
DO 46 K=1,7
46 TEMP1(I,J)=TEMP1(I,J)+PHIN(I,K)*DF(K,J)
44 TEMP1(I,J)=TEMP1(I,J)+DN(I,J)
DO 47 I=1,7
BB(I)=0.00
DO 48 J=1,4
48 BB(I)=BB(I)+TEMP1(I,J)*U(J)
47 CONTINUE
MM=1
NN=6
IAA=7
IDGT=0
CALL LEQT2F(AA,MM,NN,IAA,BB,IDGT,WKAREA,IER)
DO 49 I=1,6
49 X(I)=BB(I)
X(7)=ET-PHIF(7,1)*X(1)-PHIF(7,2)*X(2)-PHIF(7,3)*X(3)-PHIF(7,4)*
1X(4)-PHIF(7,5)*X(5)-DF(7,1)*U(1)-DF(7,2)*U(2)-DF(7,3)*U(3)-
2DF(7,4)*U(4)-PHIF(7,6)*X(6)
GO TO 900
70 CONTINUE
WRITE(6,50)
50 FORMAT(1H0,37X,' EXACT STEADY STATE VALUES,X=' )
WRITE(6,199)(X(I),I=1,7)
199 FORMAT(1H ,7F15.10)
WRITE(6,198) TOFFB
198 FORMAT(1H0,37X,' EXACT OFF TIME= ',F15.10)
WRITE(6,51) IT1
51 FORMAT(1H0,37X,' NO. OF ITERATIONS REQD.= ',I4)
C
C *****
C * CALCULATION OF THE MATRIX PSI AND ITS EIGENVALUES *
C *****
C

```

```

DO 2000 I=1,7
DO 2010 IRICH=1,4
DO 61 IZ=1,7
XA(IZ)=X(IZ)
61 XB(IZ)=X(IZ)
DX(I)=CON(IRICH)*ABS(X(I))
IF(ABS(X(I)).LE.TOLL) DX(I)=CON(IRICH)
XA(I)=X(I)+DX(I)
XB(I)=X(I)-DX(I)
TFFC1=TOFFB
IT=0
T=TOFFB
CALL STRAN(T,PHIF,DF,F2,G2,7,4,7,4,1,0,ERROR,DIFMAX,ITER,IFLSG)
1101 ZETA=0.0*XA(1)+0.0*XA(2)+PHIF(7,3)*XA(3)+PHIF(7,4)*
1XA(4)+PHIF(7,5)*XA(5)+1.0*XA(7)+0.0*U(1)+DF(7,2)*U(2)+
2DF(7,4)*U(4)-ET+PHIF(7,6)*XA(6)
IF(ABS(ZETA).LE.EPS) GO TO 1102
IF(IT.GE.NIT) GO TO 1003
DTOFF=CON(IRICH)*TFFC1
T=TFFC1+DTOFF
CALL STRAN(T,PHIFT,DFT,F2,G2,7,4,7,4,1,0,ERROR,DIFMAX,ITER,IFLAG)
ZETAN=0.0*XA(1)+0.0*XA(2)+PHIFT(7,3)*XA(3)+PHIFT(7,4
1)*XA(4)+PHIFT(7,5)*XA(5)+1.0*XA(7)+0.0*U(1)+DFT(7,2)*
2U(2)+DFT(7,4)*U(4)-ET+PHIFT(7,6)*XA(6)
DZETA=ZETAN-ZETA
SLOPE=DZETA/DTOFF
TFFC1=TFFC1-(ZETA/SLOPE)
T=TFFC1
CALL STRAN(T,PHIF,DF,F2,G2,7,4,7,4,1,0,ERROR,DIFMAX,ITER,IFLAG)
IT=IT+1
GO TO 1101
1102 DO 13 J=1,7
TEMP=0.00
DO 14 K=1,7
DO 81 MENT=1,6
81 PHIF(MENT,7)=0.0
PHIF(7,7)=1.0
PHIF(7,1)=0.0
PHIF(7,2)=0.0
14 TEMP=TEMP+PHIF(J,K)*XA(K)
DO 15 K=1,4
DF(7,1)=0.0
15 TEMP=TEMP+DF(J,K)*U(K)

```

```

13   FUN1(J)=TEMP
      CONTINUE
      TFFC2=TOFFB
      IT=0
      T=TOFFB
1103 CALL STRAN(T, PHIF, DF, F2, G2, 7, 4, 7, 4, 1, 0, ERROR, DIFMAX, ITER, IFLAG)
      ZETA=0.0*XB(1)+0.0*XB(2)+PHIF(7,3)*XB(3)+PHIF(7,4)*
      1XB(4)+PHIF(7,5)*XB(5)+1.0*XB(7)+0.0*U(1)+DF(7,2)*U(2)+
      2DF(7,4)*U(4)-ET+PHIF(7,6)*XB(6)
      IF(ABS(ZETA).LE.EPS) GO TO 1104
      IF(IT.GE.NIT) GO TO 1003
      DTOFF=CON(IRICH)*TFFC2
      T=TFFC2+DTOFF
      CALL STRAN(T, PHIFT, DFT, F2, G2, 7, 4, 7, 4, 1, 0, ERROR, DIFMAX, ITER, IFLAG)
      ZETAN=0.0*XB(1)+0.0*XB(2)+PHIFT(7,3)*XB(3)+PHIFT(7,4
      1)*XB(4)+PHIFT(7,5)*XB(5)+1.0*XB(7)+0.0*U(1)+DFT(7,2)*
      2U(2)+DFT(7,4)*U(4)-ET+PHIFT(7,6)*XB(6)
      DZETA=ZETAN-ZETA
      SLOPE=DZETA/DTOFF
      TFFC2=TFFC2-(ZETA/SLOPE)
      T=TFFC2
      CALL STRAN(T, PHIF, DF, F2, G2, 7, 4, 7, 4, 1, 0, ERROR, DIFMAX, ITER, IFLAG)
      IT=IT+1
      GO TO 1103
1104 DO 62 J=1,7
      TEMP=0.00
      DO 63 K=1,7
      DO 82 MENT=1,6
82   PHIF(MENT,7)=0.0
      PHIF(7,7)=1.0
      PHIF(7,1)=0.0
      PHIF(7,2)=0.0
63   TEMP=TEMP+PHIF(J,K)*XB(K)
      DO 64 K=1,4
      DF(7,1)=0.0
64   TEMP=TEMP+DF(J,K)*U(K)
      FUN2(J)=TEMP
62   CONTINUE
      DO 2011 J=1,7
2011 RVAL(J,IRICH)=(FUN1(J)-FUN2(J))/(2.0*DX(1))
2010 CONTINUE
      DO 65 J=1,7
      RVAL(J,5)=(RVAL(J,2)-0.25*RVAL(J,1))/0.75

```

```

65  RVAL(J,6)=(RVAL(J,3)-0.25*RVAL(J,2))/0.75
    RVAL(J,7)=(RVAL(J,4)-0.25*RVAL(J,3))/0.75
    DO 66 J=1,7
    RVAL(J,8)=(RVAL(J,6)-0.0625*RVAL(J,5))/0.9375
66  RVAL(J,9)=(RVAL(J,7)-0.0625*RVAL(J,6))/0.9375
    DO 67 J=1,7
67  TEMP2(J,1)=(RVAL(J,9)-0.015625*RVAL(J,8))/0.984375
2000 CONTINUE
    DO 17 I=1,7
    DO 17 J=1,7
    TEMP=0.00
    DO 19 K=1,7
19  TEMP=TEMP+PHIN(I,K)*TEMP2(K,J)
    PSI(I,J)=TEMP
17  CONTINUE
    WRITE(6,92)
92  FORMAT(1H0,37X,' MATRIX PSI= ')
    DO 30 I=1,7
30  WRITE(6,93)(PSI(I,J),J=1,7)
93  FORMAT(7F15.10)
    GO TO 1004
1003 WRITE(6,100) I
100  FORMAT(/,' CONVERGENCE NOT OBTAINED FOR X(I), I= ',I4)
1004 CONTINUE
    CALL EIGRF(PSI,7,7,2,W,Z,7,WK,IER)
    WRITE(6,94)
94  FORMAT(1H0,37X,' THE EIGENVALUES ARE--')
    WRITE(6,103)(W(I),I=1,7)
103  FORMAT(1H ,7F15.10)
    WRITE(6,104) WK(1),IER
104  FORMAT(1H0,37X,' CONVERGENCE TOLERANCE=',F15.10,' IER= ',I4)
905  CONTINUE
    STOP
    END

```

C  
C

```

SUBROUTINE STRAN(TAU,PHI,THETA,A,B,NA,NB,MA,MB,MODE,NTERMS,
1  TOL,DIFMAX,ITER,IFLAG)
  REAL    PHI(NA,NA),THETA(NA,NB),A(NA,NA),B(NA,NB),
1  WORK1(10,10),WORK2(10,10),DUMMY(1,1),FAC1,CON1,FAC2,CON2
  C1=1
  TS=TAU
  DO 4 I=1,MA

```

```

DO 2 J=1,MA
WORK1(I,J)=0
WORK2(I,J)=0
PHI(I,J)=0
2 CONTINUE
WORK1(I,I)=1
WORK2(I,I)=TAU
PHI(I,I)=1
4 CONTINUE
DO 6 I=1,MA
DO 6 J=1,MB
6 THETA(I,J)=0
DIFMAX=1.E8
NDO=50
IF(NTERMS.GT.0) NDO=NTERMS
FAC1=1
IFLAG=0
DO 1000 I=1,NDO
CALL MXMUL(DUMMY,WORK1,A,TS,1,1,10,10,NA,NA,MA,MA,MA,MA,1)
FAC1=FAC1*I
CON1=1./FAC1
IF(NTERMS.EQ.0.AND.I.GE.4) CALL SERROR(PHI,WORK1,CON1,NA,NA,
1 10,10,MA,MA,DIFMAX)
CALL MXADD(DUMMY,PHI,WORK1,C1,CON1,1,1,NA,NA,10,10,MA,MA,1)
IF(MODE.EQ.2) GO TO 500
FAC2=FAC1*(I+1)
CON2=TAU/FAC2
CALL MXADD(DUMMY,WORK2,WORK1,C1,CON2,1,1,10,10,10,10,MA,MA,1)
500 CONTINUE
ITER=I
IF(NTERMS.GT.0.OR.I.LT.4) GO TO 1000
IF(DIFMAX.LE.TOL) GO TO 1100
1000 CONTINUE
1100 CONTINUE
IF(MODE.EQ.1) CALL MXMUL(THETA,WORK2,B,C1,NA,NB,10,10,NA,NB,
1 MA,MA,MA,MB,2)
IF(ITER.EQ.NDO.AND.NTERMS.EQ.0) IFLAG=1
RETURN
END

```

C  
C

```

SUBROUTINE SERROR(AMX,BMX,CCC,IA,JA,IB,JB,IDO,JDO,DIFMAX)
DIMENSION AMX(IA,JA),BMX(IB,JB)

```

```

DIFMAX=1.E-30
DO 100 I=1,IDO
DO 50 J=1,JDO
IF(AMX(I,J).EQ.0.0) GO TO 50
CHANGE=ABS(BMX(I,J)*CCC/AMX(I,J))
IF(CHANGE.GT.DIFMAX) DIFMAX=CHANGE
50 CONTINUE
100 CONTINUE
RETURN
END

```

C  
C

```

SUBROUTINE MXADD(RMX,AMX,BMX,ACC,BCC,IR,JR,IA,JA,IB,JB,IDO,JDO,
1,MODE)
DIMENSION AMX(IA,JA),BMX(IB,JB),RMX(IR,JR)
IF(IA.LT.IDO.OR.JA.LT.JDO) GO TO 999
IF(IB.LT.IDO.OR.JB.LT.JDO) GO TO 999
GO TO (10,100),MODE
10 CONTINUE
DO 50 I=1,IDO
DO 50 J=1,JDO
50 AMX(I,J)=AMX(I,J)*ACC+BMX(I,J)*BCC
GO TO 300
100 CONTINUE
IF(IR.LT.IDO.OR.JR.LT.JDO) GO TO 999
DO 200 I=1,IDO
DO 200 J=1,JDO
200 RMX(I,J)=AMX(I,J)*ACC+BMX(I,J)*BCC
300 RETURN
999 CONTINUE
RETURN
END

```

C  
C

```

SUBROUTINE MXMUL(RMX,AMX,BMX,CCC,IR,JR,IA,JA,IB,JB,IDA,JDA,IDB,JDB
1,MODE)
DIMENSION AMX(IA,JA),BMX(IB,JB),RMX(IR,JR),TEMP(20)
IF(IDA>IDB*JDA>JDB.GT.IA>IDB*JA*JB) GO TO 999
IF(JDB.GT.JDA) GO TO 999
GO TO (10,210),MODE
10 DO 100 I=1,IDA
DO 20 L=1,JDA
20 TEMP(L)=AMX(I,L)

```

```
DO 80 J=1,JDB
SUM=0
DO 40 K=1,JDA
40 SUM=SUM+TEMP(K)*BMX(K,J)
AMX(I,J)=SUM*CCC
80 CONTINUE
100 CONTINUE
GO TO 600
210 CONTINUE
IF(IR.LT.IDA.OR.JR.LT.JDB) GO TO 999
DO 400 I=1,IDA
DO 380 J=1,JDB
SUM=0
DO 340 K=1,JDA
340 SUM=SUM+AMX(I,K)*BMX(K,J)
RMX(I,J)=SUM*CCC
380 CONTINUE
400 CONTINUE
600 RETURN
999 CONTINUE
RETURN
END
```

```

DTCFF=CON( I RICH)*TFFC2
T=TFFC2+DTCFF
CALL STRAN(T, PHIFT, DFT, F2, G2, 6, 4, 6, 4, 1, 0, ERROR, DIFMAX, ITER, IFLAG)
ZETAN=PHIFT(6, 3)*XB(3)+PHIFT(6, 4
1)*XB(4)+PHIFT(6, 5)*XB(5)+1.0*XB(6)+DFT(6, 1)*U(1)+DFT(6, 2)*
2U(2)+DFT(6, 3)*U(3)+DFT(6, 4)*U(4)-ET
DZETA=ZETAN-ZETA
SLOPE=DZETA/DTCFF
TFFC2=TFFC2-(ZETA/SLOPE)
T=TFFC2
CALL STRAN(T, PHIF, DF, F2, G2, 6, 4, 6, 4, 1, 0, ERROR, DIFMAX, ITER, IFLAG)
IT=IT+1
GO TO 1103
1104 DO 62 J=1, 6
      TEMP=0.00
      DO 63 K=1, 6
      DO 82 MENT=1, 5
82      PHIF(MENT, 6)=0.0
      PHIF(6, 6)=1.0
63      TEMP=TEMP+PHIF(J, K)*XB(K)
      DO 64 K=1, 4
64      TEMP=TEMP+DF(J, K)*U(K)
      FUN2(J)=TEMP
62      CONTINUE
      DO 2011 J=1, 6
2011     RVAL(J, I RICH)=( FUN1(J)-FUN2(J))/(2.0*DX( I ))
2010     CONTINUE
      DO 65 J=1, 6
      RVAL(J, 5)=(RVAL(J, 2)-0.25*RVAL(J, 1))/0.75
      RVAL(J, 6)=(RVAL(J, 3)-0.25*RVAL(J, 2))/0.75
65     RVAL(J, 7)=(RVAL(J, 4)-0.25*RVAL(J, 3))/0.75
      DO 66 J=1, 6
      RVAL(J, 8)=(RVAL(J, 6)-0.0625*RVAL(J, 5))/0.9375
66     RVAL(J, 9)=(RVAL(J, 7)-0.0625*RVAL(J, 6))/0.9375
      DO 67 J=1, 6
67     TEMP2(J, 1)=(RVAL(J, 9)-0.015625*RVAL(J, 8))/0.984375
2000     CONTINUE
      DO 17 I=1, 6
      DO 17 J=1, 6
      TEMP=0.00
      DO 19 K=1, 6
19     TEMP=TEMP+PHIN( I, K)*TEMP2(K, J)
      PSI( I, J)=TEMP

```

## BIBLIOGRAPHY

- [1] R.D.Middlebrook and S.Cuk, 'A Generalized Unified Approach to Modeling Switching Converter Power Stages', 1976 IEEE Power Electronics Specialists Conference, Conference Record, pp 18-34.
- [2] F.C.Lee and Y.Yu, 'An Adaptive Control Switching Buck Regulator Implementation, Analysis and Design', IEEE Transactions on Aerospace and Electronic Systems, vol.AES-16, No.1, January 1980.
- [3] Y.Yu and J.J.Biess, 'Some Design Aspects Concerning Input Filters for DC-DC Converters', 1971 IEEE Power Conditioning Specialists Conference, Conference Record, pp.66-76.
- [4] R.D.Middlebrook, 'Input Filter Considerations in Design and Applications of Switching Regulators', IEEE Industry Applications Society Annual Meeting, Chicago, October, 1976.
- [5] R.D.Middlebrook, 'Design Techniques for Preventing Input Filter Oscillations in Switched-Mode Regulators', Fifth National Solid State Power Conversion Conference, Proceedings, 1970
- [6] F.C.Lee and Y.Yu, 'Input Filter Design for Switching Regulators', IEEE Transactions on Aerospace and Electronic Systems, vol. AES-15, No.5, September 1979.
- [7] F.C.Lee, 'User's Design Handbook for a Standardized Control Module (SCM) for DC to DC Converters, Volume II', Virginia Polytechnic Institute and State University, April 1980.
- [8] F.C.Lee, M.F.Mahmoud and Y.Yu, 'Application Handbook for a Standardized Control Module (SCM) for DC to DC Converters, Volume I', Virginia Polytechnic Institute and State University and TRW Defense and Space Systems Group, April 1980.
- [9] F.C.Lee and R.A.Carter, 'Investigations of Stability and Dynamic Performances of Switching Regulators Employing Current Injected Control', 1981 IEEE Power Electronics Specialists Conference, Conference Record, 1981.

- [10] S.S.Kelkar and F.C.Lee, 'A Novel Input Filter Compensation Scheme for Switching Regulators', 1982 IEEE Power Electronics Specialists Conference, Conference Record, 1982.
- [11] S.S.Kelkar and F.C.Lee, 'Adaptive Feedforward Input Filter Compensation for Switching Regulators', Ninth International Power Electronics Conference and Exhibit, PowerCon 9, July 1982.
- [12] R.P.Iwens, 'ASDTIC Model: Time Domain Description and Digital Computer Program Development', TRW Interoffice Correspondence, September 1974.
- [13] F.C.Lee and Y.Yu, 'Computer-Aided Analysis and Simulation of Switched DC-DC Converters', IEEE Transactions on Industry Applications, Vol.IA-15, No.5, September 1979.
- [14] F.C.Lee, 'Digital Computer Simulation of HEAO Preregulators', TRW Interoffice Correspondence, May 1975.
- [15] R.P.Iwens, Y.Yu and J.E.Triner, 'Time Domain Modeling and Stability Analysis of an Integral Pulse Frequency Modulated DC-DC Power Converter', 1975 IEEE Power Electronics Specialists Conference, Conference Record, 1975.
- [16] R.P.Iwens, 'ASDTIC Analysis Using Discrete Time, State Space Approach', TRW Interoffice Correspondence, October 1974.
- [17] F.C.Lee, R.P.Iwens and Y.Yu, 'Generalized Computer-Aided Discrete Time Domain Modeling and Analysis of DC-DC Converters', 1977 IEEE Power Electronics Specialists Conference, Conference Record, 1977.
- [18] L.W.Johnson and R.D.Riess, 'Numerical Analysis', Addison-Wesley Publishing Company, 1977.